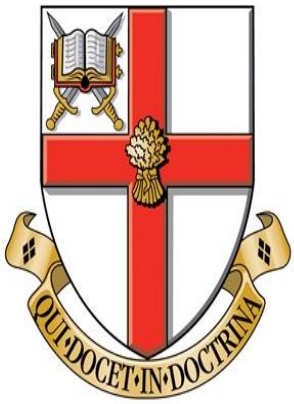

University of Chester

Faculty of Medicine, Dentistry and Life Sciences

"Changes in selective biomarkers after transurethral resection of the bladder tumour (TURBT), and their association with Non-muscle invasive bladder cancer (NMIBC) recurrence and progression"

Thesis submitted in accordance with the requirements of the University of Chester for the degree of Doctor of Philosophy

By

Peter Amona Ella-Tongwiis

September 2019

Declaration

"The material being presented for examination is my own work and has not been submitted for an award of this or another HEI except in minor particulars which are explicitly noted in the body of the thesis. Where research pertaining to the thesis was undertaken collaboratively, the nature and extent of my individual contribution has been made explicit."

Date: 16th September, 2019

Signature:

Acknowledgements

First, I would like to thank the lovely and courageous people who agreed to be recruited into this research study. In the world of research, people like you continuously contribute towards building a better world for us all.

I am also very grateful to all the staff within University of Chester and the Betsi Cadwaladr University Health Board- North Wales who supported, helped and provided professional input at various stages of this project especially staff at the arrivals ward- Wrexham Maelor Hospital, urology registrars at Wrexham Maelor Hospital and "Little Johnny" at histopathology department- Ysbyty Glan Clwyd.

I would like to acknowledge the tremendous help, advice and the many hours offered by Alexander Makanga – specialist biomedical scientist in Charge of immunohistochemistry at Ysbyty Glan Clwyd.

Thanks to Dr Gareth Elfred Jones for the making time to help and advice concerning statistical analysis.

Special thanks to Professor Stephen Fôn Hughes for the support over these years. Your friendship and mentorship before and during this research are very much appreciated. Special thanks also go to Professor Iqbal Shergill- Consultant Urological surgeon for the support and research opportunity within BCUHB.

Finally, I would like to thank my family for the continuous support and encouragement. To my wife especially, thanks for putting up with me during this time.

Table of Contents

Abstract

Introduction

Bladder Cancer (BC) is the 10th most common cancer in the UK, with about 10,000 new cases annually. It affects more men than women (ratio 3:1). Major risk factors include tobacco, chemical carcinogens, schistosomiasis infection and age. About 75-85% of BC are non-muscle invasive (NMIBC), which is associated with high recurrence and progression rates (50-60% within 7-10 years). Currently, diagnosis, treatment and management of BC is via clinical procedures such as transurethral resection of the bladder tumour (TURBT) and endoscopy. Concerning laboratory investigations, there are no routine biomarkers currently available for identifying BC patients at increased risk of developing recurrence and progression. By monitoring changes in selective biomarkers post-TURBT, any sustained changes may be a predictor of cancer recurrence or progression. The main-focus of this research study was to evaluate changes in selective novel biomarkers and their association with recurrence and progression in BC.

Materials & Methods

In this research, 40 patients (n=40) scheduled for TURBT at the Wrexham Maelor Hospital, North Wales were recruited after written informed consent. Ethical approval for the project was granted via IRAS (REC4: 14/WA/0033). Venous blood samples were taken at baseline (pre-operative) and following TURBT surgery at 1, 3 and 6 months post-operatively. Bladder tumour samples were also taken during TURBT according to standard procedure.

Selective biomarkers to assess inflammation, angiogenesis and tumour growth, were measured using commercially available ELISA and BioPlex multiplex assay kits. Tissue immunoreactivity of novel biomarkers were also assessed in BC tissues using immunohistochemistry, with clinical outcome measures being recorded for all patients.

Results

Significant increases in serum Cluster of differentiation 31 (CD31) ($p=0.003$) and Stem Cell Factor (SCF) ($p=0.032$) concentration, as well as trends of increasing concentration of serum basic Fibroblast Growth Factor (bFGF) ($p=0.14$), Vascular Endothelial Growth Factor Receptor-1 and 2 (VEGFR-1) ($p=0.15$), VEGFR-2 ($p=0.15$) and Follistatin ($p=0.40$) were observed in BC patients up to 6 months post-operative.

There were also significant decreases in serum Macrophage Inflammatory Protein -2 (MIP-2) ($p=0.001$), Platelet Derived Growth Factor (PDGF) ($p=0.012$), Matrix Metalloproteinase-9 (MMP-9) ($p=0.002$) and Vascular Endothelial Growth Factor C (VEGF-C) ($p=0.04$) serum concentration. Trends of decreasing concentration in MMP-2 ($p=0.79$), MMP-3 ($p=0.15$), interleukin-6 (IL-6) ($p=0.26$), interleukin-8 (IL-8) ($p=0.15$) and tumour necrosis factor-α (TNF-α) ($p=0.69$) were observed in BC patients up to 6 months post-operative.

There was significant immunoreactivity of CD31 ($p< 0.001$), CD34 ($p< 0.001$), Human epidermal growth factor receptor-2 (HER-2) ($p=0.032$), S100P ($p< 0.001$), Cyclooxygenase-2 (COX-2) ($p< 0.001$), VEGFR-3 ($p< 0.001$), SOX-2 ($p< 0.001$) and thrombomodulin ($p=0.010$) in bladder tumours. Although recurrence was significantly associated with cancer grade, there was no association with antibody immunoreactivity.

Conclusion

Findings from the present study may indicate an alternative approach in the monitoring and management of patients with BC. It is proposed that by allowing urological surgeons access to laboratory markers such as MIP-2, MMP-9, PDGF, SCF, HER-2, Thrombomodulin and CD31 (biomarker profile), potentially, in the future, these biomarkers may be used in addition to, or in combination with, currently used scoring systems to predict cancer recurrence and progression. However, verification and validation of these biomarkers are needed using larger cohorts.

Thesis Contents

List of Tables

List of Figures

Abbreviations

Ang-2	Angiopoietin-2
BC	Bladder Cancer
CRUK	Cancer Research UK
CC 1	Cell Conditioning 1
CC 2	Cell Conditioning 2
CD31	Cluster of differentiation 31
CD34	Cluster of differentiation 34
CEACAM-1	Carcinoembryonic Antigen-related Cell Adhesion Molecule 1
CIS	Carcinoma in situ
COX-2	Cyclooxygenase 2
CRC	Colorectal cancer
EAU	European Association of Urologists
EGF	Epidermal growth factor
EGFR	Epidermal growth factor receptor
bFGF	Basic fibroblast growth factor
FGFR	Fibroblast growth factor Receptor
H&E	Haematoxylin & Eosin
HCC	Hepatocellular carcinoma
HER-2	Human epidermal growth factor receptor 2
IHC	Immunohistochemistry
IL-6	Interleukin-6
IL-8	Interleukin-8
MIBC	Muscle Invasive Bladder Cancer
MIP-2	Macrophage inflammatory protein 2
MMP-2	Matrix metalloproteinase 2
MMP-3	Matrix metalloproteinase 3
MMP-9	Matrix metalloproteinase 9
NICE	National institute of health and care excellence

NMIBC	Non-Muscle Invasive Bladder Cancer
PDAC	Pancreatic ductal adenocarcinoma
PDGF	Platelet Derived Growth Factor
PECAM-1	Platelet Endothelial Cell Adhesion Molecule 1
PUNLMP	Papillary urothelial neoplasm of low malignant potential
SCC	Squamous cell carcinoma
SCF	Stem cell factor
SOX-2	Sex determining region Y box-2
TCC	Transitional cell carcinoma
TGF	Transforming Growth Factor
TNF-α	Tumour necrosis factor α
TURBT	Transurethral resection of the bladder tumour
VEGF-A	Vascular endothelial growth factor-A
VEGF-C	Vascular endothelial growth factor-C
VEGF-D	Vascular endothelial growth factor-D
VEGF(R)	Vascular endothelial growth factor (Receptor)

1.0 Chapter One: General Introduction

1.1 Overview

Bladder cancer (BC) is the eleventh most common cancer worldwide with an estimated 549,393 new diagnoses in 2018. Globally, it is also the fourth and thirteenth most common cancer in men and women respectively (Ferlay *et al.*, 2013, Wong *et al.*, 2018).

According to the World Health Organisation (WHO), in the UK, there were 12,218 new BC cases in 2018 and 6,101 BC related deaths whiles the 5-year prevalence was 40,146 (WHO, 2019).

Over ninety percent of all BC cases diagnosed in the UK are found in the transitional epithelium and are classified as transitional cell carcinomas (TCC). It is estimated that about 80% of TCC are non-muscle invasive (NMIBC) while about 20% may evade into the underlying detrusor muscle and are classified as muscle invasive BC (MIBC). Using the current WHO guidelines, BC is graded and staged depending on factors such as location of primary tumour, lymph node involvement and ability to spread (Babjuk *et al.*, 2017).

The current treatment/management protocols for BC involve patients undergoing endoscopy techniques (cystoscopy) and transurethral resection of the bladder tumour (TURBT) surgery to assess tumour growth and obtain biopsies for histological examination to aid diagnosis, staging and grading of patients. Cystoscopy and TURBT are repeatedly performed on the same patient during diagnosis, follow up and management. These measures are expensive, labour intensive and expose patients to repeated painful and invasive techniques.

The focus of this research was to identify changes in biomarker levels or immunoreactivity in various biological samples (serum, plasma and bladder tissues). The levels of these biomarkers at baseline were compared with levels at various post-operative stages i.e. 1, 3 and 6 months. After an assessment of the patient was made through current management protocols, the correlation between biomarker changes and BC recurrence/progression was studied. This research focussed on various markers of inflammation as well as markers of tumour growth and angiogenesis.

1.2 Bladder cancer epidemiology

1.2.1 Incidence

According to the WHO, globally, an estimated 549,393 new BC cases were reported in 2018, making BC the 11th most common cancer in the world. Geographically, differences in BC

incidence and mortality rates have been observed with the majority of all cases (59%) occurring in developed countries (Table 1.1).(Antoni *et al.*, 2017; WHO, 2019).

Table 1. 1 Estimated global incidence rates of BC by region in 2012.
Table shows high incidence rates in more developed regions of the world. ASR= age standardised ratio (Antoni *et al.*, 2017).

Area	Men	Women	M:F ASR ratio
World	330,380	99,413	4.1
Africa	17,685	6,752	3.0
Central/South America/Caribbean	17,610	7,234	3.1
North America	58,089	18,660	3.8
Asia	115,646	32,922	3.9
Europe	118,365	32,932	5.1
Oceania	2,985	913	3.9

In the UK, BC was the 9th most common cancer in the entire population in 2018. Statistically, there were 12,218 new BC cases, with 8,826 reported in men and 3,392 cases reported in women. The 5 year prevalence for the years up to 2018 was 20,146 (Antoni *et al.*, 2017, WHO, 2019).

Age is strongly associated with BC with most cases occurring in people over the age of 50. Burger *et al.* (2013) indicated that about 54% of all cases are found in people above 75 years, increasing to 90% in people aged above 60 years.

1.2.2 Mortality/Survival

Globally, about 123,000 men and 42,000 women died of BC in 2012 according to the WHO (Table 1.2). Most studies have highlighted factors such as environment, socioeconomic status, race and gender as significant contributory factors in BC mortality or survivability (Antoni *et al.*, 2017; Burger *et al.*, 2013; Ferlay *et al.*, 2013).

Table 1. 2 Estimated global mortality rates of BC by region.
Table shows high mortality rates in more developed regions of the world. ASR= age standardised ratio (Antoni *et al.*, 2017)

Area	Men	Women	M:F ASR ratio
World	123,051	42,033	3.6
Africa	9,362	3,906	2.9
Central/South America/Caribbean	7,078	3,069	3.0
North America	13,285	5,307	3.3
Asia	52,816	16,478	4.2
Europe	39,522	12,889	4.7
Oceania	988	384	3.2

According to the Office of national statistics (ONS), for the period 2012- 2017, the age standardised 1-year and 5-year net survival rates for men in England are 78.4% and 58.6% respectively. In the same period, the 1-year and 5-year net survival rates for women in England are 65.7% and 46.0% respectively (ONS, 2019)

For the 2007-2011 in Wales, 1-year survival rates were 77% (men) and 63% (women). These rates declined for five year rates to about 58% (men) and 50% (women) (Huddart, Jones, & Choudhury, 2015).

In the United States, a recent study reported significant associations between risk of BC death and a person's gender, ethnicity and environmental location. Tobacco use, employment status, access to portable water, house location and involvement in mining presented a significant risk of BC death ($p<0.05$) (Smith *et al.*, 2016).

1.2.3 Recurrence

In terms of quality of life and cost of treatment, recurrence plays a major role in BC. The National Cancer Institute defines recurrence as *"Cancer that has recurred (come back), usually after a period of time during which the cancer could not be detected".*

Recurrence rates in BC may vary according to the type, stage or grade of the cancer. In a large study of 7,410 subjects with high grade NMIBC, recurrence occurred in 2897 subjects while 2449 observed a cancer progression to advanced stages (Chamie *et al.*, 2013). Out of the 2449

cases, 981 died of BC related complications. Upon further analysis, the researchers reported an increased recurrence rate in women, people of black origin and BC stage T1. Furthermore, follow up data from the same study showed a 74.3% recurrence rate in 10 years in people with high grade NMIBC. In that same group, a 33.3% progression rate and a 12.3% BC related death rate were reported (Chamie *et al.*, 2013). This important study therefore highlights a complex association between BC recurrence and outcome.

1.3 Risk Factors in BC

Risk factors identified in BC include tobacco, exposure to chemical carcinogens (Table 1.3), chronic inflammatory infections, genetic modification, and lifestyle choices (Burger *et al.*, 2013; Cumberbatch *et al.*, 2018). Overall, an estimated 42% of all BC cases are attributed to lifestyle choices. More importantly, tobacco plays a significant role in up to 47% of all BC cases in the UK (Ng et al., 2013; Burger et al., 2013).

Table 1. 3 Risk factors associated with BC.
Risk factors are grouped based on levels of evidence (convincing versus limited) based on data produced from various studies. (Adapted from the International Agency for Research on Cancer (IARC) and World Cancer Research Fund/American Institute for Cancer Research (WCRF/AICR) classifications, 2018).

Evidence	Risk factors
'Sufficient' or 'Convincing' evidence	Aluminium production 4-Aminobiphenyl Arsenic/inorganic arsenic compounds Auramine production Benzidine Chlornaphazine Cyclophosphamide Magenta production 2-Naphthylamine Painting Rubber production industry Schistosoma haematobium Tobacco smoking ortho-Toluidine X-radiation, gamma-radiation
'Limited' or 'probable' evidence	4-Chloro-ortho-toluidine Coal-tar pitch Dry cleaning Engine exhaust, diesel Hairdressers and barbers, occupational exposure 2-mercaptobenzothiazole Pioglitazone Printing processes Soot Textile manufacturing Tetrachloroethylene

1.3.1 Tobacco

Chemical residues present in tobacco are filtered through urine and deposited in the bladder and may act as carcinogens for BC. Tobacco has been implicated as the most significant risk factor in the development of BC (Burger *et al.*, 2013), accounting for almost 37% of UK cases in 2010 (Parkin, 2011).

Several comprehensive Surgeon General's reports have concluded that there is a causal relationship between smoking and cancers in various organ systems (Health & Services, 2004; Health & Services, 2014; Smith *et al.*, 2016). Most of these cancers develop through a series of complex mechanisms such as gene mutation, activation of oncogenes and suppression of tumour suppressor genes as shown in Figure 1.1.

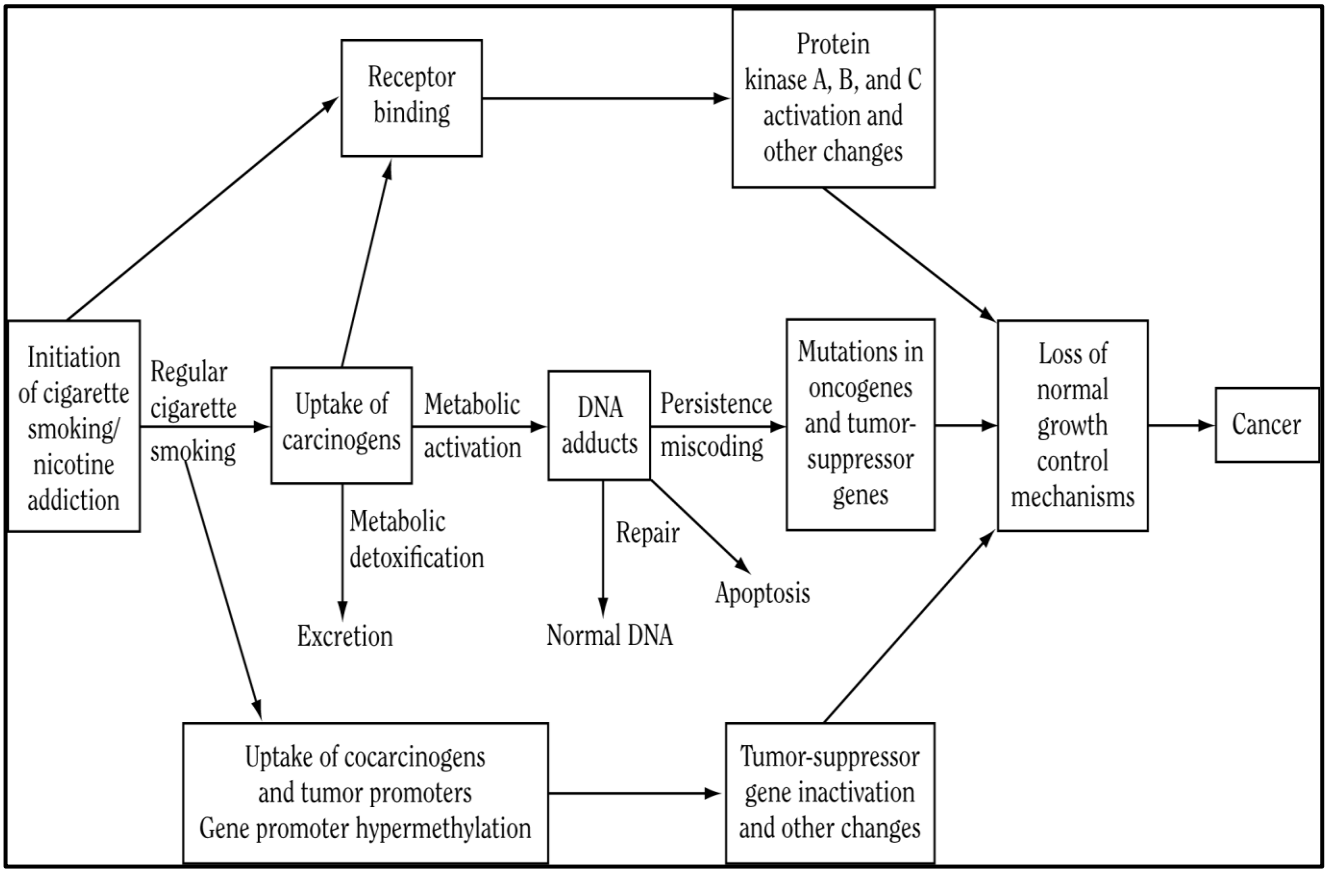

Figure 1. 1 Smoking-associated mechanisms in Cancer (Adapted from the US department of Health and Human Services, 2014).

Several studies have observed higher BC risk in smokers compared to non-smokers (Alberg *et al.*, 2007; McCormack *et al.*, 2010; van Osch *et al.*, 2018). This risk is also directly associated with quantity and duration of smoking (Ditre *et al.*, 2011; Freedman, Silverman, Hollenbeck, Schatzkin, & Abnet, 2011). Tobacco use was estimated to be a risk factor in up to 50% of the BC cases. Both former smokers (HR, 2.22; 95% confidence interval [CI], 2.03-2.44) and

current smokers (HR, 4.06; 95% CI, 3.66-4.50) were observed to have a significantly higher BC risk compared to those who had never smoked (Freedman *et al.*, 2011).

A recent study by Liss *et al* (2016) using a large sample size (N=222,163) implicated tobacco in BC specific deaths. In that study, there was an increased chance of BC specific death for active smokers (4-fold) and former smokers (3-fold) when compared to people who had never smoked. This study however did not make a stage by stage or grade by grade analysis of the BC (Liss, White, Natarajan, & Parsons, 2016).

In a systematic review of 14 research studies (n=5990), Crivelli *et al.* (2014) analysed the relationship between smoking status/exposure and various urological malignancies and conditions such as urothelial carcinoma, upper tract urothelial carcinoma (UTUC) treated with TURBT, radical cystectomy (RC), or radical nephroureterectomy (RNU). They reported a significant association between smoking and disease recurrence whilst some studies provided a link between smoking cessation and good prognosis.

In the UK, as part of BC management protocols, services are offered to BC patients who smoke to encourage smoking cessation. This recommendation, supported by the NICE guidelines, is aimed at reducing the harmful effects of tobacco, which has been well documented to play an integral role in the pathogenesis of BC.

1.3.2 Genetic Influence

There is limited evidence linking BC to inherited genetic variations. Currently, there is heightened interest in molecular genetics to understand the role of mutations in the development of BC (Kwan *et al.*, 2019; Zhang *et al.*, 2018a).

In many patients, mutations in the fibroblast growth factor receptor-3 (FBFR3), retinoblastoma protein (RB), HRAS and TP53 genes have been shown to increase BC risk (Apollo *et al.*, 2019; Zhang *et al.*, 2018a). These genes and proteins play specific functions in regulating cell cycle and growth. The resulting mutants have diminished capacity and therefore results in uncontrolled cell growth.

In an epidemiological study of microRNA variants, researchers reported a significant link between people who possessed these microRNAs and BC development (Yang *et al.*, 2008). The researchers included 746 Caucasians who had BC and a further 746 controls and studied 41 single-nucleotide polymorphisms in each group. They observed that a variant genotype of a gene called GEMIN3 presented a significantly higher risk of developing BC (OR = 2.40; 95% CI = 1.04 –5.56). Furthermore, using haplotype analysis, it was observed that the GEMIN4

gene also presented a higher chance of developing BC (OR= 1.25; 95% CI= 1.01–1.54). Even though this was an experimental study, together with other recent studies (Lee *et al.*, 2018; Mazoochi, Karimian, Ehteram, & Karimian, 2019) they highlight the suspected link between gene variants and BC.

1.3.3 Occupational Environment

Work exposure to several chemicals can significantly increase the risk of BC (Table 1.3) with some studies putting the risk at 5-6% (Parkin, 2011). In the dye industry, chemicals like 4-Aminobiphenyl, 2-Naphthylamine and benzene are routinely used and have been implicated in BC (Brown, Slack, Rushton, & Group, 2012). Some aromatic amines present in textiles, rubber and pesticides are carcinogenic and expose workers in those industries to BC. In the rubber industry alone, workers risk for BC is 29% more than the rest of the population (Reulen, Kellen, Buntinx, Brinkman, & Zeegers, 2008).

In a prospective study of 57,310 people who use pesticides, Koutros *et al.* (2016) have reported an elevated BC risk. Using Poisson regression analyses, a higher BC risk was found in people who had used bentazon (RR= 1.55, 95% CI= 1.10, 2.19), Bromoxynil (RR= 1.51, 95% CI= 1.04, 2.20), Chloramben (RR= 1.56, 95% CI= 1.10, 2.22) and diclofob-methyl (RR= 1.85, 95% CI= 1.01, 3.42) at least once. There was also a positive link between dichlorodipheyltrichloroethane (DDT) (RR= 1.40, 95% CI= 1.10, 1.80) and heptachlor (RR= 1.30, 95% CI= 0.98, 1.74) and BC. From this study Koutros *et al.* (2016) successfully established the relationship between various aromatic amines.

A recent study in two Italian case cohorts observed that prolonged exposure to carcinogens such as cadmium and trichloroethylene were associated with BC. They also observed an increased association between occupations such as chemical engineering and postal services and BC (Sciannameo *et al.*, 2018).

1.3.4 Medications/Conditions

Some medical conditions have been implicated in BC as either a primary factor or secondary to the carcinogenic influence of drug treatment. Conditions like urine retention may significantly increase the risk of BC (Jiang, 2007). In certain regions like North Africa and Asia, the high cases of a parasitic infection known as schistosomiasis, which causes inflammation in the urinary system, may be an etiologic factor in BC (Burger *et al.*, 2013).

BC is reported to be the most common in Egypt primarily due to the prevalence of an infection; schistosomiasis (Burger *et al.*, 2013). Schistosomiasis is an infection caused by a parasite

known as *Schistosoma haematobium*. It is characterised by chronic inflammation of the bladder and other components of the urinary tract and very common in Egypt and other countries in the Mediterranean (Parkin *et al.*, 2008). BC arising from Schistosomiasis are usually squamous cell carcinomas (SCC). Even though over 90% of all BC are TCC Babjuk *et al.* (2013), relatively rare forms such as SCC may also occur.

1.4 Structure of the bladder, Staging, Grading and Risk stratification in BC

1.4.1 Structure of the bladder

The urinary bladder is surrounded by layers of adipose and connective tissues. Females possess a slightly smaller bladder due to the presence of the uterus which sits directly above and slightly towards the back of the bladder and increases in size during pregnancy and therefore reduces the storage capacity of the bladder (Dixon & Gosling, 1983).

The bladder may be divided into two parts (Figure 1.2). The "body" is found superior to the ureteral openings whilst the base is found superior to the urethral opening and made up of the trigone, deep detrusor and urethrovesical wall (Andersson & Arner, 2004).

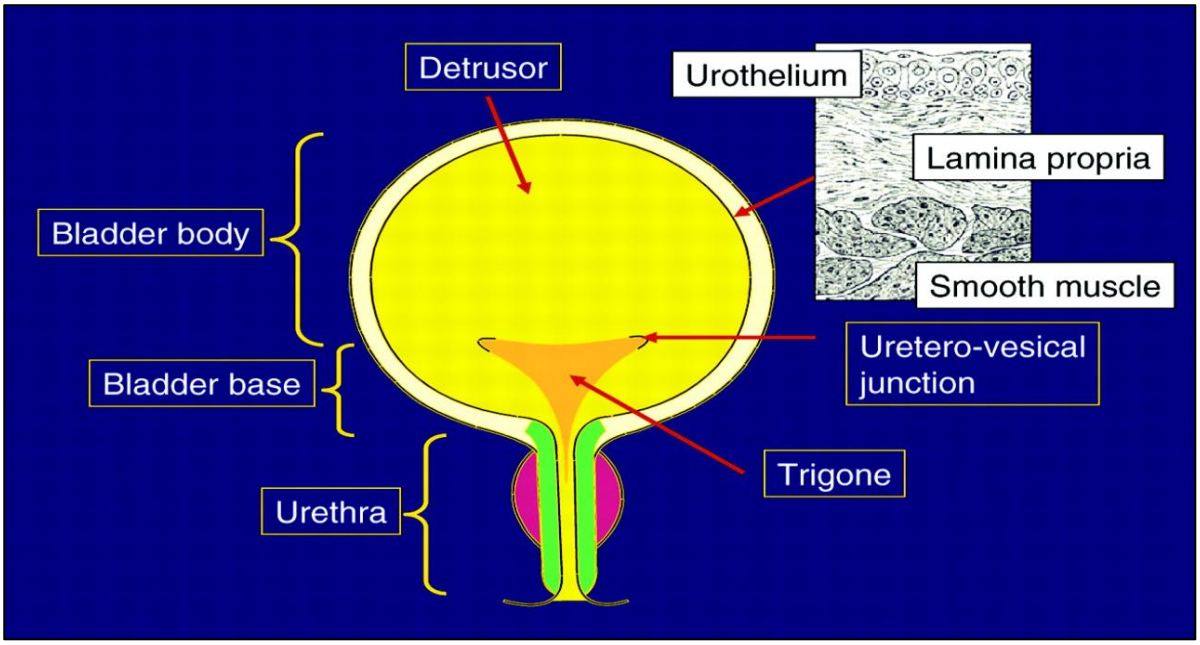

Figure 1. 2 Layers of the Urinary Bladder. Adapted from (Andersson & Arner, 2004)

Anatomically, the bladder consists of 3-6 layers, all of which play significant roles in tumour classification and staging.

The mucosa makes up the topmost layer of the bladder. This mucosa is different from those found in other parts of the body by its ability to stretch and hold large quantities of urine. The

epithelium covers the mucosa and is the layer usually in contact with urine. It may also be called the urothelium or transitional epithelium. This transitional epithelium is distinct as it contains multiple layers of cells (Figure 1.3). It has an innermost layer, about 2-5 middle layers and a topmost (superficial) layer (Jost, Gosling, & Dixon, 1989). The various layers contain different cell sizes and nuclei content, with innermost and intermediate layers showing distinctly thicker nuclei, stains more intently and varying cell sizes (Jost *et al.*, 1989).

Most BC arise from cells in the epithelium. Other components of the urinary system contain similar epithelial cells and may therefore develop similar cancers as the bladder (Guo, Liu, & Teng, 2016; Humphrey *et al.*, 2016; Mostofi, Sobin, Torloni, & Organization, 1973).
Located immediately beneath the epithelium is the lamina propria consisting of connective tissue and blood vessels. The lamina propria also contains a layer of smooth muscle known as muscularis mucosae. This is usually a monolayer and different in structure from the main muscular tissue of the bladder (Humphrey *et al.*, 2016; Jost *et al.*, 1989).
The muscularis propria also known as detrusor muscle makes up the inner wall of the bladder. It is primarily made of smooth muscle and is important for determining cancer grade and stage. The deepest bladder tissue layer is the perivesical tissue and usually comprises blood vessels, fat layers and fibrous tissue (Humphrey *et al.*, 2016; Jost *et al.*, 1989).

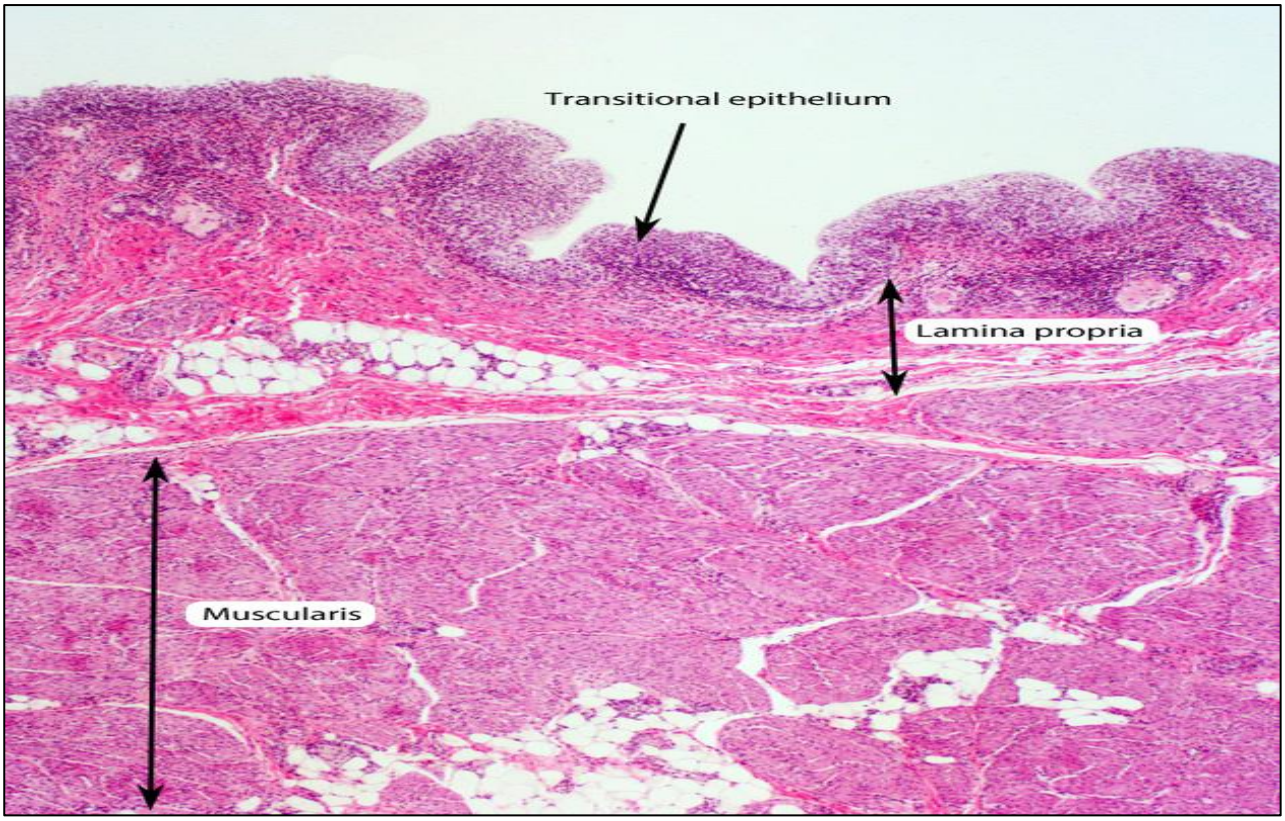

Figure 1. 3 Histological structure of the urinary bladder
H&E staining showing histological distinctions of the urinary bladder. Top most layer consist of multiple layers of epithelial cells (transitional epithelium). Lamina propria contains connective tissue and vascular network. Underlying muscularis (also called detrusor muscle) lies below the lamina propria and contains blood vessels and smooth muscle cells (Humphrey, Moch, Cubilla, Ulbright, & Reuter, 2016)**.**

1.4.2 Staging

Staging is one of the classification techniques employed for the treatment and management of BC. The most important staging system is known as Tumour Node Metastasis (TNM) classification. It uses tumour information, lymph node involvement and metastatic ability to classify Bladder tumours (Figure 1.4).

Majority of BC cases develop in the superficial layers of the transitional epithelium and lamina propria and have been termed superficial or non-muscle invasive BC (NMIBC). It occurs mostly in the mucosa and submucosal layer (Ta, T1 or CIS) (Babjuk *et al.*, 2013). An estimated 75-85% of all BC cases are NMIBC. Specifically, stage Ta is responsible for about 80% of NMIBC, whiles muscle invasive BC (MIBC) accounts for 20% (Colquhoun & Mellon, 2002).

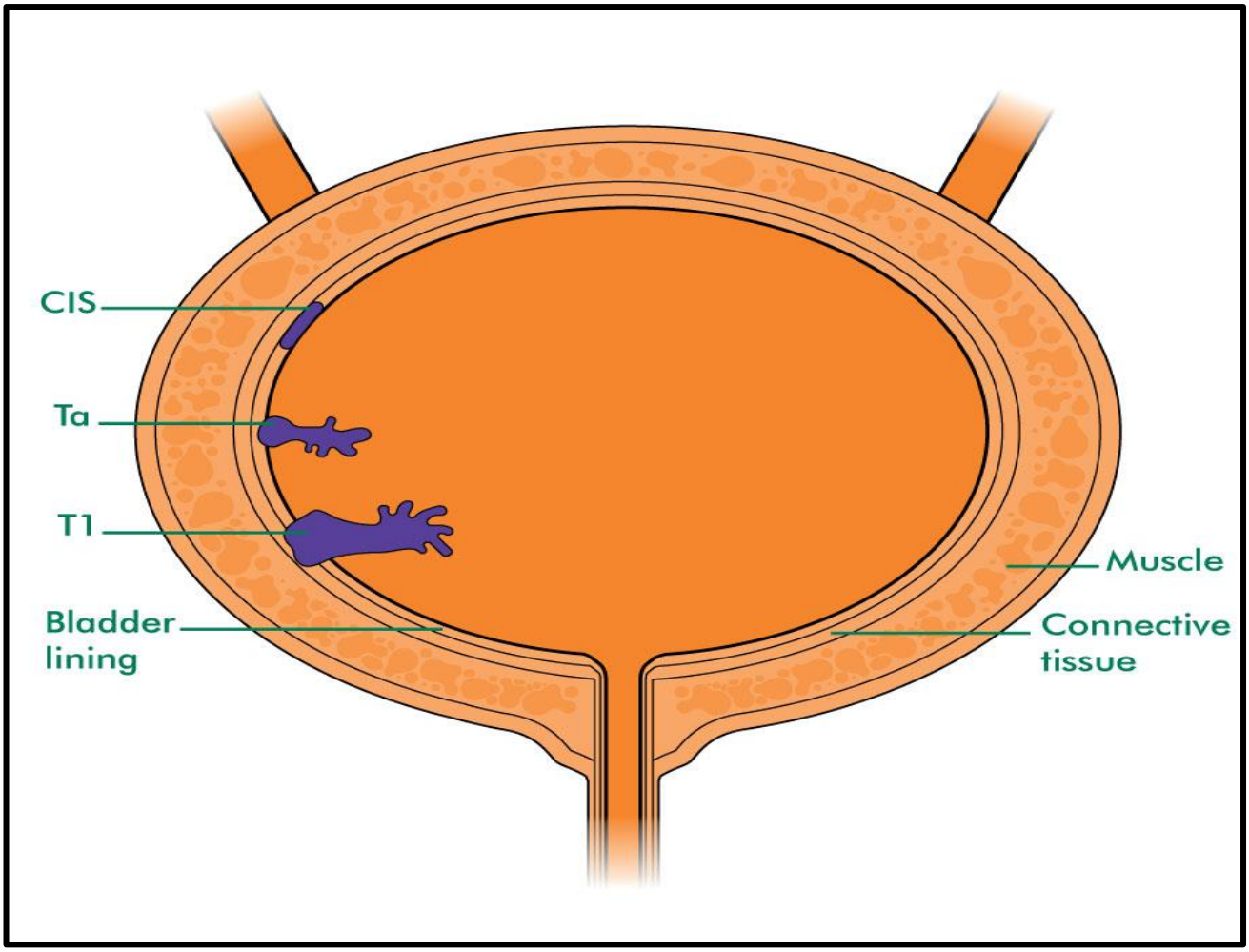

Figure 1. 4 Staging of BC
Staging BC is based on location of the tumours. CIS and Ta are located on the urothelium whilst T1 is located epithelium and lamina propria (Reproduced from Macmillan Cancer support, 2019)

The TNM classification is used to categorise BC depending on three main factors; Tumour, lymph node involvement and ability to metastasize (Table1.4 and Figure 1.4). Stage Ta are localised in the epithelium and does not spread to the underlying tissues like the lamina propria. Progression rate is low even though most tumours recur after treatment. Stage Ta tumours are also mostly low grade, however, 3-18% present as high grade (Sylvester *et al.*, 2005).

Stage T1 BCs usually arise from the epithelium but spread into the lamina propria. They however do not penetrate enough to reach the detrusor muscle. (Stein *et al.*, 2001) reports that about 30% of stage T1 tumours were re-classified as muscle invasive even though there were initially reported as NMIBC.

CIS tumours occur only in the epithelium, are usually high grade and may appear as little reddish projections even though some are not detected easily. They are also usually associated with advanced grade invasive lesions. When treatment is not initiated, a high number of CIS

cases (40-80%) usually spread into muscle tissues. Patients diagnosed with both CIS and T1 cancers are reported to have severe outcomes than those presenting with other stages of NMIBC (Losa, Hurle, & Lembo, 2000).

With respect to this thesis, patients diagnosed with NMIBC will be the focus by investigating the role of novel biological biomarkers that may be able to predict cancer recurrence and progression.

Table 1. 4 TNM BC classification 2009 (Babjuk *et al.*, 2013)

T	Primary tumour
Ta	Non-invasive papillary carcinoma
Tis	Tumour in situ (carcinoma in situ)
T1	Tumour invades sub-epithelial connective tissue
T2	tumour invades muscularis a: superficial muscle (inner half) b: deep muscle (outer half)
T3	Tumour invades perivesical tissue (beyond muscularis) a: microscopically b: macroscopically (extravesical mass)
T4	Tumour invades any of the following: prostate, uterus, vagina, pelvic wall, abdominal wall a: Prostate, uterus, vagina b: Pelvic wall, abdominal wall
N	Lymph nodes
Nx	Regional lymph nodes cannot be assessed
N0	No regional lymph nodes metastases
N1	Metastasis in a single lymph node in the true pelvis (hypogastric, obturator, external iliac or presacral)
N2	Metastasis in multiple lymph nodes in the true pelvis
N3	Metastasis in common iliac lymph node
M	Distant metastasis
M0	No distant metastasis
M1	Distant metastasis

1.4.3 Grading and risk stratification

Grading classification of BC is important in the management of BC and used as an effective tool in prognosis. The WHO classified BC into 3 grades in 1973; grades 1-3 based on cellular anaplasia ie alterations in differentiation (Table 1.5) (Mostofi *et al.*, 1973).

A histological form of grading NMIBC initially proposed by the WHO in 1973 was later updated in 2004 (Table 1.5) (Epstein, Amin, Reuter, Mostofi, & Committee, 1998; Sauter *et al.*, 2004). Even though both have been successfully used to grade patients and improved prognosis, patient stratification continue to overlap in both systems and opinion among

researchers and clinicians is divided concerning universal usage and integration into clinical trials (Babjuk *et al.*, 2013).

In subsequent reviews, the WHO introduced the 2004 grading system for non-invasive urothelial tumours based on tissue architecture and cytological features (Eble, Sauter, Epstein, & Sesterhenn, 2004; Lopez-Beltran & Montironi, 2004). This grading system gives clearer definitions of tumours and distinguishes between malignancies and lesions with low malignant potential.

The high recurrence rates in NMIBC has highlighted the need to adopt models to aid in the prediction of recurrence and progression. Even though an exact risk classification template is not currently available, some generally accepted guidelines have been formulated. In this regard, the European association of Urology (EAU), European Organization for Research and Treatment of Cancer (EORTC) and the Spanish Club Urológico Español de Tratamiento Oncológico (CUETO) are important institutions that have developed models for risk stratification. In terms of disease progression, cancer grade is considered a higher risk factor than cancer stage. This observation is due to the fact that similar disease progression rates have been reported in BC patients who presented with high grade T1 or Ta (Millan-Rodriguez, Chechile-Toniolo, Salvador-Bayarri, Palou, & Vicente-Rodriguez, 2000).

Table 1. 5 Risk stratification in NMIBC.
This model was developed based on evidence review and clinical opinion and places BC cases in 3 risk groups based on stage, grade and clinical history (Huddart & Choudhury, 2015).

Low Risk NMIBC	Intermediate Risk NMIBC	High Risk NMIBC
▪ Solitary pTaG1 <3cm ▪ Solitary pTaG2 (low grade) <3cm ▪ Any PUNLMP	▪ Solitary pTaG1 >3cm ▪ Multifocal pTaG1 ▪ Solitary pTaG2 (low grade) >3cm ▪ Multifocal pTaG2 (low grade) ▪ pTaG2 (high grade) ▪ Any pTaG2 (grade not further specified) ▪ Any low risk recurring within 12 months from last tumour occurrence	▪ pTaG3 ▪ pT1G2 ▪ pT1G3 ▪ pTis (Cis) ▪ aggressive variants of urothelial carcinoma, for example micropapillary or nested variants

Table 1. 6 1973 and 2004 WHO histological grading of BC (Mostofi et al., 1973 Sauter et al., 2004

1973 WHO grading
Urothelial papilloma
Grade 1; well differentiated
Grade 2; moderately differentiated
Grade 3; poorly differentiated
2004 WHO grading
Flat lesions
Hyperplasia (flat lesion without atypia or papillary)
Reactive atypia (flat lesion with atypia)
Atypia of unknown significance
Urothelial dysplasia
Urothelial carcinoma in situ
Papillary lesions
Urothelial papilloma (which is a completely benign lesion)
Papillary urothelial neoplasm of low malignant potential (PUNLMP)
Low-grade papillary urothelial carcinoma
High-grade papillary urothelial carcinoma

The NICE guidelines identify three risk categories for patients with NMIBC; low risk, intermediate risk and high risk (Table 1.6). In risk stratification and treatment, all BC management guidelines encourage clinicians to take into consideration patients' previous recurrence information, size/number of tumours, stage/grade, CIS presence and invasion of the lymph nodes (Huddart & Choudhury, 2015). This stratification, suggested by the NICE were based on analysis of EORTC tables as well as other research studies (Lammers *et al.*, 2014; Sylvester *et al.*, 2006).

1.5 Clinical techniques for the management of BC

Currently, there is no approved/recommended and widely used laboratory-based diagnostic technique specifically developed for the diagnosis of BC. Non-specific symptoms of BC, which includes blood in the urine (haematuria), lower abdominal pain and fatigue, are most often associated with other conditions.

The diagnosis and subsequent management/monitoring of BC cases therefore require a combination of several laboratory-based, clinical and technological techniques for effective treatment and management. These include imaging and surgical techniques, laboratory examination of biological samples, radiotherapy and immunotherapy.

1.5.1 Imaging Techniques

Flexible or rigid cystoscopy, performed under local or general anaesthesia are important imaging techniques used in the assessment, treatment and management of bladder conditions (Figure 1.5). The most common form is conducted using white light (known as white light cystoscopy (WLC)) even though different light sources are available and are being used with varying results (Grossman *et al.*, 2007; Herr & Donat, 2008). Variations in the detection of recurrences in low risk patients have been observed in some types of cystoscopy (Chou *et al.*, 2017). Marginal differences between WLC and Narrow Band Imaging has recently been reported (Drejer *et al.*, 2017). There has also been reports of low sensitivity in cystoscopy compared to other imaging techniques (Mowatt *et al.*, 2010). These observations further highlight the need to investigate novel biomarkers capable of identifying recurrence and progression in BC.

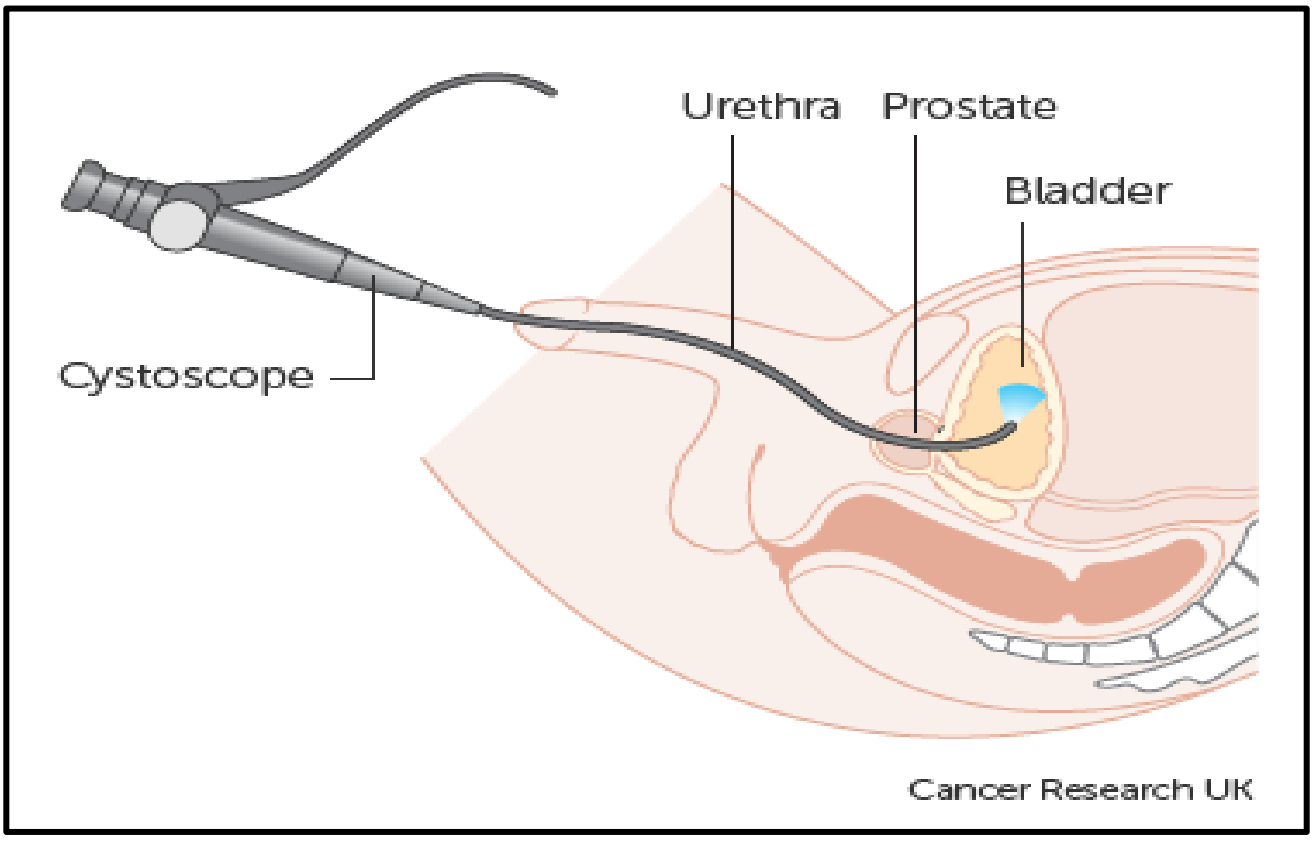

Figure 1. 5 Cystoscopy in Men. [Adapted from CRUK, 2016)].

1.5.2 Transurethral Resection of a Bladder tumour (TURBT)

TURBT is a fundamental treatment option for BC and is usually done after a diagnosis of NMIBC has been made using imaging, cytological and histological techniques. Before a TURBT session however, flexible cystoscopy (together with CT scan or MRI in patients with suspected MIBC) is conducted to assess the size and location of the tumour (Huddart & Choudhury, 2015).

There is evidence to suggest that, patients whose Bladder tumours were resected without removing detrusor muscle, have an increased risk of early recurrence (Mariappan, Zachou, & Grigor, 2010). This later research highlights the findings of (Brausi *et al.*, 2002) on the quality and accuracy of bladder samples for histology. In the latest NICE guidelines however, more high quality research using higher samples sizes, is encouraged to assess the relationship between TURBT and outcomes in new and recurrent BC (Huddart & Choudhury, 2015).

These undesirable outcomes of TURBT, which is currently the gold standard for the diagnosis and treatment of BC, highlights the need for more research into identifying biomarkers in BC, which is a focus of our present study.

1.6 Role of the laboratory in BC Management

There are currently no routinely used blood or tissue-base biomarkers for the management of BC. Diagnosis and management of BC are currently done by examining haematoxylin and eosin (H&E) stained microscope slides of bladder biopsies.

1.6.1 Urine cytology and molecular markers

Urine cytology has been used for several years as a screening tool to identify BC in high-risk individuals, i.e. people with haematuria, the aged and people with a previous history of BC. The utility of cytology however is questionable since it has low sensitivity in low grade tumours and is prone to variations such as experience of the scientist examining the specimen (Lotan & Roehrborn, 2002).

For patients with high grade TCC or carcinoma in situ (CIS), examination of voided urine through urine cytology is reported to be useful in diagnosis. Sensitivity of urine cytology in high grade TCC and CIS has been estimated to be as high as 90-100% in some cases. In low grade TCC however, low sensitivities have been reported (Yafi *et al.*, 2015). High false negative rates due to infections, inflammation, chemotherapy surgery and stones have been associated with urine cytology (Gupta *et al.*, 2019). These factors, together with initial high cost, reduce the utility of urine cytology for the routine management of BC.

Urine based molecular biomarkers, such as Bladder tumour antigen (BTA) and Nuclear Matrix Protein 22 (NMP22) have been developed based on ELISA techniques (Table 1.7). These tumour specific biomarkers identified in Bladder tumours present with higher sensitivities (Yafi *et al.*, 2015).

Table 1. 7 Urinary Molecular markers for BC diagnosis/management.
Table represents current urine-based markers in BC and highlights variations in both sensitivity and specificity for all BC and high-grade tumours. Some markers have been approved by FDA for clinical use; however, none is currently routinely used in BC management. Adapted from (Babjuk *et al.*, 2017). BTA= Bladder specific antigen.

Biomarkers/Test	Overall Sensitivity (%)	Overall Specificity (%)	Sensitivity for high-grade tumours (%)
UroVysion (FISH)	30-86	63-95	66-70
Microsatellite analysis	58-92	73-100	90-92
Immunocyt/uCyt +	52-100	63-79	62-92
Nuclear matrix Protein 22	47-100	55-98	75-92
BTA stat	29-83	56-86	62-91
BTA TRAK	53-91	28-83	74-77
Cytokeratin	12-88	73-95	33-100

According to the NICE guidelines (Huddart & Choudhury, 2015), urinary biomarkers should not be exclusively used for the investigation of suspected BC cases or for monitoring BC patients post-treatment. The use of urine biomarkers in the diagnosis or monitoring of BC treatment could however be encouraged in exceptional cases such as clinical research studies.

1.6.2 Haematoxylin & Eosin examination

In histopathology, the haematoxylin and Eosin (H&E) stain is one of the most widely used tools for the evaluation and confirmation of pathological conditions. It is routinely performed on tissue sections that have been adequately processed and sectioned. Currently, H&E is the gold standard for the confirmation of most cancers, including BC.

The fundamental element in H&E staining in histology is the use of two or more stains to colour different cell or tissue components. In pathological conditions, due to changes or divisions in the nucleus, the H&E stain is used to highlight these changes and helps in decision-making. Haematoxylin, a component of the H&E stain, is purple dye that stains the nuclear material in the nucleus whiles the Eosin component stains the cytoplasmic material.

In the diagnosis and management of BC, pathologists routinely use H&E stained tissue slides. Indeed, all BC grading systems are based on the examination of H&E slides (Gupta *et al.*,

2019). Interpretation of H&E slides must therefore be done by trained histologists and pathologists, taking into account patient history, clinical presentation and other laboratory investigations.

1.6.3 Immunohistochemistry (IHC)

In histology, IHC is an immunoassay used to explore antigen (protein) presence in tissue sections using specific antibodies. The principle is based on the interaction between antigens and antibodies and ability to detect these interactions using various detection systems. IHC is a multi-step process (Figure 1.6) starting from the theatre/clinic (sample collection) to the laboratory and may therefore be influenced by several factors.

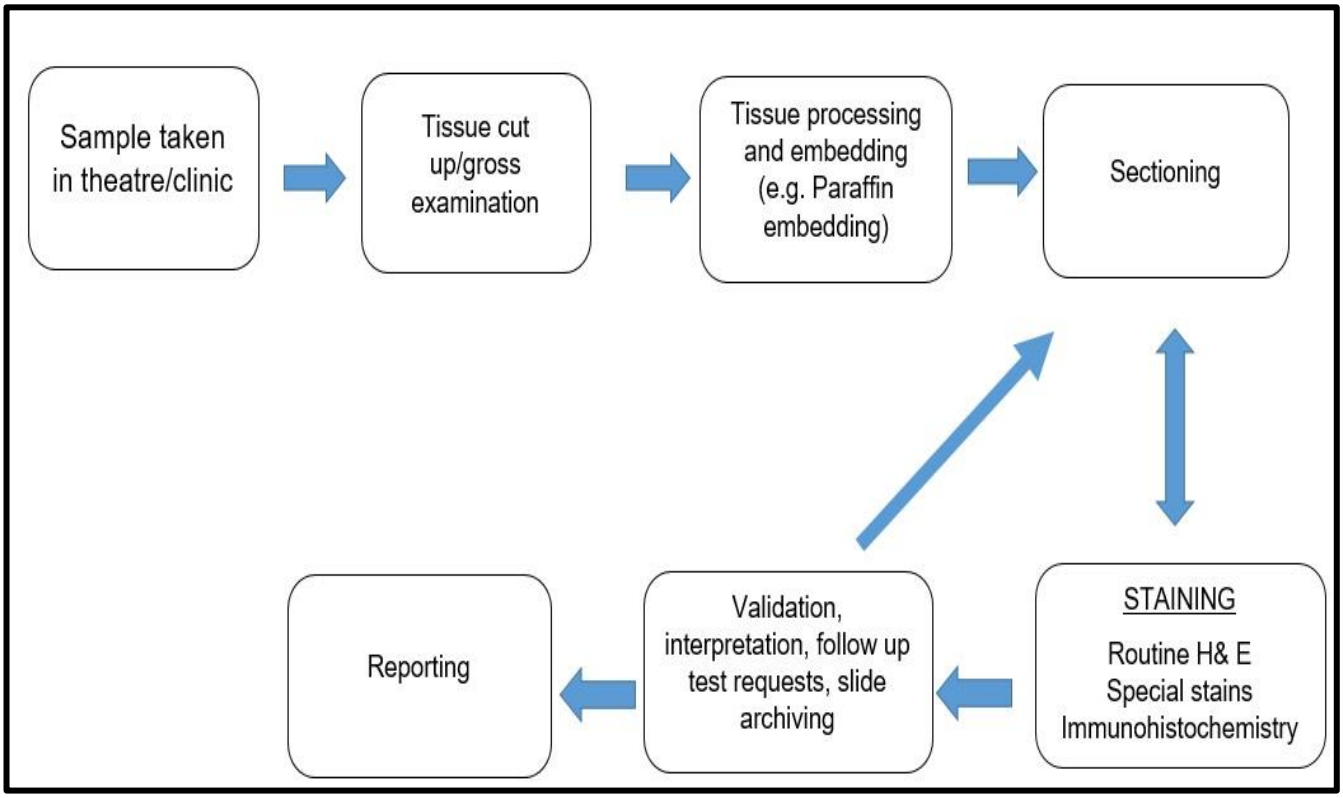

Figure 1. 6 Workflow in a typical histopathology laboratory.
The multi-step process begins with sample preservation (using formalin for example) and ends with the release of a laboratory report for the requesting physician. Prepared slides can be re-sectioned in cases where there is poor staining or for follow up test requests.

IHC evaluation of cancer tissue samples has led to development of treatment therapies in some cancers. In breast cancer treatment and management, immunoreactivity of a panel of antibodies (estrogen receptor, progesterone receptor, and human epidermal growth factor receptor 2) is valuable in deciding treatment options (Dede *et al.*, 2013; Xu, Guo, Jing, & Sun, 2018).

A study of 93 BC patients have identified IHC as a potential tool for sub-classifying T1 tumours (Mhawech, Iselin, & Pelte, 2002). Another has highlighted the immunohistochemical characteristics in various disorders of the bladder (Rajcani *et al.*, 2013).

1.7 Hallmarks of Cancer

A depth of knowledge, gained through intense research using tissue culture, animal models and human tissues, has increased our understanding of tumourigenesis, treatment and subsequent management of several human tumours.

Previous research has shown that tumourigenesis is a complex multi-step process of molecular and genetic changes resulting in the conversion of normal tissue cells into malignant tumour cells (Foulds, 1954; Nowell, 1976). Most of these tumour cells in humans have also been shown to be traditionally linked with several rate limiting reactions or events (Balmain, Barrett, Moses, & Renan, 1993).

Hanahan & Weinberg (2000) proposed a framework upon which the complex properties of cancer could be clearly organised. This framework grouped cancer features into six broad hallmarks (Figure 1.7);

- The ability of cancer cells to be self-sufficient in producing growth signals,
- The ability to evade programmed self-death
- Insensitivity to signals regulating cell growth
- Unlimited cell growth
- The ability of cancer cells to invade near and distant tissues and metastasis
- Uncontrolled blood vessels production (angiogenesis) (Hanahan & Weinberg, 2000).

This research focussed on the role inflammation and angiogenesis play in BC recurrence and progression and will be discussed in the next section (Hanahan & Weinberg, 2011; Mantovani, 2009).

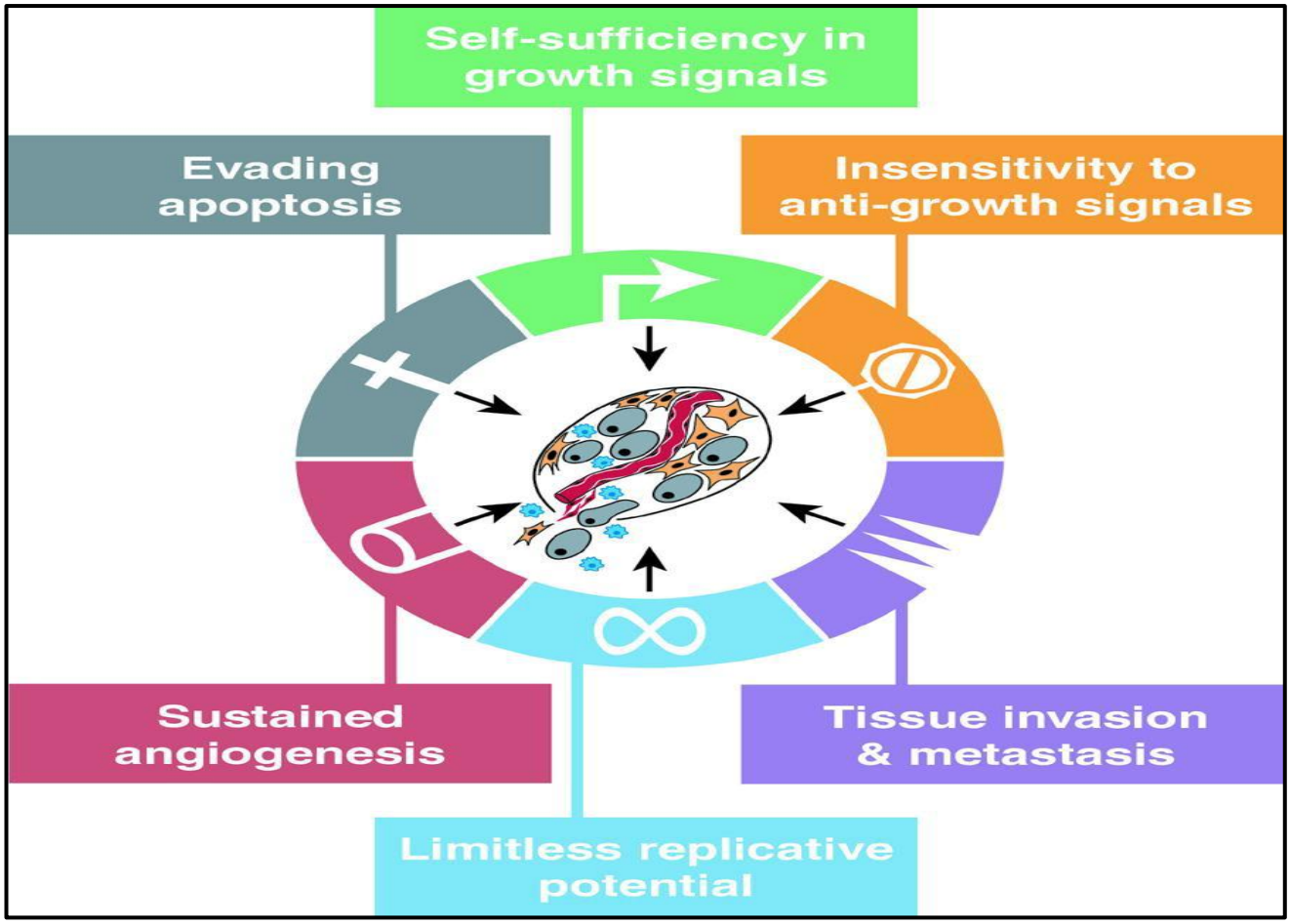

Figure 1. 7 Hallmarks of cancer.
The six initial hallmarks of cancer proposed by Hanahan and Weinberg are cells' ability to evade programmed death, uncontrolled angiogenesis, unlimited replicative potential, tumour cells ability to invade underlying tissues and metastasis, ability to evade anti-growth signals and ability to continuously produce growth signals. These complex multi-step processes are exhibited by most tumour cells. Adapted from (Hanahan & Weinberg, 2000).

1.7.1 Sustained Angiogenesis

Angiogenesis (also loosely called angiopoiesis) refers to the production of new blood vessels (Risau, 1997; Simons *et al.*, 2018). It is an essential feature in organ formation and growth as it ensures adequate distribution of nutrients and oxygen to all cells or tissues (Potente & Carmeliet, 2017).

There is evidence, from earlier research, that normal endothelial cells lack the ability (they are quiescent) whereas early cancer cells acquire the ability to induce angiogenesis (Bouck, Stellmach, & Hsu, 1996). In conditions such as diabetic retinopathy, psoriasis and rheumatoid arthritis, increased angiogenesis has been implicated in disease development and severity (Colville-Nash & Scott, 1992).

In tumour pathology, angiogenesis is an essential hallmark for tumour growth in which tumour cells are unable to grow in the absence of new blood vessels (Folkman, 1971; Potente & Carmeliet, 2017).

The so called 'angiogenic switch', which refers to positive and negative angiogenic signals has been extensively discussed in a bid to explain angiogenesis (Baeriswyl & Christofori, 2009; Huijbers *et al.*, 2016). Angiogenic signals may be initiated by soluble factors or receptors located on the surfaces of endothelial cells resulting in the deregulation of cell-cell and cell-matrix interactions. Examples of positive angiogenic signals are VEGF, FGF and MMP which may interact with receptor tyrosine kinases found on the surfaces of endothelial cells (Kessenbrock, Wang, & Werb, 2015; Liang & Ferrara, 2016). Angiogenesis can also be inhibited or stopped in the presence or through the activities of several negative factors or inhibitors, such as thrombospondin-1 (Moens, Goveia, Stapor, Cantelmo, & Carmeliet, 2014).

With regards to angiogenesis and vascular permeability, VEGF-A, together with receptor tyrosine kinases (VEGFR-1 and VEGFR-2) are the most prominent and have been extensive studied (De Palma, Biziato, & Petrova, 2017). VEGF-A has been shown to induce angiogenesis, vascular permeability and cell migration by activating VEGFR-1 and VEGFR-2 (Shibuya & Claesson, 2006) (Hanahan & Weinberg, 2011).

There is also a strong association between VEGF and the extracellular matrix. Indeed Hardbower, de Sablet, Chaturvedi, & Wilson (2013) have observed that inactive forms of VEGF ligands located within the ECM may be activated by collagenases such MMP-9. This link between ECM degradation and VEGF signalling further highlights the role angiogenesis plays in tumour progression.

Another important proangiogenic factor that plays an important role in tumour development and progression is FGF and its receptors. These factors and receptors sustain angiogenesis in tumours through positive angiogenic signalling (Baeriswyl & Christofori, 2009).

The activities of anti-angiogenic proteins in the behaviour of malignant cells have been identified as an opportunity to develop treatment therapies. In genetically altered mice deficient in tumstatin (an anti-angiogenic protein), there was an exponential growth in tumour size of 300% and a markedly increased microvessel density. Subsequent adjustment of tumstatin to normal physiologic levels resulted in reduced tumour growth (Maeshima *et al.*, 2000).

The significant links identified between angiogenesis and cancer have highlighted the need to identify angiogenesis-associated biomarkers that can be used for managing human cancers. With respect to BC, any identification of a potential biomarker that can be utilised for

management or monitoring initial treatment outcome, can enhance patient care since there are currently no routinely used biomarkers for that purpose.

1.7.2 Inflammation

An inflammatory response may be initiated by external influences such as microbes or toxins and internal influences such as necrotic tissues. These influences initially result in dilation of blood vessels, increased vascular permeability and recruitment of host defence mediators and cells such as dendritic cells, macrophages and mast cells, to the site of inflammation (Balkwill & Mantovani, 2012).

Due to advances in technology, most of the principal characteristics of inflammation can now be explained. For example, during tissue injury or microbial infection, activation of inflammatory molecules such as cytokines, enzymes, nitric oxide and TNF eventually lead to dilation of blood vessels. This fundamental change is believed to be the cause of redness, heat and swelling of inflamed tissues (Munn, 2017). Table 1.8 lists some mediators of inflammation, their sources of production as well as their functions.

Table 1. 8 Mediators of Inflammation.
(Barden *et al.*, 2018; Dmitrieva, Shilovskiy, Khaitov, & Grivennikov, 2016).

Mediators	Source	Effect on inflammation
Histamine	Mast cells, basophils, platelets	Vasodilation, increased permeability, endothelial action
Prostaglandins	Mast cells, leucocytes	Vasodilation, pain, fever
leukotrienes	Mast cells, leucocytes	Increased permeability, chemotaxis, leucocyte adhesion, leucocyte activation
Cytokines (TNF, IL-1, IL-6)	Macrophages, endothelial cells, mast cells	Endothelial activation (immunoreactivity of adhesion
Chemokines	Leucocytes, mast cells	Chemotaxis, leucocyte activation
Platelet activation factor	Leucocyte, mast cells	Vasodilation, increased permeability, leucocyte adhesion,
Complement	Plasma	Direct target killing, vasodilation, leucocyte chemotaxis and activation

Ever since the relationship between inflammation and cancer was identified in 1863 by Rudolf Virchow, researchers have frequently located inflammatory cells within tumour biopsies (Figure 1.8) and observed that a high number of tumours occurred in areas associated with chronic inflammation (Balkwill & Mantovani, 2001). Furthermore, increased presence of microRNAs, cytokines, prostaglandins and other molecules are known to cause angiogenesis, genetic mutations and cell proliferation (Munn, 2017; Schetter, Heegaard, & Harris, 2009).

Importantly, inflammation has been shown to enhance several other cancer hallmarks. For example, inflammation can enhance the function of growth factors involved in proliferative

signalling, whilst in other instances, it can stimulate the production or secretion of positive angiogenic signals leading to increased tumour growth, invasion and metastasis (Li *et al.*, 2019; Presta, Foglio, Churruca Schuind, & Ronca, 2018; Savant, Sriramkumar, & O'Hagan, 2018).

Indeed some estimates indicate that infections and inflammatory responses account for about 15-20% of cancer mortalities worldwide (Aggarwal, Vijayalekshmi, & Sung, 2009; Parkin, 2008).

During chronic inflammation, several initiators have been implicated in the development of cancer. For example, chronic inflammation arising from a *Helicobacter pylori* microbial infection has been implicated in gastric cancer (Hardbower *et al.*, 2013) whilst prostatitis, an inflammatory condition increases the risk of prostate cancer (Doat *et al.*, 2018; Perletti *et al.*, 2017).

Even though most research into inflammation-related cancer has focussed on the tissue microenvironment and tissue immunoreactivity of inflammatory proteins, there is renewed effort to identify serum-based inflammatory markers. In this approach, presence of CRP, CXCL9/MIG, CRP and serum amyloid A have been associated with an increased risk of lung cancer (Shiels *et al.*, 2015). In ovarian cancer, an assessment of prognostic inflammation score can be evaluated using serum albumin, lymphocyte and neutrophil concentration (Wang *et al.*, 2016a).

This research will assess the importance of various serum and tissue-based inflammatory markers in identifying BC recurrence and progression.

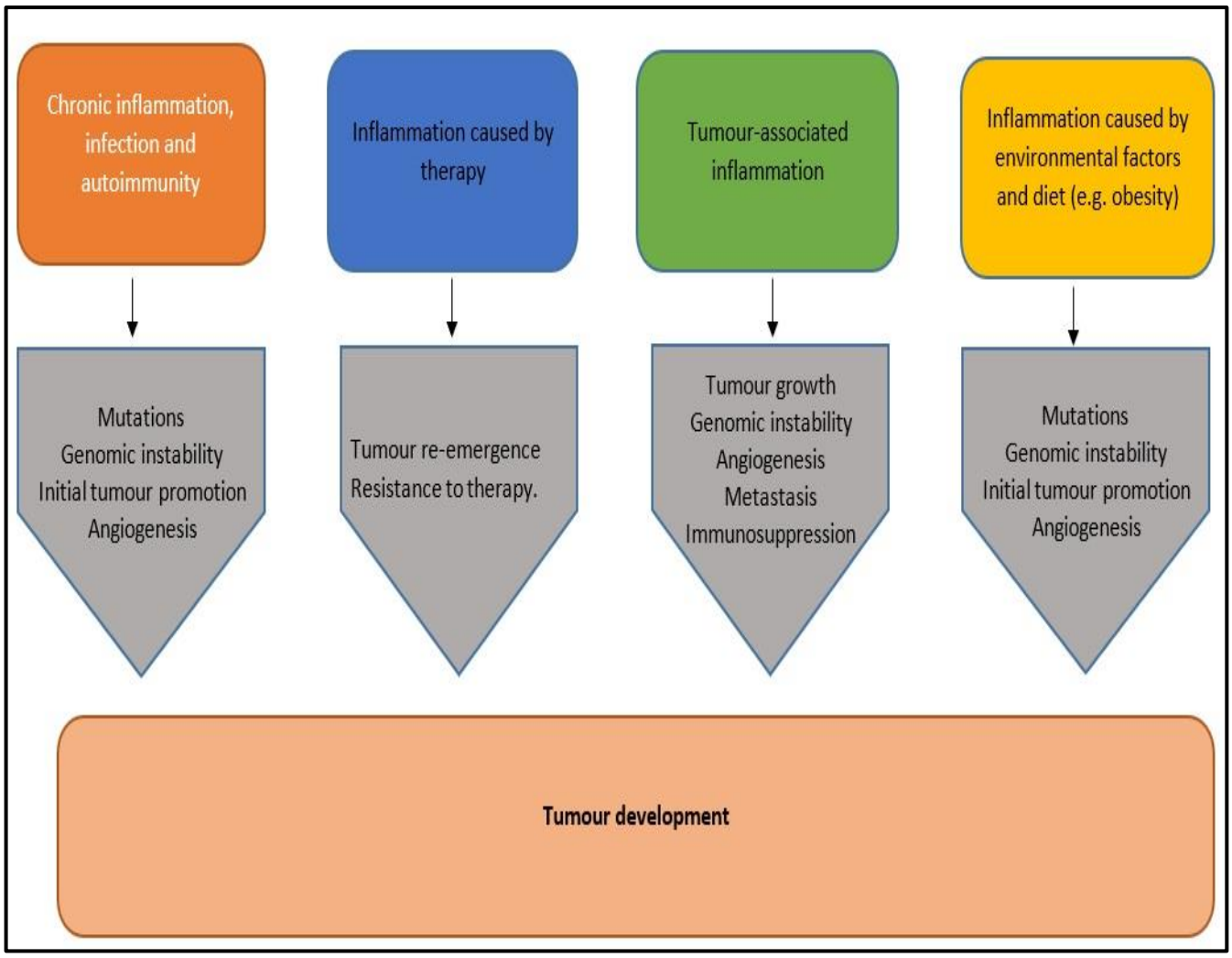

Figure 1. 8 Types of Inflammation in tumour development.
Presence of inflammatory cells within tumour microenvironment may be caused by different types of inflammation. Chronic inflammation (potentially due to infection or autoimmunity) has downstream effects such as angiogenesis, genetic instability etc. other types of inflammation such as tumour-associated inflammation, therapy-associated inflammation and inflammation due to diet and other environmental factors may lead to angiogenesis, promote tumour growth and genetic instability. Adapted from (Balkwill & Mantovani, 2001; Coussens & Werb, 2002; Mantovani, Allavena, Sica, & Balkwill, 2008)

1.8 Biomarkers in BC

The identification and utility of any Biomarker for the diagnosis or management of any pathological condition relies on intense research, optimisation and validation of the biomarker. Figure 1.9 highlights some of the steps involved in biomarker discovery.

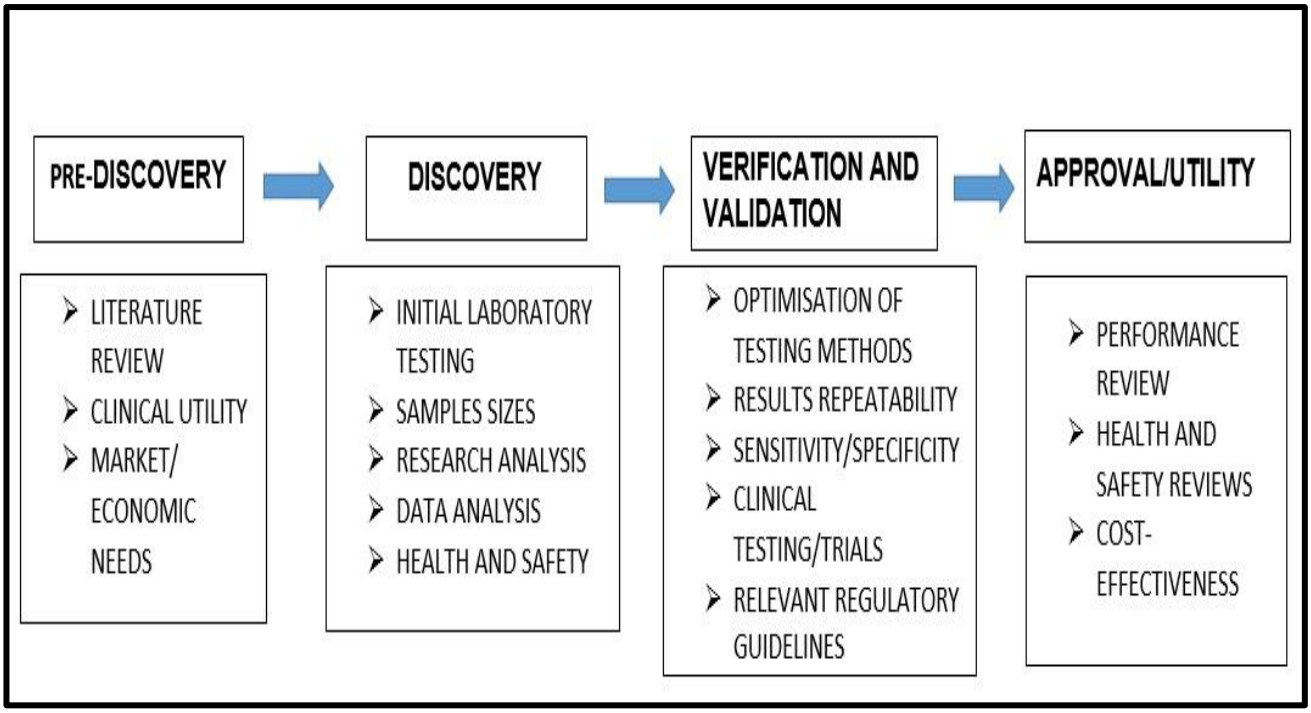

Figure 1. 9 Processes involved in Biomarker discovery
Biomarker discovery is a multistep process beginning with research, validation, approval, regulation and utility.

Anti-cancer mechanisms have been developed by studying the various hallmarks possessed by cancer cells (Hanahan & Weinberg, 2000). This approach may also be used to develop methods for the screening, diagnosis, prognosis and management of BC.

In the absence of an ideal biomarker for BC diagnosis, a combination of urine cytology, histological observation and imaging techniques are being employed to diagnose BC. Cytological/histological examination is also used in monitoring recurrence and reaction to treatment but only as a supplement to cystoscopy (Babjuk *et al.*, 2017).

1.8.1 Inflammatory biomarkers in BC

Even though the roles of inflammation in various cancers have been extensively researched, understanding of its role in NMIBC development, recurrence prediction or progression is not as vast. Several inflammatory biomarkers of interest to this research will be discussed. These will include novel serum and tissue-based biomarkers undergoing research and validation.

1.8.1.1 Interleukin 6 (IL-6), Interleukin 8 (IL-8) and Tumour Necrosis Factor-α (TNF-α)

Cytokines are low molecular weight proteins usually released by white blood cells in response to stimuli. Even though their roles vary, their main function is to help build up host defence to infection or disease. Various proteins such as chemokines, interferons, interleukins, growth factors and tumour necrosis factors make up cytokines (Bridge, Lee, Daud, Wells, & Bluestone,

2018). Depending on their function, some may be classified as proinflammatory (e.g. they activate/sustain inflammation) or anti-inflammatory (e.g. they deregulate cells that promote inflammation) (Sathishkumar *et al.*, 2016; Zhu, Miao, Zhu, Wang, & Zhou, 2017b).

IL-6 is a proinflammatory cytokine that may be produced in response to inflammation, immune response or malignancy (Bridge *et al.*, 2018; Gasche, Hoffmann, Boland, & Goel, 2011). Its proinflammatory functions include promotion of the JAK1/STAT3, MAPK and PI3K pathways (Colomiere *et al.*, 2009; Coquet, Rausch, & Borst, 2015; Wang *et al.*, 2015). It plays a significant role in regulating CRP levels and bone metabolism and is located on the long arm of chromosome 7 and contains 184 amino acids (Bowcock *et al.*, 1988).

Interactions between IL-6 and its receptor (IL-6Rα) in the tumour microenvironment, leads to activation of signalling pathways such as JAK/STAT3 (Colomiere *et al.*, 2009). Through a complex series of reactions, this activation results in increased cell proliferation, cell migration, angiogenesis and tumour cell survival (Abubaker *et al.*, 2014; Wang *et al.*, 2012b).

An important proinflammatory role of IL-8 is activation of G proteins involved in signalling pathways. One of these pathways is the mitogen-activated protein kinase (MAPK) which imparts on cancer cells, the ability to multiply and spread into other tissues (Karashima *et al.*, 2003).

The gene encoding TNF-α is located on chromosome 6 and has sometimes been called a tumour-promoting agent due to its role in cell survival (Balkwill, 2002). When activated through Toll-like receptors, TNF-α initiates an inflammatory process leading to the release/arrival of other inflammatory markers at the source of stimuli (Beutler, 1999).

The prevalence of inflammation at the site of the tumour could initiate angiogenesis since proinflammatory cells as well as growth and angiogenetic factors will be activated (Colomiere *et al.*, 2009). In BC tissues, some researchers have observed an increased presence of inflammatory infiltrates compared with normal bladder control tissues (Cresswell, Robertson, Neal, Griffiths, & Kirby, 2001).

There is currently a heightened interest to identify biomarkers for the management of BC with many studies being published. However, there is a difficulty in translating research into useful clinical value, hence the continuous reliance of imaging techniques such as cytology. Promising results have been observed in serum and genetic examinations of CRP and other inflammatory markers in MIBC. Similar results are however lacking in NMIBC patients undergoing TURBT.

1.8.1.2 Cyclooxygenase 2 (COX-2)

Cyclooxygenase-2 (COX-2) also known as prostaglandin-endoperoxide synthase 2 (PTGS2) is an enzyme homodimer (70kda each) which plays important roles in the inflammatory response (Yu & Kim, 2010). It is an important enzyme involved in the production of prostaglandins through the conversion of arachidonic acid. This pathway of conversion leads to the formation of several prostaglandins which are involved in many physiological as well as pathologic processes in humans (Mead, Alfin-Slater, Howton, & Popjak, 1986).

One of the earliest prominent studies linking COX-2 with inflammation were murine studies in which elevated COX-2 immunoreactivity resulted in higher PG levels in inflamed joint tissues (Anderson *et al.*, 1996).

In cell culture, proinflammatory activities of COX-2 have been reported. Specifically, proinflammatory factors such as IL-1, LPS and TNF-α can induce COX-2 immunoreactivity whilst its levels are reduced in the presence of anti-inflammatory factors like IL-4 and IL-13 (Crofford, 1997).

Inhibition of COX-2 activities have been exploited for the development of therapeutic interventions in BC. In this regard, many large studies have reported a significant reduction (40-50%) in colorectal cancer risks due to aspirin and NSAID use (Giovannucci *et al.*, 1995; Giovannucci *et al.*, 1994). Aspirin and NSAID are drugs, which inhibit inflammation by controlling COX-2 activities.

In a study of 40 tissue samples from patients with BC, significantly higher COX-2 immunoreactivity rates were reported in both MIBC (86%) and NMIBC (78%) (Mohammed *et al.*, 1999).

In a recent study, the immunoreactivity of COX-2 was evaluated in 40 patients with colorectal cancer. In comparison to normal tissues, they observed significantly higher COX-2 immunoreactivity in colonic adenocarcinoma sample tissues. Furthermore, high stage and high grade patients presented with high staining intensity and percentage of tumour cells (Hedaya, Helmy, Ezzat, & Hammam, 2015).

In another study, COX-2 immunoreactivity was studied in a retrospective study of 183 patients with endometrial carcinoma. In 68% of the patients, COX-2 immunoreactivity was increased and this was also associated with tissue differentiation, stage and myometrial invasion depth ($p< 0.05$)(Cai, Zhang, Han, & Ding, 2017)

1.8.1.3 Macrophage Inflammatory Protein-2 (MIP-2)

The macrophage inflammatory protein 2 (MIP-2) is also know by several names such as chemokine (C-X-C motif) ligand 2 (CXCL-2), growth regulated protein beta or gro-oncogene 2. MIP-2 belongs to the CXC chemokine ligand family and thus play various important functions in inflammation, angiogenesis, leucocyte migration, and tumourigenesis (Kollmar, Menger, & Schilling, 2006; Luster, 1998). It is released by monocytes, macrophages, epithelial cells and stem cells (David *et al.*, 2017; Ohtsuka, Lee, Stamm, & Sanderson, 2001a).

During inflammation and in the presence of the right stimuli (such as IL-1α), epithelial cells release MIP-2. The presence of MIP-2 creates an environment for the recruitment/activation of neutrophils to the site of inflammation (Proudfoot *et al.*, 2003). Leucocyte activation is thought to occur when bound to G protein-coupled transmembrane receptors (CXCR). This binding of a chemokine to CXCR causes leucocytes to move towards the site of inflammation (Rot & Andrian, 2004).

Using Murine studies Ohtsuka, Lee, Stamm, & Sanderson (2001b) observed a significant link between the release of MIP-2 by intestinal epithelial cells and an enhanced recruitment of neutrophils. This study, demonstrated a clearer insight into the role of intestinal epithelial cells in immune regulation of the mucosa.

A recent study investigated the relationship between myeloid-derived suppressor cells and BC prognosis (Zhang *et al.*, 2017). They observed that, in BC cells with high MIP-2 immunoreactivity levels, there was an associated increase in CD33+ myeloid-derived suppressor cells. Furthermore, patients with tumour-associated myeloid-derive suppressor cells presented with high circulating MIP-2 levels compared with healthy controls (Zhang *et al.*, 2017).

In another study, tumour cells and tumour-associated fibroblasts in breast carcinoma cell lines secreted higher MIP-2 levels whiles increased immunoreactivity of CXCR-2 (which possesses anti-proliferative properties), resulted in low MIP-2 secretion (Erin, Nizam, Tanriover, & Koksoy, 2015).

With regards to BC, there is limited research highlighting the role MIP-2 plays in cancer recurrence and progression. Although a large body of evidence exists which links MIP-2 to tumour-associated angiogenesis, most of this information was obtained from animal models and cell culture techniques. This present study therefore seeks to provide more information by identifying changing levels of serum MIP-2 in patients undergoing TURBT for the treatment of BC.

1.8.1.4 Thrombomodulin

Thrombomodulin as a 74kDa membrane receptor expressed on endothelial cells with important roles in physiological coagulation (Esmon, Owen, & Esmon, 1982; Greineder *et al.*, 2017). Thrombomodulin also plays several essential roles in inflammation and cancer promotion (Greineder *et al.*, 2017; Song *et al.*, 2018).

The effects of Thrombomodulin activity in cancer have been linked to its roles in anticoagulation, anti-inflammation and tissue adhesion and proliferation (Figure 1.10) (Wu, Chang, Lin, Chen, & Chen, 2014).

Several research studies using cell lines, animals and human tissue samples, have highlighted a link between Thrombomodulin and cancer (Chang *et al.*, 2016; Shirai *et al.*, 2017; Wu *et al.*, 2014; Yang, Cheng, & Lu, 2017). In a recent research study using lung cancer cell lines (95D & SPC-A-1), an increased immunoreactivity of Thrombomodulin was observed. This high immunoreactivity of Thrombomodulin resulted in a lower tumourigenic potential of the lung cells as well as a reduced colony forming potential. The researchers further reported a reduction in cell invasion and migration in cells that had high Thrombomodulin immunoreactivity (Zheng *et al.*, 2016).

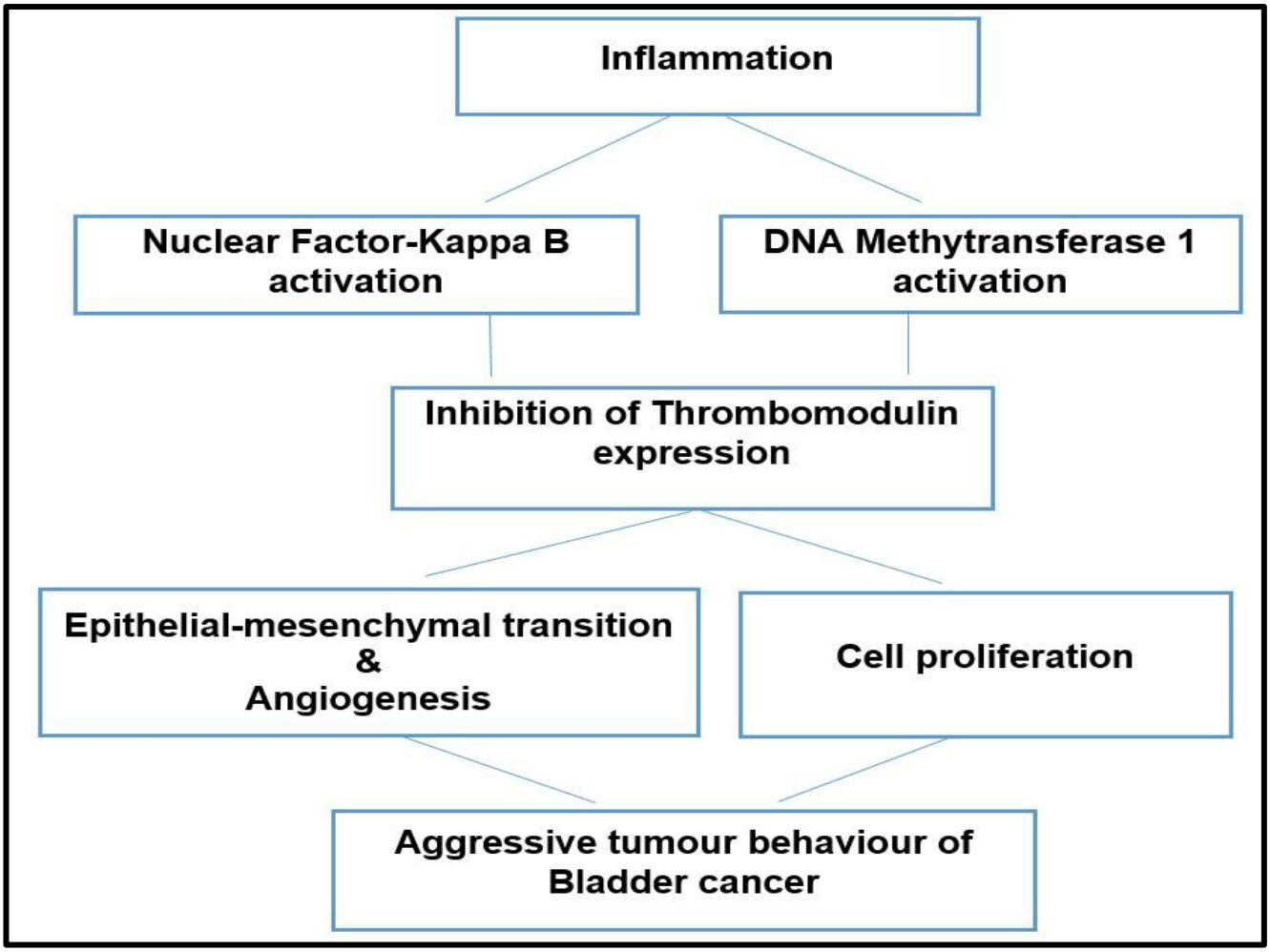

Figure 1. 10 Role of Thrombomodulin and its association with BC. (Adapted from Wu et al., 2014)

In a research study of 100 patients (60 with MIBC and 40 with NMIBC) and 4 BC cell lines (HT1376, HT1197, T24 & J82), (Wu *et al.*, 2014) reported an inverse relationship between Thrombomodulin immunoreactivity and cell invasion *in vitro*. When Thrombomodulin silencing vector was introduced in to HT1376 and HT1197 cell lines, which traditionally have a high Thrombomodulin rates, higher rates of cancer invasion were observed in vivo. In mice, higher tumour implantation rates and bigger tumour sizes were observed when a similar silencing vector was introduced (Wu *et al.*, 2014).

These studies demonstrate an association between thrombomodulin and cancer and warrants further investigation.

1.8.1.5 S100 Calcium binding protein P (S100P)

The S100 proteins are associated with roles in cellular processes like regulation of cell cycle, growth, transcription and differentiation (Jiang *et al.*, 2016). These proteins may be localised in different cellular compartments and are activated and relocated through calcium activation.

The S100P is a 10 kDa protein which was initially purified from placenta tissue (Emoto, Kobayashi, Akatsuka, & Hidaka, 1992).

It is thought that, when secreted, S100P may have paracrine or autocrine signalling effects (Gibadulinova, Tothova, Pastorek, & Pastorekova, 2011) while cellular immunoreactivity of S100P may interact with growth factors, receptors leading to several effects such as proliferation (Jiang *et al.*, 2016)
The association between S100P and cellular processes such as cell survival, proliferation, tumour invasion and angiogenesis have been studied by various researchers (Guo *et al.*, 2014a; Jiang *et al.*, 2016; Liu *et al.*, 2017; Tabrizi *et al.*, 2018).

Several experimental studies showed that S100P, involved in processes of proliferation, survival, angiogenesis and metastasis, may contribute to development of a malignant phenotype (Wang et al., 2006; Surowiak et al., 2007).

In a study of 68 patients with transitional cell carcinoma (TCC), S100A8 was significantly immunoreactive in TCC tissues than normal tissues (P=0.05). Comparing the various stages, there was 78.9% immunoreactivity in pT2-pT4, 46.9% in pTa-pT1, 29.2% in low grade PUNLMP and 70.5% in high grade PUNLMP. Immunoreactivity also correlated with increasing stage and grade (Cui, Shi, & Xu, 2012).

Another study using a sample size of 90 employed two dimensional electrophoresis, mass spectrometry, western blots and ELISA and reported a significant difference between S100A8/S100A9 levels in low grade and high grade bladder tumours (Bansal, Gupta, Sankhwar, & Mahdi, 2014).

1.8.1.6 sCD40L

CD40 ligand (CD40L) is a 33kDa transmembrane protein member of the larger TNF superfamily and usually located on the surfaces of platelets, activated B and T cells (van Kooten & Banchereau, 2000). Under certain conditions, such as inflammatory response during immune activation, it may also be expressed on the surfaces of basophils, mast cells and NK cells (Blumberg, Gettings, Turner, Heal, & Phipps, 2006).

As a costimulatory molecule, CD40L interaction with CD40, has been shown stimulate the functions of endothelial cells, B cells and other cells located within the vascular network (Blumberg *et al.*, 2006). Indeed it has been suggested that the CD40/CD40L network may

contribute to endothelial cell and germinal cell B cell survival in both physiological and inflammatory conditions (Bishop, Moore, Xie, Stunz, & Kraus, 2007)

Through induction of the so-called Tumour necrosis factor receptor-associated factors (TRAFs), the CD40/CD40L complex plays further downstream roles in various pathways such as the MAPK pathway and the phosphoinositide 3-kinase (PI3K) pathway (Bishop *et al.*, 2007; Säemann *et al.*, 2003).

In tumour pathology, CD40/CD40L-associated regulation of tissue factor on endothelial cells is one of the fundamental associations between CD40L and potential cancer growth and metastasis. In this regard, (Miller, Yaron, & Yellin, 1998) have reported that, CD40L-related activities resulted in increased immunoreactivity of tissue factor in human umbilical vein endothelial cells.

In a study of 139 patients with hepatocellular carcinoma undergoing liver transplantation, higher pre-operative sCD40L serum levels were associated with patients who did not survive following transplantation (Lorente *et al.*, 2018).

1.8.1.7 Angiopoietin-2

Angiopoietin-2 is an angiogenic mediator expressed on the surfaces of endothelial cells and on monocytes (Lefere *et al.*, 2018). Angiopoietin-2 activity may be influenced by the presence of VEGF through tissue remodelling and increased vascular vessel diameter. Indeed, it has been demonstrated that when VEGF is absent, angiopoietin-2 causes cell death and suppressed breast cancer proliferation (Liang, Li, & Chung, 2017).

Through its receptor (TIE-2), it has been suggested that angiopoietin-2 initiates angiogenesis by enhancing growth and proliferation of endothelial cells (Ju *et al.*, 2014). Due to their roles in inflammation, high serum levels of both angiopoietin-2 and TIE-2 have been observed in several inflammation related conditions (van Sleen *et al.*, 2019; Yang *et al.*, 2018b).

In a study of 117 BC patients and 64 healthy controls, preoperative serum angiopoietin-2 and TIE-2 were analysed. Even though there was no correlation between serum angiopoietin-2 levels and tumour stage or grade, serum TIE-2 levels were significantly higher in NMIBC compared to patients with MIBC. Furthermore, angiopoietin-2 and TIE-2 levels were lower in BC patients compared to healthy controls (Szarvas *et al.*, 2008).

It can therefore be appreciated that, even though angiopoietin-2 also has inflammatory functions, its role in potential tumour growth is of interest to this present study.

1.8.1.8 Osteopontin

Initial isolation and characterisation of Osteopontin was performed by studying secreted proteins from malignant mammalian cells (Senger, Wirth, & Hynes, 1979). When initially secreted, it occurs as a 34kDa glycoprotein before undergoing transformation into a 40 to 75 kDa protein in various cells (Wei, Wong, & Kwok, 2017). Although Osteopontin plays a key role in biomineralization when highly immunoreactive in osteoblasts (Giachelli & Steitz, 2000), it has also been involved in chronic inflammation (Lund, Giachelli, & Scatena, 2009) and regulation of cell-cell interactions (Villanueva *et al.*, 2019). It is therefore a multifunctional protein involved in several physiological and pathological processes. However, this research will focus on its role as an inflammatory marker involved in tumour growth.

In a research study (n= 241), an assessment of osteopontin immunoreactivity revealed a significant association with MMP-3 in ovarian cancer. In that study, the presence of osteopontin and MMP-3 were indicators of early disease progression in ovarian cancer (Fisher, Jain, Tayback, & Fedarko, 2004). Indeed earlier research has shown that osteopontin activates proteolytic functions of MMP-3 when they are expressed together (Fedarko, Jain, Karadag, & Fisher, 2004). These activities further highlight the angiogenic potential of osteopontin and MMPs (Hirama *et al.*, 2003)

In a study of 72 patients with TCC, plasma osteopontin concentrations were significantly increased in TCC patients compared to normal controls. Within patients with TCC, those presenting with metastasis and high stage cancers, had higher osteopontin concentrations compared to other groups (Ang, Chambers, Tuck, Winquist, & Izawa, 2005).

There is currently limited research about changes in Osteopontin concentration in BC patients following treatment. This therefore, warrants further study and could potentially be used as part of a biomarker profile for the management or monitoring of BC patients after TURBT treatment.

1.8.2 Growth and Angiogenic markers in BC

1.8.2.1 Epidermal growth factors/ receptors (EGF, EGFR) and human epidermal growth factor receptor 2 (HER-2)

This family of growth factors are part of the larger family of tyrosine kinase receptors. Physiologically, they are involved in the regulation of cell growth and regeneration by influencing signalling pathways (Alexander *et al.*, 2014; Pereira, Bersano, Rocha, & Lopes, 2018).

Earlier researchers identified a higher immunoreactivity of EGFR in high grade BC (Korkolopoulou *et al.*, 1997; Wright *et al.*, 1991). Some studies also found a higher progression and fatality rate in patients presenting with significantly elevated levels of EGFR in tissues (Lipponen & Eskelinen, 1994; Liukkonen *et al.*, 1999).

The human epidermal growth factor receptor 2 (HER-2) is also called CD340 or Erbb2 (when isolated in rodents) or HER-2/neu or ERBB2 (when isolated in humans) (Iqbal & Iqbal, 2014; Riese & Stern, 1998). Earlier original studies by various research groups observed that HER-2 is structurally dissimilar to the EGFR and is found on the longer arm of chromosome 17 where it encodes for an 185kDa transmembrane protein (Coussens *et al.*, 1985; Semba, Kamata, Toyoshima, & Yamamoto, 1985).

As an oncogene, HER2 over-amplification causes tumourigenesis due to activation of signalling pathways such as MAPK (Siddiqa, Long, Li, Marciniak, & Kazhdan, 2008; Wang *et al.*, 2016b).

Research using animal models, has provided significant information about the relationship between HER-2 immunoreactivity pattern and tumour development. (Muller, Sinn, Pattengale, Wallace, & Leder, 1988) reported an increased rate of breast adenocarcinoma in transgenic mice with mutated HER-2 genes. In a similar study, increased tumourigenesis was reported in nude mice in the presence of high HER-2 immunoreactivity or over amplifications of a HER-2/neu gene (Hudziak, Schlessinger, & Ullrich, 1987).

In human pathology, HER2 gene amplification and higher protein immunoreactivity occurs in about 25% of people with metastatic breast cancer (Blackwell *et al.*, 2012).

In a recent study, (Hammam *et al.*, 2015) reported higher HER-2 immunoreactivity in high grade and high stage BC compared to low grade.

Two treatment strategies exploiting HER-2 immunoreactivity using IHC FISH, have been used in the management of breast cancer. One of these strategies target HER-2 positive tumours with specific anti-HER-2 antibodies; e.g. Trastuzumab (Slamon *et al.*, 2001; Smith *et al.*, 2007). These improved statistics in breast cancer management through HER-2 targeted protocols provided evidence that more research on HER-2 could lead to strategies that are more successful.

The second HER-2 related treatment strategy in breast cancer management aims to reduce cell proliferation and increase apoptosis using oral tyrosine kinase inhibitors. These inhibitors such as neratinib, afatinib and lapatinib bind the cytoplasmic domain of the HER-2 structure and

reduces subsequent phosphorylation and signal transduction (Blackwell *et al.*, 2010; Gril *et al.*, 2008; Rabindran *et al.*, 2004).

1.8.2.2 Vascular endothelial growth factors

The vascular endothelial growth factors (VEGFs), together with their receptors have been widely studied and are known to play various critical roles in normal physiology and disease states (Shigetomi *et al.*, 2018). They have been implicated in vasculogenesis and angiogenesis (Benjamin, Golijanin, Itin, Pode, & Keshet, 1999; Gerhardt *et al.*, 2003).

About 7 genes encode for the VEGFs, however the main factors are VEGF-A, VEGF-B, VEGF-C, placental growth factor (PLGF) and VEGF-D (Figure 1.11). With regards to the receptors, three main receptors have been identified ie VEGFR-1, VEGFR-2 and VEGFR-3 (Shibuya, 2011; Yang, Wang, & Ma, 2018a) (Figure 1.11).

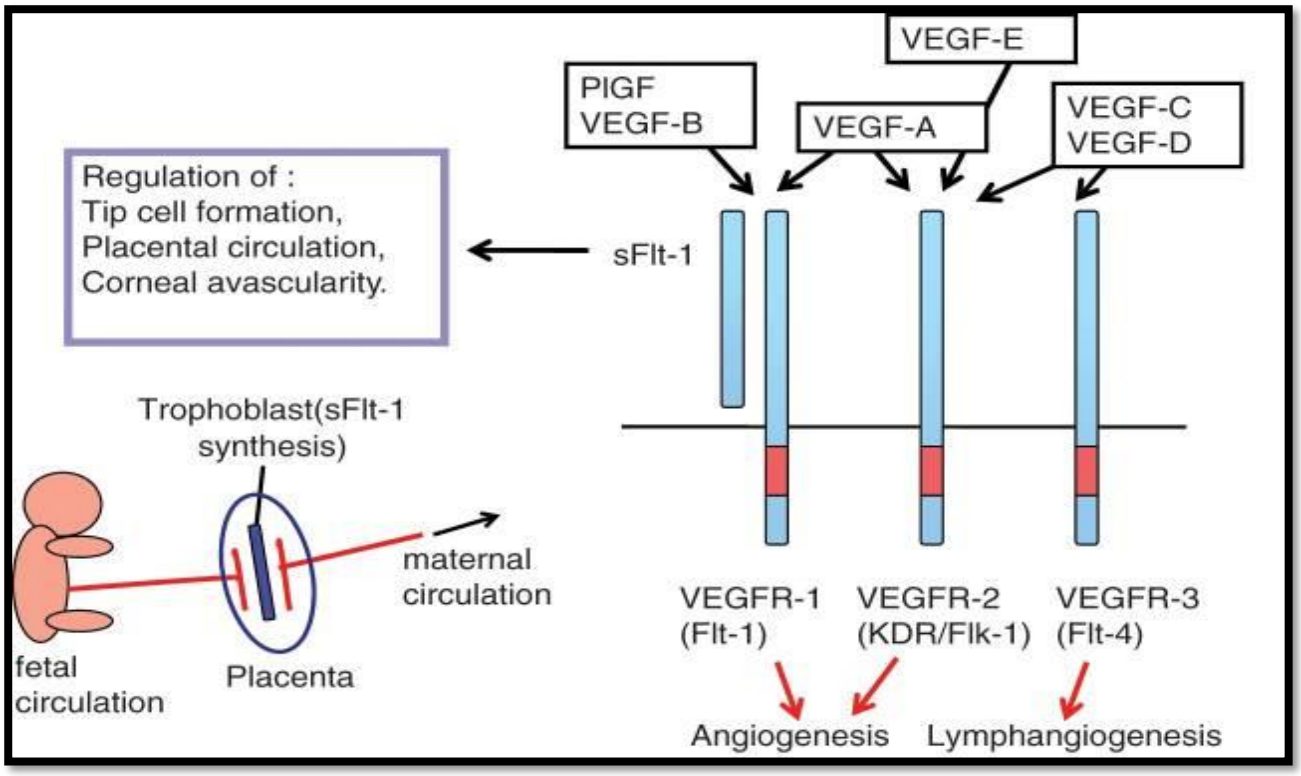

Figure 1. 11 The vascular endothelial growth factors and their receptors.
Summary of the three VEGF receptors and the factors they interact with. Their activities mostly result in the induction of angiogenesis and lymphangiogenesis in many cancers. Adapted from (Shibuya, 2011).

VEGF, which may also be called VEGF-A, was initially identified when researchers using murine studies purified and studied fluids from tumours (Senger *et al.*, 1983). Some Studies have shown that VEGF-A plays important physiological roles such as enhancing vascular permeability, angiogenesis and promoting cell migration in endothelial cells and macrophages (Cartland, Genner, Zahoor, & Kavurma, 2016; Shibuya, 2011). The role of VEGF-A in the

regulation of embryogenesis was highlighted in earlier studies. Cerdan, Rouleau, & Bhatia (2004) reported that in the absence of a single copy of VEGF-A gene, embryos died prematurely; highlighting the important role it plays in the vasculature.

In another study, Lee *et al.* (2007) investigated the role of VEGF-A and its receptors in the functioning of vascular endothelial cells. They showed that in a healthy homeostatic state, autocrine production of VEGF was needed to maintain normal functioning of the circulatory system. They further observed that mice that had a genetic depletion of VEGF resulted in endothelial degeneration, intravascular thrombosis and higher death rates in mutant mice (Lee *et al.*, 2007).

The most important signalling receptor for VEGF-A is the VEGFR-2, which is present on endothelial cells and initiates cell migration and angiogenesis (Gerhardt *et al.*, 2003). Due to its role in tumourigenesis, inhibition of VEGF-A activity provides an opportunity for the development of anti-cancer interventions (Drewes *et al.*, 2012; Hurwitz *et al.*, 2004).

VEGF-C and VEGF-D are mostly released as immature isoforms which can be proteolytically cleaved to produce active forms (McColl *et al.*, 2007). Their interactions with VEGFR-3 has been shown to induce angiogenesis within lymphatic endothelial cells (Eroglu, Ersoz, Karasoy, & Sak, 2017).

Even though VEGFR-3 immunoreactivity is usually located on endothelial cells within the lymphatic system (Gerhardt *et al.*, 2003) and has been mainly involved in lymphangiogensis (Eroglu *et al.*, 2017), some studies have observed that any inhibition of VEGFR-3 activity, reduces Angiogenic sprouting and vascular network formation (Tammela *et al.*, 2008).

Due to the high recurrence rates in BC, measurement of VEGF and their receptors may provide useful for predicting recurrence and progression.

1.8.2.3 Basic fibroblast growth factor (bFGF)

The basic Fibroblast Growth Factor (bFGF), also known as Fibroblast Growth Factor-2 (FGF-2) is a member of the larger FGF family of protein (Basilico & Moscatelli, 1992; De Palma *et al.*, 2017). These proteins are structurally similar and together with their receptors, are involved in several physiological and pathological conditions (Okada-Ban, Thiery, & Jouanneau, 2000). bFGF is a 13kda protein which was initially purified from bovine pituitary gland (Gospodarowicz, 1975).

bFGF may be secreted or membrane bound and therefore has pleiotropic effects on several cells and systems though complex signalling cascades, most of which are not fully understood (De

Palma *et al.*, 2017). Physiologically, bFGF is known to have mitogenic effects on fibroblast cells, which usually occur in tissue remodelling and regeneration (Zhang *et al.*, 2016). Pathologically however, bFGF is suspected to have strong angiogenic properties especially in tumour progression and invasion (Cartland *et al.*, 2016; Sun *et al.*, 2017). When produced by mast cells located in the tumour microenvironment, bFGF together with other pro-angiogenic regulators such as VEGFA, PLGF, MMPs and IL-6, promote proliferation of ECs, ECM remodelling and angiogenesis (Harney *et al.*, 2015; Lewis, Harney, & Pollard, 2016)

In 134 patients with endometrial cancer Dobrzycka, Mackowiak-Matejczyk, Kinalski, & Terlikowski (2013), reported increased serum bFGF concentrations in cancer patients compared with normal controls. They further reported a significant association between high preoperative serum bFGF levels and shorter overall survival, suggesting that, bFGF could potential be useful in assessing treatment outcome.
In BC, an earlier study using 32 patients observed high preoperative serum bFGF levels in high-grade tumours and high-risk patients compared to normal controls (Gazzaniga *et al.*, 1999). Currently, there is limited research evaluating changes in serum bFGF concentrations in patients undergoing TURBT for the treatment of BC.

1.8.2.4 Carcinoembryonic antigen-related cell adhesion molecule 1 (CEACAM1)

The CEACAM-1 is also known as biliary glycoprotein 1 or CD66a. Immunoreactivity of this cell adhesion molecule has been observed in endothelial cells, epithelial cells and myeloid cells of several human organ systems (Prall *et al.*, 1996). The role of CEACAM-1 in inducing angiogenesis has been studied using both in vivo and *in vitro* models (Kilic *et al.*, 2005). Specifically, in chicken embryos, CEACAM-1 presence was strongly associated with increased vascularisation of the chorioallantoic membrane. Furthermore increased VEGF, a known pro-angiogenic factor, induces CEACAM-1 immunoreactivity, highlighting its link with angiogenesis (Ergün *et al.*, 2000).

With regards to cancer, CEACAM-1 has been associated with tumour suppressor activities. Specifically, this tumour suppressive function has been attributed to a cytoplasmic isoform of CEACAM-1 (Kuespert, Pils, & Hauck, 2006). Using cell culture studies, tumour suppressive properties of CEACAM-1 have been assessed. In DU145 prostate cancer cells, the presence of CEACAM-1 significantly prevented tumourigenesis and tumour cell proliferation (Luo *et al.*, 1999).

Pathologically, CEACAM-1 activities have been implicated in cancer invasion and metastasis. In oncology, several previous studies have reported a decreased immunoreactivity, down

regulation or loss of CEACAM-1 immunoreactivity in tumour cells (Luo *et al.*, 1999; Neumaier, Paululat, Chan, Matthaes, & Wagener, 1993).

In a study of 48 patients with hepatocellular carcinoma, loss of CEACAM-1 immunoreactivity was significantly associated with high grade and poor survival. In that study, although 25 hepatocellular carcinoma patients presented with CEACAM-1 immunoreactivity, this did not have any relationship with patient outcome (Sha *et al.*, 2012).

In another study of 139 patients with hepatocellular carcinoma, loss of CEACAM-1 within tumour cells was strongly associated with high-grade tumours as well as cancer stage. There was also a correlation between loss of immunoreactivity and short survival and tumour invasion (Cruz, Wakai, Shirai, Yokoyama, & Hatakeyama, 2005).

Other studies have, however, observed increased CEACAM-1 immunoreactivity in cancer cells. For example, high serum concentrations were reported in gastrointestinal cancer patients compared to healthy controls. In that study, increased CEACAM-1 immunoreactivity was observed within invasive tumours compared to other tissues (Zhou *et al.*, 2017).
In another study, higher CEACAM-1 immunoreactivity was reported in gastric adenocarcinoma compared to normal mucosa. High immunoreactivity was also linked with lymph node metastasis and cancer stage and no association was observed between immunoreactivity and tumour grade (Shi, Xu, He, & Xi, 2014).

1.8.2.5 Matrix metalloproteinases (MMPs)

The matrix metalloproteinases (MMPs), also known as matrixins, are a group of proteinases playing various important roles in normal physiology such as angiogenesis, would healing, and embryogenesis (Littlepage *et al.*, 2010; Lv *et al.*, 2018).

The MMP superfamily of proteinases are categorised into several groups based on their substrates and structure and include gelatinases, collagenases, matrilysins, stromelysins, membrane-type MMPs and other MMPs (Boyanton & Blick, 2002; Newby, 2005). For the purposes of this research MMP-2, MMP-3 and MMP-9 will be discussed even though inferences may be made to other MMPs.

MMPs possess a basic structure which contains a propeptide domain, a catalytic domain, a linker peptide and hemopexin-like domains and may be grouped based on localisation, sequence components, substrate specificity or associated motifs (Vihinen & Kähäri, 2002). MMP mediates degradation of the extracellular matrix (ECM) through processes such as catalysation and proteolytic activities. ECM degradation undermines several normal

physiological functions like embryogenesis, and tissue repair (Hadler-Olsen, Fadnes, Sylte, Uhlin-Hansen, & Winberg, 2011; Hammam *et al.*, 2015).

MMP-3 (also known as stromelysin-1) is categorised in the same group as MMP-10, MMP-11 and MMP-12. MMP-2 and MMP-9 are also known as gelatinase-A and gelatinase-B, respectively. They have a significant association with tumour invasion and play important roles in the degradation of the basement membrane(Newby, 2005).

In pathology, MMP-related degradation of the ECM has resulted in conditions such as periodontitis, osteoarthritis and cancer (Boyanton & Blick, 2002; Slamon *et al.*, 2001). Indeed, increased ECM degradation of the vasculature, due in part, to the activity of MMP, plays a part in cardiovascular conditions such as heart failure, atherosclerosis, aneurysms etc (Newby, 2005; Spinale, 2002).

There is evidence that MMP-2 is initially produced as an inactive proMMP-2 and forms a complex with TIMP-2. Through a series of complex steps, MTI-MMP interactions occurring within their hemopexin domains lead to activation of proMMP-2 on cell surfaces (Nagase, Visse, & Murphy, 2006). Some reviews have also highlighted a relationship between proMMP-2 activation and TIMP-3 although the significance of this association is not clearly understood (Vihinen & Kähäri, 2002).

In pathological states, both earlier and current studies on the activities of MMPs have highlighted a significant relationship with tumourigenesis, tumour vascularisation, disease severity etc (Masson *et al.*, 2005; Sinnamon, Carter, Fingleton, & Matrisian, 2008; Wu, He, Zhao, & Wang, 2018).

(Sinnamon *et al.*, 2008) observed reduced intestinal tumourigenesis in MMP-9 deficient mice compared to littermate controls. In a study using 2 animal models,(Masson *et al.*, 2005) reported an increased immunoreactivity of MMP-9 by neutrophils principally located within the tumour microenvironment. They further reported that in mice deficient in both MMP-2 and MMP-9, there was no tumour angiogenesis and invasion was minimal. A more recent study of two mouse models reported that, even though there was lower tumour angiogenesis and tumour growth in genetically deficient MMP-9, there was an increased rate of tumour invasion. In that study, they also observed an increased presence of inflammatory cells caused by the increased tumour invasiveness due to MMP-9 deficiency (Shchors *et al.*, 2013).

Similarly, in MMP-2 deficient mice, several researchers have reported adverse disease effects. For example, there was a reduced retinal angiogenesis in MMP-2 deficient mice (Ohno-Matsui *et al.*, 2003). In choroidal neovascularization, MMP-2 protein was highly immunoreactive within tumours in wild-type mice compared to MMP-9 deficient mice (Berglin *et al.*, 2003).

These findings indicate that the absence of these MMPs seems to reduce tumour growth and reduces disease severity.

In colorectal cancer tissues, a study observed high MMP-2 immunoreactivity compared with adjacent noncancerous tissue (Deng *et al.*, 2017). They also observed a significant relationship between MMP-2 immunoreactivity and reduced overall survival. In a large study of 939 patients with BC, Chan *et al.* (2017), also reported a significant relationship between MMP-2 immunoreactivity and progression-free survival and a shorter overall survival.

In a recent study, protein and gene expressions of MMP-2, MMP-9 and TIMP-2 were evaluated in 50 patients. It was observed that in both urine and blood samples, there was high immunoreactivity of both MMP-2 and MMP-9 in patients with malignant disease compared with patients with non-malignant diseases and healthy controls (Fouad, Salem, Ellakwa, & Abdel-Hamid, 2018).

Since MMPs can be secreted or membrane-expressed, several laboratory methods can be used for their measurement. In this present study, we studied serum MMPs using a modified ELISA technique (bioplex Luminex technique).

1.8.2.6 SOX-2

SOX-2 (Sex determining region Y box-2), is a member of the sex determining Y-related high motility box (SOX) family. It is a transcription factor and plays important roles in the development of embryonic stem stems and other growth processes (Masui *et al.*, 2007; Sarkar & Hochedlinger, 2013).

In oncology, increased SOX-2 immunoreactivity has been reported in different cancer types. In cervical squamous cell carcinoma (SCC), SOX-2 was observed to be highly immunopositive in the SCC tissues compared with normal cervical tissues (Chang *et al.*, 2015). In non-small cell lung cancer, SOX-2 was reported to be a sensitive diagnostic marker of squamous cell carcinoma (Tsuta *et al.*, 2011).

The association between SOX-2 and BC was investigated by (Kitamura *et al.*, 2013). In a comprehensive study which included IHC, gene analysis and transfection studies, they observed a significantly increased association between SOX-2 and BC. Specifically, when nude mice were transplanted with highly purified Cancer stem cells, SOX2+ cells exhibited higher tumourigenic ability compared to SOX2- cells (Kitamura *et al.*, 2013).

In another study of SOX-2 related cancer activities in both human and mouse tissues, (Zhu *et al.*, 2017a) observed that tumour cells reactive to anti-SOX-2, contributed to increased BC tumour proliferation.

In the light of our current understanding of SOX-2 activities in cancer, it may be utilised as a prognostic tool or therapeutic intervention.

1.8.2.7 Follistatin

Follistatin is a regulatory glycoprotein associated with tissue repair, inflammation and embryogenesis. The regulatory functions of follistatin are mainly achieved through its bind to activin (Stamler *et al.*, 2008).

In cancer cell lines, studies have highlighted the inhibitory effects of follistatin binding to activin. Specifically, in breast cancer, follistatin indirectly suppresses tumour proliferation by inhibiting the activities of activin (An *et al.*, 2017; Razanajaona *et al.*, 2007)

Serum follistatin levels were significantly higher in ovarian cancer patients compared to normal controls in a study by (Ren *et al.*, 2012). Relatively high sensitivity and specificity observed in that study suggested possible use of follistatin as a biomarker for ovarian cancer.

In a recent study using both cell lines and human tissues, (Zabkiewicz, Resaul, Hargest, Jiang, & Ye, 2017), demonstrated that increased follistatin cell immunoreactivity and high serum levels are significantly associated with reduced invasion and better survival at 5 years.

1.8.2.8 CD31

CD31, also called platelet endothelial cell adhesion molecule-1 (PECAM-1), is a 140kDa protein located on chromosome 17 usually localised on the surfaces of neutrophils, monocytes, platelets and endothelial cells (Righi *et al.*, 2003; Stockinger *et al.*, 1990; van Mourik, Leeksma, Reinders, De Groot, & Zandbergen-Spaargaren, 1985).

Physiologically, CD31 plays various roles in angiogenesis, leucocyte migration and activation of integrins (O'Brien, Lim, Sun, & Albelda, 2003). CD31 may be secreted, membrane bound or localised intracellularly but it is most importantly utilised as a marker of angiogenesis by evaluating its immunoreactivity on the surfaces of endothelial cells (Deliu *et al.*, 2016; Qian, Yang, Zhao, Chen, & He, 2018).

Since its discovery in 1990 (Stockinger *et al.*, 1990), more research has focussed on understanding CD31 as a pro-inflammatory protein by studying its effect in leucocyte transmigration. CD31 is believed to enhance leucocyte migration towards localised inflammation and injury, by regulating cell motility and directionality in an adhesion cascade (Wu, Stabach, Michaud, & Madri, 2005). CD31 located on endothelial cells may also interact

either directly with CD31 located on leucocytes or indirectly with the help of neutrophil CD177 (O'Brien *et al.*, 2003).

Further insight into the role CD31 plays in promoting angiogenesis in human tumours has been provided in an earlier study by (Cao *et al.*, 2002). Using a mouse model transfected with skin cancer, they observed reduced vessel density in human skin tumours when CD31 was absent. Furthermore, when antibodies against CD31 were present, tube formation was truncated in human umbilical vein endothelial cells.

El Gehani *et al.* (2011) analysed the immunoreactivity of CD31 in 42 BC samples and measured their association with tumour angiogenesis using microvessel density. They reported significantly increased CD31 immunoreactivity in BC tumour cells compared to bladder tissues. More importantly, there was increased angiogenesis in invasive tumours compared to non-musical invasive tumours.

The roles CD31 plays in angiogenesis and the inflammatory cascade has generated several research interests in terms of disease pathogenesis. In 82 patients with TCC of the renal pelvis, immunoreactivity PECAM-1 and two other proteins (p53 and MIB-1) were recently evaluated using tissue microarrays (García-Tello *et al.*, 2014). Significant correlations were reported between factors such as PECAM-1 immunopositivity ($p= 0.0036$) and worst cancer specific survival. However, PECAM-1 immunoreactivity was not identified as a primary predictor of prognosis (García-Tello *et al.*, 2014).

In colorectal cancer, an assessment of the role of CD31 in tumour angiogenesis was conducted by Mohamed et al. (2017a). In their study of 50 patients with colorectal cancer, they reported a significant association between CD31-assisted microvessel density counting and poor prognosis ($p= 0.023$).

1.8.2.9 CD34

CD34 is an 115kDa transmembrane protein expressed on hematopoietic stem cells, vascular endothelial progenitors and embryonic fibroblasts (Brown, Greaves, & Molgaard, 1991; Fina *et al.*, 1990; Patry *et al.*, 2018).

In a recent study (n=60) of patients with various forms of benign and malignant oral conditions, cell proliferation due to angiogenesis was analysed using IHC (Sheelam *et al.*, 2018). The researchers directed specific antibodies against various proteins involved in cell proliferation and vascularity such as proliferating cell nuclear antigen (PCNA), vascular endothelial growth factor and CD34 and analysed their immunoreactivity using IHC. The microvessel density; calculated from CD34 immunoreactivity, was significantly higher in oral squamous cell

carcinoma compared with other benign oral conditions. They also observed significant increases in CD34 and VEGF protein immunoreactivity as oral cells progress from normal mucosa cells to dysplasia to Oral squamous cell carcinoma (Sheelam *et al.*, 2018).

1.8.2.10 Other growth factors (PDGF, SCF)

The stem cell factor (SCF) is also known as mast cell factor or steel factor and is 45kDa cytokine found in plasma membranes (Roskosli, 2005). SCF is a ligand for c-kit and together, they are implicated in the activation of various signalling pathways (such as MAPK, PI3K,) resulting in several downstream effects such as cell proliferation, angiogenesis and metastasis (Cardoso, Figueira, & Socorro, 2017). As a hematopoietic growth factor, SCF activity usually results in proliferation of hematopoietic cells. However earlier studies suggests SCF and other hematopoietic growth factors are capable of stimulating proliferation in tumour cells (Turner *et al.*, 1992). Furthermore, there is evidence to suggest that some malignant cells secrete large quantities of hematopoietic cytokines which may be measured in serum (McDermott *et al.*, 2002).

Research studies in various cancers have reported diverse findings with regards to serum SCF concentrations and immunoreactivity. In cultured cell lines, addition of SCF resulted in a 2.4-fold increase in cell proliferation (Lemoli *et al.*, 1994). In patients with colorectal cancer, serum SCF concentrations were lower compared to normal controls (Mroczko, Szmitkowski, WereszczyńSka-Siemiątkowska, & Okulczyk, 2005). In a similar study, serum SCF concentrations were also lower in patients with pancreatic cancer compared to normal controls (Vasiliades *et al.*, 2012).

With regards to BC, few studies have been conducted to assess SCF involvement in proliferation or recurrence. A study using BC T24 cell lines reported increased proliferation cells stimulated by SCF compared to unstimulated cells. The presence of SCF was also associated with invasiveness in these cells (Guo *et al.*, 2014b).

It can therefore be appreciated that, SCF may play a significant role in the high BC recurrence rates. This current research therefore seeks to measure serum SCF concentrations in patients undergoing treatment for BC. No previous research study has been performed to our knowledge on patients undergoing TURBT and followed for up to 6-months post-operatively.

PDGF is a glycoprotein located on chromosome 7 and may exist in dimeric forms; PDGF-AA and PDGF-BB or in a unified form; PDGF-AB (Raica & Cimpean, 2010). As a growth factor, PDGF plays crucial roles in physiological angiogenesis and also pathologically associated with angiogenesis in several human diseases cancers (Holleran, Hall, O'Regan, Smith, & McNamara, 2015; Jitariu, Raica, Cimpean, & Suciu, 2018; Yuge *et al.*, 2015)

Several studies performed using both cell lines and human tissues have attempted to identify the roles PDGF and its receptors play in cell proliferation and cancer. In human adipose stem cells, the presence of high PDGF concentrations in human serum, is positively associated with increased proliferation of human adipose stem cells. High concentrations of PDGF-AB in human serum had a significant positive effect on cell proliferation (Josh *et al.*, 2013). In another study using colorectal cancer cell lines (SW480, DLD-1 & Caco-2), obstruction of PDGF receptor β resulted in reduced cell proliferation as well as slowed activation of various downstream signalling pathways (Kaulfuβ *et al.*, 2013). This therefore provides an opportunity to use inhibitors of PDGF and their receptors in developing therapeutic agents for treatment.

In pathology, high concentrations of PDGF-AA in patients with colorectal cancer have been associated with development of liver metastasis (Pan, Peng, Xiao, & Gu, 2017). In these patients, increased metastatic disease could potentially be due to increased cell proliferation, invasion and tumour growth.

These studies provide evidence of the role PDGF plays in cell proliferation. In this regard, serum measurement of PDGF concentration could provide useful information in BC patients undergoing surgical treatment.

1.9 Assessing recurrence

Following recruitment, patients underwent for TURBT for the diagnosis and treatment of BC. Post-operatively, and in accordance with standard management guidelines, patients had several follow up clinics for the assessment of surgical outcome. Depending on stage, grade and risk stratification, patients may be offered 6 weeks, 3-months, 6-months or 9-months post-operative cystoscopy, to assess presence or absence of residual or recurrent bladder tumours, following TURBT.

In all patients recruited into this research study, follow up data immediately available from follow up clinics was retrieved. This information was obtained from outpatient clinic as well as BCUHB clinical portal.

Investigating the long-term overall survival rates, 5-year and 10-year recurrence and progression data are, however, beyond the scope of this research. However, the short-term information available (up to 2 years post TURBT) will be discussed in relation to the biomarkers measured, and may ultimately provide sufficient and accurate clinical data that may help predict or forecast NMIBC recurrence and progression.

1.10 Aims and Objectives

Current management guidelines for BC patients, involve surveillance and follow-up programmes using imaging procedures. Specifically, NMIBC is associated with high recurrence and progression rates. Currently, there is no laboratory-based tests for monitoring treatment and identifying patients at increased risk of cancer recurrence or progression.

This research study aimed to investigate the role of novel biomarkers in patients who had TURBT, for the diagnosis and treatment of NMIBC. Following the initial optimisation of methods, four pilot clinical studies were performed with the aim of identifying,

1. Changes in serum-based inflammatory markers in BC patients and their association with recurrence and progression

2. Changes in serum matrix metalloproteinase 2, 3 and 9 (MMP-2, MMP-3 and MMP-9) and CEACAM-1 concentration in patients undergoing TURBT for the treatment of BC

3. The role of various serum-based angiogenic and growth biomarkers in non-muscle invasive BC recurrence/progression

4. The role of novel antibody immunoreactivity and their association with BC recurrence and progression

Ultimately, it is anticipated that changes to certain biomarkers may be associated with NMIBC recurrence and progression. Verification and validation of these biomarkers could potentially be used in addition to or in combination with current management protocols for the identification of patients at risk of developing recurrence and progression. Additionally, the identification of potential biomarkers for BC recurrence would potentially reduce the frequency of imaging and surgical surveillance systems currently employed for the management of BC. Ultimately, our research findings may help modify or revise BC post-operative care for the benefit of the patients.

2.0 Chapter Two: Methods

2.1 Synopsis

The main aim of this chapter was to present all the materials and methods used during the research study. This research was a multi-centre project and was carried out at various locations within the Betsi Cadwaladr University Health Board (BCUHB) and the University of Chester.

The chapter therefore includes details of the ethical approval, patient selection and recruitment and sample/tissue collection. These three initial research steps were undertaken within various sites at the BCUHB.

Antibody optimisation/validation together with tissue processing and staining were carried out in the histopathology department at Ysbyty Glan Clwyd. Detailed descriptions of these processes have been provided in subsequent sections/chapters. Tissue staining of the various antibodies were evaluated at Ysbyty Glan Clwyd and Wrexham Maelor Hospital, with the help of experienced histopathologists and consultant pathologists. General research investigations involving ELISA and Bio-plex assays were performed at the North Wales Clinical Research Centre.

Data manipulation was done using various statistical models and tools with guidance from departmental statistician based at the University of Chester.

2.2 Equipment

0.5 ml flat cap microcentrifuge tubes

Thermofisher Scientific Product No. AB0350

1.5 ml Pierce Microcentrifuge Tubes

Thermofisher Scientific Product No. 69715

2.0 ml Pierce™ Microcentrifuge Tubes

Thermofisher Scientific Product No. 69720

3.0 ml Plastic whole blood tube with spray-coated K2EDTA

Becton Dickinson Product No.: 367856

3.0 ml Plastic citrate tubes

Becton Dickinson Product No.:363083

5.0 ml SST tube with silica clot activator

Becton Dickinson Product No.: 367986

BD Vacutainer Eclipse blood collection needle

Becton Dickinson Product No.: 368607

BD Vacutainer one-use holder

Becton Dickinson Product No.: 364815

BD Vacutainer Safety-Lok blood collection set

Becton Dickinson Product No.: 367287

BenchMark ULTRA (Automated IHC/ISH slide staining system)

Ventana Medical Systems Product No. 05342716001

BenchMark XT (Automated IHC/ISH slide staining system)

Ventana Medical Systems Product No.

Bio-plex 200

Bio-Rad Laboratories Inc:

Array reader Product No. 171000201
Microplate platform
High-throughput fluidics (HTF)
Calibration and validation kits
Bio-Plex MCV plate
PC and monitor
Bio-Plex Manager™ software

Dako Coverslipper

Agilent Dako Product No: CR100

EZ Read 400 Microplate Reader

Biochrom Product No: 80-4001-40

Finese ME+ Microtome

Thermofisher Scientific Product No. 902100A

Fisherbrand™ ZX4 IR Vortex Mixer

Thermofisher Scientific Product No: 13284769

Genlab Vertical Stainless Steel Digital Incubator

Thermofisher Scientific Product No: 12853416

Handheld Magnetic Washer

Bio-Rad Laboratories, Inc Product No. 171020100

HydroFlex™ microplate washer for 96-well format

Tecan Product No:

ID-Incubator 37 S I

Bio-Rad Laboratories Inc Product No: 009690

Lexicon® II Ultra-low Temperature Freezer

ESCO Product No.: UUS-714A-3-SS

PELORIS tissue processor

Thermofisher Scientific Product No: 26.0003

Prep kits

Ventana Medical Systems Product No: 783-3457

Precision circulating water bath

Thermofisher Scientific Product No: TSCIR35

Quick Release Tourniquet

DS MEDICAL

SL 8 small benchtop centrifuge

Thermofisher Scientific Product No: 75007221

SlideMate AS Slide Printer

Thermofisher Scientific Product No: A83900001

StuartMini Microtitre Plate Shaker

Cole-Parmer Product No: WZ-51707-08

TOMO® Adhesion Microscope Slides

Jencons (a VWR Division) Product No. 631-1109E

2.3 Reagents

10% Neutral Buffered Formalin

CellPath Product No. BAF-6000-08A

Bio-Plex Pro™ Human Cancer Biomarker Panel 1, 16-plex

Bio-Rad Laboratories Inc Product No. 171AC500M

Bio-Plex Pro™ Human Cancer Biomarker Panel 2, 18-plex

Bio-Rad Laboratories Inc Product No. 171AC600M

Bio-Plex Pro™ Human MMP-2 Singleplex set

Bio-Rad Laboratories Inc Product No. 171BM002M

Bio-Plex Pro™ Human MMP-3 Singleplex set

Bio-Rad Laboratories Inc Product No. 171BM003M

Bio-Plex Pro™ Human MMP-9 Singleplex set

Bio-Rad Laboratories Inc Product No. 171BM006M

CD31 (JC70) Antibody

Ventana Medical Systems Product No. 760-4378

CD34 (QBEnd/10) Antibody

Ventana Medical Systems Product No. 760-2927

COX-2 (SP21) Antibody

Ventana Medical Systems Product No. 760-4254

Dako REAL Antibody Diluent

Dako. Product No. S2022

HER-2/neu (4B5) Antibody

Ventana Medical Systems Product No. 790-2991

Human CEACAM-1 SimpleStep ELISA kit

Abcam Product No. 215540

Human CEACAM-1/CD66a Antibody

R&D Systems, Inc. Product No. MAB22441-100

Human S100A8 Antibody

R&D Systems, Inc. Product No. MAB4570

Human FGF R3 (IIIc) Antibody

R&D Systems, Inc. Product No. MAB7662-100

Human MIP2 ELISA Kit (CXCL2)

Abcam Plc Product No. ab184862

Human VEGF R2/KDR/Flk-1 Antibody

R&D Systems, Inc. Product No. MAB3571-100

Human VEGF R3/Flt-4 Antibody

R&D Systems, Inc. Product No. MAB3491-100

Podoplanin (D2-40) Antibody

Ventana Medical Systems Product No. 760-4395

Sheath Fluid

Bio-Rad Laboratories Inc Product No. 171000055

S100P Antibody

Ventana Medical Systems Product No. 760-4620

SOX-2 (SP76) Antibody

Ventana Medical Systems Product No. 760-4621

Thrombomodulin Antibody

Cell Marque Product No. CMC33921040

ultraView Universal DAB Detection Kit

Ventana Medical Systems Product No. 760-500

Ventana Amplification Kit

Ventana Medical Systems. Product No. 760-080

Ventana Hematoxylin

Ventana Medical Systems. Product No. 760-2021

Ventana protease 1

Ventana Medical Systems. Product No. 760-2018

Ventana Antibody Diluent with Casein

Ventana Medical Systems. Product No. 760-219

2.4 Buffers and solutions

2.4.1 Cell conditioning 1 (CC1)

The Ventana CC1 (Ventana Medical Systems) is a ready to use buffer in the initial stages of immunohistochemistry (IHC) on the ventana benchmark XT analyser. In the presence of heat, CC1 is used for antigen retrieval (Heat induced epitope retrieval). The basic pH and tris-based buffer in CC1 enhances antibody binding in tissues by hydrolysing covalent bonds at high temperature. Prior to use, the solution was stored at room temperature (15 to 30° C) and used within 3 months of purchase as recommended by manufacturers. During IHC, CC1 was applied to 5 µm tissue sections cut from 10% buffered neutral formalin fixed tissues using the mild (30 minutes) and standard (60 minutes) cell conditioning options.

2.4.2 Cell conditioning 2 (CC2)

The Ventana CC2 (Ventana Medical Systems) is a ready to use buffer for pre-treatment of tissue slides for IHC on the ventana benchmark XT analysers. CC2 has an acidic pH, contains citrate base, ProClin 300 preservative and used to hydrolyse formalin and formaldehyde related covalent bonds in tissues leading to enhanced antibody binding and improved results in IHC. Prior to usage, the solution was stored at room temperature (15 to 30° C) and was used within 3 months of purchase.

2.4.3 The EZ prep (10X)

During IHC, deparaffinization was performed using the ventana EZ prep solution (1X) solution (EZ prep) (Ventana Medical Systems, UK). EZ prep solution (1X) was prepared by diluting all contents of EZ prep concentrate (10X) in nine parts of distilled water. The EZ Prep solution contains a detergent and 0.5% ProClin 300 preservative. Tissue slides were dewaxed by using EZ prep (1X), heat and vortex mixing. Heated paraffin wax floated out from tissue sections through the aqueous solution and was efficiently removed by vortex mixing. Prepared solution was kept at room temperature and used within expiry date.

2.4.4 Liquid cover slip (high temperature) and Liquid coverslip (low temperature)

During IHC, evaporation was minimized by using liquid cover slip (LCS) (Ventana medical systems). This prevents tissue sections from drying up during the IHC. Liquid coverslip is applied between segments of IHC procedure. The Liquid cover slip (high temperature) solution contains paraffinic hydrocarbon and mineral oil whilst Liquid cover slip (low temperature) contains paraffinic hydrocarbon tinted with Oil Red O. These organic oils have relatively lower density compared to water and therefore serve as a barrier between aqueous solutions on

microscope slides and air. This eventually reduces the rate of evaporation and enhances the staining process. Solutions were stored at room temperature ((15°-30°C) and used within the expiry date.

2.4.5 Reaction Buffer (10X)

Reaction buffer (1X) (Ventana medical systems) was prepared by mixing one part reaction buffer concentrate (10X) with nine parts of distilled water and mixed thoroughly. Reaction buffer (1X) is a tris-based solution with a slightly basic pH of 7.6 ± 0.2. Reaction buffer (1X) was used as a wash medium during the various steps in IHC on the Ventana Benchmark XT and Ventana ULTRA. Solution was stored at room temperature (15°-30°C) and used within the expiry date.

2.4.6 Phosphate buffered saline (PBS)

1 litre of 20X PBS stock solution was made as follows

1. 800 ml of distilled water in a 1 litre beaker
2. A stir bar was placed in the beaker and placed on a magnetic stirrer
3. 160g of Sodium Chloride was weighed and added to beaker and totally dissolved
4. 6.8g of Potassium dihydrogen phosphate (Sigma-Aldrich, UK) was weighed and added to beaker and totally dissolved
5. 24.2g of Dipotassium hydrogenphosphate (Sigma-Aldrich, UK) was weighed and added to beaker and totally dissolved
6. Final volume was adjusted to 1 litre using distilled water
7. Solution was stored in a larger beaker and until required. Stock has a shelf life of 6 months. Before usage, stock solution was diluted 1:20 with distilled water.

2.5 Methods

2.5.1 Ethical approval

Permission for this research study was sought from the Research Ethics Service (REC reference 14/WA/0033. see appendix). The IRAS project ID for the project is 150558. All patient recruitment procedures and laboratory investigations were conducted in conformity with the provisions of the RES. All samples, patient demographics and patient data were completely anonymised to ensure confidentiality.

2.5.2 Subject recruitment

Subjects recruited for this research attended the Betsi Cadwaladr University Health Board (BCUHB) Wrexham Maelor Hospital, North Wales for elective procedures for the treatment/management of BC.

The author reviewed medical records of potential subjects scheduled for surgical procedures for the treatment or management of BC. Specifically, patients' treatment history, current medication, previous surgery, previous cancer, smoking status and diabetic status were carefully reviewed. Patients who had other cancers were not included in the study to avoid conflicting results.

After screening case notes, the author approached patients eligible for inclusion into the study to begin the recruitment process. To obtain an informed consent for participation in the study, the author discussed with each patient detailed requirement necessary for inclusion into the study. A copy of the patient information sheet (PIS) and consent form was then given to each recruited patient after discussing it in detail. The patient information sheet contained detailed information about the research ie. Purpose of study and consent form. Patients who agreed to participate in the research study filled and signed a consent form and retained their copies.

40 patients (average age= 72.9, males= 33 and females= 7) prospective patients scheduled for a Transurethral Resection of the Bladder tumour (TURBT) for the treatment of BC, were recruited into this research study after informed consent.

For each of these patients, serum blood samples were taken pre-operatively and at 1-month, 3-months and 6-months post-operatively. During TURBT procedure, tissue samples were taken as per standard guidelines for histopathological analysis. This study was conducted concurrently with ongoing BC treatment/management for recruited patients. As such all tissue blocks were subsequently retrieved from the histopathology department of the Ysbyty Glan Clwyd hospital following routine H&E staining by biomedical scientists and reporting by histologists and consultant pathologists. All histology reports produced from H&E staining were individually examined before IHC was conducted.

2.5.3 Blood sampling

Venous blood samples were obtained through standard venepuncture from all patients who consented to participate in the study. Blood sampling was done through venepuncture of the ante-cubital vein (where practically possible) into various blood collection Vacutainer tubes.

Specifically, for citrated plasma, blood was taken into 3 ml plastic citrated tubes (Becton Dickinson) whilst normal plasma was obtained by using spray-coated K2EDTA plastic whole blood Vacutainer tubes (Becton Dickinson, UK).

For serum, venous blood samples were collected into 5 ml SST tubes with silica clot activator (Becton Dickinson), and left at room temperature for at least 2 hours. Tubes were then centrifuged at 1500xg for 10minutes to adequately separate serum from whole blood cells, as per standard operating procedure. For plasma, blood tubes were centrifuged within 30 minutes after venepuncture. All serum and plasma samples were aliquoted into 1 ml eppendorff tubes and stored at -80^{o}C until analysed.

Post-operatively, venous blood samples were taken at 1-month, 3-months and 6-months. During post-operative sampling, patients' medical history, as well as vital statistics (i.e. blood pressure, temperature and urine dipstick), were assessed.

During blood collection and storage, strict protocols were followed to minimize variations in analyte concentrations. For plasma samples, venous blood samples were centrifuge without delay and stored in -80^{o}C freezers immediately.

2.5.4 Tissue preservation and processing

For the purposes of these research studies, Formalin fixed, paraffin embedded (FFPE) tissue blocks of recruited patients were retrieved from storage at the histopathology department of Ysbyty Glan Clwyd.

During surgery, BC tissue samples were taken in theatre by the consultant urological surgeon at the Wrexham Maelor Hospital, a standard requirement for the treatment of BC. Tissues were immediately placed in 10% Formalin preservative solution, transported within 24-72 hours to the histopathology department of Ysbyty Glan Clwyd and then processed into tissues blocks by BCUHB staff, according to standard protocol. Briefly, tissue processing involves several steps of dehydration in ethanol, clearing and embedding in paraffin wax. This was done according to standard protocol. Tissue blocks were then used in the management of patients and stored at room temperature in the dark until retrieved for this study.

2.5.5 Cutting Tissue sections (Microtomy)

At least 12 sections (4 µm each) were cut from each patient tissue block using a microtome. Each tissue block was placed on ice for at least 10 minutes prior to sectioning. This technique cools paraffin, maintains tissue integrity and aids easy sectioning. Each cut section was floated on a water bath in which the temperature was maintained at 40-45^{0} C to stretch out embedded formalin and remove wrinkled tissue. Sections were then placed on positively charged glass

tomoslides and incubated at 55-60^0 C for at least 30 minutes before proceeding with IHC. This process enhances fixation of the tissue to the glass slides and ensures stability of the tissue. Slides can also be incubated at 37^0 C overnight for fixation.

In this research, both control and study tissues (Patient tissue) slides were placed on the same slide before proceeding with IHC (Figure 2.1). This approach ensures that, both tissues are treated with the same conditions i.e. temperature, length of incubation and therefore eliminates any inconsistencies. It also validates the staining process and serves as a control mechanism for the entire IHC protocol. Concerning reporting, histologists and pathologists report on the patient tissues by referring to all control tissues thereby enhancing the quality of the reports.

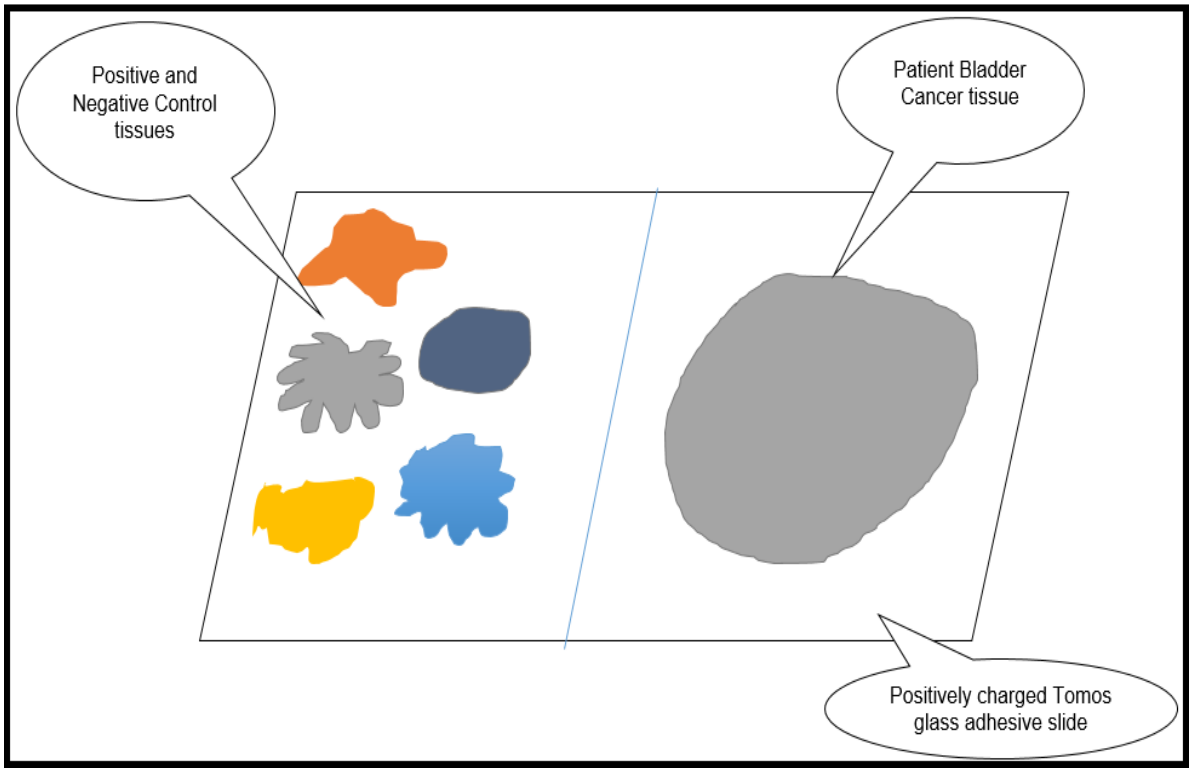

Figure 2. 1: Representation of tissue arrangement on a slide.

Both control tissues and patient tissues being analysed were placed on the sample positively charged glass slide for IHC.

2.5.6 Measurement of cancer panel-1 and cancer panel-2 using Bio-Rad Luminex 200

Bio-Rad Bio-plex techniques are based on a unique combination of three core components of the xMAP technology. The first component is based on the ability of fluorescently labelled beads to identify specific analytes in a biological specimen. These beads possess unique colour codes for specific identification and analysis. The second component quantifies the amount of analyte bound to each bead using a flow cytometer. The final component is a digital processor

capable of accurately analysing high volumes of fluorescent data produced from the two components.

The principle of the immunoassays employed by the Bio-Plex technique operate like a conventional sandwich ELISA. Capture antibodies linked to specific magnetic beads target the biomarker of interest. The 96-well plate is then washed several times to remove unbound protein before a biotinylated detection anybody is added to create a sandwich complex. The addition of a streptavidin-phycoerythrin (SA-PE) conjugate creates a detection complex. A dedicated flow cytometer then measures the final reaction complex.

A vial of Bio-Rad Bio-Plex Pro Human Cancer panel 1 standard was reconstituted with 781 µl of standard diluent HB. One vial each of Bio-Rad Bio-Plex Pro Human Cancer 1 quality control high and quality control low was reconstituted with 250 µl standard diluent HB and mixed gently and thoroughly. Reconstituted standards and controls were gently vortexed for 5 seconds and placed on ice for 30 minutes before use. Reconstituted standards were serially diluted fourfold before performing the assay. Each well of a 96 well plate requires 2.5 µl of 20x stock coupled beads adjusted to a total volume of 50 µl in assay buffer. To prepare 1x coupled beads, 20x stock coupled beads were vortexed for 30 seconds at mid speed. 288 µl of 20x beads were mixed with 5.47 ml of assay buffer to prepare a total volume of 5.76 ml.

Prior to running assay, 1x diluted coupled beads were vortexed for 30 seconds and 50 µl was added to each well of the 96 well plate. The plate was washed twice in 100 µl wash buffer per well using a Bio-Rad Bio-Plex handheld magnetic washer. Diluted standards, controls and samples (diluted fourfold in sample diluent HB) were vortexed for 5 seconds and 50 µl was added to appropriate wells after which the plate was incubated for 1 hour in the dark at room temperature with shaking at 850 ± 50 rpm.

Each well of a 96 well plate requires 1.25 µl of 20x stock detection antibody adjusted to a total volume of 25 µl in detection antibody diluent. 15 minutes prior to use, 1x detection antibody was prepared by vortexing 20x stock detection antibody for 30 seconds and then spun at low speed for 30 seconds. 145 µl of 20x stock detection antibody was then mixed with 2.76 ml of detection antibody diluent to prepare a total volume of 2.9 ml 1x detection antibody. At the end of the 1-hour incubation period for standards, controls and samples, the plate was washed three times with 100 µl wash buffer per well using the Bio-plex handheld magnetic washer to remove any unbound proteins. Diluted 1x detection antibodies were vortexed for 5 seconds and 25 µl added to each well. The plate was incubated at room temperature for 30 minutes in the dark with shaking at 850 ± 50 rpm.

10 minutes prior to use, 1x SA-PE conjugate was prepared by vortexing 100x stock SA-PE conjugate for 30 seconds and then spun at low speed for 30 seconds. 60 µl of 100x stock SA-PE conjugate was then mixed with 5.94 ml of assay buffer to prepare a total volume of 6 ml 1x SA-PE conjugate. At the end of the 30-minute incubation period for detection antibodies, the plate was washed three times with 100 µl wash buffer per well using the Bio-plex handheld magnetic washer to remove any unbound detection antibody. Diluted 1x SA-PE conjugate was vortexed for 5 seconds and 50 µl added to each well. The plate was incubated at room temperature for 10 minutes in the dark with shaking at 850 ± 50 rpm.

At the end of the 10-minute incubation period, plate was washed three times with 100 µl wash buffer per well using the Bio-plex handheld magnetic washer. Beads were re-suspended with 125 µl assay buffer per well, covered with a new sealing tape and placed on a plate shaker at 850 ± 50 rpm for 30 seconds. Data from the plate was analysed on the Bio-plex 200 instrument using the Bio-Plex manager 6.0 software. The mean fluorescent intensity (MFI) for each well was acquired using the software. This information was subsequently used in creating a standard curve as well as calculation sample concentrations.

2.5.7 Measurement of MMP-2, MMP-3 & MMP-9 using Bio-Rad luminex 200

Bio-Rad Bio-plex techniques are based on a unique combination of three core components of the xMAP technology. The first component is based on the ability of fluorescently labelled beads to identify specific analytes in a biological specimen. These beads possess unique colour codes for specific identification and analyses. The second component quantifies the amount of analyte bound to each bead. This Bio-Plex 200 contains a dedicated a flow cytometer. The third component is a digital processor for high-speed quality data processing.

The principles of the immunoassays employed by the Bio-Plex technique operate like a conventional sandwich ELISA. Capture antibodies linked to specific magnetic beads target the biomarker of interest. The 96-well plate is then washed several times to remove unbound protein before a biotinylated detection anybody is added to create a sandwich complex. The addition of a streptavidin-phycoerythrin (SA-PE) conjugate creates a detection complex. A dedicated flow cytometer then measures the final reaction complex.

781 µl of 10% serum-based standard diluent (prepared by diluting 1 part standard diluent HB with 1.5 parts of sample diluent HB) was used to reconstitute a vial of Bio-Rad Bio-Plex Pro Human MMP standard. Reconstituted standard was gently vortexed for 5 seconds and placed on ice for 30 minutes before being serially diluted threefold. Each well of a 96 well plate requires 2.5 µl of 20x stock coupled beads adjusted to a total volume of 50 µl in assay buffer. To prepare 1x coupled beads, 20x stock coupled beads were vortexed for 30 seconds at mid

speed. 288 µl of 20x MMP-2 beads, 288 µl of 20x MMP-3 beads and 288 µl of 20x MMP-9 beads were mixed with, 4,896 µl of assay buffer to prepare a total volume of 5.76 ml.

Prior to running assay, 1x diluted coupled beads were vortexed for 30 seconds and 50 µl was added to each well of the 96 well plate. Plate was washed two times in 100 µl 1% wash buffer (dilute 1 part 10x stock solution with 9 parts distilled water) per well using a Bio-Rad Bio-Plex handheld magnetic washer. Diluted standards and samples (diluted fivefold in sample diluent HB) were vortexed for 5 seconds and 50 µl was added to appropriate wells after which the plate was incubated for 1 hour in the dark at room temperature with shaking at 850 ± 50 rpm.

Each well of a 96 well plate requires 1.25 µl of 20x stock detection antibody adjusted to a total volume of 25 µl in detection antibody diluent. 15 minutes prior to use, 1x detection antibody was prepared by vortexing 20x stock detection antibody for 30 seconds and then spun at low speed for 30 seconds. 150 µl each of 20x MMP-2, MMP-3 AND MMP-9 stock detection antibody was then mixed with 2.56 ml of detection antibody diluent to prepare a total volume of 3 ml 1x detection antibody. At the end of the 1-hour incubation period for standards and samples, plate was washed three times with 100 µl 1% wash buffer per well using the Bio-plex handheld magnetic washer to remove any unbound proteins. Diluted 1x detection antibodies were vortexed for 5 seconds and 25 µl added to each well. The plate was incubated at room temperature for 30 minutes in the dark with shaking at 850 ± 50 rpm.

10 minutes prior to use, 1x SA-PE conjugate was prepared by vortexing 100x stock SA-PE conjugate for 30 seconds and then spun at low speed for 30 seconds. 60 µl each of 100x stock MMP-2, MMP-3 and MMP-9 SA-PE conjugate was added to 5.82 µl of assay buffer to prepare a total volume of 6 ml 1x SA-PE conjugate. At the end of the 30-minute incubation period for detection antibodies, the plate was washed three times with 100 µl 1% wash buffer per well using the Bio-plex handheld magnetic washer to remove any unbound detection antibody. Diluted 1x SA-PE conjugate was vortexed for 5 seconds and 50 µl added to each well. The plate was incubated at room temperature for 10 minutes in the dark with shaking at 850 ± 50 rpm.

At the end of the 10-minute incubation period, the plate was washed three times with 100 µl wash buffer per well using the Bio-plex handheld magnetic washer. Beads were re-suspended with 125 µl assay buffer per well, covered with a new sealing tape and placed on a plate shaker at 850 ± 50 rpm for 30 seconds. . Data from the plate was analysed on the Bio-plex 200 instrumant using the Bio-Plex manager 6.0 software. The mean fluorescent intensity (MFI) for each well was acquired using the software. This information was subsequently used in creating a standard curve as well as calculation sample concentrations.

2.5.8 Measurement of MIP-2 concentration using ELISA

MIP-2 concentration was quantitatively determined in serum using a commercially available ELISA kit [Human MIP-2 ELISA kit (CXCL2), (Abcam Plc)].

The antibody cocktail was prepared by mixing equal volumes (600 µL) of 10X capture antibody and 10X detector antibody in 4,800 µL of Antibody diluent 4BI and mixed thoroughly and gently. MIP-2 human lyophilized recombinant protein was reconstituted by adding 1000 µl sample diluent 25BP to produce a stock standard solution of 300 pg/ml. Starting with a 150 pg/ml solution, a serial dilution of standards was prepared (0 – 150 pg/ml) using standard diluent 25BP.

A 98 well microplate pre-coated with anti-MIP-2 human monoclonal antibody was used for this assay. 50 µl/well of standards and samples (diluted 1:4 in sample diluent 25BP) are added to plate. 50 µl/well of antibody cocktail (prepared as indicated above) was then added to the plate and incubated at room temperature for 1 hour on a plate shaker set to 400rpm. Plate was washed three times with 350 µl 1X wash buffer PT ensuring complete liquid removal by blotting. 100 µl/well of TMB substrate was added to plate and incubated in the dark on a plate shaker set to 400 rpm. The colour development was stopped by adding 100 µl/well of stop solution to plate.

The optical density of each well was read using a plate reading set to 450 nm. This was an endpoint reading. A standard curve was constructed and used to determine the concentrations of MIP-2 in unknown samples.

2.5.9 Measurement of CEACAM-1 concentration using ELISA

The concentration of CEACAM-1 was quantitatively determined in serum using a commercially available ELISA kit (Human CEACAM-1 simplestep ELISA kit, Abcam plc UK).

Antibody cocktail was prepared by mixing equal volumes (600 µL) of 10X human CEACAM-1 capture antibody and 10X human CEACAM-1 detector antibody in 4,800 µL of Antibody diluent 4BI and mixed thoroughly and gently. CEACAM-1 human lyophilized recombinant protein was reconstituted by adding 500 µl sample diluent NS to produce a stock standard solution of 6000 pg/ml. Starting with a 3000 pg/ml solution, a serial dilution of standards was prepared (zero – 3000 pg/ml) using standard diluent NS.

A 98 well microplate pre-coated with anti-CEACAM-1 human monoclonal antibody is used for this assay. 50 µl/well of standards and samples (diluted 1:4 in sample diluent NS) was added to the plate. 50 µl/well of antibody cocktail (prepared as indicated above) was then added to

the plate and incubated at room temperature for 1 hour on a plate shaker set to 400rpm. The Plate was washed three times with 350 µl 1X wash buffer PT ensuring complete liquid removal by blotting. 100 µl/well of TMB substrate was added to plate and incubated in the dark on a plate shaker set to 400 rpm. The colour development was stopped by adding 100 µl/well of stop solution to the plate.

Optical density each well was read using a plate reading set to 450 nm. This was an endpoint reading. A standard curve was constructed and used to determine the concentrations of CEACAM-1 in unknown samples.

2.5.10 Immunohistochemistry (IHC)

Due to recent advances in research and technology, IHC is now widely used as a diagnostic tool in various NHS pathology departments. During this research, a modified indirect IHC used in a UKAS accredited NHS pathology department was used to stain all tissue sections.
All tissue samples were stained using either the Ventana BenchMark ULTRA (Automated IHC/ISH slide staining system) or the Ventana BenchMark XT (Automated IHC/ISH slide staining system). Both analysers operate on the same principle of identifying proteins or antigens in tissue samples using specifically labelled primary antibodies through activations of antibody-antigen interactions. The standard IHC protocol is a multi-step process that begins with deparaffinization and ends with counterstaining. In this research, although the principles were followed, a modified IHC protocol was used. The differences between the two methods are highlighted in Figure 2.2. Furthermore, the various steps in the IHC protocol will be discussed in the next sections

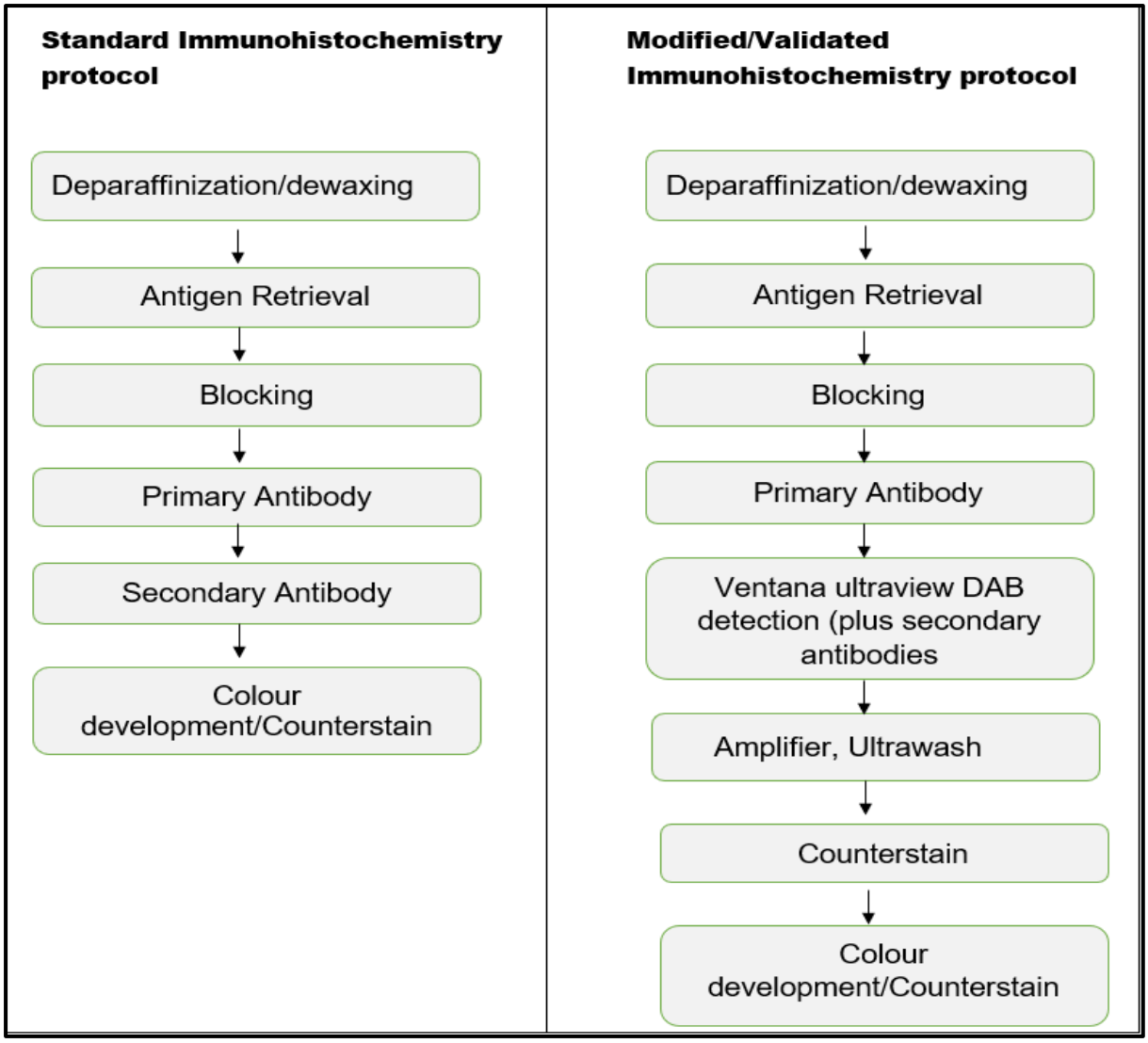

Figure 2. 2: Standard IHC protocol versus the modified protocol used in this research

Deparaffinisation (dewaxing)

The focus of this step is to "bring slides down to water" (rehydrate) through a series of steps and washes in alcohol and water. Prior to deparaffinization, 4 µm thick tissue sections cut from neutral-buffered formalin-fixed, paraffin-embedded routinely processed tissue blocks were placed on positively charged glass slides (TOMOSlides) and placed in a 55°C oven for about 2 hours. Deparaffinization begins with placing slides in 2 to 3 baths of xylene for 5-10 minutes followed by rehydration in absolute alcohol (100%) and several decreasing alcohol concentrations (i.e. 95%, 70%, 50% etc) for 5-10 minutes each.

Blocking

Blocking endogenous peroxidase activity in tissues may be done by immersing slides in a low concentration of 3% hydrogen peroxide solution for 5-10 minutes with gentle vortexing. This

is followed by rinsing in running water for about 5 minutes. If required, non-specific binding may also be prevented by blocking in diluted normal goat serum. In this research protocol, endogenous proteins and peroxides were blocked by covering slides with Ventana diluent/option 1 for 4 minutes.

Antigen Retrieval

Depending on the protein being investigated, heat-induced or enzymatic epitope retrieval methods may be used. During tissue fixation, formation of methylene bridges results in crosslinks, an effect which masks antigenic sites. This step is important for unmasking antigenic sites in proteins being investigated. In this research, antigen retrieval was performed using the heat induced epitope retrieval method by exposing the slides to cell conditioning 1 (standard CC1) at 95-100ºC for 52 minutes. CC1 is a tri-based EDTA buffer with a pH of 7.8 (section 2.4.1).

Primary and secondary antibodies

Details of primary antibodies used in this study are summarised in table 2.1. Detailed description and discussion of antibody validation for IHC has also been provided in chapter 3. In this research, an indirect IHC method was used. Unlabelled primary antibodies, which were mouse or rabbit monoclonal IgG antibodies, were applied to tissues sections during the IHC staining process. HRP-labelled secondary antibodies (goat anti-mouse IgG, goat anti-mouse IgM, and goat anti-rabbit) were then added to the slides. The selected secondary antibodies were against antibodies from the species in which the primary antibodies were raised. Schematic diagram of an indirect IHC is presented in Figure 2.3.

Table 2. 1 Immunohistochemical Staining localisations for various antibodies

Primary Antibody	Control tissues	Localization
CEACAM-1	Colon	Cytoplasmic, Membranous
CD31	Appendix, Tonsil	Cytoplasmic, Membranous
CD34	Appendix, Tonsil	Membranous, nucleus
COX-2	Colon, appendix, placenta	Cytoplasmic, membranous
HER-2/neu	Breast	Membranous
S100P	Placenta, Colon, Appendix	Cytoplasmic, Nuclear
SOX-2	Fallopian tube, Umbilical cord	Nuclear
thrombomodulin	Bladder	Cytoplasmic, membranous
VEGFR-3	Fallopian tube, Umbilical cord	Nuclear

Detection system (ultraView Universal DAB Detection Kit)

The detection kit used in this research; the ventana Ultraview DAB universal detection kit (Ventana medical systems) is an indirect biotin-free kit capable of identifying mouse and rabbit IgG and IgM antibodies in PPFE tissue sections during IHC (table 2.2).

Table 2. 2 Components of the UltraView Universal DAB detection kit

Universal DAB Inhibitor	3% hydrogen peroxide solution.
Universal HRP Multimer	HRP-labelled antibodies (goat anti-mouse IgG, goat anti-mouse IgM, and goat anti-rabbit) (<50 μg/ml) in a buffer containing protein with ProClin 300, a preservative.
Universal DAB Chromogen	0.2% 3, 3'-diaminobenzidine tetrahydrochloride in a proprietary stabilizer solution with a proprietary preservative.
Universal DAB H_2O_2	*ultra*View Universal DAB H2O2 (0.04% hydrogen peroxide in a phosphate buffer solution)
Universal Copper	Copper sulphate (5g/L) in an acetate buffer with proprietary preservative.

Following exposure to primary antibody and HRP-labelled secondary antibody, 3, 3'-diaminobenzidine (DAB) was used for colour development. DAB is catalysed to form a brown precipitate (oxidised form of DAB) in the presence of hydrogen peroxide (Figure 2.3). This is then visualised using light microscopy.

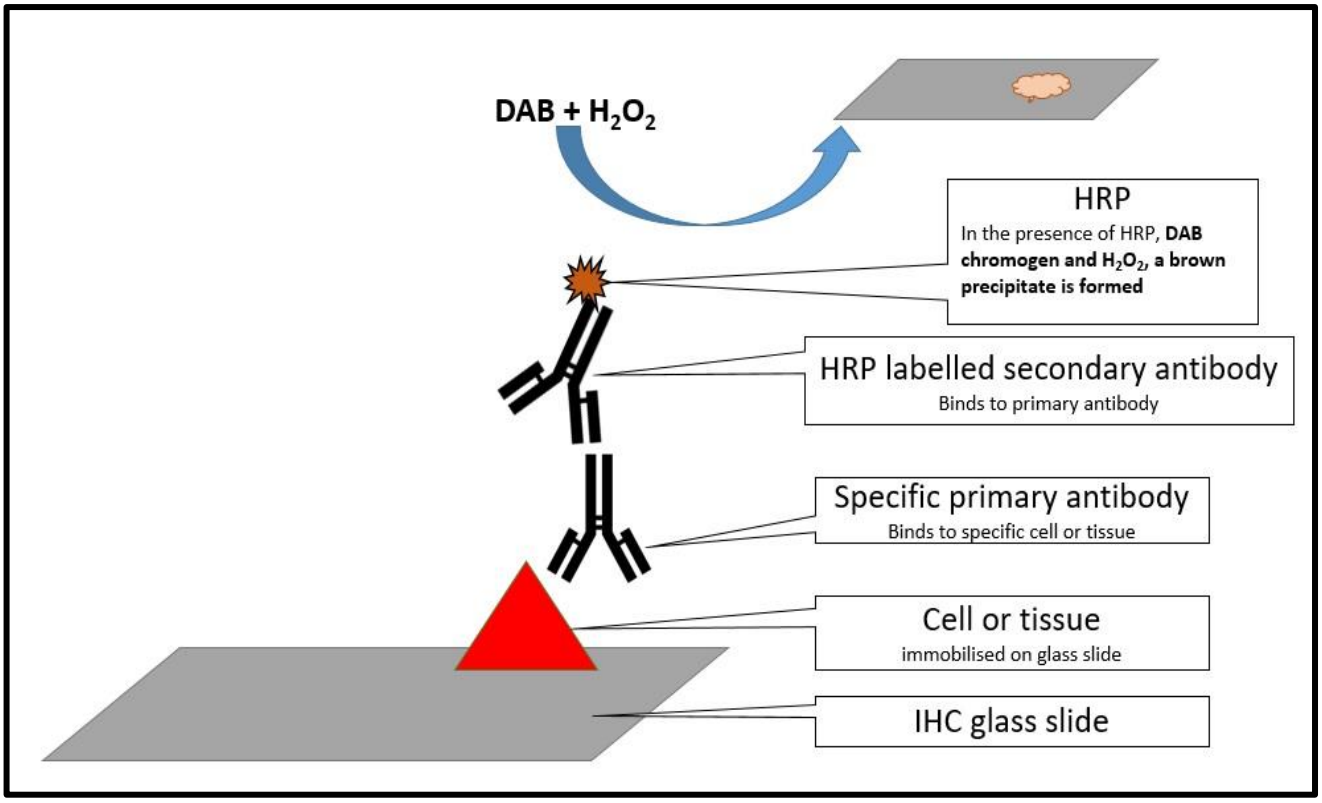

Figure 2. 3 Graphical representation of ultraview detection system

Counterstaining

Following primary antibody staining in tissue samples, counterstaining is usually used to highlight other components of cell/tissue to aid visualisation. In this research, the Ventana haematoxylin was used as counterstain and stains nuclei blue by reacting with a dye complex in the presence of nucleic acids and histone proteins

Dehydration and cover slipping

Dehydration of the slides was carried out using an automated instrument, Coverstainer (Dako, England). Slides were dehydrated by immersing in a series of graded alcohols and finally clearing in xylene as follows;

1. 2-3 baths of 70% alcohol for 5 minutes each
2. 2-3 baths of 90% alcohol for 5 minutes each
3. 2-3 baths of 95% alcohol for 5 minutes each
4. 2-3 baths of 100% alcohol for 5 minutes each
5. 2-3 baths of xylene for 5 minutes each

Slides are drained and blotted after each bath to reduce contamination and coverslips were then applied. The Dako coverstainer maintains consistent dehydration of the slides and avoids

bubbles after coverslipping. It also avoids damaging the tissues, less time consuming and avoids marking the coverslips.

2.6 Statistical Analysis

With regards to statistical analysis, professional advice was sought from Dr Gareth Elfred Jones, department of biological Sciences statistician based at the University of Chester. Analysis was carried out using SPSS for windows version 25 (licensed by the University of Chester).

With regards to data generated from serum analysis, normality tests were performed on all data sets to determine whether there was normal distribution. Normal distribution was observed were in cases where $p \geq 0.05$.

Normally distributed data were analysed using the repeated measures one-way analysis of variance (ANOVA) using $p \geq 0.05$ to determine significance. Further statistical testing (Post hoc) was performed using the Bonferoni test, in cases where a significant variation was observed in the ANOVA test. Normally distributed data were presented in bar graphs using mean and SDs.

Data sets that were not normally distributed were analysed using the Friedman test. In cases were a significant variance was observed with regards to the Friedman test, further post hoc testing was performed using the Wilcoxon's signed test. Data that was not normally distributed were presented in box plots using median and interquartile ranges.

With regards to tissue analysis, a chi-square test was performed to determine the difference between antibody staining in bladder tumour cells in comparison with normal urothelium. A Kruskal Wallis test was used to determine the association between clinopathological features (such as cancer grade and stage) and immunoreactivity. In cases where there was a significant difference, further post-hoc testing was performed using the Mann-Whitney test.

Data that were normally distributed are presented in bar charts using mean values and errors bars represent standard error mean. Non-parametrically distributed are presented in box plots using median and interquartile ranges.

3.0 Chapter Three: Validation of Immunohistochemistry

3.1 Antibody optimisation for Immunohistochemistry

The main aim of this chapter was to provide in detail, the processes undertaken to verify and validate the staining protocols used in this study. Validation of the IHC protocol for each of the primary antibodies studied was carried out prior to staining any patient tissues.

For the purposes of this research, CEACAM-1, CD31, CD34, COX-2, HER-2, S100P, SOX-2, Thrombomodulin and VEGFR-3 antibodies were optimised for IHC, using the ventana benchmark ULTRA (automated IHC/ISH slide staining system) (Roche, UK) and the ventana benchMark XT (automated IHC/ISH slide staining system) (Roche, UK) at the department of histopathology at Ysbyty Glan Clwyd. Preliminary IHC investigations (adjustments for antibody dilution, incubation times, temperature alterations, etc.), were undertaken to optimise staining conditions for each antibody. IHC protocol used in this project was based on a modified IHC technique employed on the ventana ultra and ventana XT automated analysers (Section 2.5.10).

As previously discussed (section 2.5.5), each positively charged glass slide used for staining patient tissues contained at least 2 controls tissues, for quality assurance and validation purposes. This validation technique ensured that both sample and control tissues were exposed to the same staining conditions. This novel addition to IHC staining is unique to this research study, since no current literature reported similar modifications.

3.1.1 Optimisation of S100P antibody immunoreactivity in tissues using IHC

Anti-S100P mouse monoclonal antibody (16/f5) was optimised for IHC using human placenta tissue samples from Ysbyty Glan Clwyd. Sections were cut as previously described (sections 2.5.5). Sectioned tissue slides were placed in an incubator (set to 60^{o}C) for 30-60 minutes and then transferred to the ventana benchmark XT (Automated IHC/ISH slide staining system) for IHC. In the first step, slides were deparaffinised at 72^{o}C for 4 minutes using ventana EZ prep solution (section 2.4.3).

Antigen retrieval was performed using the enzymatic method by exposing the slides to ventana protease 1 solution for 8 minutes.

Anti-S100P mouse primary monoclonal antibodies, (purchased pre-diluted from ventana medical systems), was applied to slides and incubated for 24 minutes at 37^{o}C. Staining was amplified by adding one drop of ventana amplifier. After series of washes, slides were incubated in hydrogen peroxidase, universal HRP multimer (which contains labelled secondary antibodies) and universal DAB chromogen for colour development.

Slides were then counterstained in haematoxylin 1 for 12 minutes before applying a blueing reagent for 4 minutes.

During optimisation, the first IHC staining protocol used for S100P contained the manufacturer commended staining options (Experimental protocol 1 in table 3.1). A representative histological picture of each protocol has also been provided (figure 3.1-3.3)

Table 3. 1 IHC Experimental protocols for anti-S100P monoclonal antibody.
Since the primary antibody was supplied pre-diluted, these Experimental protocols varied the length of incubation for the primary antibody. Experimental protocol 2 also included an amplification step and a longer counterstain incubation.

Experimental protocol 1	Experimental protocol 2 (Optimised protocol)
Control tissue- Placenta	Control tissue- Placenta
Deparaffinization- 72ºC for 4 minutes	Deparaffinization- 72ºC for 4 minutes
Antigen retrieval- Protease 1 for 8 minutes	Antigen retrieval- Protease 1 for 8 minutes
CC1 not required	CC1 not required
Ab incubation at 37ºC for 16 Minutes	Ab incubation at 37ºC for 24 minutes
Amplification- not required	Amplification- Ventana amplifier
Detection kit- Ultraview	Detection kit- Ultraview
Counterstain for 8 minutes	Counterstain for 12 minutes
blueing reagent (4 Minutes)	blueing reagent (4 Minutes)

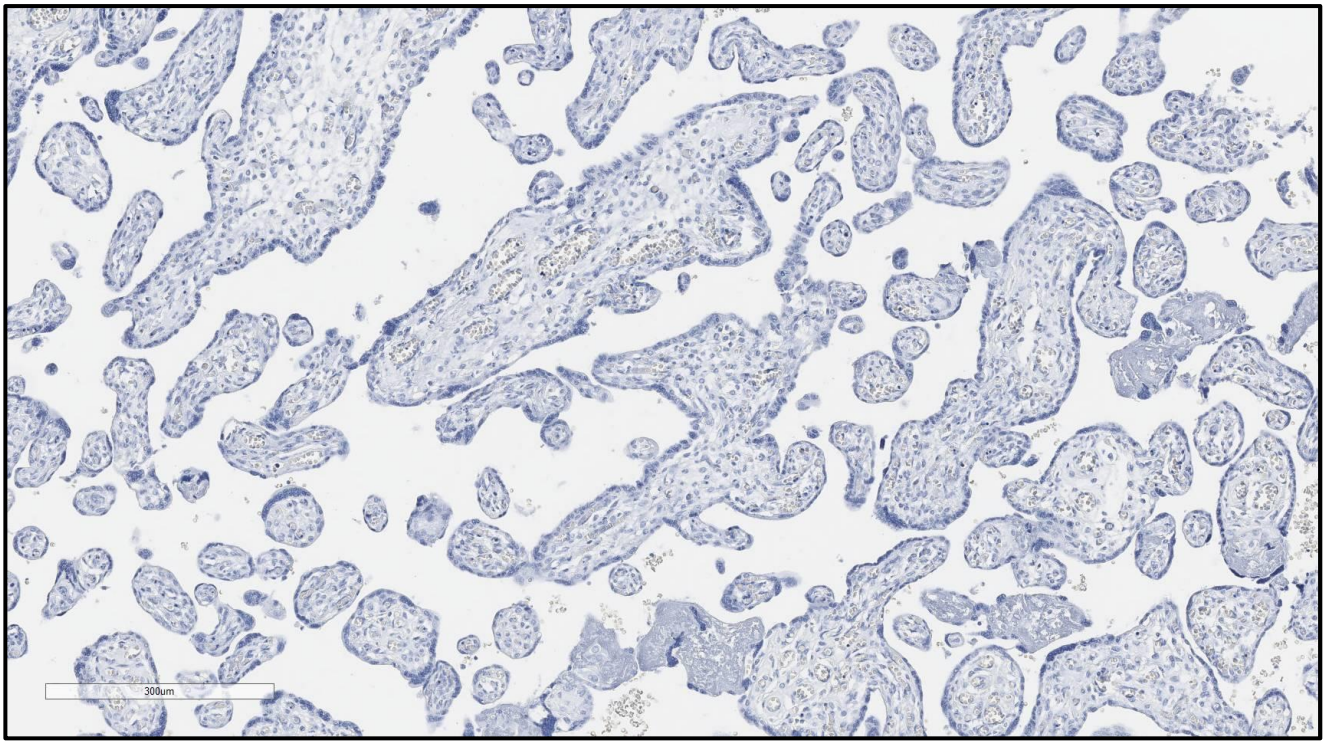

Figure 3. 1 Anti-S100P IHC optimisation using negative control.
Immunohistochemical staining of anti-S100P (16/f5) mouse monoclonal primary antibody in FFPE human placenta tissues. Ventana ultraview DAB detection. No nuclear and cytoplasmic IHC staining in epithelial cells of trophoblasts. X100 magnification

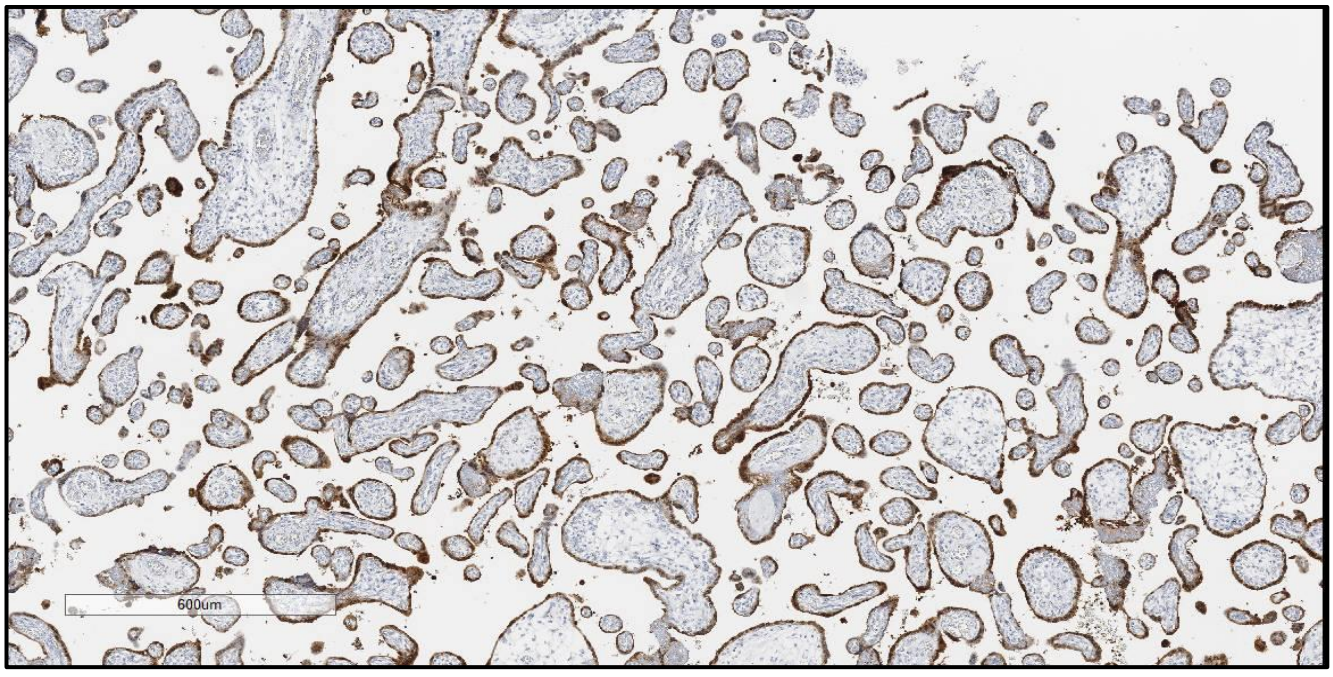

Figure 3. 2 Anti-S100P IHC optimisation using Experimental protocol 1.
IHC staining of anti-S100P (16/f5) mouse monoclonal primary antibody in FFPE human placenta. Antigen retrieval = protease (8 Minutes), Antibody incubation= 16 Minutes, No amplification, Ventana ultraview DAB detection. Note the positive nuclear and cytoplasmic Immunohistochemical staining (brown) in epithelial cells of trophoblasts. X100 magnification

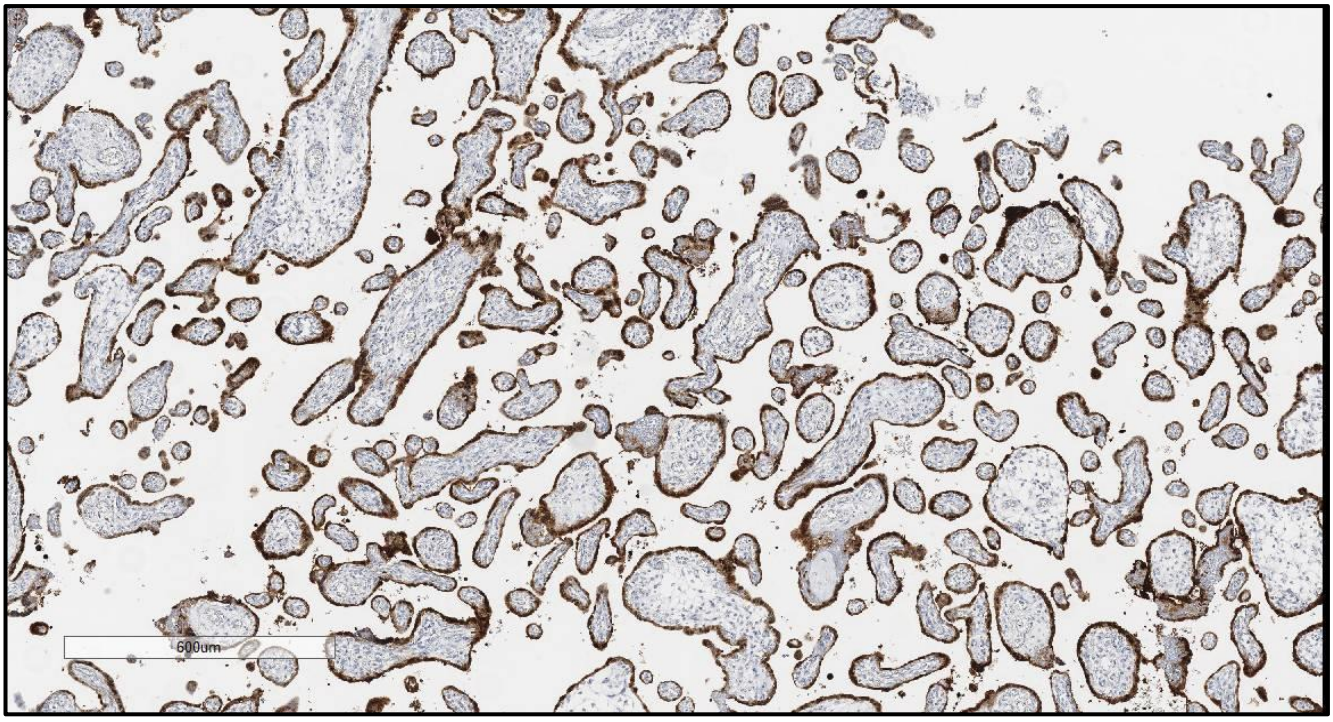

Figure 3. 3 Anti-S100P IHC optimisation using Experimental protocol 2 (optimised protocol).
IHC staining of anti-S100P (16/f5) mouse monoclonal primary antibody in FFPE human placenta. Antigen retrieval= protease (8 Minutes), Antibody incubation= 24 Minutes, amplification, Ventana ultraview DAB detection. This staining protocol had a longer primary antibody incubation time, longer counterstaining time and an amplification step. Positive nuclear and cytoplasmic Immunohistochemical staining in epithelial cells of trophoblasts. Staining in this protocol are sharper with fewer background staining. X100 magnification.

3.1.2 Optimisation of COX-2 antibody immunoreactivity in tissues using IHC

Anti-COX-2 (SP21) rabbit monoclonal primary antibody was optimised for IHC using colon sample tissues from Ysbyty Glan Clwyd. Sections were cut as previously described (sections 2.5.5). Sectioned tissue slides were placed in an incubator (set to 60ºC) for 30-60 minutes then transferred to the ventana benchmark ULTRA (Automated IHC/ISH slide staining system) for IHC. In the first step, slides were deparaffinised at 72ºC for 4 minutes using ventana EZ prep solution (section 2.4.3).

Antigen retrieval was performed using the heat induced epitope retrieval method by exposing the slides to cell conditioning 1 (standard CC1) at 95-100ºC for 64 minutes. CC1 is a tri-based EDTA buffer with a pH of 7.8. (Section 2.4.1).

Anti-COX-2 (SP21) rabbit monoclonal primary antibodies, (purchased prediluted from Ventana medical systems), was applied to slides and incubated for 32 minutes at 37ºC. Staining was amplified by adding one drop of Ventana amplifier.

After series of washes, slides were incubated in hydrogen peroxidase, universal HRP multimer (which contains labelled secondary antibodies) and universal DAB chromogen for colour development. Slides were then counterstained in haematoxylin 1 for 12 minutes before applying a blueing reagent for 4 minutes.

Starting with the product insert (contains initial recommended protocol), we varied various stages of the staining process such as incubation time, heat, counterstain, amplification and blocking. Each summary has been provided (Table 3.2). A representative histological picture of each protocol has also been provided (figures 3.4- 3.7).

Table 3. 2 IHC Experimental protocols for anti-COX monoclonal antibody.
Three variations of the protocol were used in optimising anti-COX-2 antibody. Optimum staining was achieved with protocol 2, which showed high intensity staining with little background noise. Protocol 2 had 32 minutes primary antibody incubation and did not require amplification.

Experimental protocol 1	Experimental protocol 2 (Optimised protocol)	Experimental protocol 3
Control tissue- Colon adenocarcinoma	Control tissue- Colon adenocarcinoma	Control tissue- Colon adenocarcinoma
Deparaffinization- 72^{o}C for 4 minutes	Deparaffinization- 72^{o}C for 4 minutes	Deparaffinization- 72^{o}C for 4 minutes
Antigen retrieval- CC1 95-100^{o}C for 32 minutes	Antigen retrieval- CC1 95-100^{o}C for 64 minutes	Antigen retrieval- CC1 95-100^{o}C for 64 minutes
Ab incubation at 37^{o}C for 16 Minutes	Ab incubation at 37^{o}C for 32 minutes	Ab incubation at 37^{o}C for 32 minutes
Amplification- not required	Amplification- not required	Amplification- Ventana amplifier
Detection kit- Ultraview	Detection kit- Ultraview	Detection kit- Ultraview
Counterstain for 8 minutes	Counterstain for 12 minutes	Counterstain for 12 minutes
blueing reagent (4 Minutes)	blueing reagent (4 Minutes)	blueing reagent (4 Minutes)

With regards to the various protocols, Experimental protocol 2 produced the best IHC staining outcome. Staining intensity was optimum with little background staining. Even though Experimental protocol 3 had the highest staining intensity, there was some background staining and the procedure that a longer overall length.

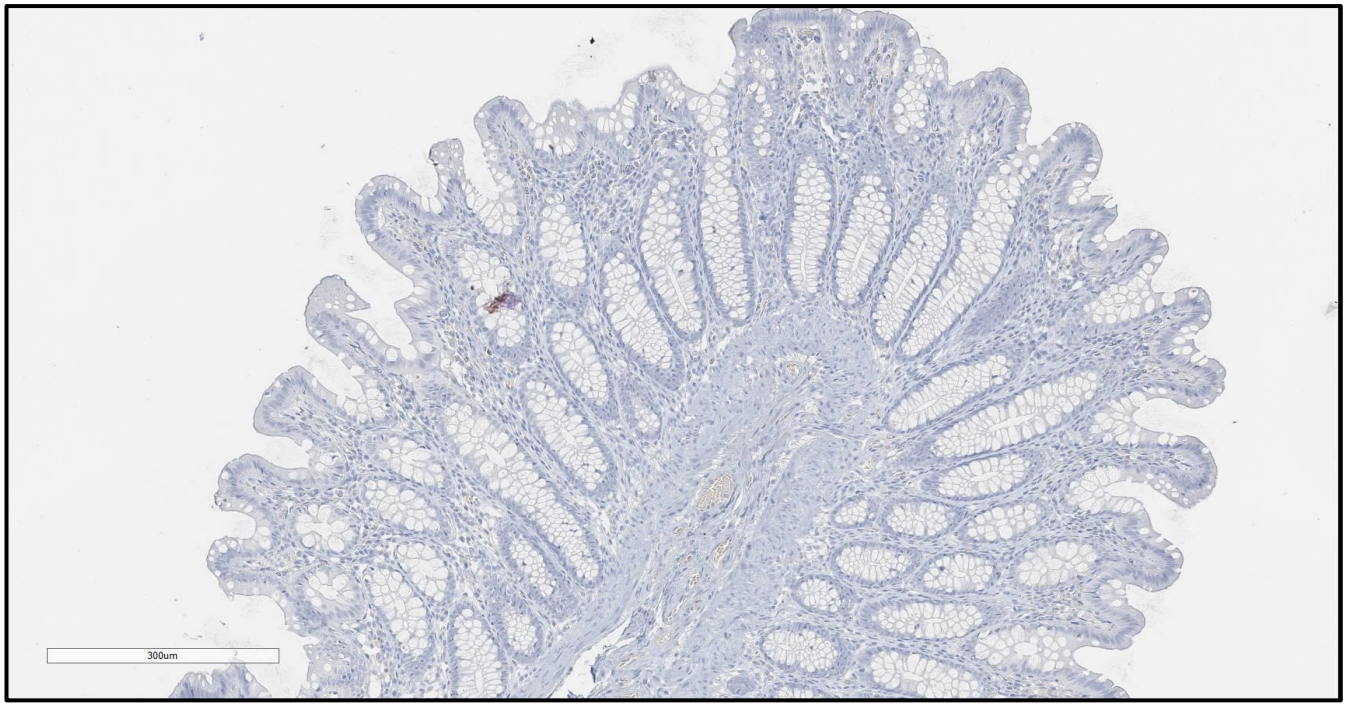

Figure 3. 4 Anti-COX-2 IHC optimisation using negative control.
IHC staining of COX-2 (SP21) rabbit monoclonal primary antibody in FFPE Colon adenocarcinoma tissue. Ventana ultraview DAB detection. No staining in colon tissues. X100 magnification.

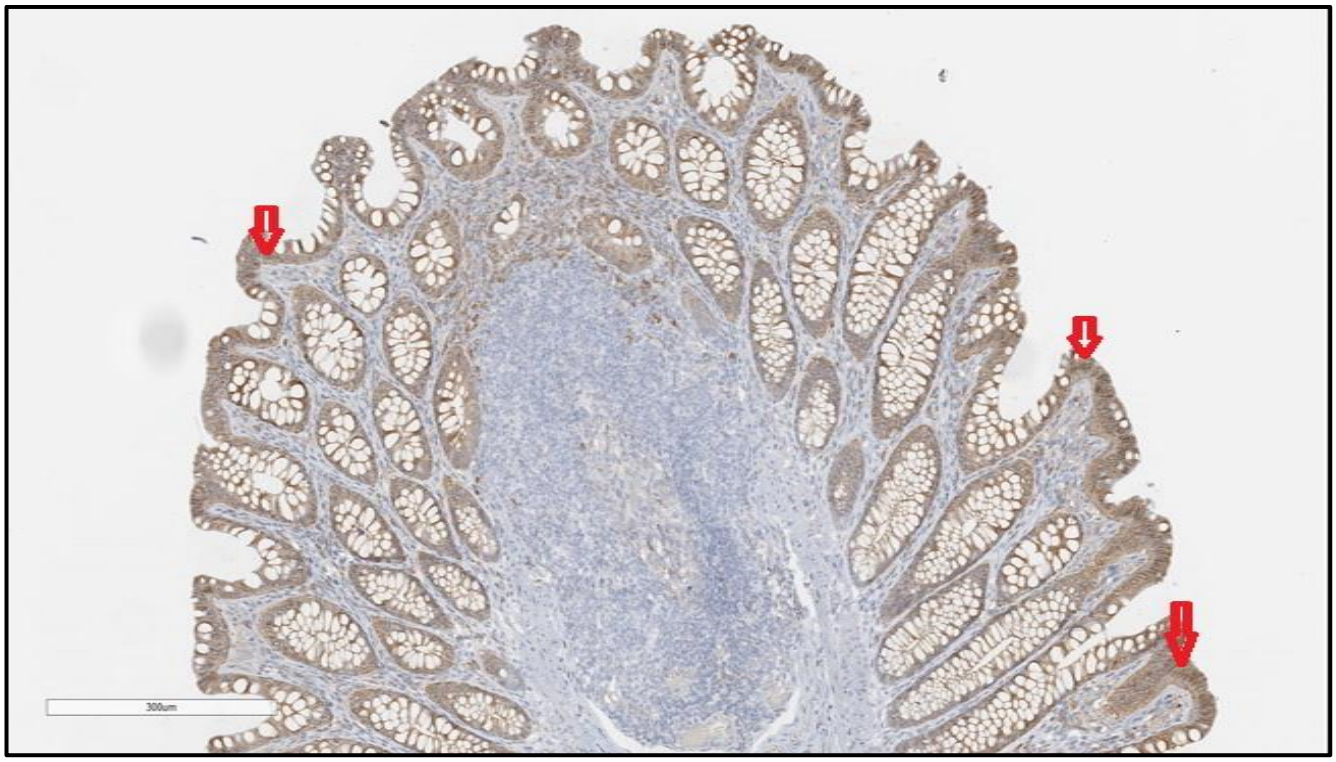

Figure 3. 5 Anti-COX-2 IHC optimisation using Experimental protocol 1.
IHC staining of COX-2 (SP21) rabbit monoclonal primary antibody in FFPE human Colon adenocarcinoma tissue. CC1= 32 Minutes, antibody incubation= 16 Minutes, No amplification, Ventana ultraview DAB detection. Positive cytoplasmic and membranous IHC staining (red arrows) within epithelial cells in colonic crypts. X100 Magnification

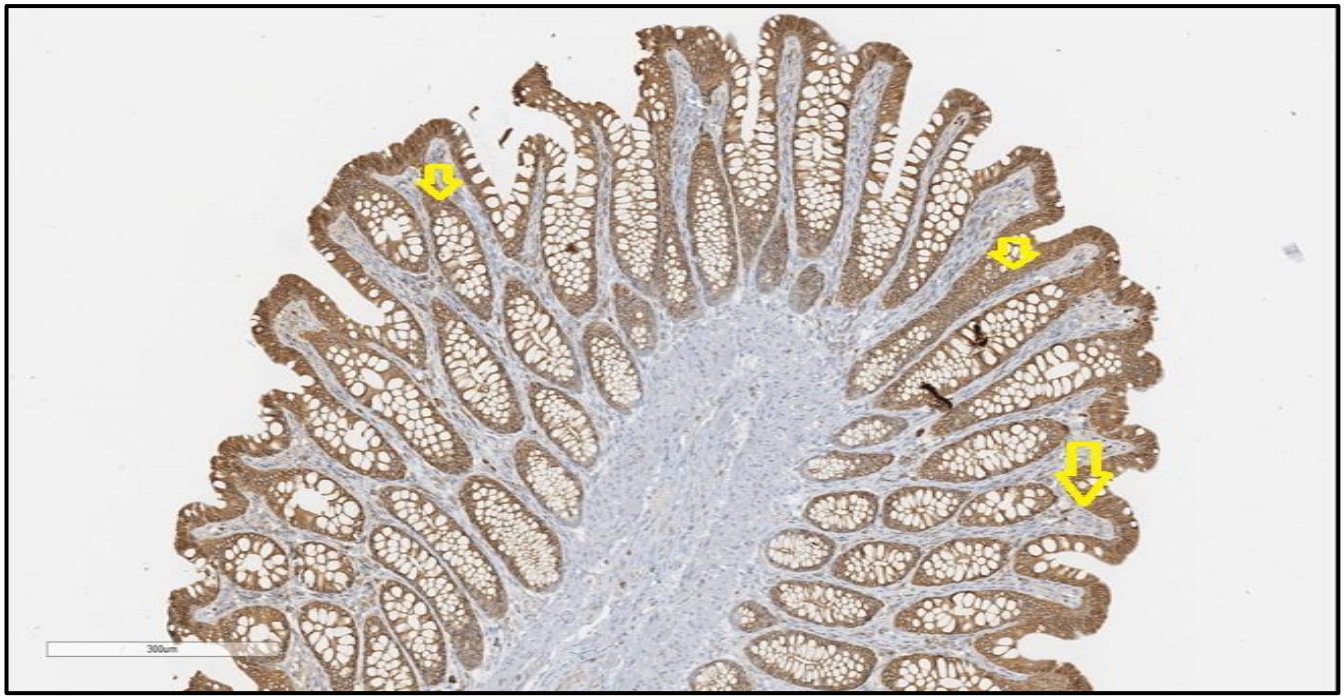

Figure 3. 6 Anti-COX-2 IHC optimisation using Experimental protocol 2 (Optimised protocol)
IHC staining of COX-2 (SP21) rabbit monoclonal primary antibody in FFPE human Colon adenocarcinoma tissue. CC1= 64 Minutes, antibody incubation= 32 Minutes, No amplification, Ventana ultraview DAB detection. Positive cytoplasmic and membranous IHC staining (yellow arrows) within epithelial cells in colonic crypts. note the high colour intensity. X100 Magnification.

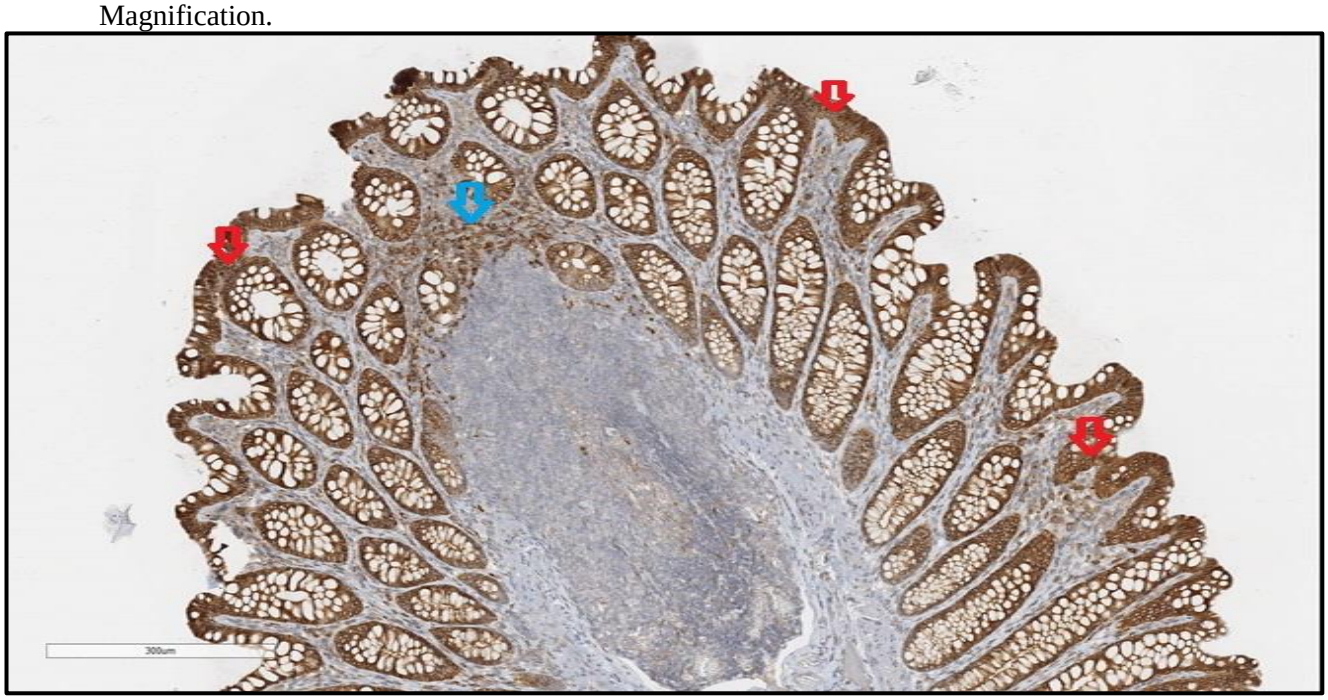

Figure 3. 7 Anti-COX-2 IHC optimisation using Experimental protocol 3
IHC staining of COX-2 (SP21) rabbit monoclonal primary antibody in FFPE human Colon adenocarcinoma tissue. CC1= 64 Minutes, antibody incubation= 32 Minutes, amplification applied, Ventana ultraview DAB detection. Positive cytoplasmic and membranous IHC staining (red arrows) within epithelial cells in colonic crypts. Also note the deeper intensity and background staining (blue arrows). X100 Magnification.

3.1.3 Optimisation of HER-2 antibody immunoreactivity in tissues using IHC

Anti-HER-2/neu (4B5) rabbit monoclonal primary antibody (Ventana medical systems) was optimised for IHC using breast sample tissues from Ysbyty Glan Clwyd. Sections were cut as previously described (sections 2.5.5). Sectioned tissue slides were placed in an incubator (set to 60^{o}C) for 30-60 minutes and then transferred to the ventana benchmark ULTRA (automated IHC/ISH slide staining system) for IHC.

Slides were deparaffinised at 72^{o}C for 4 minutes using EZ prep solution (Section 2.4.3). Antigen retrieval was performed using the heat induced epitope retrieval method by exposing the slides to cell conditioning 1 (mild CC1) at 95-100^{o}C for 8 minutes. CC1 is a tri-based EDTA buffer with a pH of 7.8 (Section 2.4.1).

Anti HER-2 antibodies, (purchased pre-diluted from Ventana medical systems) was applied to slides and incubated for 20 minutes at 37^{o}C. To prevent background staining, endogenous proteins and peroxides were blocked using Ventana diluent/option 1. Staining was enhanced by adding a post-antibody incubation amplification step using Ventana amplifier.

After series of washes, slides were incubated in hydrogen peroxidase, universal HRP multimer (which contains labelled secondary antibodies) and universal DAB chromogen for colour development. Slides were then counterstained in haematoxylin 1 for 12 minutes before applying a blueing reagent for 4 minutes.

Starting with the product insert (contains initial recommended protocol), we varied various stages of the staining process such as incubation time, heat, counterstain, amplification and blocking. Each summary has been provided (Table 3.3). Subsequently, a representative picture of each protocol has also been provided (figure 3.8- 3.11)

With regards to the various protocols, Experimental protocol 2 produced the best IHC staining outcome. Staining intensity was optimum with little background staining.

Table 3. 3 IHC Experimental protocols for Anti HER-2/neu (4B5) rabbit monoclonal primary antibody.

Experimental protocol 1	Experimental protocol 2 (Optimised protocol)	Experimental protocol 3
Control tissue- Breast carcinoma	Control tissue- Breast carcinoma	Control tissue- Breast carcinoma
Deparaffinization- 72ºC for 4 minutes	Deparaffinization- 72ºC for 4 minutes	Deparaffinization- 72ºC for 4 minutes
Antigen retrieval- CC1 95-100ºC for 32 minutes	Antigen retrieval- CC1 95-100ºC for 4 minutes	Antigen retrieval- CC1 95-100ºC for 64 minutes
Blocking- Not added	Block-Ultra block with Ventana diluent	Block-Ultra block with Ventana diluent
Ab incubation at 37ºC for 16 Minutes	Ab incubation at 37ºC for 20 minutes	Ab incubation at 37ºC for 32 minutes
Amplification- not required	Amplification- Ventana amplifier	Amplification- not required
Detection kit- Ultraview	Detection kit- Ultraview	Detection kit- Ultraview
Counterstain for 8 minutes	Counterstain for 12 minutes	Counterstain for 12 minutes
blueing reagent (4 Minutes)	blueing reagent (4 Minutes)	blueing reagent (4 Minutes)

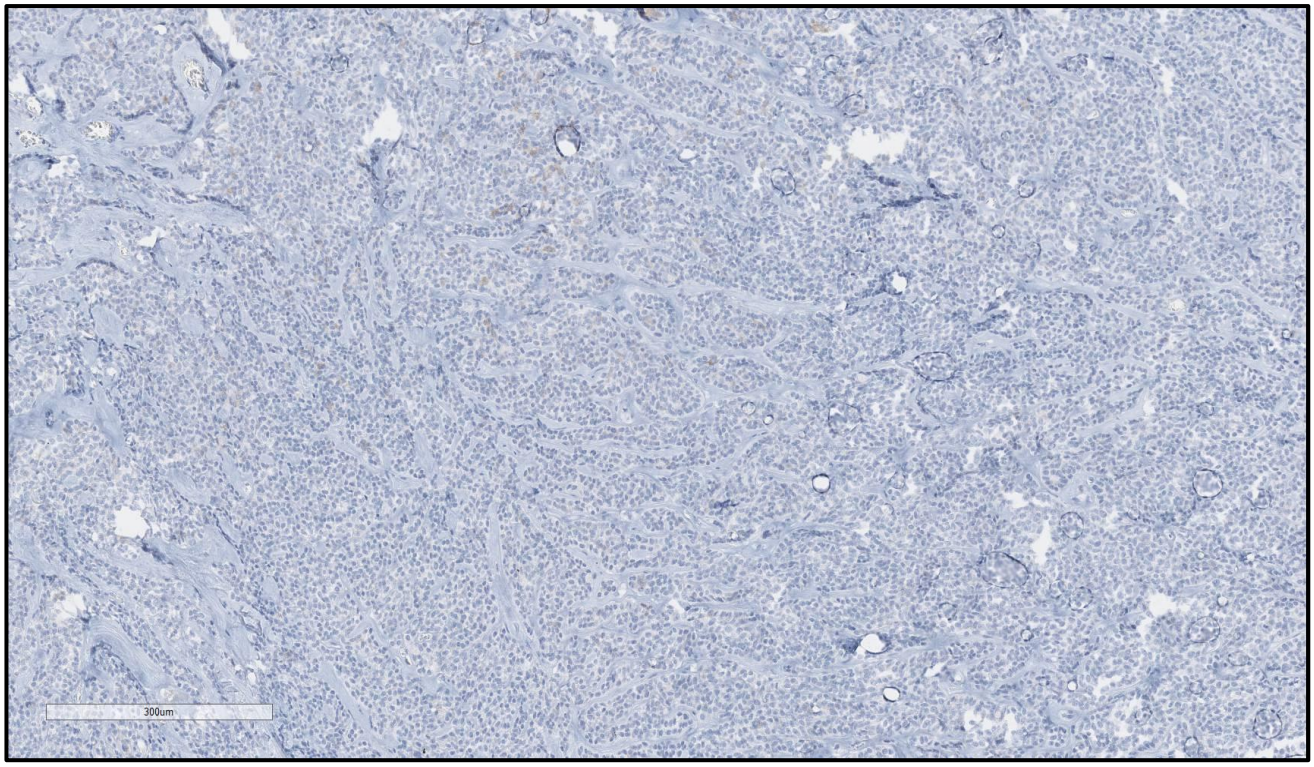

Figure 3. 8 Anti-HER-2/neu IHC optimisation using negative control
IHC staining of anti-HER-2 (4B5) rabbit monoclonal primary antibody in FFPE human breast carcinoma tissue. Ventana ultraview DAB detection. Negative staining in breast carcinoma X100.

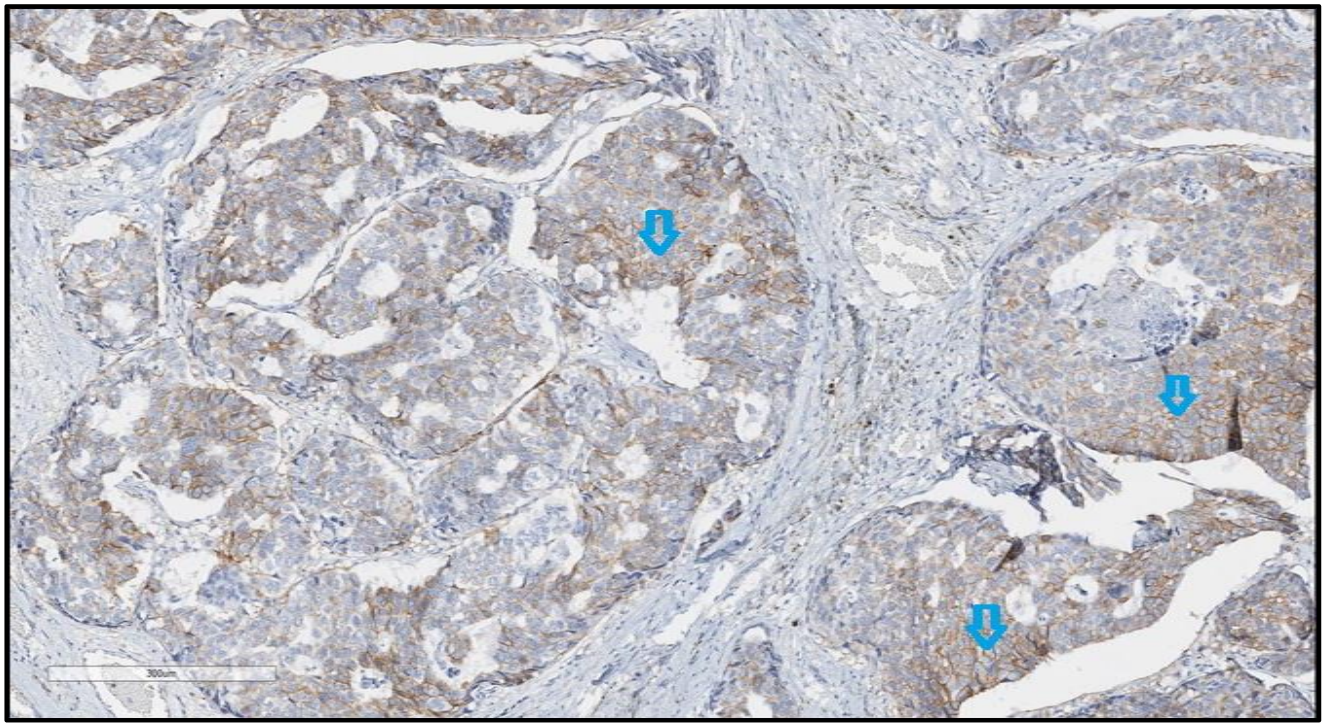

Figure 3. 9 Anti-HER-2/neu IHC optimisation using Experimental protocol 1
IHC staining of anti-HER-2 (4B5) rabbit monoclonal primary antibody in FFPE human breast carcinoma tissue. CC1= 32 Minutes, Ab incubation= 16 Minutes, No amplification, Ventana ultraview DAB detection. Weak membranous staining (Arrows) in breast carcinoma tissues. X100 magnification.

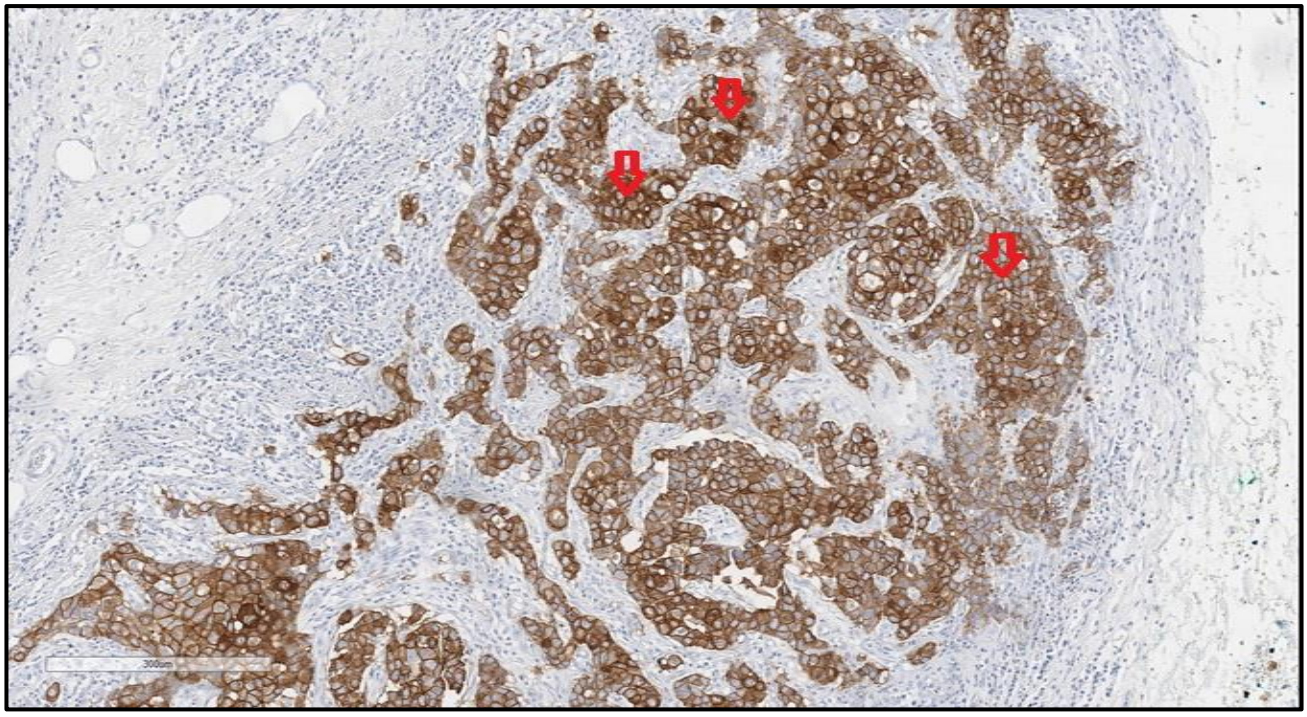

Figure 3. 10 Anti-HER-2/neu IHC optimisation using Experimental protocol 2 (Optimised protocol)
IHC staining of anti-HER-2 (4B5) rabbit monoclonal primary antibody in FFPE human breast carcinoma tissue. CC1= 32 Minutes, blocking, Ab incubation= 20 Minutes, Amplification added, Ventana ultraview DAB detection. Optimum membranous staining (arrows) in breast carcinoma tissues. X100 magnification.

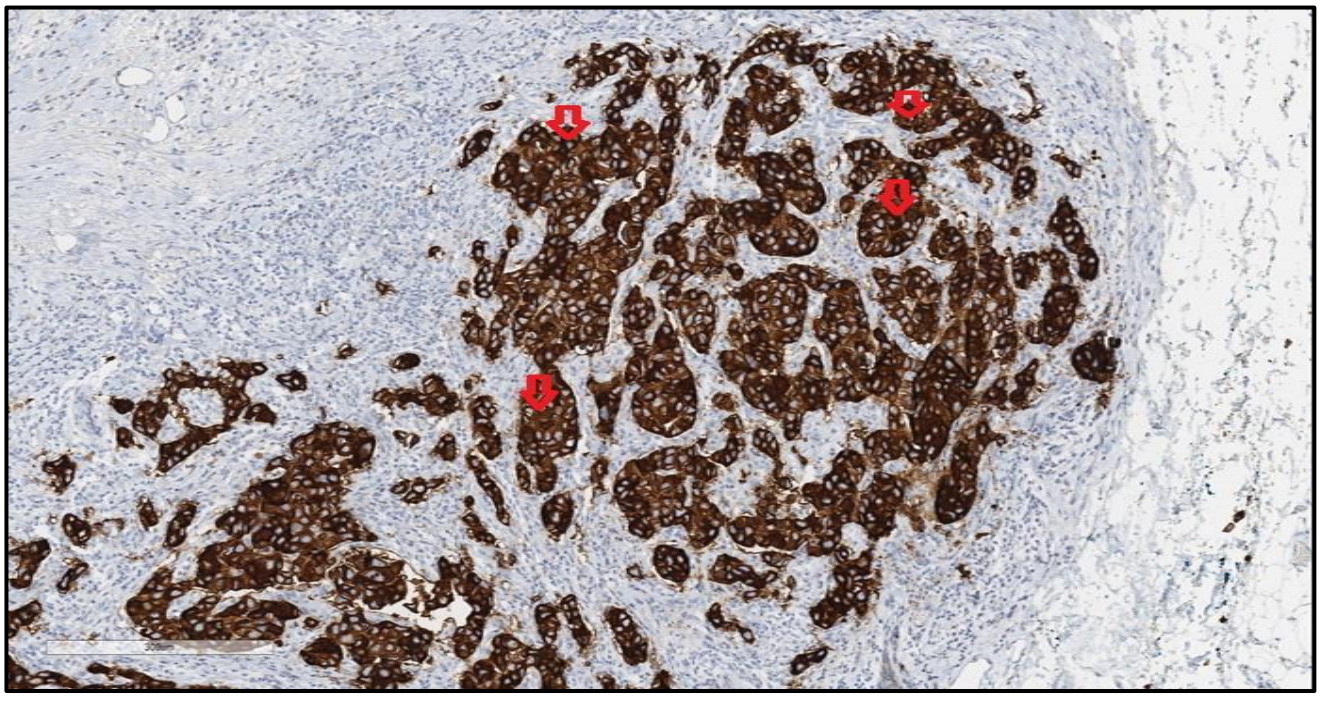

Figure 3. 11 Anti-HER-2/neu IHC optimisation using Experimental protocol 3
IHC staining of anti-HER-2 (4B5) rabbit monoclonal primary antibody in FFPE human breast carcinoma tissue. CC1= 64 Minutes, blocking, Ab incubation= 32 Minutes, No amplification, Ventana ultraview DAB detection. Strong membranous staining (arrows) in breast carcinoma tissues. X100 magnification

3.1.4 Optimisation of SOX-2 antibody immunoreactivity in tissues using IHC

Anti-SOX-2 (SP76) rabbit monoclonal primary antibody (Cell marque, UK) was optimised for IHC using human fallopian tube tissue samples from Ysbyty Glan Clwyd. Sections were cut as previously described (sections 2.5.5). Sectioned tissue slides were placed in an incubator (set to 60^{o}C) for 30-60 minutes and then transferred to the Ventana Benchmark ULTRA (Automated IHC/ISH slide staining system) for IHC.

Slides were deparaffinised at 72^{o}C for 4 minutes using EZ prep solution (Section 2.4.3). Antigen retrieval was performed using the heat induced epitope retrieval method by exposing the slides to cell conditioning 1 (standard CC1) at 95-100^{o}C for 72 minutes. CC1 is a tri-based EDTA buffer with a pH of 7.8 (Section 2.4.1).

Anti-SOX2 primary monoclonal antibodies, (Cell marque, UK) was applied to slides and incubated for 32 minutes at 37^{o}C. To prevent background staining, endogenous proteins and peroxides were blocked using Ventana diluent/option 1.

After series of washes, slides were incubated in universal HRP multimer (which contains labelled secondary antibodies) and universal DAB chromogen for colour development. Slides were then counterstained in haematoxylin 1 for 12 minutes before applying a blueing reagent for 4 minutes.

Starting with the product insert (contains initial recommended protocol), we varied various stages of the staining process such as incubation time, heat, counterstain, amplification and blocking. Each summary has been provided (Table 3.4). Subsequently, a representative picture of each protocol has also been provided (figures 3.12-3.14)

Table 3. 4 IHC Experimental protocols for Anti-SOX2 (SP76) rabbit monoclonal primary antibody.
Optimum staining was achieved by increasing antigen retrieval time, length of primary antibody incubation and adding a blocking and amplification step.

Experimental protocol 1 (product insert)	Experimental protocol 2 (Optimised protocol)
Control tissue- Fallopian tube	Control tissue- Fallopian tube
Detection kit- Ultraview	Detection kit- Ultraview
Deparaffinization- 72ºC for 4 minutes	Deparaffinization- 72ºC for 4 minutes
Antigen retrieval- CC1 95-100ºC for 32 minutes	Antigen retrieval- CC1 95-100ºC for 76 minutes
Ab incubation at 37ºC for 16 minutes	Ab incubation at 37ºC for 32 minutes
Blocking- Not required	Block-Ultra block with Ventana diluent
Amplification- not required	Amplification- Ventana amplifier
Counterstain (8 minutes)	Counterstain (12 minutes)
blueing reagent (4 minutes)	blueing reagent (4 minutes)

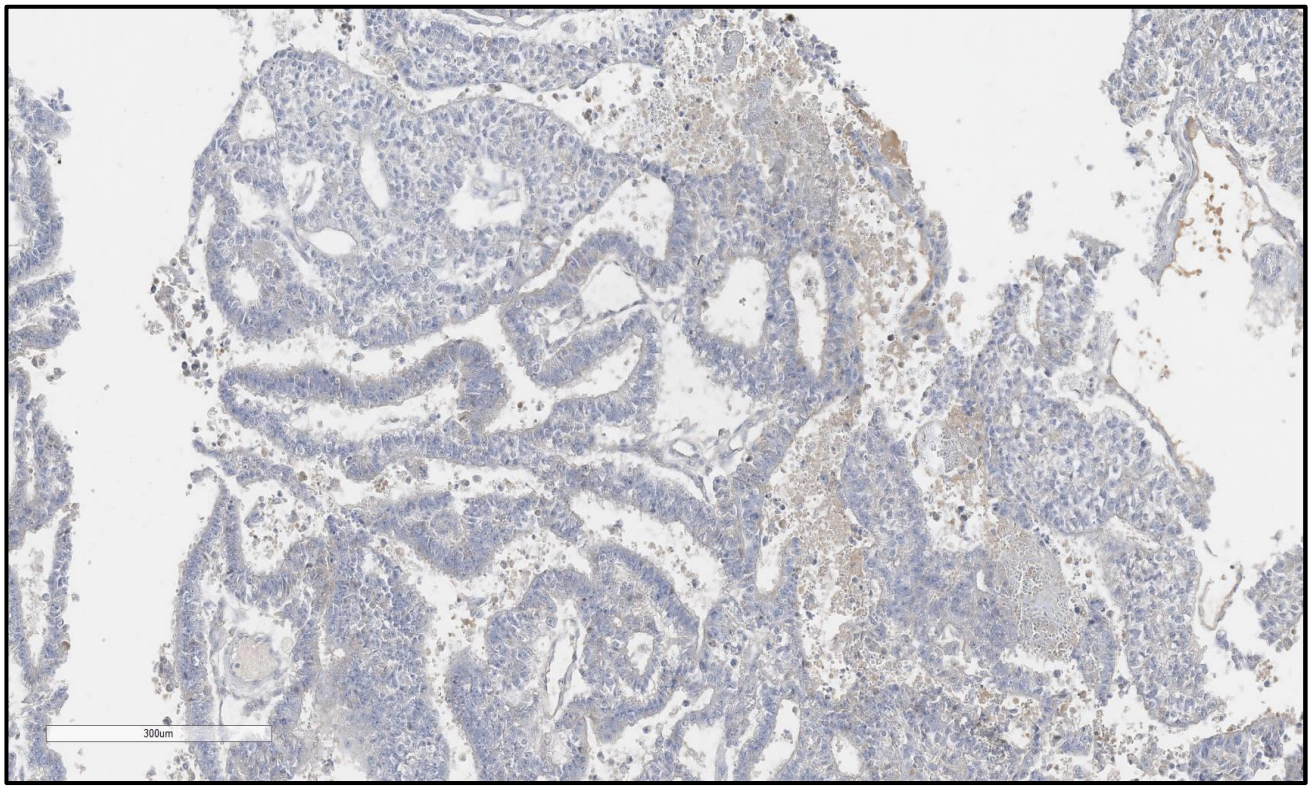

Figure 3. 12 Anti-SOX-2 IHC optimisation using negative control
IHC staining of anti-SOX-2 monoclonal primary antibody in FFPE human fallopian tube tissue. Ventana ultraview DAB detection. No staining X100.

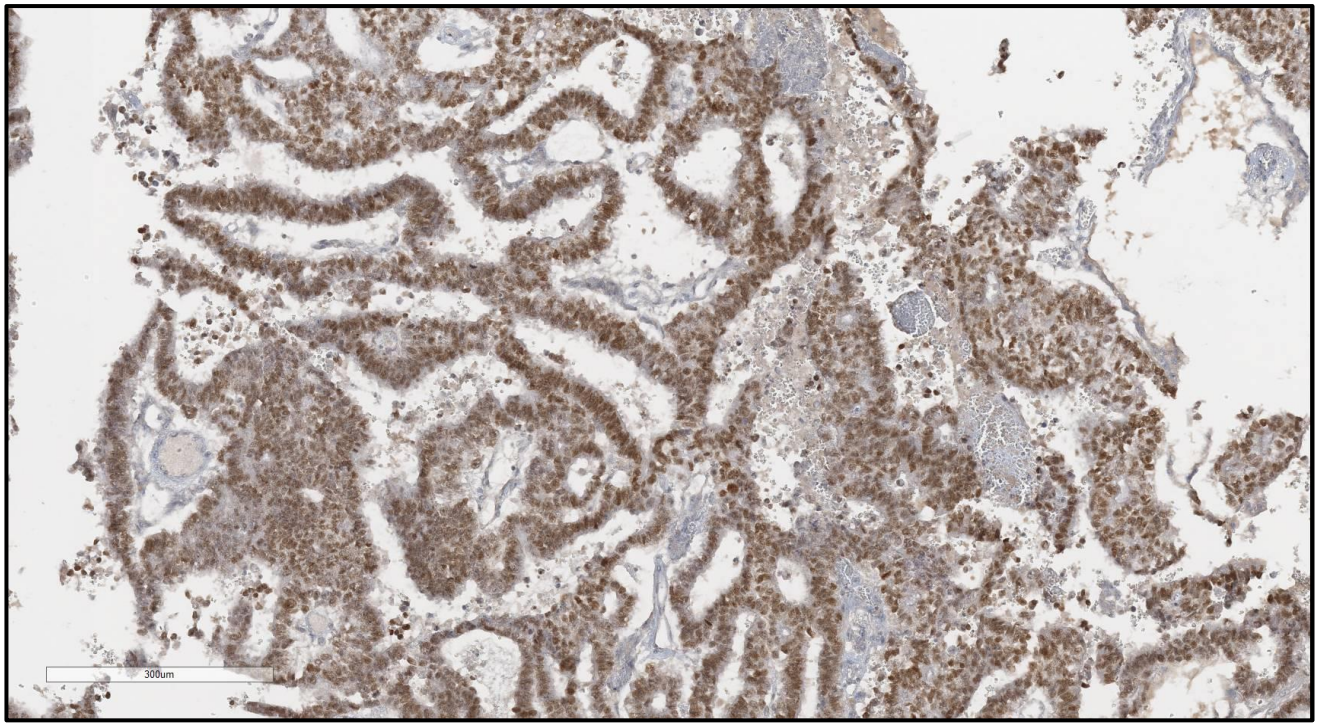

Figure 3. 13 Anti-SOX-2 IHC optimisation using Experimental protocol 1 (Package insert)
IHC staining of anti-SOX-2 (SP76) rabbit monoclonal primary antibody in FFPE human fallopian tube tissue. CC1= 32 Minutes, blocking, Ab incubation= 16 Minutes, No amplification, Ventana ultraview DAB detection. Nuclear and cytoplasmic staining (brown) in fallopian tissues. X100 magnification

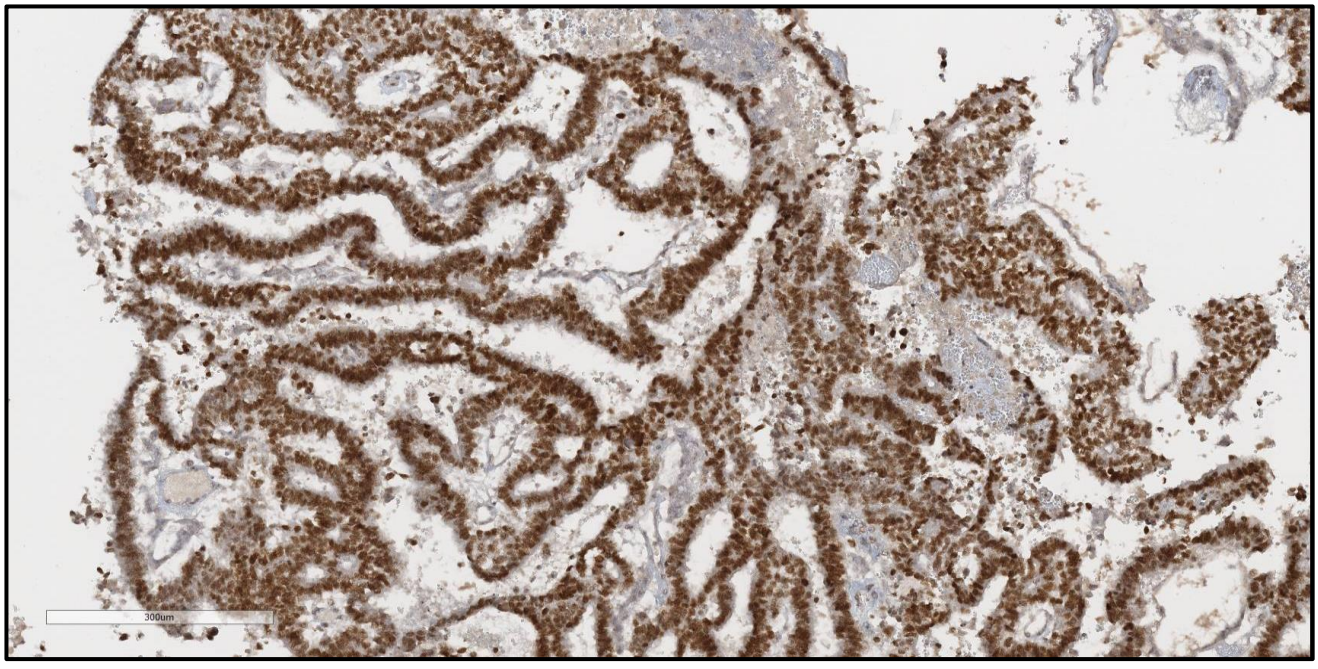

Figure 3. 14 Anti-SOX-2 IHC optimisation using Experimental protocol 2 (Optimised protocol)
IHC staining of anti-SOX-2 (SP76) rabbit monoclonal primary antibody in FFPE human fallopian tube tissue. CC1= 76 Minutes, blocking, Ab incubation= 32 Minutes, amplification added, Ventana ultraview DAB detection. Nuclear and cytoplasmic staining (brown) in fallopian tissues. Reduced background staining. X100 magnification.

3.1.5 Optimisation of VEGFR-3 antibody immunoreactivity in tissues using IHC

Mouse anti-human VEGFR-3 monoclonal primary antibody (R &D systems, UK) was optimised for IHC using umbilical cord tissue samples from Ysbyty Glan Clwyd. Sections were cut as previously described (sections 2.5.5). Sectioned tissue slides were placed in an incubator (set to 60^{o}C) for 30-60 minutes and then transferred to the Ventana Benchmark ULTRA (Automated IHC/ISH slide staining system) for IHC.

Slides were deparaffinised at 72^{o}C for 4 minutes using EZ prep solution (Section 2.4.3). Antigen retrieval was performed using the heat induced epitope retrieval method by exposing the slides to cell conditioning 1 (mild CC1) at 95-100^{o}C for 52 minutes. CC1 is a tri-based EDTA buffer with a pH of 7.8 (Section 2.4.1).

Anti-VEGFR-3 mouse monoclonal primary antibody (R & D medical systems, UK) was applied to slides (1:50 initial dilution) and incubated for 16 minutes at 37^{o}C. To prevent background staining, endogenous proteins and peroxides were blocked using Ventana diluent/option 1.

After series of washes, slides were incubated in universal HRP multimer (which contains labelled secondary antibodies) and universal DAB chromogen for colour development. Slides were then counterstained in haematoxylin 1 for 12 minutes before applying a blueing reagent for 4 minutes.

Starting with the product insert (contains initial recommended protocol), we varied various stages of the staining process such as incubation time, heat, counterstain, amplification and blocking. Each summary has been provided (Table 3.5). Subsequently, a representative picture of each protocol has also been provided (Figure 3.15-3.19)

Table 3. 5 IHC Experimental protocols for anti-VEGFR-3 primary antibody

Experimental protocol 1	Experimental protocol 2	Experimental protocol 3	Experimental protocol 4 (optimised protocol)
Control tissue- Umbilical cord	Control tissue- Umbilical cord	Control tissue- Umbilical cord	Control tissue- Umbilical cord
Deparaffinization- 72^{o}C	Deparaffinization- 72^{o}C	Deparaffinization- 72^{o}C	Deparaffinization- 72^{o}C
CC1 at 100^{o}C for 32 Minutes	CC1 at 100^{o}C for 32 Minutes	CC1 at 100^{o}C for 52 Minutes	CC1 at 100^{o}C for 52 Minutes
Blocking- not included	Blocking- not included	Blocking- Ventana diluent	Blocking- Ventana diluent
Ab incubation at 37^{o}C for 16 Minutes (1:50 dilution)	Ab incubation at 37^{o}C for 16 Minutes (1:100 dilution)	Ab incubation at 37^{o}C for 4 Minutes (1:100 dilution)	Ab incubation at 37^{o}C for 16Minutes (1:200 dilution)
No ultrawash	Ultrawash	Optiview HRP multimer-8Minutes	Ultrawash
Detection kit- Ultraview	Detection kit- Ultraview	Detection kit- optiview	Detection kit- Ultraview
Counterstain (12 Minutes)	Counterstain (12 Minutes)	Counterstain (12 Minutes)	Counterstain (12 Minutes)
blueing reagent (4 Minutes)	blueing reagent (4 Minutes)	blueing reagent (4 Minutes)	blueing reagent (4 Minutes)

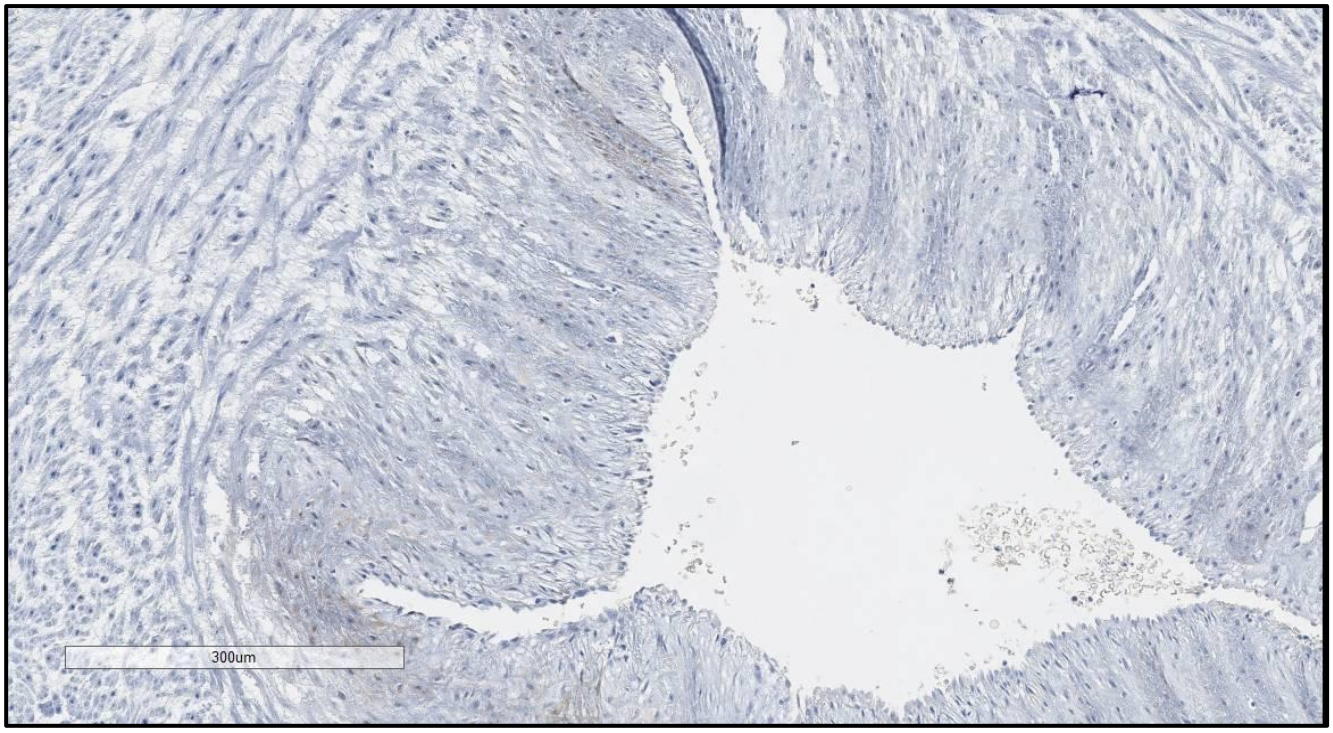

Figure 3. 15 Anti-VEGFR-3 IHC optimisation using negative control
IHC staining of anti-VEGFR-3 mouse monoclonal primary antibody in FFPE human umbilical cord tissues. Ventana ultraview DAB detection. No staining in nuclei of endothelial cells within umbilical cord tissues X100.

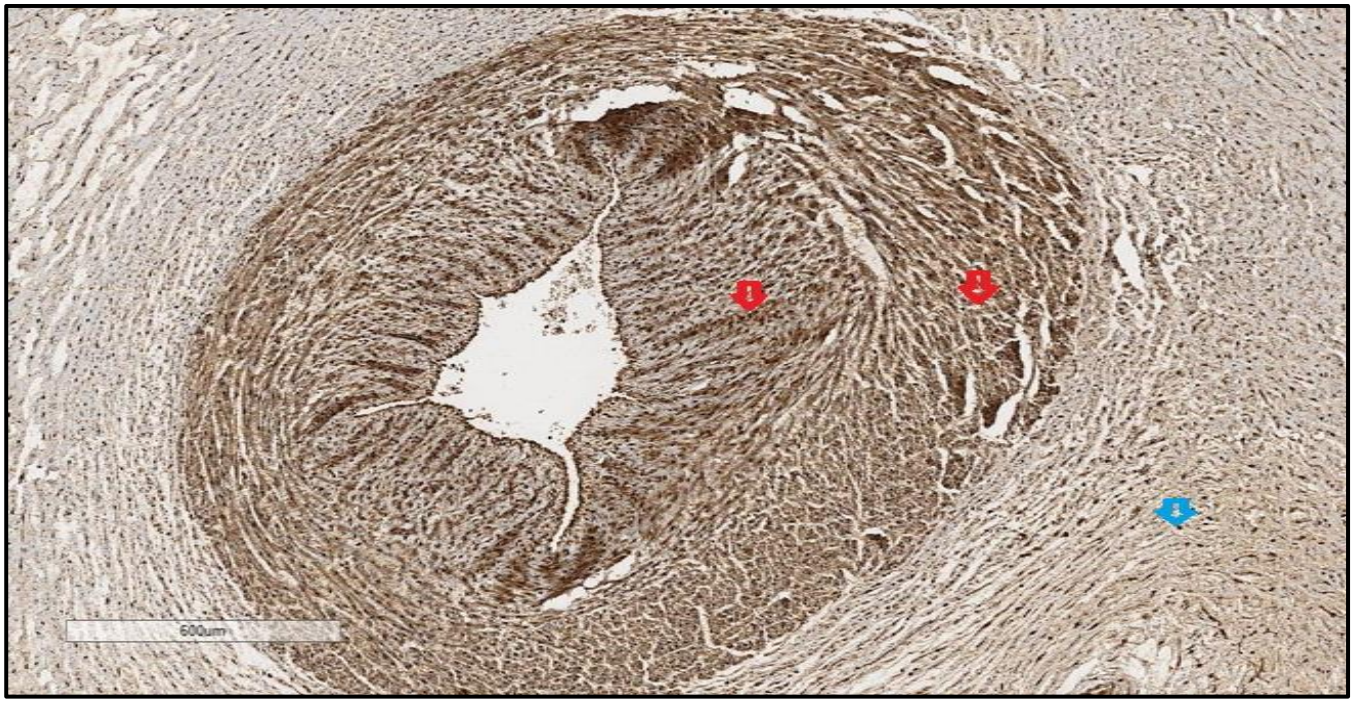

Figure 3. 16 Anti-VEGFR-3 IHC optimisation using Experimental protocol 1
IHC staining of VEGFR-3 mouse monoclonal primary antibody in FFPE human umbilical cord samples. Antibody incubation= 16 Minutes, 1:50 dilution. Ventana ultraview DAB detection. Positive nuclear and cytoplasmic staining in endothelial cells (Red arrows). Note the nonspecific staining (blue arrows) within underlying stroma and muscle cell. X100 magnification.

Figure 3. 17 Anti-VEGFR-3 IHC optimisation using experimental protocol 2
IHC staining of anti-VEGFR-3 mouse monoclonal primary antibody in FFPE human umbilical cord samples. Antibody incubation= 16 Minutes, 1:100 dilution, Ultrawash, Ventana ultraview DAB detection. Positive nuclear and cytoplasmic staining in endothelial cells (red arrows). Note the nonspecific staining (blue arrow) within underlying stroma and muscle cell. Nonspecific staining is reduced compared with Experimental protocol 1. X100 magnification.

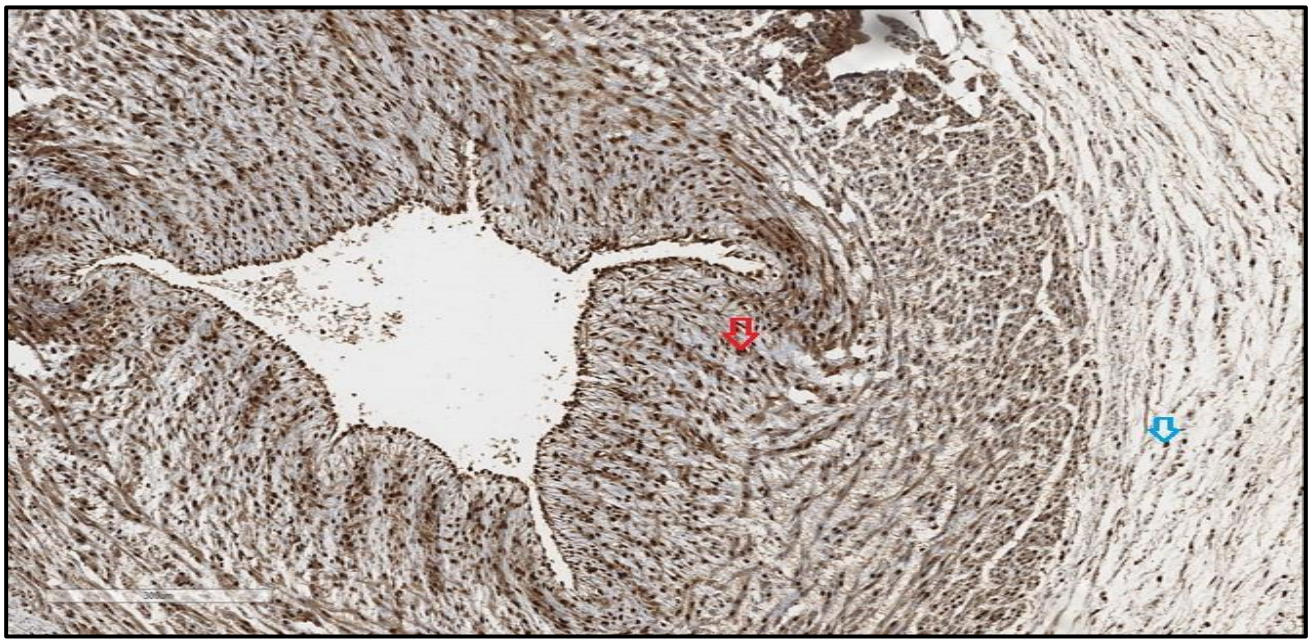

Figure 3. 18 Anti-VEGFR-3 IHC optimisation using experimental protocol 3
IHC staining of VEGFR-3 mouse monoclonal primary antibody in FFPE human umbilical cord samples. Antibody incubation= 4 Minutes, 1:100 dilution, Ultrawash, Ventana optiview DAB detection. Positive nuclear and cytoplasmic staining in endothelial cells (red arrow). Note the nonspecific staining (Blue arrow) within underlying stroma and muscle cell. Results from Experimental protocol 3 not significantly different from Experimental protocol 2. Nonspecific staining present in both protocols.

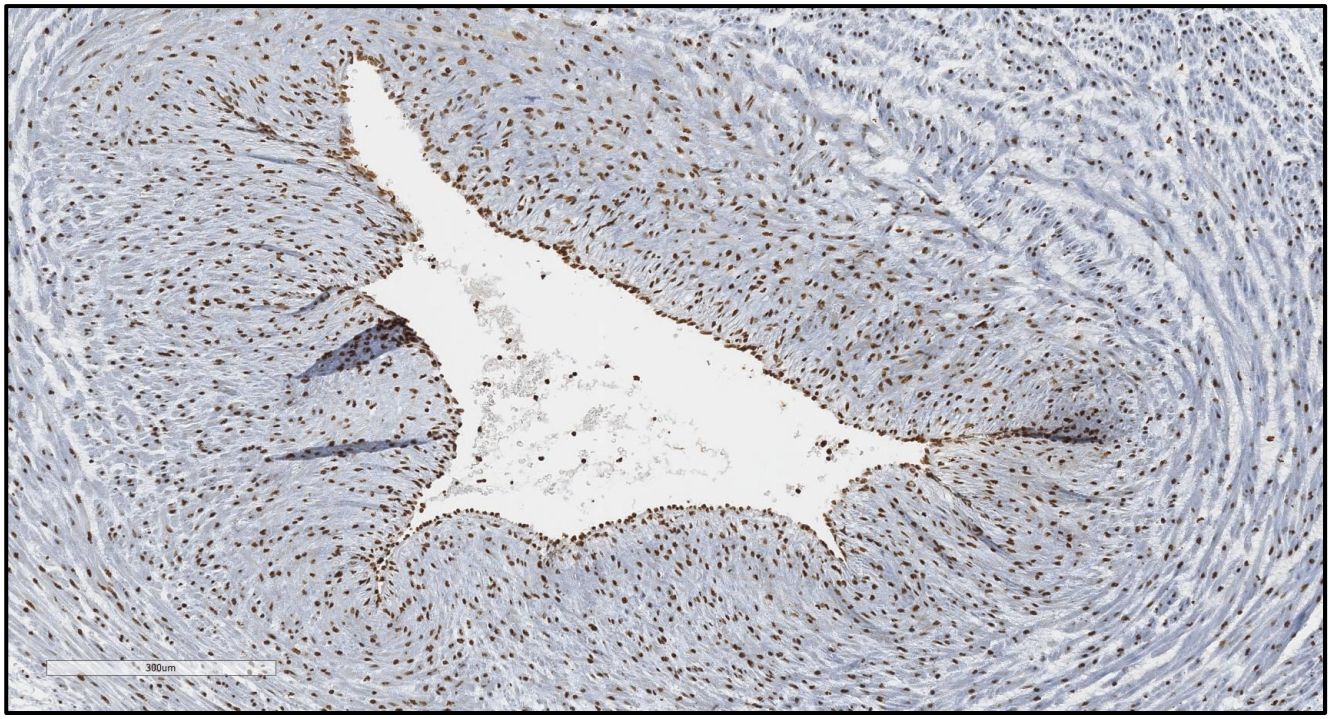

Figure 3. 19 Anti-VEGFR-3 IHC optimisation using Experimental protocol 4 (Optimised protocol)
IHC staining of VEGFR-3 mouse monoclonal primary antibody in FFPE human umbilical cord samples. Antibody incubation= 16 Minutes, 1:200 dilution, Ultrawash, Ventana ultraview DAB detection, post-staining amplification. Positive nuclear staining in endothelial cells (brown). Note the significantly reduced nonspecific staining within underlying stroma and muscle cell.

3.1.6 Optimisation of CEACAM-1 antibody immunoreactivity in tissues using IHC

Anti-CEACAM-1 mouse polyclonal primary antibody (R &D systems, UK) was optimised for IHC using colon carcinoma tissue samples from Ysbyty Glan Clwyd. Sections were cut as previously described (sections 2.5.5). Sectioned tissue slides were placed in an incubator (set to 60^{o}C) for 30-60 minutes and then transferred to the Ventana Benchmark ULTRA (Automated IHC/ISH slide staining system) for IHC.

Slides were deparaffinised at 72^{o}C for 4 minutes using EZ prep solution (Section 2.4.3). Antigen retrieval was performed using the heat induced epitope retrieval method by exposing the slides to cell conditioning 1 (mild CC1) at 95-100^{o}C for 36 minutes. CC1 is a tri-based EDTA buffer with a pH of 7.8 (Section 2.4.1).

Anti-CEACAM-1 mouse polyclonal primary antibody (R & D medical systems, UK) was applied to slides (1:20 initial dilution, optimum dilution was 1:200) and incubated for 28 minutes at 37^{o}C. To prevent background staining, endogenous proteins and peroxides were blocked using Ventana diluent/option 1. A post-staining amplification step was included in the Optimised protocol.

After series of washes, slides were incubated in universal HRP multimer (which contains labelled secondary antibodies) and universal DAB chromogen for colour development. Slides were then counterstained in haematoxylin 1 for 12 minutes before applying a blueing reagent for 4 minutes.

Starting with the product insert (contains initial recommended protocol), we varied various stages of the staining process such as incubation time, heat, counterstain, amplification and blocking. Each summary has been provided (Table 3.6). Subsequently, a representative picture of each protocol has also been provided (figures 3.20-3.23).

Table 3. 6 IHC Experimental protocols for anti-CEACAM-1 primary antibody

Experimental protocol 1	Experimental protocol 2 (optimised protocol)	Experimental protocol 3
Control tissue- Colon	Control tissue- Colon	Control tissue- Colon
Deparaffinization- 72ºC	Deparaffinization- 72ºC	Deparaffinization- 72ºC
CC1 at 100ºC for 36 Minutes	CC1 at 100ºC for 36 Minutes	CC1 at 100ºC for 36 Minutes
Blocking- Not added	Blocking- Option 1	Blocking- Option 1
Anti CEACAM-1 Ab at 37ºC for 8 Minutes (1:50 dilution)	Anti CEACAM-1 Ab at 37ºC for 8 Minutes (1:100 dilution)	Anti CEACAM-1 Ab at 37ºC for 28 Minutes (1:200 dilution
	amplify	Amplify
Detection kit- Ultraview	Detection kit- Optiview	Detection kit- Ultraview
Counterstain (12 Minutes)	Counterstain (12 Minutes)	Counterstain (12 Minutes)
blueing reagent (4 Minutes)	blueing reagent (4 Minutes)	blueing reagent (4 Minutes)

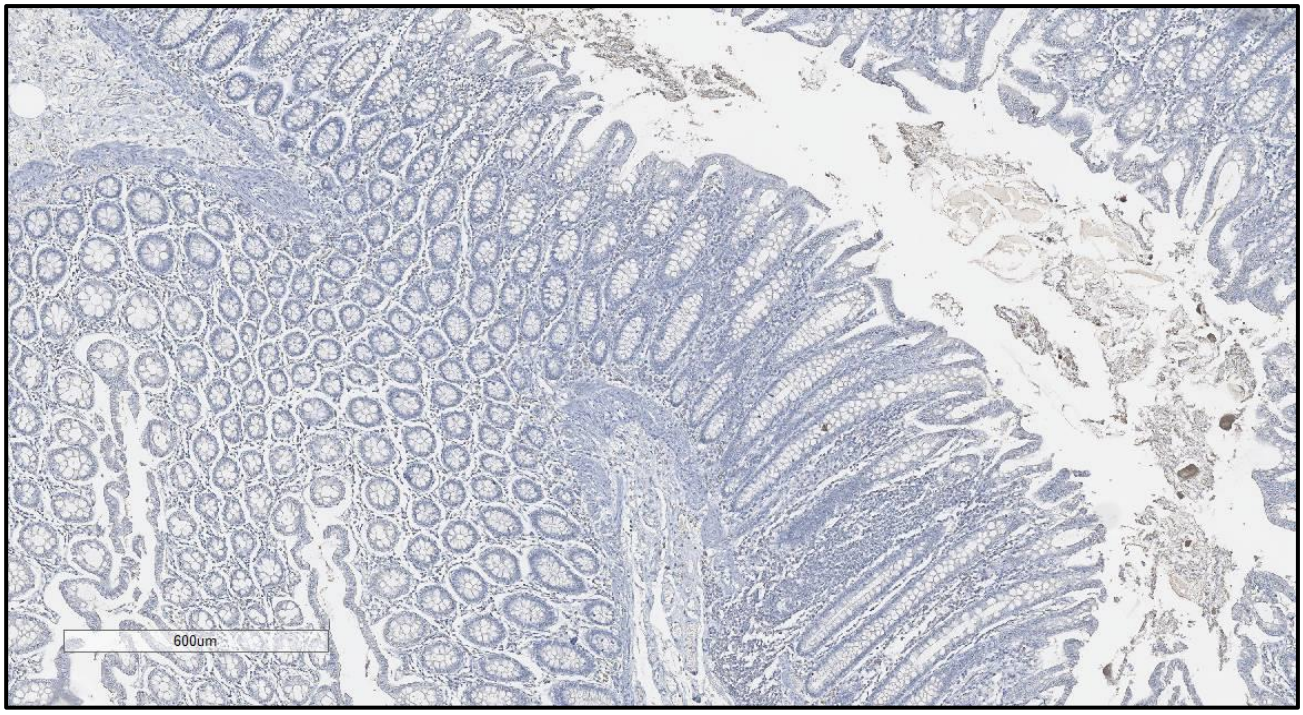

Figure 3. 20 Anti-CEACAM-1 IHC optimisation using negative control
IHC staining of anti-CEACAM-1 mouse polyclonal primary antibody in FFPE human umbilical cord tissues. Ventana ultraview DAB detection. No staining in nuclei of endothelial cells within umbilical cord tissues. X100 magnification.

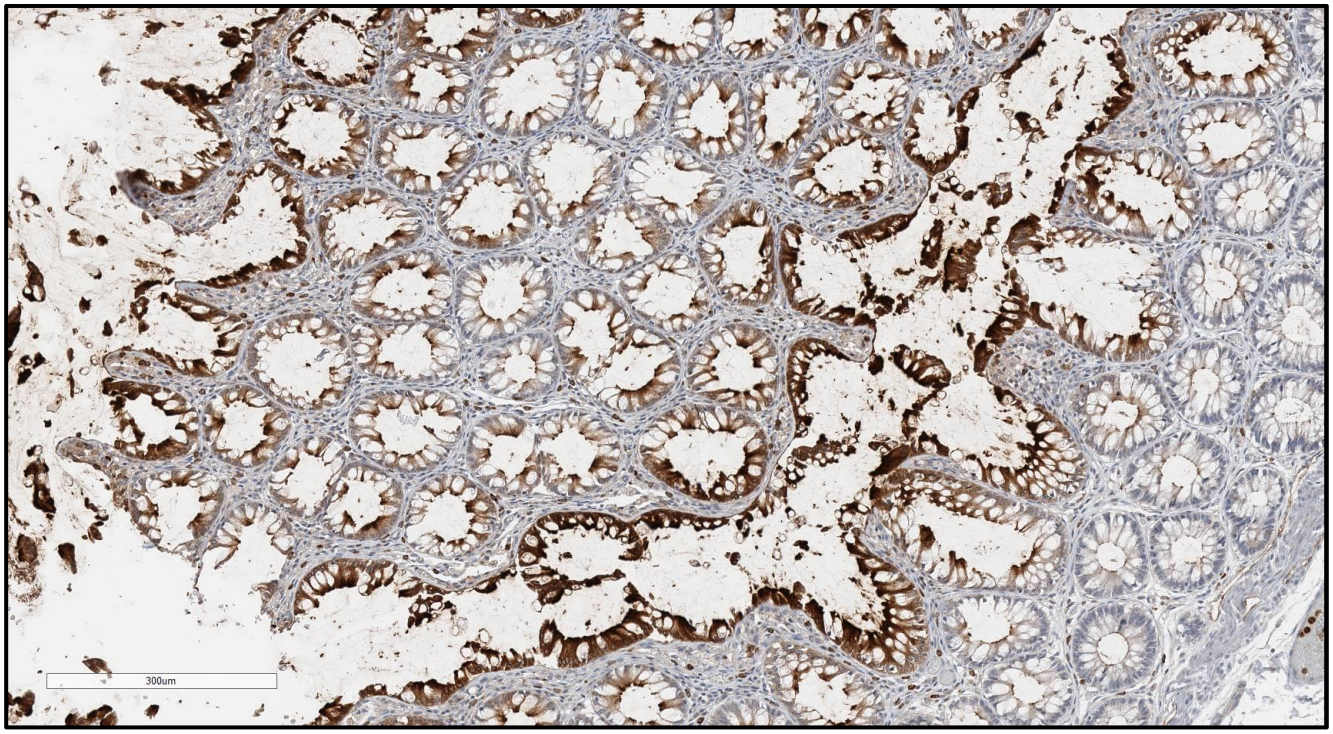

Figure 3. 21 Anti-CEACAM-1 IHC optimisation using experimental protocol 1
IHC staining of CEACAM-1 mouse polyclonal primary antibody in FFPE human colon carcinoma samples. Antibody incubation= 8 Minutes, 1:50 dilution. Ventana ultraview DAB detection. Positive membranous and cytoplasmic staining in colon epithelial cells (brown). X100 magnification.

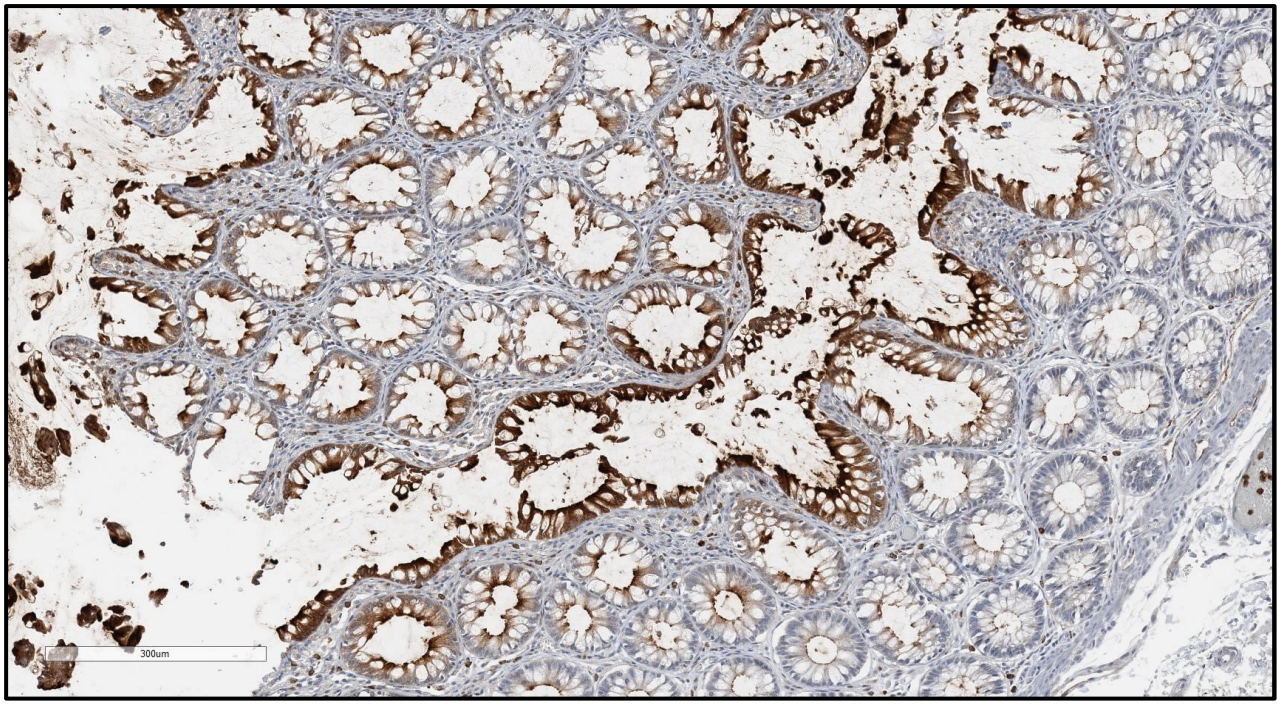

Figure 3. 22 Anti-CEACAM-1 IHC optimisation using experimental protocol 2 (optimised protocol)
IHC staining of CEACAM-1 mouse polyclonal primary antibody in FFPE human colon carcinoma samples. Antibody incubation= 8 Minutes, 1:100 dilution. Ventana ultraview DAB detection. Positive membranous and cytoplasmic staining in colon epithelial cells (brown). X100 magnification.

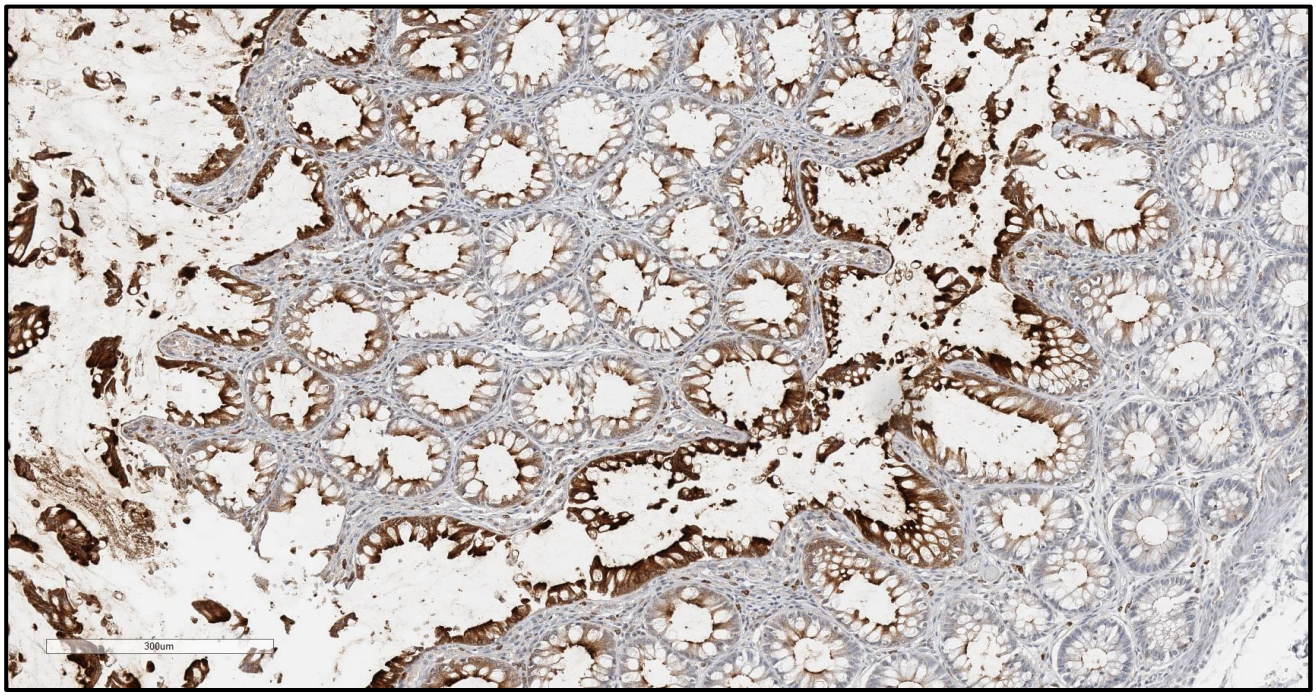

Figure 3. 23 Anti-CEACAM-1 IHC optimisation employing experimental protocol 3
IHC staining of CEACAM-1 mouse polyclonal primary antibody in FFPE human colon carcinoma samples. Antibody incubation= 23 Minutes, 1:200 dilution. Ventana ultraview DAB detection. Positive membranous and cytoplasmic staining in colon epithelial cells (brown). X100 magnification.

3.1.7 Optimisation of Thrombomodulin antibody immunoreactivity in tissues for IHC

Anti-Thrombomodulin (1009) mouse monoclonal antibody was optimised for IHC using human bladder tissues samples from Ysbyty Glan Clwyd. Sections were cut as previously described (section 2.5.5). Sectioned tissue slides were placed in an incubator (set to 60ºC) for 30-60 minutes and then transferred to the Ventana Benchmark XT (Automated IHC/ISH slide staining system) for IHC. In the first step, slides were deparaffinised at 72ºC for 4 minutes using Ventana EZ prep solution (section 2.4.3).

Antigen retrieval was performed using the heat induced epitope retrieval method by exposing the slides to cell conditioning 1 (Standard CC1) at 95-100ºC for 64 minutes. CC1 is a tri-based EDTA buffer with a pH of 7.8 (Section 2.4.1).

Anti-Thrombomodulin mouse primary monoclonal antibodies, (cell Marque, UK), was applied to slides and incubated for 32 minutes at 37ºC. After series of washes, slides were incubated in hydrogen peroxidase, universal HRP multimer (which contains labelled secondary antibodies) and universal DAB chromogen for colour development. Following antibody incubation, staining was amplified by using Ventana amplifier. Furthermore, an ultrawash step was included in the Optimised protocol

Slides were then counterstained in haematoxylin 1 for 12 minutes before applying a blueing reagent for 4 minutes.

Summarised optimisation information for anti-Thrombomodulin is provided in table 3.9 and examples of staining outcome using the various protocols are provided in figures 3.24, 3.25, 3.26

Table 3. 7 IHC Experimental protocols for anti-Thrombomodulin primary monoclonal antibody.

Experimental protocol 1	Experimental protocol 2 (optimised protocol)
Control tissue- Bladder	Control tissue- Bladder
Deparaffinization- 72°C for 4 minutes	Deparaffinization- 72°C for 4 minutes
Antigen retrieval- CC1 for 72 minutes	Antigen retrieval- CC1 for 8 minutes
Blocking- Not applied	Blocking- option 1
Ab incubation at 37°C for 16Minutes	Ab incubation at 37°C for 32 minutes
Amplification- not required	Amplification- Ventana amplifier
	Ultrawash
Detection kit- Ultraview	Detection kit- Ultraview
Counterstain for 8 minutes	Counterstain for 12 minutes
blueing reagent (4 Minutes)	blueing reagent (4 Minutes)

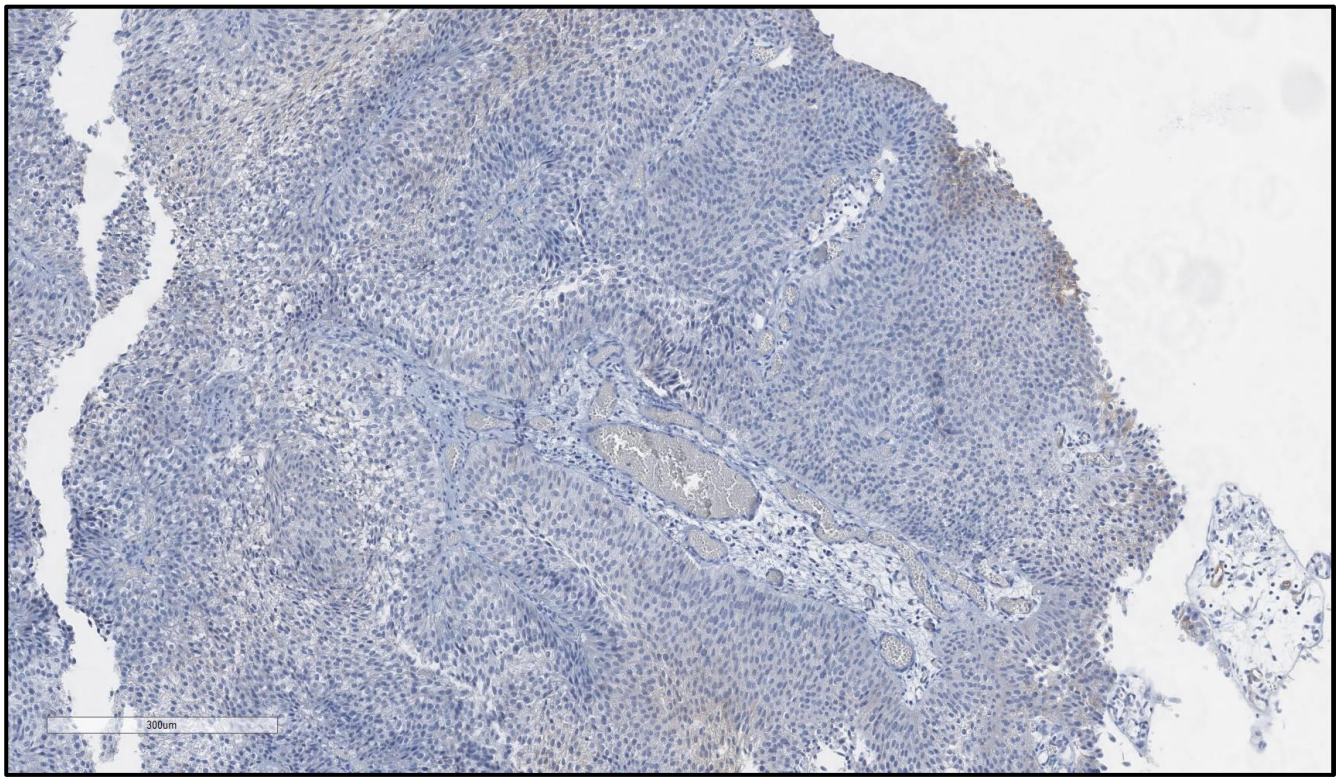

Figure 3. 24 Anti-Thrombomodulin IHC negative control
IHC staining of anti-Thrombomodulin mouse polyclonal primary antibody in FFPE human Bladder tissues. Ventana ultraview DAB detection. No staining in cytoplasmic or membranous staining in epithelial cells within bladder tissues. X100 magnification.

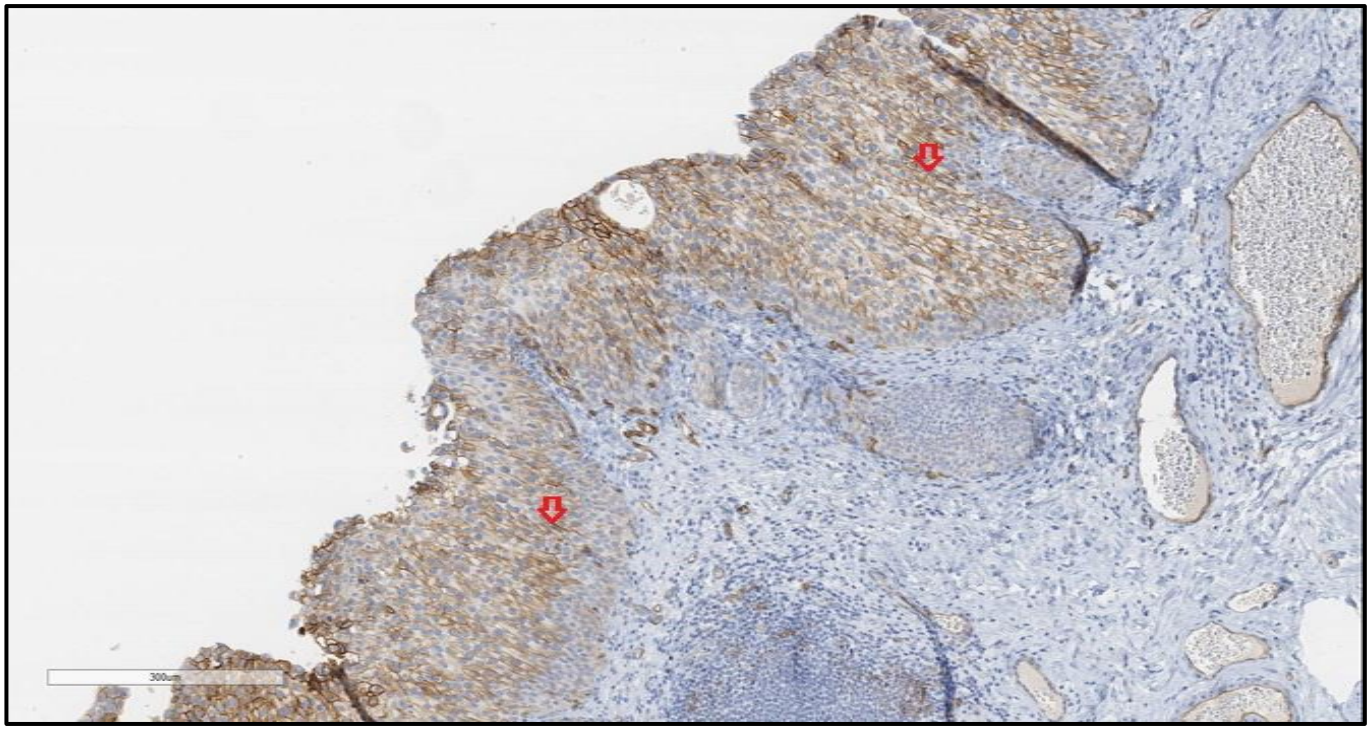

Figure 3. 25 Anti-Thrombomodulin IHC protocol 1
IHC staining of anti-Thrombomodulin mouse polyclonal primary antibody in FFPE human Bladder tissue. Antibody incubation= 16 Minutes, no amplification, Ultrawash added, Ventana ultraview DAB detection. Positive membranous and cytoplasmic staining in Bladder epithelial cells (Red arrows). X100 magnification.

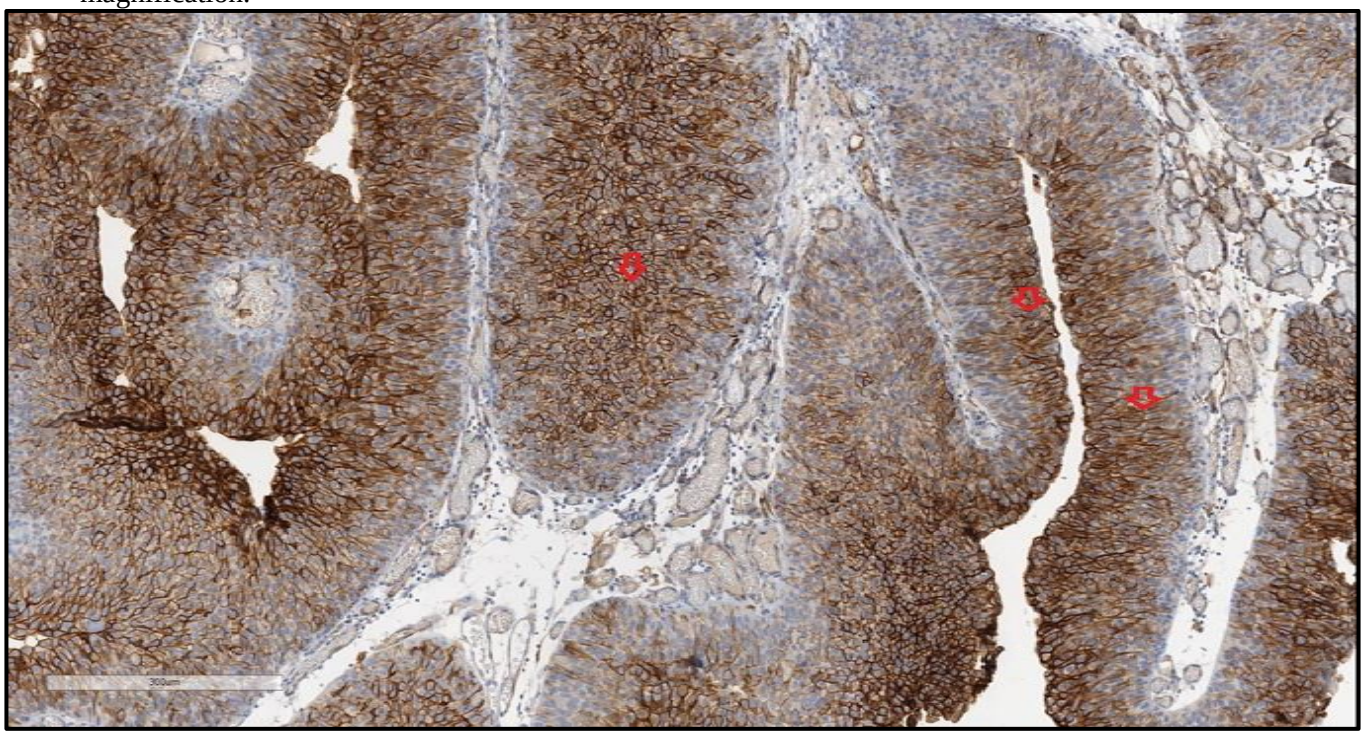

Figure 3. 26 Anti-Thrombomodulin IHC protocol 2 (optimised protocol)
IHC staining of anti-Thrombomodulin mouse polyclonal primary antibody in FFPE human Bladder tissue. Antibody incubation= 32 Minutes, amplification step added, Ultrawash step added, Ventana ultraview DAB detection. Strong Positive membranous and cytoplasmic staining in Bladder epithelial cells (Red arrows). X100 magnification.

3.1.8 Optimisation of anti-CD31 antibody immunoreactivity in tissues using IHC

Anti-CD31 (JC70) mouse monoclonal antibody was optimised for IHC using placenta tissue samples from Ysbyty Glan Clwyd. Sections were cut as previously described (section 2.3.5). Sectioned tissue slides were placed in an incubator (set to 60ºC) for 30-60 minutes and then transferred to the Ventana Benchmark XT (Automated IHC/ISH slide staining system) for IHC. In the first step, slides were deparaffinised at 72ºC for 4 minutes using Ventana EZ prep solution (section 2.2.3).

Antigen retrieval was performed using the heat induced epitope retrieval method by exposing the slides to cell conditioning 1 (Standard CC1) at 95-100ºC for 64 minutes. CC1 is a tri-based EDTA buffer with a pH of 7.8 (Section 2.2.1).

Anti-CD31 mouse primary monoclonal antibodies, (purchased prediluted from Ventana medical systems), was applied to slides and incubated for 32 minutes at 37ºC. After series of washes, slides were incubated in hydrogen peroxidase, universal HRP multimer (which contains labelled secondary antibodies) and universal DAB chromogen for colour development.

Slides were then counterstained in haematoxylin 1 for 12 minutes before applying a blueing reagent for 4 minutes. Figures 3.27-3.28 show representative pictures of optimised CD34 staining in control tissue.

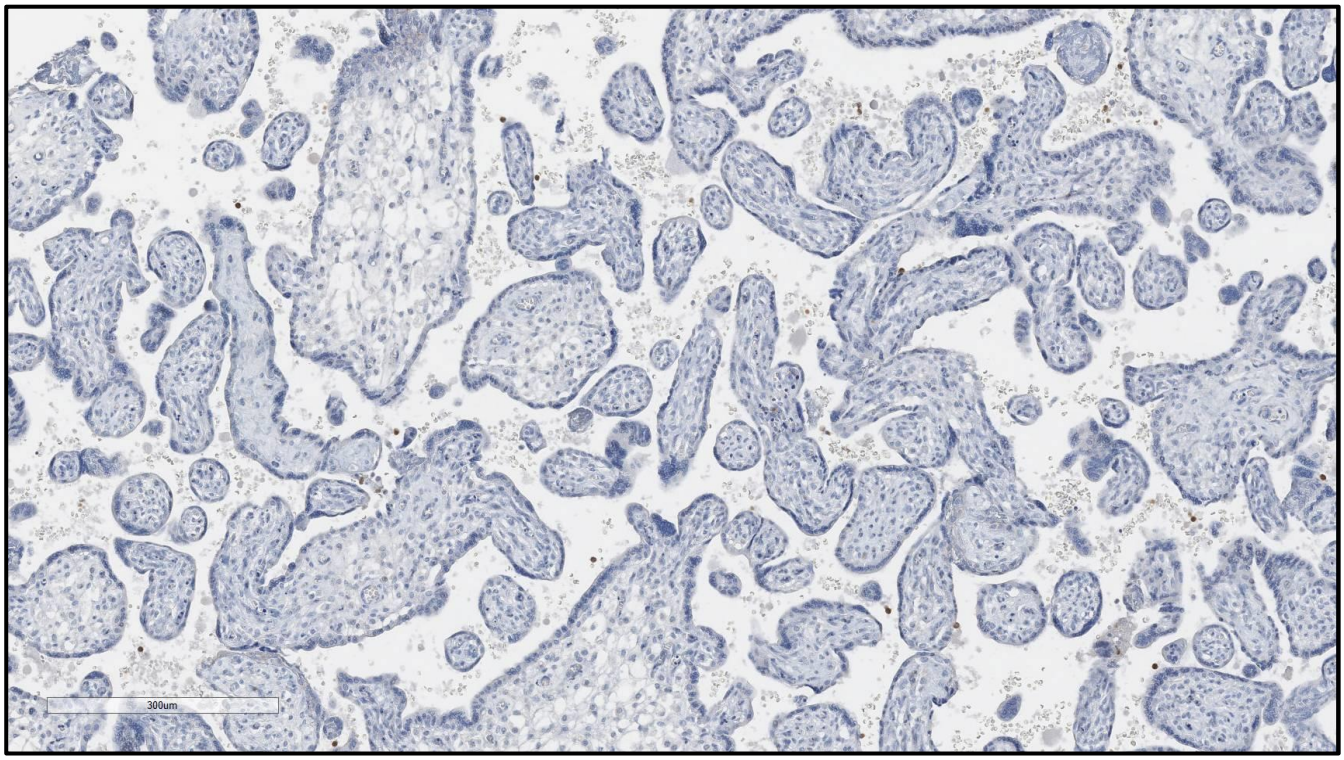

Figure 3. 27 Anti-CD31 IHC negative control
IHC staining of CD31 mouse polyclonal primary antibody in FFPE human placenta samples. Negative control slide. No membranous and cytoplasmic staining in vascular endothelial cells. X100 magnification.

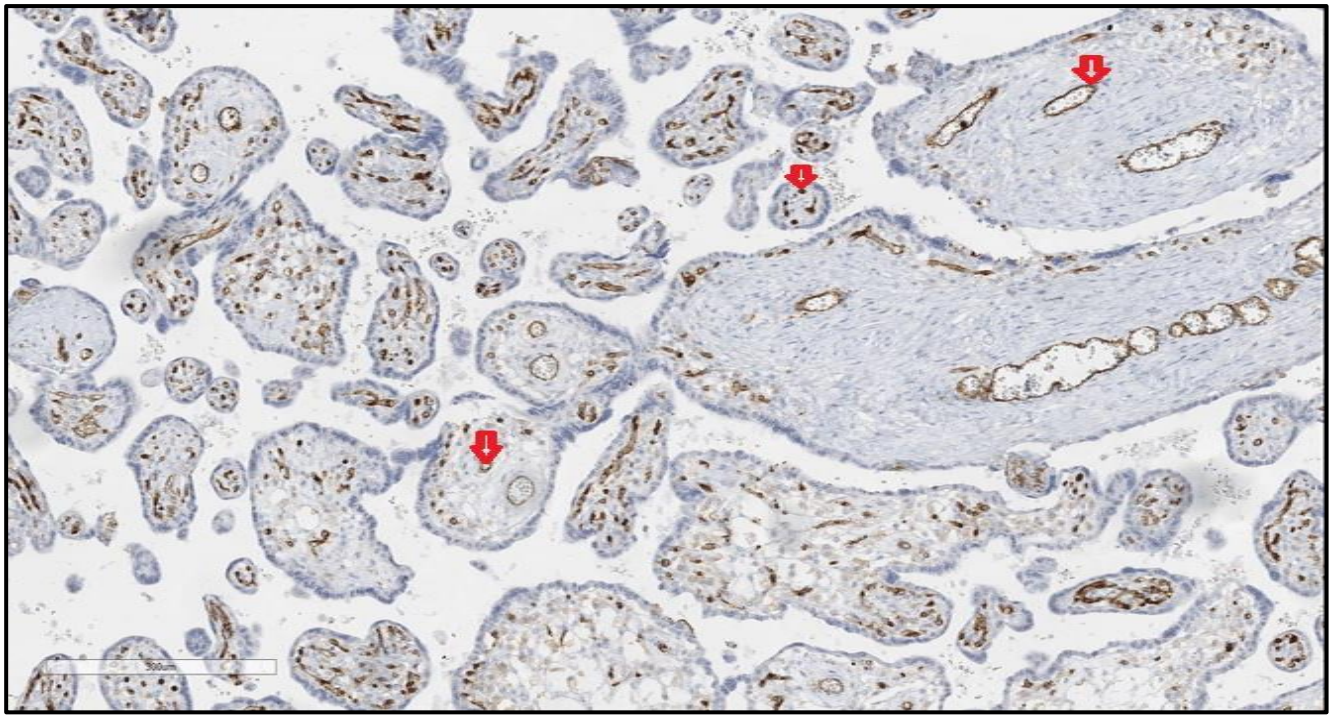

Figure 3. 28 Anti-CD31 IHC optimisation using optimised protocol
IHC staining of CD31 mouse polyclonal primary antibody in FFPE human placenta samples. Antibody incubation= 32 Minutes. Ventana ultraview DAB detection. Positive membranous and cytoplasmic staining in vascular endothelial cells (Red arrows). X100 magnification.

3.1.9 Optimisation of anti-CD34 antibody immunoreactivity in tissues using IHC

Anti-CD34 (QBEnd/10) mouse monoclonal antibody was optimised for IHC using appendix, Tonsil tissue samples from Ysbyty Glan Clwyd. Sections were cut as previously described (section 2.3.5). Sectioned tissue slides were placed in an incubator (set to 60ºC) for 30-60 minutes and then transferred to the Ventana Benchmark XT (Automated IHC/ISH slide staining system) for IHC. In the first step, slides were deparaffinised at 72ºC for 4 minutes using Ventana EZ prep solution (section 2.2.3).

Antigen retrieval was performed using the heat induced epitope retrieval method by exposing the slides to cell conditioning 1 (Standard CC1) at 95-100ºC for 64 minutes. CC1 is a tri-based EDTA buffer with a pH of 7.8 (Section 2.2.1).

Non-specific binding was prevented by blocking in ventana option 1 solution. Anti-CD34 mouse primary monoclonal antibodies, (purchased prediluted from Ventana medical systems), was applied to slides and incubated for 32 minutes at 37ºC. Staining was amplified by adding post-stain amplification step.

After series of washes, slides were incubated in hydrogen peroxidase, universal HRP multimer (which contains labelled secondary antibodies) and universal DAB chromogen for colour development. Slides were then counterstained in haematoxylin 1 for 12 minutes before applying a blueing reagent for 4 minutes. Figures 3.29-3.30 show representative pictures of optimised CD34 staining in control tissue.

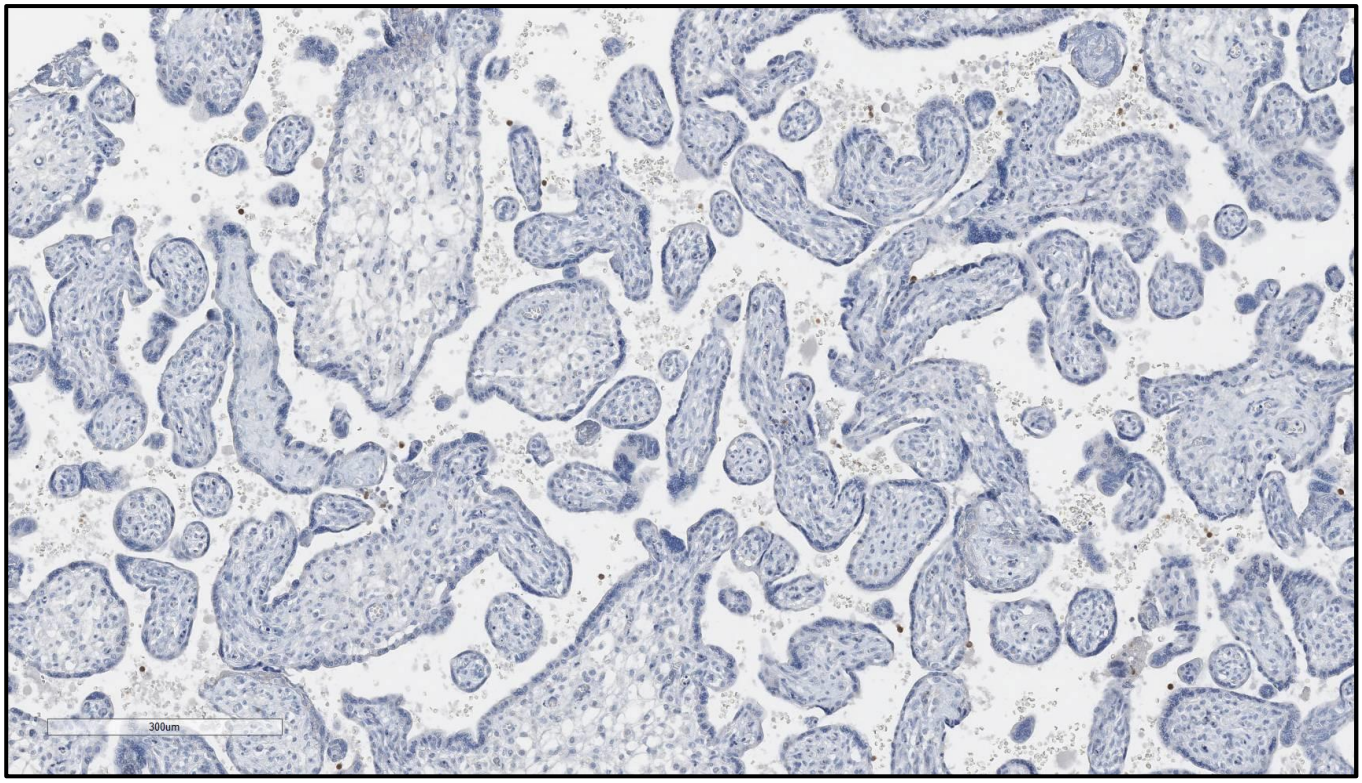

Figure 3. 29 Anti-CD34 IHC negative control
IHC staining of CD34 mouse polyclonal primary antibody in FFPE human placenta samples. Negative control slide. No membranous and cytoplasmic staining in vascular endothelial cells. X100 magnification

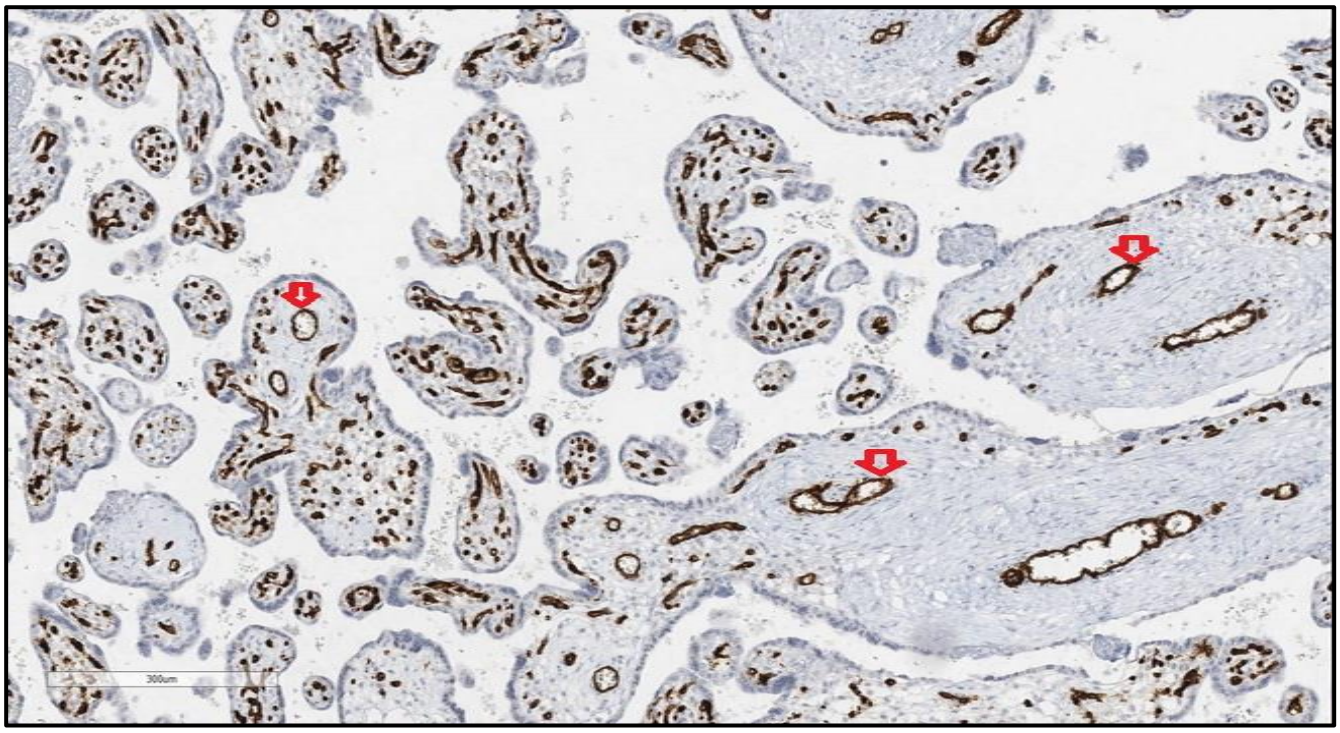

Figure 3. 30 Anti-CD34 IHC optimisation using optimised protocol
IHC staining of CD34 mouse polyclonal primary antibody in FFPE human placenta samples. Endogenous blocking Antibody incubation= 32 Minutes, post-stain amplification. Ventana ultraview DAB detection. Positive membranous and cytoplasmic staining in vascular endothelial cells (Red arrows). X100 magnification

3.2 Summary of antibody and IHC optimisation

In summary, results from the optimisation of IHC methods are provided in Table 3.8. For each antibody, manufacturer recommended protocols were modified and several IHC assays were performed on various control tissues for optimum performance.

These optimised protocols were used as templates for staining FFPE bladder tissues obtained during TURBT for the treatment of BC. Optimisation, verification and IHC analysis of all tissues and protocols were performed to enhance the overall quality, validation and reliability of the IHC results. The identification of a good biomarker profile may enhance management and monitoring of BC patients following surgical treatment via TURBT.

Table 3. 8 Summarised optimised protocols for IHC.

Optimised S100P protocol	Optimised COX-2 protocol	Optimised HER-2 protocol	Optimised SOX-2 protocol	Optimised VEGFR-3 protocol	Optimised CEACAM-1 protocol	Optimised CD31 protocol	Optimised CD34 protocol	Optimised Thrombomodulin protocol
Control tissue-Placenta	Control tissue-Colon adenocarcinoma	Control tissue-Breast carcinoma	Control tissue-Fallopian tube	Control tissue-Umbilical cord	Control tissue-Colon	Control tissue-Placenta	Control tissue-placenta	Control tissue-Bladder
Detection kit-Ultraview	Detection kit-Ultraview	Detection kit-Ultraview	Detection kit-Ultraview	Detection kit-Ultraview	Detection kit-Ultraview	Detection kit-Ultraview	Detection kit-Ultraview	Detection kit-Ultraview
Deparaffinization-72ºC for 4 minutes	Deparaffinization-72ºC for 4 minutes	Deparaffinization-72ºC for 4 minutes	Deparaffinization-72ºC for 4 minutes	Deparaffinization-72ºC for 4 minutes	Deparaffinization-72ºC for 4 minutes	Deparaffinization-72ºC for 4 minutes	Deparaffinization-72ºC for 4 minutes	Deparaffinization-72ºC for 4 minutes
Antigen retrieval-Protease 1 for 8 minutes	Antigen retrieval-CC1 95-100ºC for 64 minutes	Antigen retrieval-CC1 95-100ºC for 4 minutes	Antigen retrieval-CC1 95-100ºC for 76 minutes	CC1 at 100ºC for 52 minutes	CC1 at 100ºC for 36 minutes	CC1 at 100ºC for 64 minutes	CC1 at 100ºC for 64 minutes	Antigen retrieval-CC1 for 8 minutes
Blocking- not required	Blocking- not required	Block-Ultra block with Ventana diluent	Block-Ultra block with Ventana diluent	Blocking-Ventana diluent	Blocking-Ventana diluent	Blocking- Not required	Blocking-Ventana diluent	Blocking-Ventana diluent
Ab incubation at 37ºC for 24 minutes	Ab incubation at 37ºC for 32 minutes	Ab incubation at 37ºC for 20 minutes	Ab incubation at 37ºC for 32 minutes	Ab incubation at 37ºC for 16 Minutes (1:200 dilution)	Anti CEACAM-1 Ab at 37ºC for 28 Minutes (1:200 dilution	Anti CEACAM-1 Ab at 37ºC for 32 Minutes	Anti CEACAM-1 Ab at 37ºC for 32 Minutes	Ab incubation at 37ºC for 32 minutes
Amplification-Ventana amplifier	Amplification-not required	Amplification-Ventana amplifier	Amplification-Ventana amplifier	Ultrawash	Amplify	Amplification-not required	Amplification-Ventana amplifier	Amplification-Ventana amplifier & Ultrawash
Counterstain for 12 minutes	Counterstain for 12 minutes	Counterstain for 12 minutes	Counterstain (12 minutes)	Counterstain (12 Minutes)	Counterstain (12 Minutes)	Counterstain (12 Minutes)	Counterstain (12 Minutes)	Counterstain for 12 minutes
blueing reagent (4 Minutes)	blueing reagent (4 Minutes)	blueing reagent (4 Minutes)	blueing reagent (4 minutes)	blueing reagent (4 Minutes)	blueing reagent (4 Minutes)	blueing reagent (4 Minutes)	blueing reagent (4 Minutes)	blueing reagent (4 Minutes)

4.0 Chapter Four: Changes in serum-based inflammatory markers in BC patients, and their association with recurrence and progression

4.1 Synopsis

During this study, the association between various inflammatory biomarkers and BC recurrence and progression was investigated. 40 patients (n=40) scheduled for a transurethral resection of the Bladder tumour (TURBT) surgery were recruited after informed consent (section 2.5.2). Blood sampling collection procedures were undertaken pre-operatively and at 1 month, 3 months and 6 months post-operatively (section 2.5.3).

Blood samples were analysed for the detection of MIP-2, CD31, IL-6, IL-8, TNF-α, CD40L, TGF-α, angiopoietin-2 and Osteopontin. The concentrations of these inflammatory markers were analysed using commercially available ELISA (sections 2.5.8) and the Bioplex multiplex system (section 2.5.6).

The main aim of this pilot clinical study was to assess the relationship between changing levels of serum inflammatory markers in patients undergoing treatment for BC and BC recurrence/progression. Due to the high rates of recurrence in BC, it is anticipated that significant changes in biomarker levels could help predict patients who are at an increased risk of recurrence.

4.2 Results

4.2.1 Changes in MIP-2 concentration following TURBT for NMIBC treatment

Figure 4.1 represents changes to macrophage inflammatory protein 2 (MIP-2) concentrations (pg/ml) in patients who had TURBT for the treatment of NMIBC. There was a significant decrease in MIP-2 concentration up to 6 months after TURBT ($X^2(3) = 14.44$, $p=0.001$), as determined by the Friedman test. Data are presented in box plots using median (interquartile ranges). MIP-2 concentration increased from 347 pg/ml, (308-499) at baseline, to 389 pg/ml, (303-536) at 1-month post-operative. The MIP-2 concentrations then decreased to 285 pg/ml, (235-530) at 3-months post-operative and further decreased to 206 pg/ml (189-320) at 6-months post-operative. On further statistical analysis using the Wilcoxon's signed test, there was a significant difference between baseline and 6-month post-operative MIP-2 concentrations ($Z=-3.26$, $p=0.001$, $r= 0.75$).

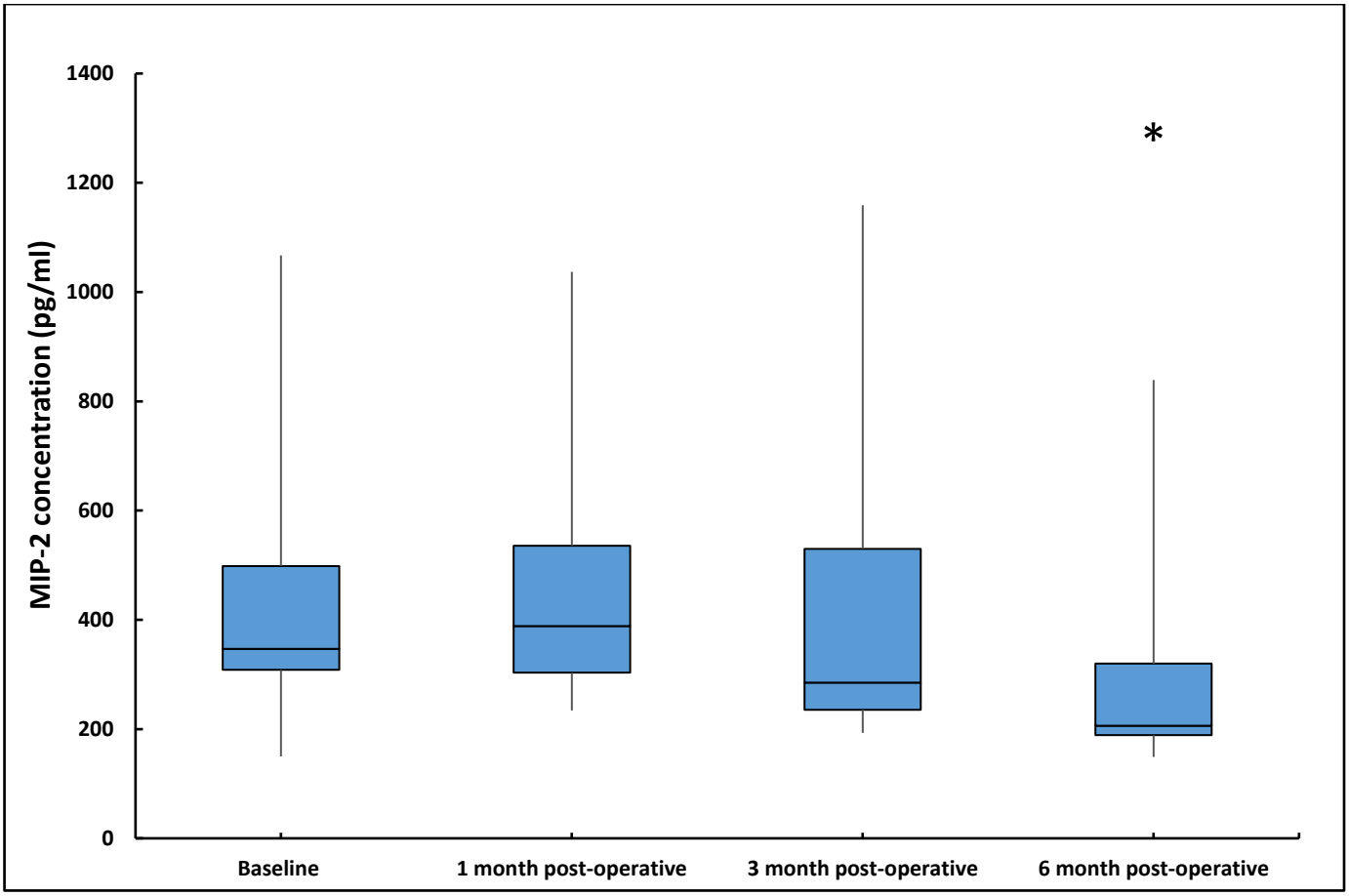

Figure 4. 1 Changes in MIP-2 concentration following TURBT for NMIBC treatment. The results show [Median, (interquartile range)], X2(3) = 14.44, p=0.001 as determined by Friedman, significant difference (*) between baseline and 6 months post-operative (Z=-3.26, p=0.001, r= 0.75) as determined by Wilcoxon's signed test, n=40.

4.2.2 Changes in CD31 (PECAM-1) concentration following TURBT for BC treatment.

Figure 4.2 represents changes to CD31 concentrations (pg/ml) in patients who had TURBT for the treatment of NMIBC. This parameter was measured as a potential biomarker for inflammation and angiogenesis, hallmarks of tumour growth. There was a statistically significant increase in CD31 concentration ($X^2(3) = 13.94$, p=0.003) up to 6-months post-operative, as determined by the Friedman test. Data are presented in box plots using median (interquartile ranges). Baseline levels of 9004 pg/ml (7546-12247), CD31 concentration increased at 1-month post-operative [12254 pg/ml, (8570-14862)] and at decreased 3-months post-operative [10717 pg/ml, (9845-17196)]. At 6-months post-operative however, CD31 concentrations slightly increased to 11160 pg/ml, (10052-14692). On further statistical analysis using the Wilcoxon's signed test, there as a statistically significant difference between baseline versus 3-months post-operative (Z= -3.10, p=0.002, r= 0.75) and 6-months post-operative (Z= -3.20, p=0.001, r= 0.78).

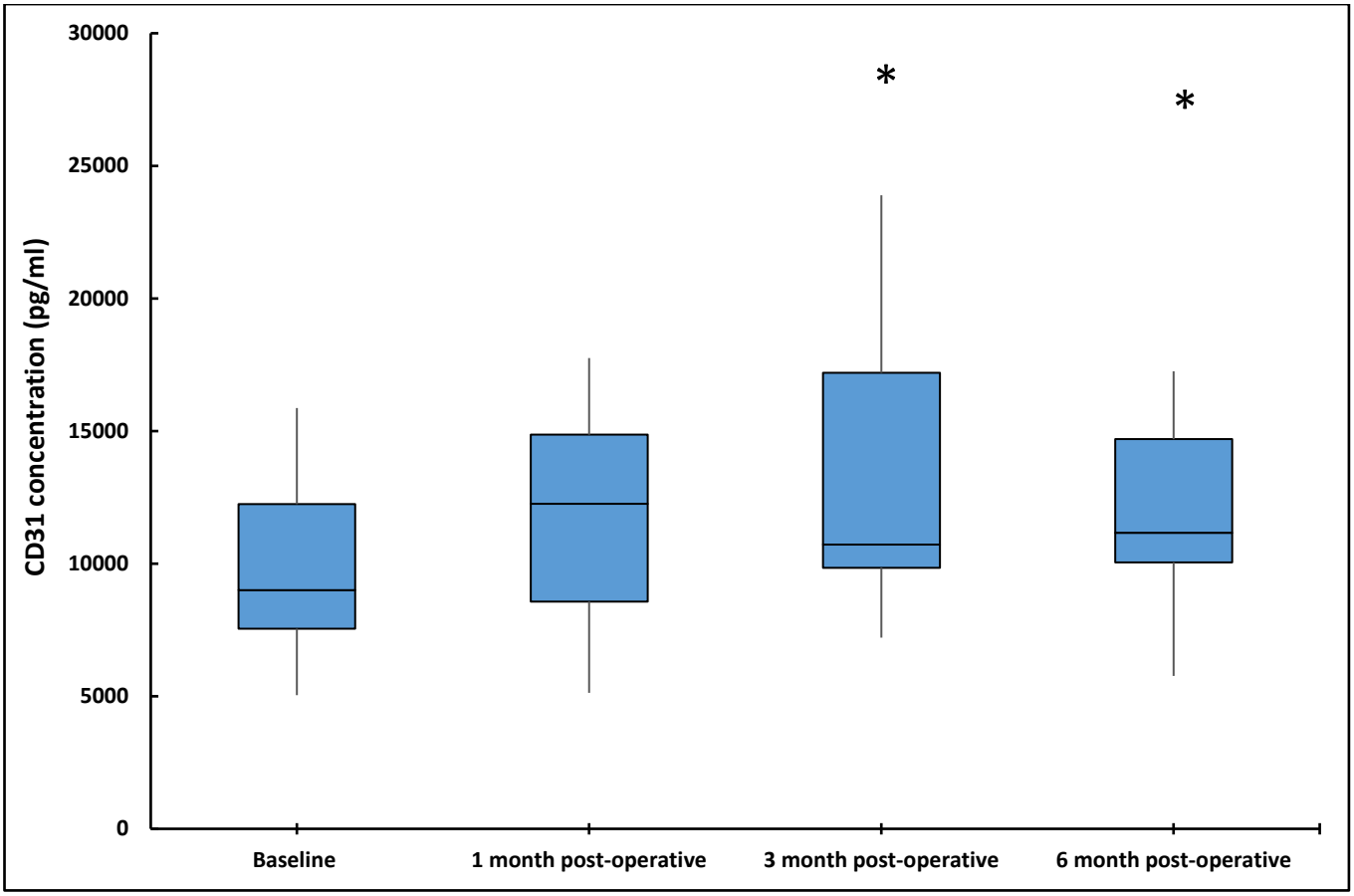

Figure 4. 2 Changes in CD31 concentration following TURBT for NMIBC treatment.
The results show [Median, (interquartile range)], p=0.003 as determined by Friedman, significant difference (*) between baseline & 3 months (Z= -3.10, p=0.002, r= 0.75) and baseline & 6 months (Z= -3.20, p=0.001, r= 0.78) post-operative as determined by Wilcoxon's signed, n=40

4.2.3 Changes in Interleukin-6 (IL-6) concentration following TURBT for BC treatment.

Figure 4.3 represents changes to IL-6 concentration (pg/ml) in patients who had TURBT for the treatment of NMIBC. This parameter was measured due to its roles in inflammation and the potential role this plays in tumour growth. The serum IL-6 concentration showed a decreased trend up to 6 months post-operatively. Data are presented in box plots using median (interquartile ranges). Serum IL-6 concentrations increased from 179 pg/ml (35-250) at baseline, to 181 pg/ml (46-261) at 1-month post-operative. IL-6 concentration then decreased at 3-months post-operative to 166 pg/ml (37-228), and further decreased at 6-months post-operative to 163 pg/ml (34-209). There was no statistical significance, as determined by the Friedman test ($X^2(3) = 4.059$, p=0.255).

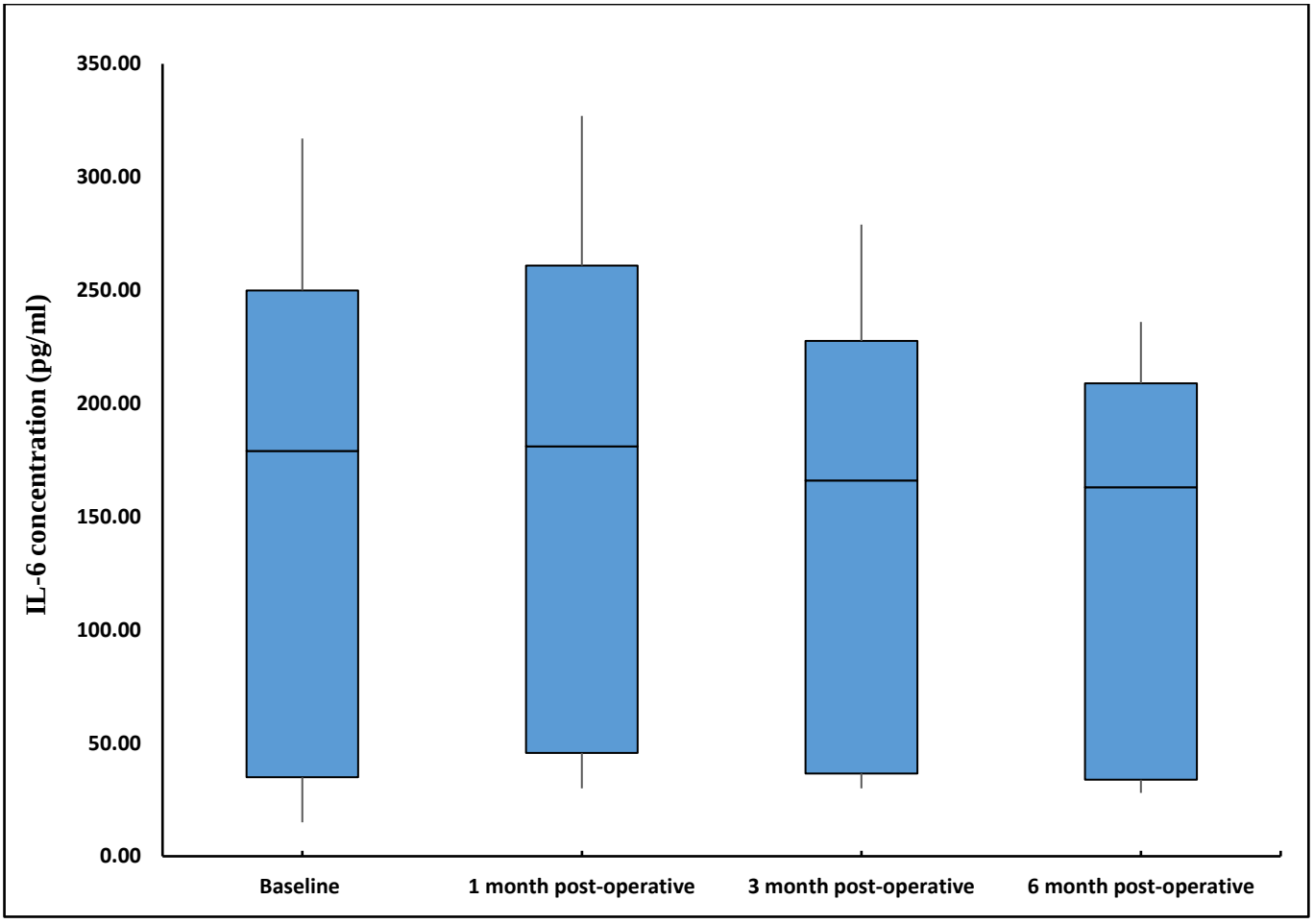

Figure 4. 3 Changes in IL-6 concentration following TURBT for BC treatment.
The results show [Median, (interquartile range)], $X^2(3) = 4.059$, p=0.25 as determined by Friedman, n=40.

4.2.4 Changes in Interleukin-8 (IL-8) concentration following TURBT for BC treatment.

Figure 4.4 represents changes to serum IL-8 concentration (pg/ml) in patients who had TURBT for the treatment of NMIBC. This parameter was measured due to its roles in inflammation and the potential role this plays in tumour growth. The serum IL-8 concentration showed a decreased trend up to 6 months post-operatively. Data are presented in box plots using median (interquartile ranges).

IL-8 concentration decreased from 66 pg/ml (13-82) at baseline, to 63 pg/ml (16-94) at 1-month post-operative and further decreased to 40 pg/ml (13-75) at 3-months post-operative. IL-8 concentration however increased to 52 pg/ml (13-77) at 6-months post-operative. There was no statistical significance, as determined by the Friedman test ($X^2(3) = 5.400$, p=0.15).

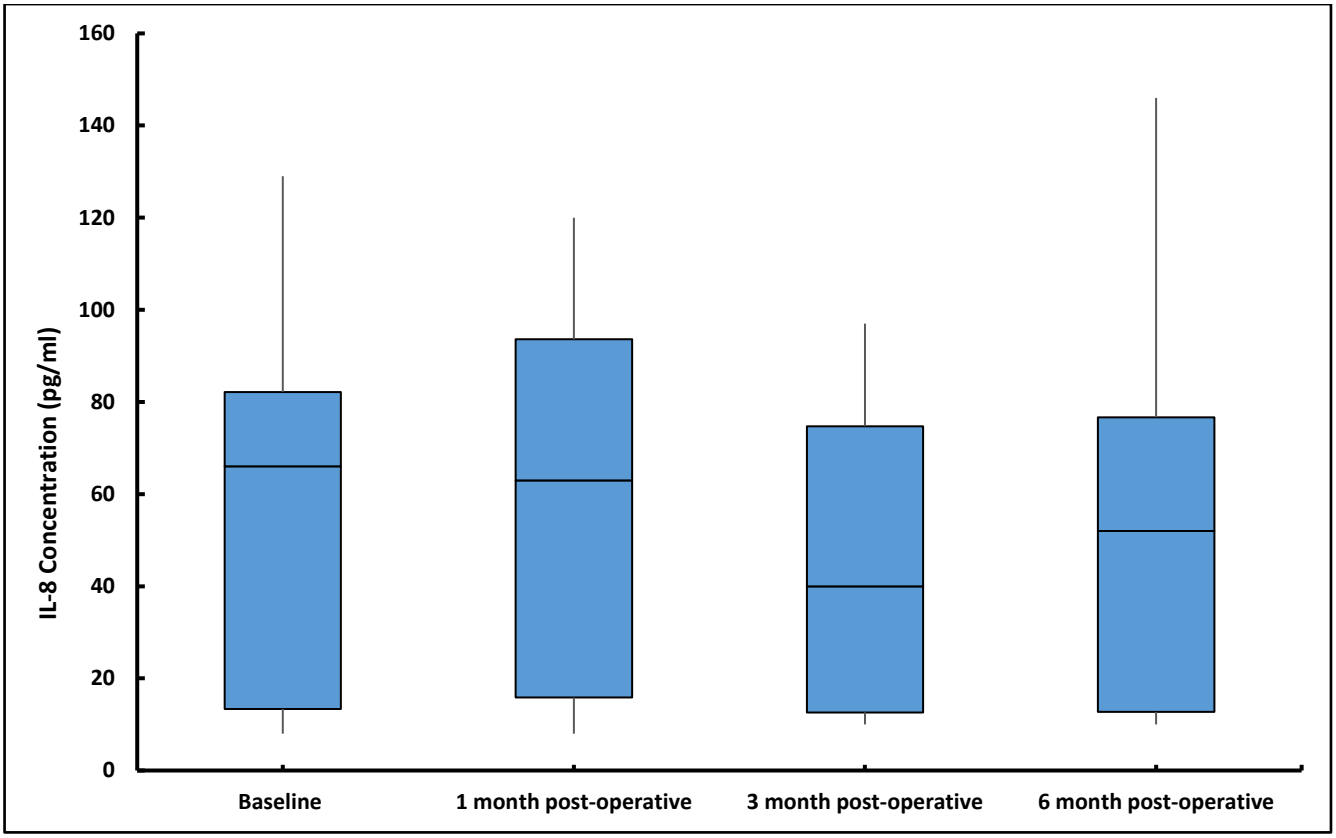

Figure 4. 4 Changes in IL-8 concentration following TURBT for BC treatment.
The results show median, (interquartile range), $X^2(3) = 5.400$, p=0.15 as determined by Friedman, n=40.

4.2.5 Changes in Tumour Necrosis Factor- α (TNF-α) concentration following TURBT for BC treatment.

Figure 4.5 represents changes to serum TNF-α concentration (pg/ml) in patients who had TURBT for the treatment of NMIBC. This parameter was measured due to its roles in inflammation and the potential role this plays in tumour growth. The serum TNF-α concentration showed a decreased trend up to 6 months post-operatively. Data are presented in box plots using median (interquartile ranges).

TNF-α serum concentration initially increased from 80 pg/ml (30-103) at baseline to 86 pg/ml (34-115) at 1-month post-operative. The concentrations decreased at 3-months post-operative [70 pg/ml (26-101) and finally increased at 6-months post-operative 75 pg/ml (27-96). There was no statistical significance, as determined by the Friedman test ($X^2(3) = 1.447$, p=0.69).

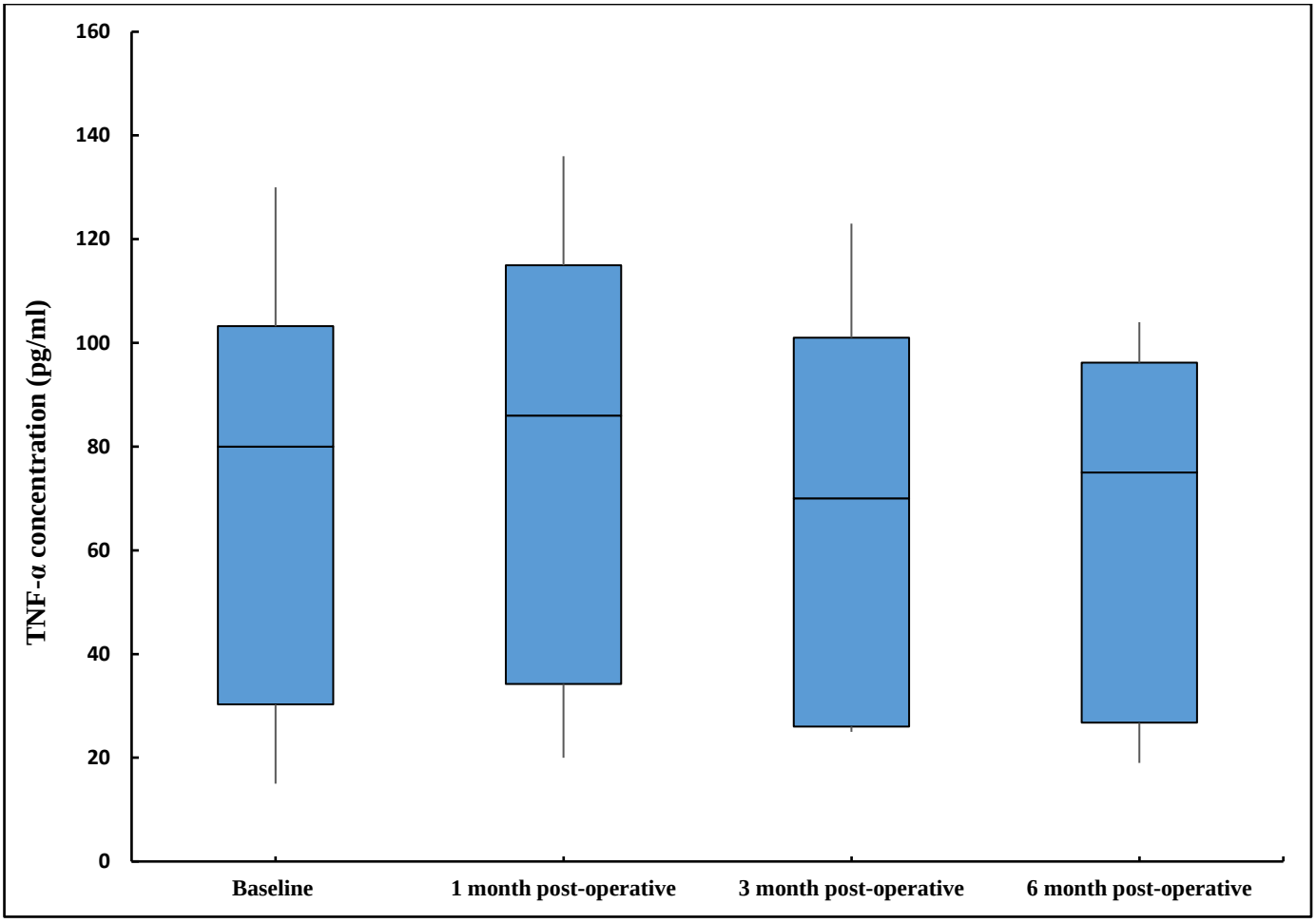

Figure 4. 5 Changes in TNF-α concentration following TURBT for BC treatment.
The results show [Median, (interquartile range)], $X^2(3) = 1.447$, p=0.69 as determined by Friedman, n=40.

4.2.6 Changes in sCD40L concentration following TURBT for BC treatment

Figure 4.6 represents changes to sCD40L concentrations (pg/ml) in patients who had TURBT for the treatment of NMIBC. This parameter was measured as a marker of inflammation in patients undergoing treatment for NMIBC. Data are presented in box plots using median (interquartile ranges). There was a trend of decreasing sCD40L concentration up to 6 months following TURBT. Serum sCD40L concentration decreased from baseline [913 pg/ml (398-1071)] to 887 pg/ml (379-1136), at 1-month post-operative and further decreased to 800 pg/ml (227-1017) at 3-months post-operative, before increasing to 827 pg/ml (277-968) at 6-months post-operative. Using the Friedman test, there was no statistically significant change ($X^2(3) =7.376$, p=0.06) in sCD40L concentration following TURBT.

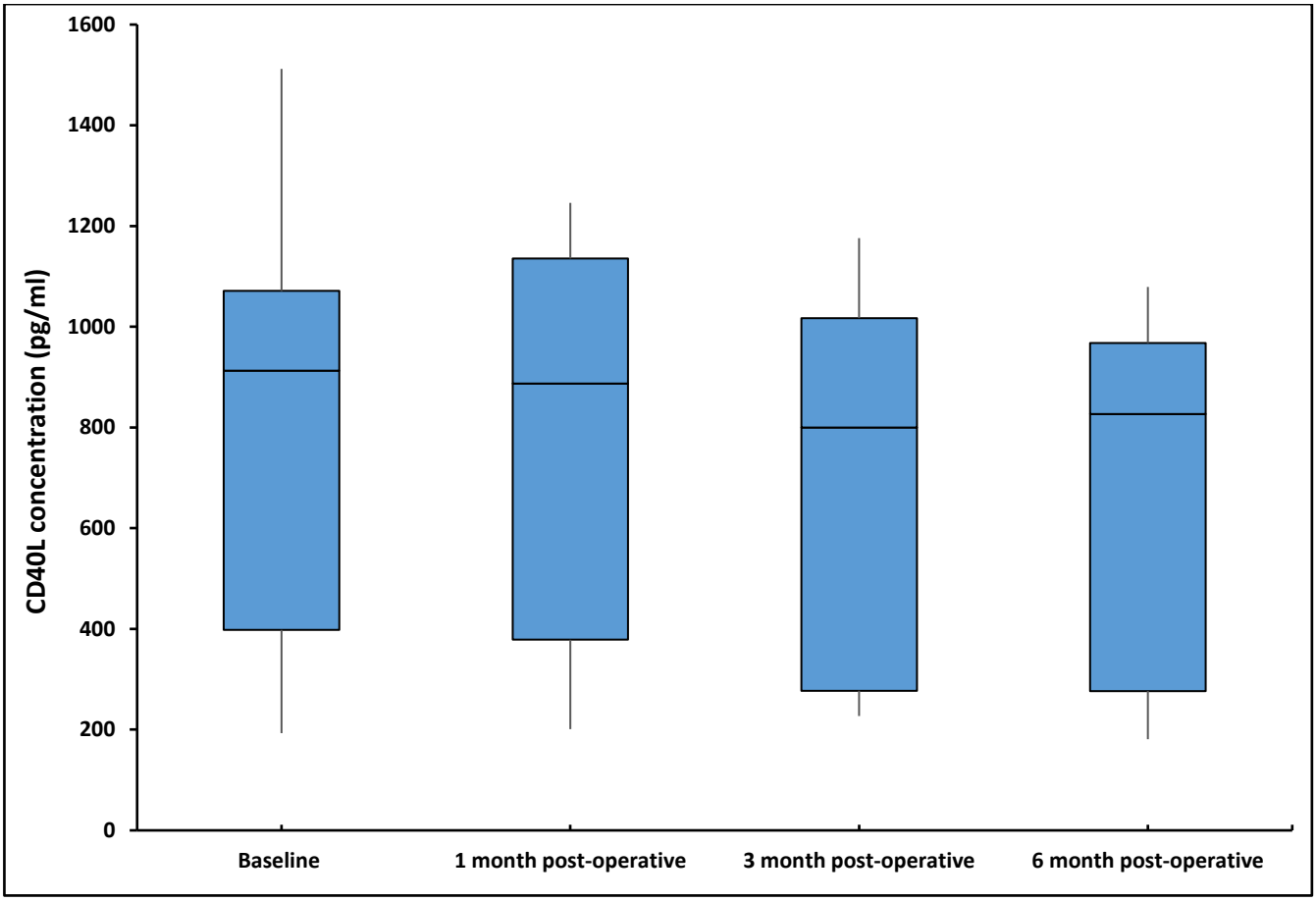

Figure 4. 6 Changes in sCD40L concentration following TURBT for NMIBC treatment. The results show Median, (interquartile range), $X^2(3)$ =7.376, p=0.06 as determined by Friedman. n=40.

4.2.7 Changes in Angiopoietin-2 concentration following TURBT for NMIBC treatment

Figure 4.7 represents changes to angiopoietin-2 concentrations (pg/ml) in patients who had TURBT for the treatment of NMIBC. This parameter was measured as a marker of inflammation in patients undergoing treatment for NMIBC. Data are presented in box plots using median (interquartile ranges). Angiopoietin-2 concentration increased from baseline [1924 pg/ml (1142-2324)] to 2114 pg/ml (1381-2715) at 1-month post-operative before decreasing to 1760 pg/ml (1097-2597), at 3-months post-operative. The angiopoietin-2 concentration, however, slightly increased to 1842 pg/ml (1178-2120) at 6-months post-operative. Using the Friedman test, there was no statistically significant change ($X^2(3) = 1.970$, p=0.57) in angiopoietin-2 concentration up to 6-months following TURBT.

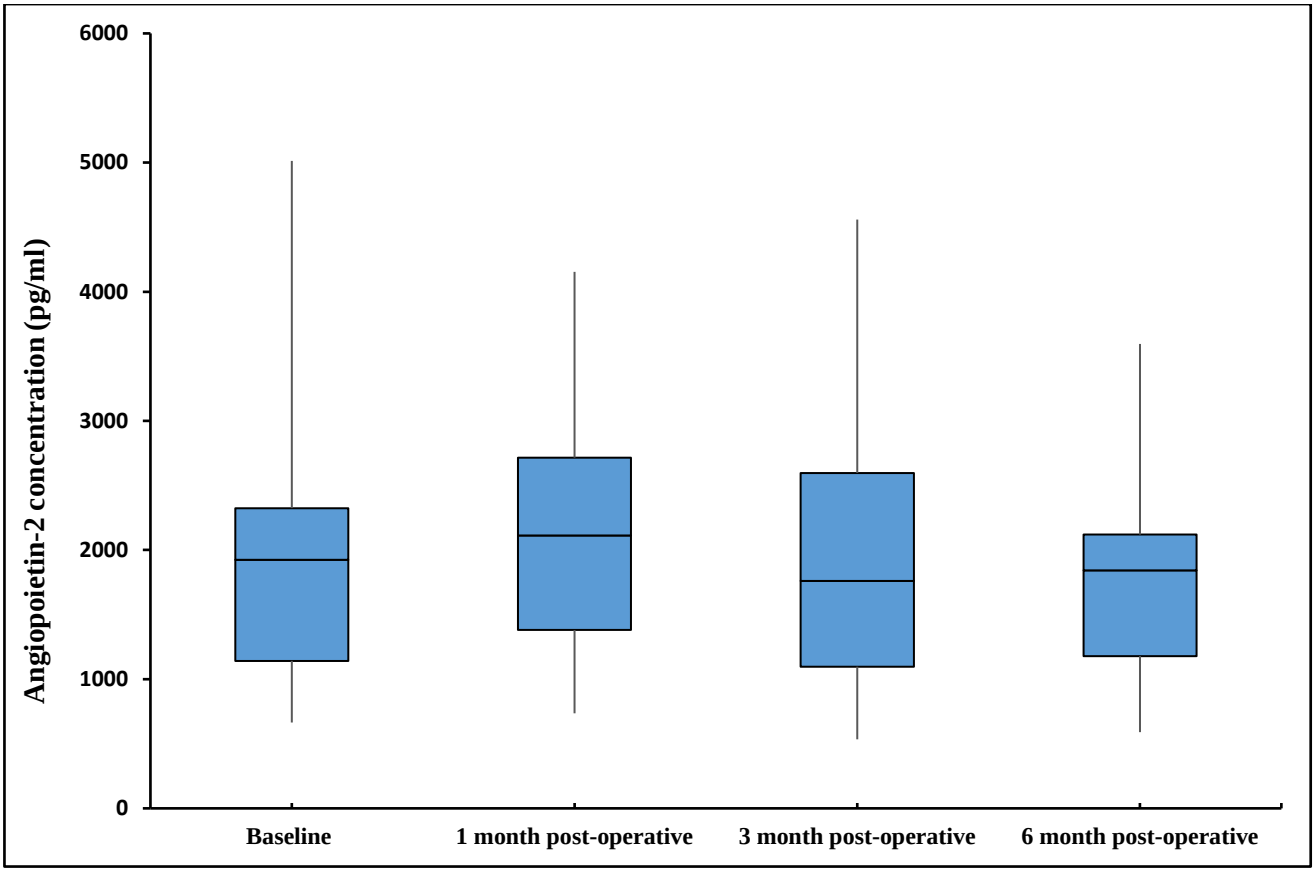

Figure 4. 7 Changes in Angiopoietin-2 concentration following TURBT for NMIBC treatment. The results show median, (interquartile range), $X^2(3) = 1.970$, p=0.57 as determined by Friedman, n=40.

4.2.8 Changes in Osteopontin concentration following TURBT for NMIBC treatment

Figure 4.8 represents changes to osteopontin concentrations (pg/ml) in patients who had TURBT for the treatment of NMIBC. This parameter was measured as potential biomarker for inflammation and cancer growth. Data are presented in box plots using median (interquartile ranges). Osteopontin concentration increased from baseline levels [64068 pg/ml (44838-127748)] to 64756 pg/ml (56123-91427) at 1-month post-operative and 77135 pg/ml (48278-92111), at 3-months post-operative. At 6-months post-operative however, concentrations decreased below baseline levels to 57634 pg/ml (49102-69191). No statistical significance was achieved ($X^2(3) = 3.49$, p=0.32) as determined by the Friedman Test.

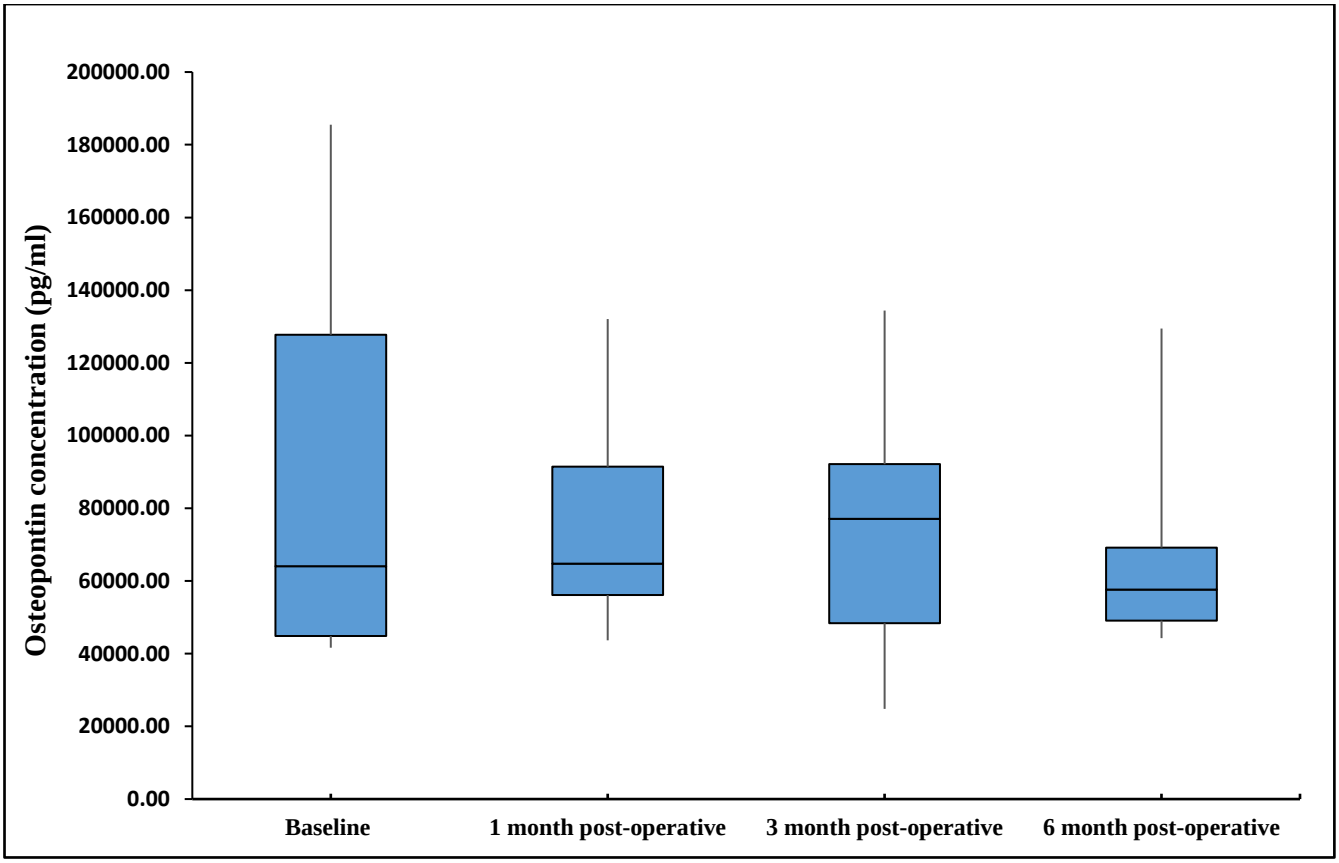

Figure 4. 8 Changes in Osteopontin concentration following TURBT for NMIBC treatment. The results show [Median, (interquartile range)], X2(3)= 3.49, p=0.32 as determined by Friedman.

4.3 Summary of results

Significant changes to two inflammatory biomarkers were reported in BC patients up to 6 months following TURBT. Specifically,

- Serum MIP-2 concentration decreased significantly following TURBT for treatment of BC ($X^2(3) = 14.44$, p=0.001). There was also significant difference between baseline and 6-month post-operative MIP-2 concentrations (Z=-3.26, p=0.001, r= 0.75).

- Serum CD31 concentration significantly increased following TURBT for treatment of BC ($X^2(3) = 13.94$, p=0.003). There was also a statistically significant difference between baseline versus 3-months post-operative (Z= -3.10, p=0.002, r= 0.75) and baseline versus 6-months post-operative (Z= -3.20, p=0.001, r= 0.78).

- There was a trend of decreasing concentration in serum IL-6 and IL-8. These changes were however not statistically significant.

- There was no statistically significant change in serum TNF-α [($X^2(3) = 1.447$, p=0.69], sCD40L [$X^2(3) = 7.376$, p=0.06], angiopoietin-2 [$X^2(3) = 1.970$, p=0.57] and Osteopontin [$X^2(3) = 3.49$, p=0.32] concentrations up to 6-months post-operatively.

5.0 Chapter Five: Changes in serum MMP-2, MMP-3, MMP-9 and CEACAM-1, in patients undergoing TURBT, for the treatment of NMIBC

5.1 synopsis

This chapter seeks to examine the changes in the levels of serum MMP-2, MMP-3, MMP-9 and CEACAM-1 in patients scheduled for TURBT at Wrexham Maelor Hospital, for the treatment of NMIBC. Venous blood samples were taken pre-operatively, and at 1-month, 3-months and 6-months post-operatively.

The MMPs are a group of zinc-binding proteins implicated in the degradation of the extra-cellular matrix through their proteolytic activities (Lv *et al.*, 2018). As a group, they have also been implicated in several physiological activities, such as wound healing and embryogenesis and pathological conditions such as arthritis, cardiovascular conditions, kidney disorders and cancer (Hadler-Olsen *et al.*, 2011). CEACAM-1 is a glycoprotein expressed on various cells including endothelial cells, epithelial cells and myeloid cells (Prall *et al.*, 1996), and has been associated with angiogenesis (Kilic *et al.*, 2005).

The main aim of this clinical pilot-study was to investigate the relationship between changes in levels of MMP-2, MMP-3, MMP-9 and CEACAM-1 in patients undergoing TURBT for the treatment of BC. It is envisaged that any changes in MMP serum levels could help in predicting cancer recurrence and/or progression in current BC patients undergoing treatment.

5.2 Results

5.2.1 Changes in Matrix Metalloproteinase 2 (MMP-2) Concentration following TURBT for the treatment of NMIBC

Figure 5.1 represents changes to serum MMP-2 concentrations (pg/ml) in patients who had TURBT for the treatment of NMIBC. Data are presented in box plots using median (interquartile ranges). Serum MMP-2 concentration showed a decreasing trend up to 6 months after TURBT for the treatment of BC. MMP-2 concentrations decreased from 17197 pg/ml, (12729-23288) at baseline (pre-operative) to 17020 pg/ml, (11120-23218) at 1-month post-operative. MMP-2 concentration demonstrated minimal changes at 3 months [17145 pg/ml, (12540-25515) before decreasing to 13130 pg/ml, (8965-25847) at 6-months post-operative. These changes were not statistically significant ($X^2(3) = 1.06$, $p=0.787$) as determined by Friedman test.

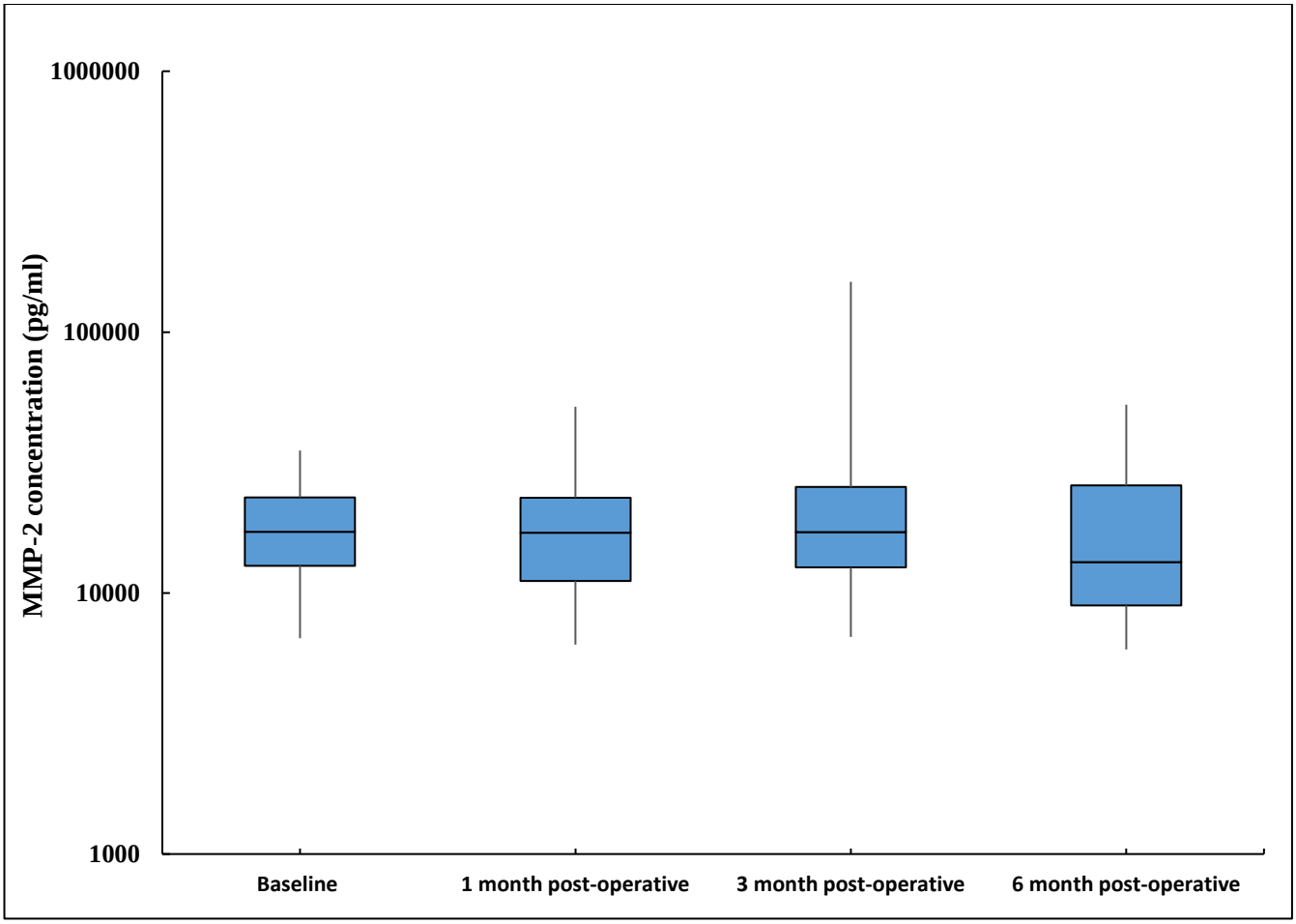

Figure 5. 1 Changes in MMP-2 following TURBT for NMIBC treatment.
The results show median, (interquartile range), $X^2(3) = 1.06$, p=0.787 as determined by Friedman, n=40.

5.2.2 Changes in Matrix Metalloproteinase 3 (MMP-3) Concentration following TURBT for the treatment NMIBC

Figure 5.2 represents changes to serum MMP-3 concentrations (pg/ml) in patients who had TURBT for the treatment of NMIBC. Data are presented in box plots using median (interquartile ranges). Serum MMP-3 concentration showed a decreasing trend up to 6 months after TURBT for the treatment of BC. MMP-3 concentration initially increased from 6693 pg/ml, (4184-9483) at baseline pre-operative to 7760 pg/ml (3050-9598) at 1-month post-operative. At 3-months post-operative, however, MMP-3 concentration decreased below pre-operative levels to 6403 pg/ml, (4324-9963) before decreasing further to 5640 pg/ml, (3541-9395) at 6 months post-operative. These changes were not statistically significant ($X^2(3) = 5.22$, p=0.156) as determined by Friedman test.

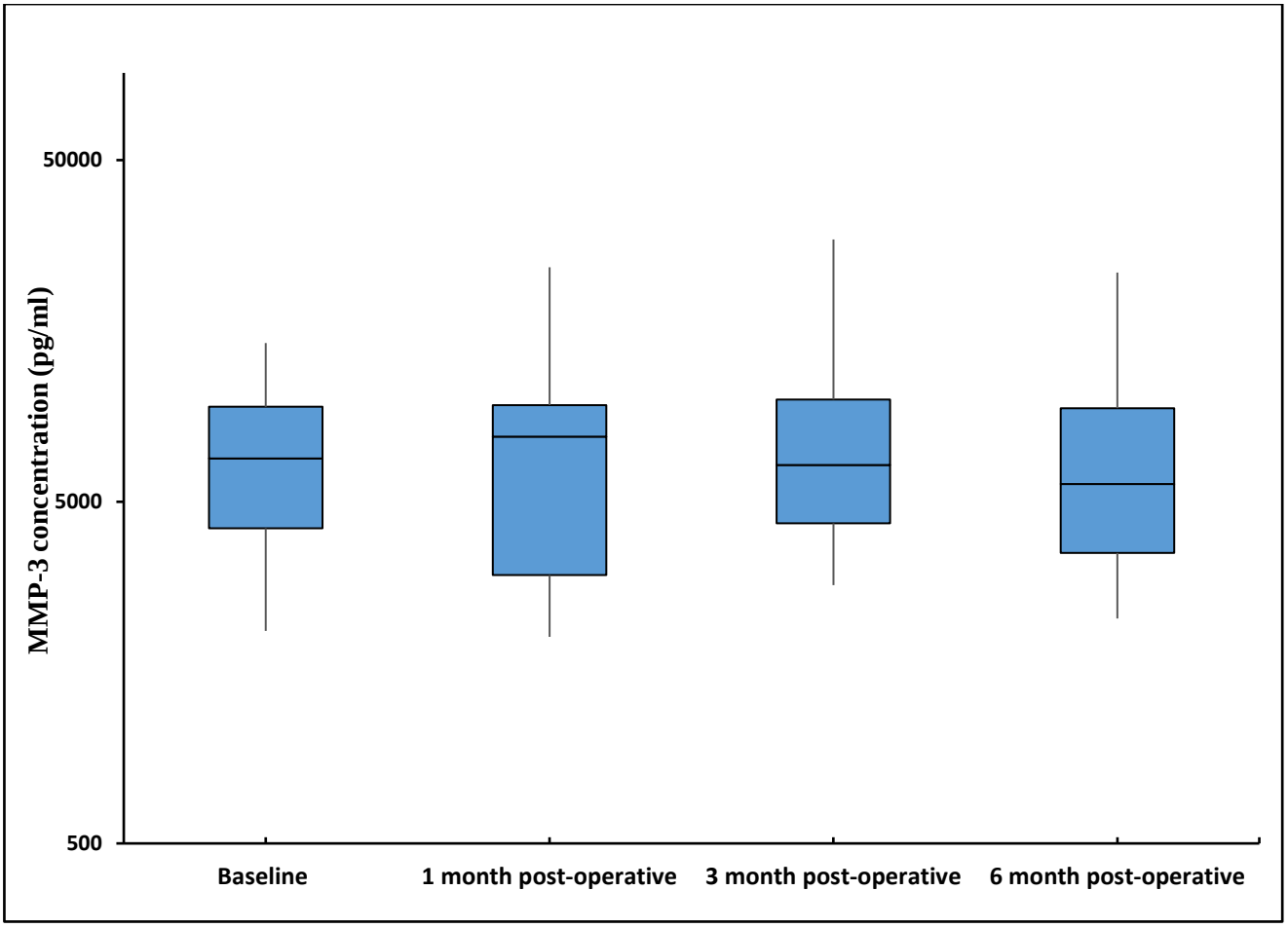

Figure 5. 2 Changes in MMP-3 following TURBT for NMIBC treatment. The results show median, (interquartile range), $X^2(3) = 5.22$, p=0.156 as determined by Friedman, n=40.

5.2.3 Changes in Matrix Metalloproteinase 9 (MMP-9) concentration following TURBT for the treatment of NMIBC

Figure 5.3 represents changes to MMP-9 concentrations (pg/ml) in patients who had TURBT for the treatment of NMIBC. Data are presented in box plots using median (interquartile ranges). There was a significant decrease ($X^2(3) = 14.43$, p=0.002, as determined by Friedman) in MMP-9 concentration up to 6 months after TURBT for the treatment of NMIBC. The baseline (pre-operative) serum MMP-9 concentrations decreased from 4141 pg/ml, (3058-11322) to 2700 pg/ml, (1242-3515) at 1-month post-operative. At 3 months post-operative however, MMP-9 concentration increased slightly to 3121 pg/ml, (1168-4801) before finally decreasing to 2257 pg/ml, (1515-3503) at 6 months post-operative. Upon further statistical analysis using the Wilcoxon's signed test, there was a significant change between baseline *vs* 1-month post-operative MMP-9 concentrations (Z= -2.59, p=0.010, r= 0.565). There was also a significant change between baseline *vs* 6-month post-operative MMP-9 concentrations (Z= -3.22, p=0.001, r= 0.703).

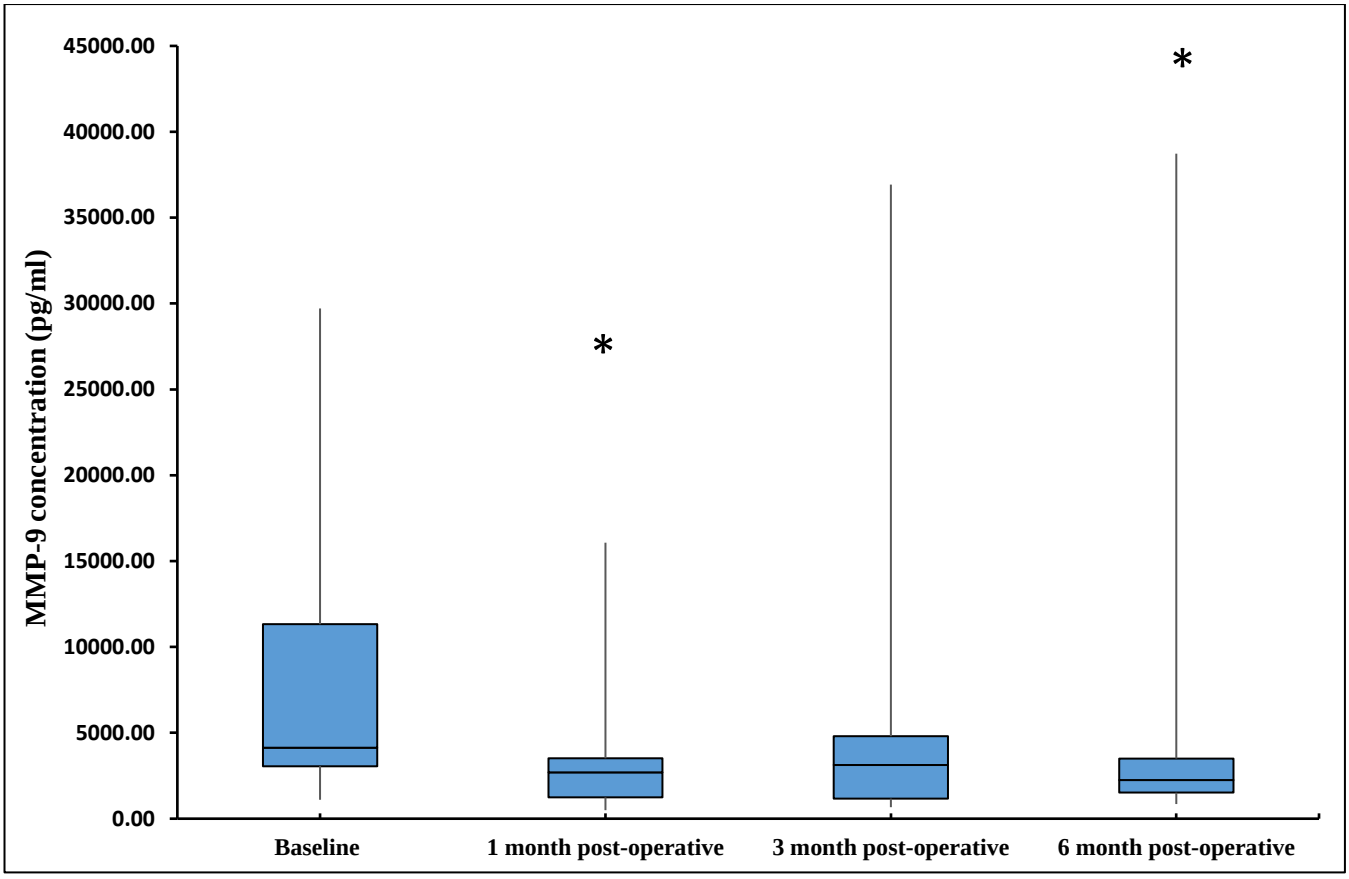

Figure 5. 3 Changes in MMP-9 following TURBT for NMIBC treatment. The results show median, (interquartile range), $X^2(3) = 14.43$, p=0.002 as determined by Friedman, significant changes between baseline and 1-month post-operative (Z= -2.59, p=0.010, r= 0.565) and between baseline and 6-months post-operative (Z= -3.22, p=0.001, r= 0.703) n=40.

5.2.4 Changes in CEACAM-1 concentration following TURBT for the treatment of NMIBC

Figure 5.4 represents changes to MMP-9 concentrations (pg/ml) in patients who had TURBT for the treatment of NMIBC. Data are presented in box plots using median (interquartile ranges). Baseline (pre-operative) CEACAM-1 concentrations decreased from 1639 pg/ml, (1205-2566) to 1555 pg/ml, (1382-2222) at 1-month post-operative. At 3-months post-operative however, CEACAM-1 concentration increased to 1613 pg/ml, (1392-2366) and further increased at 6-months post-operative to 1706 pg/ml, (1413-2237). These changes were not statistically significant ($X^2(3) = 1.67$, p=0.64) as determined by Friedman test.

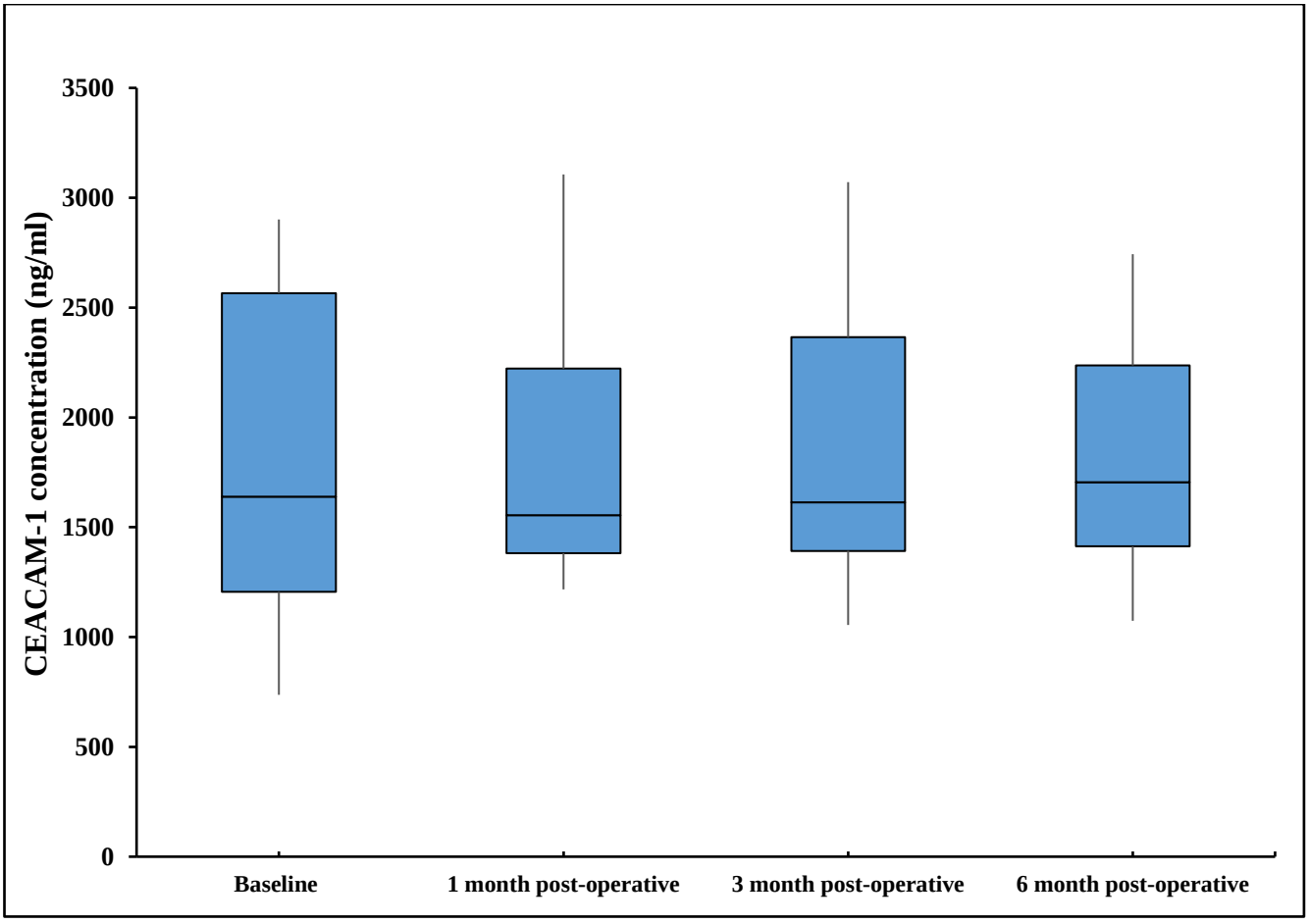

Figure 5. 4 Changes in CEACAM-1 following TURBT for NMIBC treatment. The results show [Median, (interquartile range)], $X^2(3) = 1.67$, p=0.64 as determined by Friedman, n**=40**

5.3 Summary of results

No significant changes were observed in MMP-2 [$X^2(3) = 1.06$, p=0.787], MMP-3 [$X^2(3) = 5.22$, p=0.156] and CEACAM-1 [$X^2(3) = 1.67$, p=0.64] serum concentrations up to 6 months following TURBT for the treatment of NMIBC.

There was however a significant decrease in serum MMP-9 concentration [$X^2(3) = 14.43$, p=0.002] up to 6 months following TURBT for the treatment of NMIBC.

With respect to MMP-9 and its association with angiogenesis and tumour growth, this marker may be considered to form part of a biomarker profile, for which NMIBC patients could be monitored as part of their follow-up and surveillance programmes.

6.0 Chapter Six: The role of various serum-based angiogenic and growth biomarkers in patients undergoing TURBT, for the treatment of NMIBC

6.1 Synopsis

With regards to this chapter, the major focus was to investigate changes in various serum-based biomarkers that associate with cancer growth and progression. 40 patients scheduled for TURBT for the treatment of NMIBC were recruited after informed consent (section 2.5.2). Blood sampling collection procedures were undertaken pre-operatively and at 1 month, 3 months and 6 months post-operatively (section 2.5.3).

Using commercially available assay kits (sections 2.5.6), serum concentrations of various cancer growth markers were measured. Specifically, markers investigated included: basic fibroblast growth factor (bFGF), Follistatin, human epidermal growth factor receptor 2 (HER-2/neu), platelet derived growth factor (PDGF), Stem cell factor (SCF), soluble epidermal growth factor receptor (sEGFR), TIE-2 and vascular endothelial growth factors A, C and D (VEGF-A, VEGF-C and VEGF-D) and VEGF receptors 1 and 2 (VEGFR-1 and VEGFR-2).

The main aim of this study was to investigate the effect of TURBT for the treatment of BC on novel biomarkers, which may ultimately provide key information that could help predict cancer recurrence and progression in BC patients following treatment.

6.2 Results

6.2.1 The effect of TURBT on Basic Fibroblast Growth Factor concentration (bFGF)

Figure 6.1 represents changes to serum bFGF (pg/ml) in patients who had TURBT for the treatment of NMIBC. This parameter was measured as a potential biomarker for angiogenesis, due to its role as a signalling marker for the FGF gene, which is highly expressed in BC. Data are presented in bar charts using mean (± Standard deviation). Baseline bFGF concentration increased from 414 (± 163) pg/ml to 456 (±123) pg/ml at 1-month post-operative. bFGF levels further increased at 3-months post-operative 494 (±155) pg/ml, peaking at 6-months post-operative 523 (±119) pg/ml. Even though bFGF concentration increased from baseline up to 6 months post-operatively, no statistical significance was achieved (Wilks' Lambda= 0.67, $F_{(3,48)}$ = 1.933, p=0.137) as determined by the ANOVA Test.

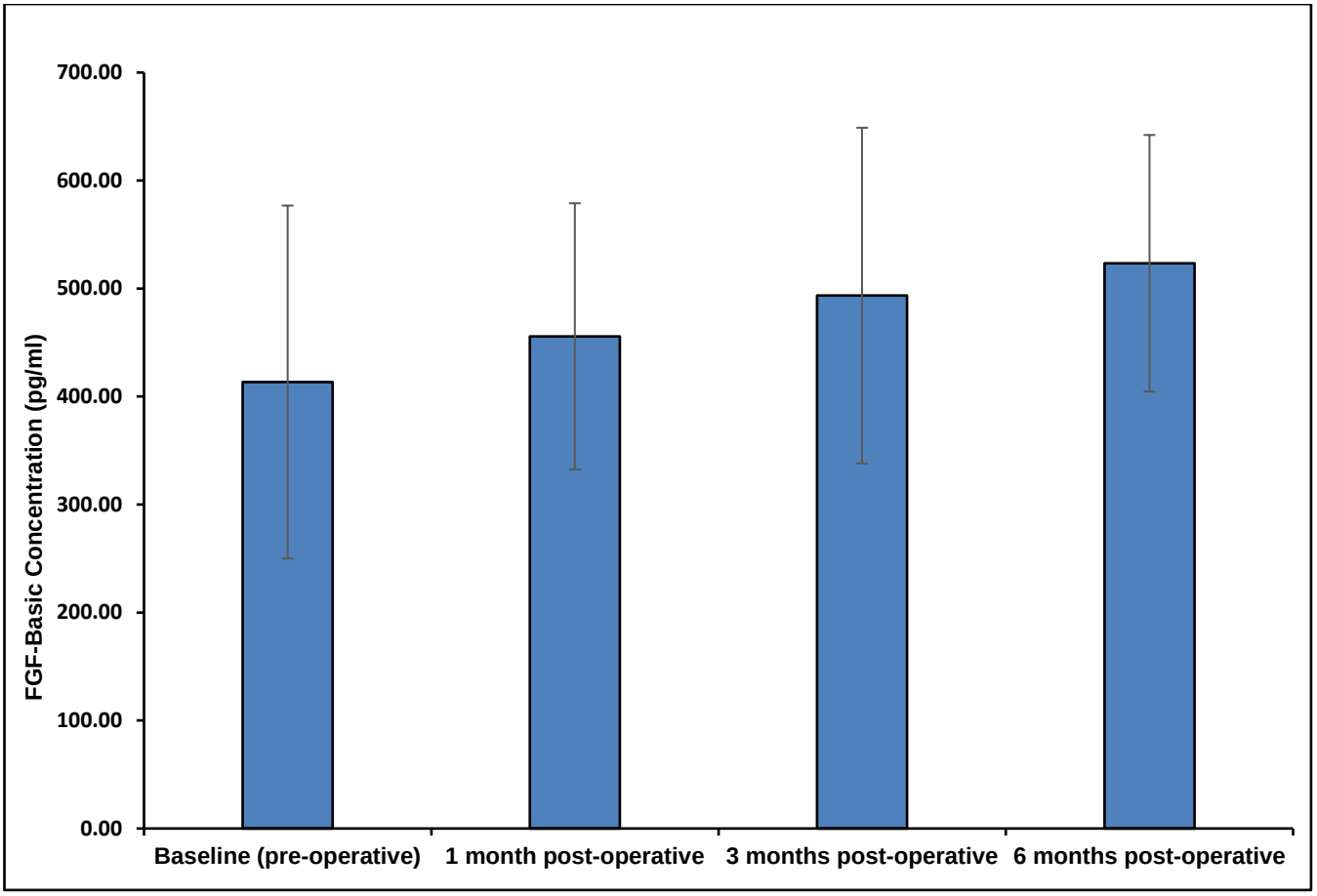

Figure 6. 1 The effect of TURBT on serum basic Fibroblast growth factor concentration. The points represent [mean ± SD) as determined by Anova, (Wilks' Lambda= 0.67, $F_{(3,48)}$ = 1.933, p=0.137), n=40.

6.2.2 The effect of TURBT on PDGF concentration

Figure 6.2 represents changes to PDGF concentration (pg/ml) in patients who had TURBT for the treatment of NMIBC. PDGF was measured due to its role as a potential biomarker for assessing angiogenesis, an important hallmark of cancer growth. Data are presented in box plots using median (interquartile ranges). There was a significant decrease in serum PDGF concentration up to 6 months after TURBT [($X^2(3)$ = 10.91, p=0.012), as determined by the Friedman test]. PDGF concentration decreased from 1714 pg/ml, (1128-2632) at baseline to 1594 pg/ml, (783-2119) at 1-month post-operative and 1331 pg/ml, (702-1496) at 3-months post-operative. At 6-months post-operative however, PDGF concentration increased to 1431 pg/ml, (903-1932). On further statistical analysis using the Wilcoxon's signed test, there was a significant difference between baseline and 3-months post-operative PDGF concentrations (Z= -2.20, p=0.028, r= 0.534).

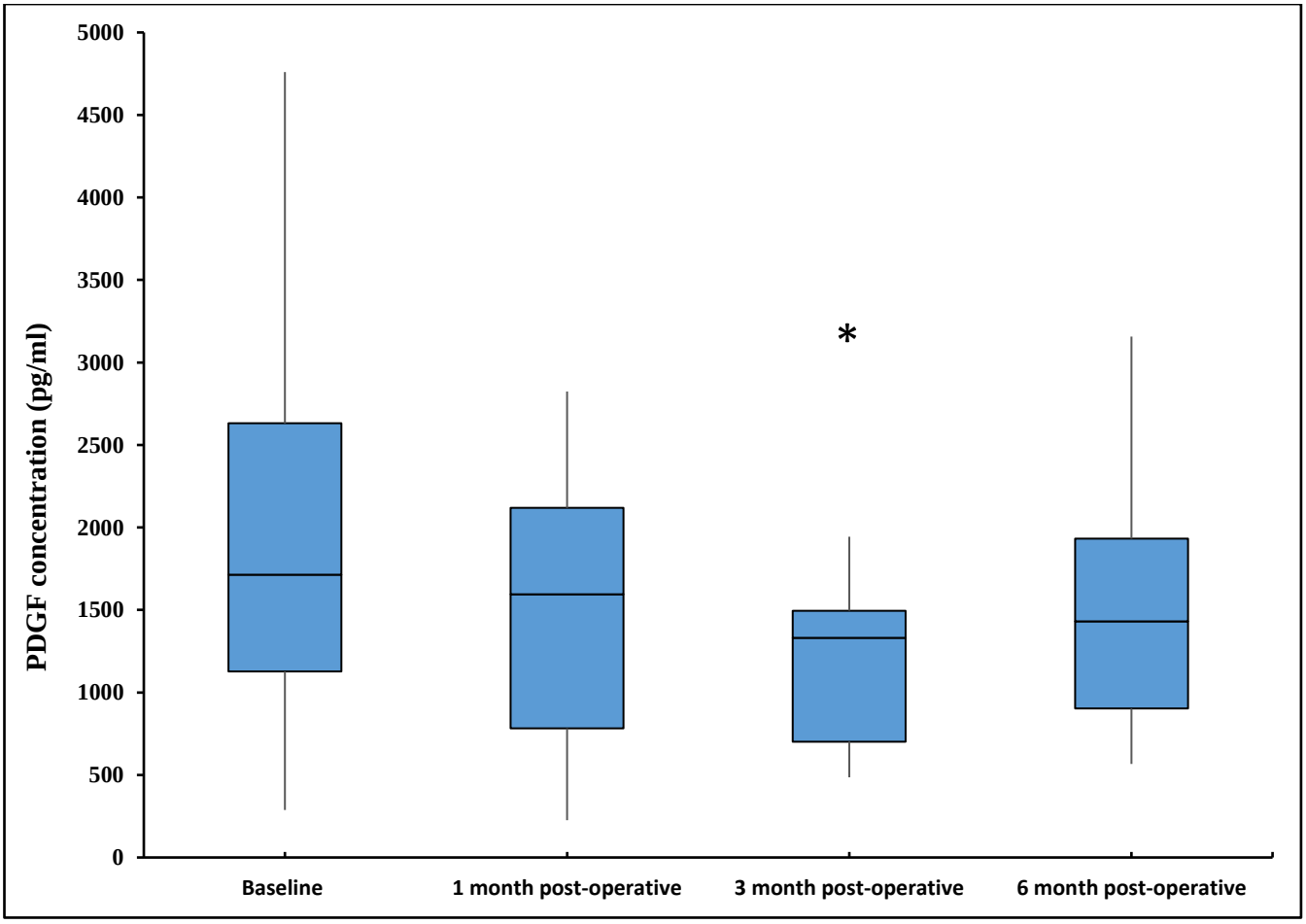

Figure 6. 2 The effect of TURBT on serum PDGF concentration.
The points represent [Median, (interquartile range) p=0.012 as determined by Friedman, significant difference (*) between baseline Vrs 3-months post-operative ((Z= -2.20, p=0.028, r= 0.534), n=40.

6.2.3 The effect of TURBT on SCF concentration

Figure 6.3 represents changes to SCF concentrations (pg/ml) in patients who had TURBT for the treatment of NMIBC. SCF was measured as a potential biomarker for cancer growth. Data are presented in box plots using median (interquartile ranges). There was a significant increase in SCF concentration up to 6-months after TURBT [($X^2(3) = 8.79$, p=0.032), as determined by Friedman test]. SCF concentration increased from 516 pg/ml, (430-617) at baseline to 598 pg/ml, (396-652) at 1-month post-operative. At 3-months post-operative, SCF concentration decreased to 539 pg/ml, (508-713) before finally increasing to 546 pg/ml, (480-671) at 6-months post-operative. On further statistical analysis using the Wilcoxon's signed test, there was a significant change between baseline and 3-months post-operative (Z= -2.82, p=0.005, r= 0.65).

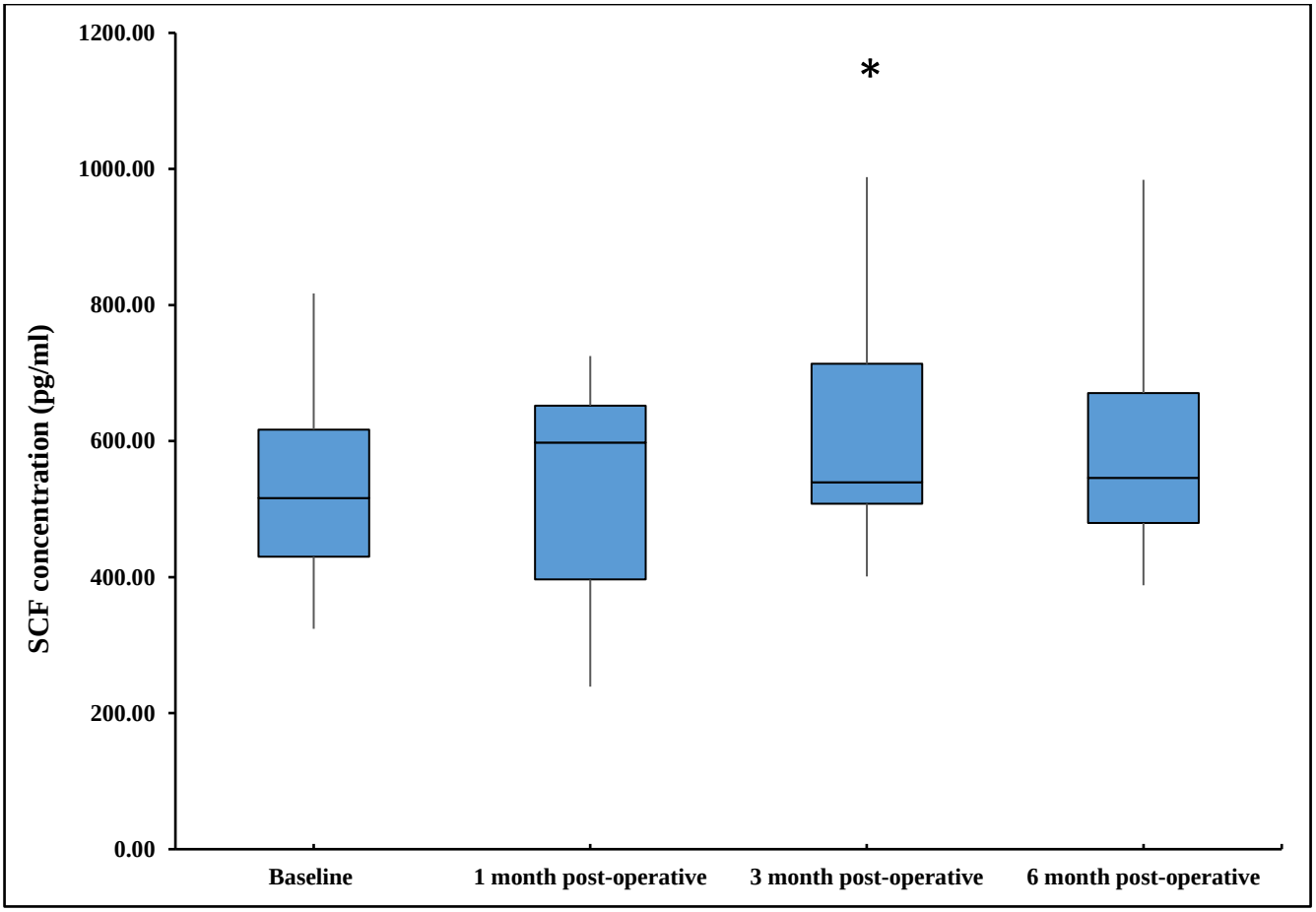

Figure 6. 3 The effect of TURBT on serum SCF concentration.
The points represent [Median, (interquartile range), $X^2(3) = 8.79$, p=0.032 as determined by Friedman, significant difference (*) between baseline versus 3-months post-operative (Z= -2.82, p=0.005, r= 0.65), determined by Wilcoxon's signed test, n=40.

6.2.4 The effect of TURBT on Follistatin concentration

Figure 6.4 represents changes to Follistatin concentrations (pg/ml) in patients who had TURBT for the treatment of NMIBC. The parameter was measured as a potential biomarker for assessing cancer growth following surgical treatment for BC. Data are presented in box plots using median (interquartile ranges). The serum Follistatin concentration remained relatively unchanged between baseline 1074 pg/ml, (769-1237) and 1-month post-operative 1057 pg/ml, (644-1567). The concentration, however, increased at 3-months post-operative 1301 pg/ml, (812-1516) and at 6 months post-operative 1257 pg/ml, (839-1348). Statistical analysis was performed using the Friedman test, although no statistical significance was achieved ($X^2(3) = 2.91$, p=0.403).

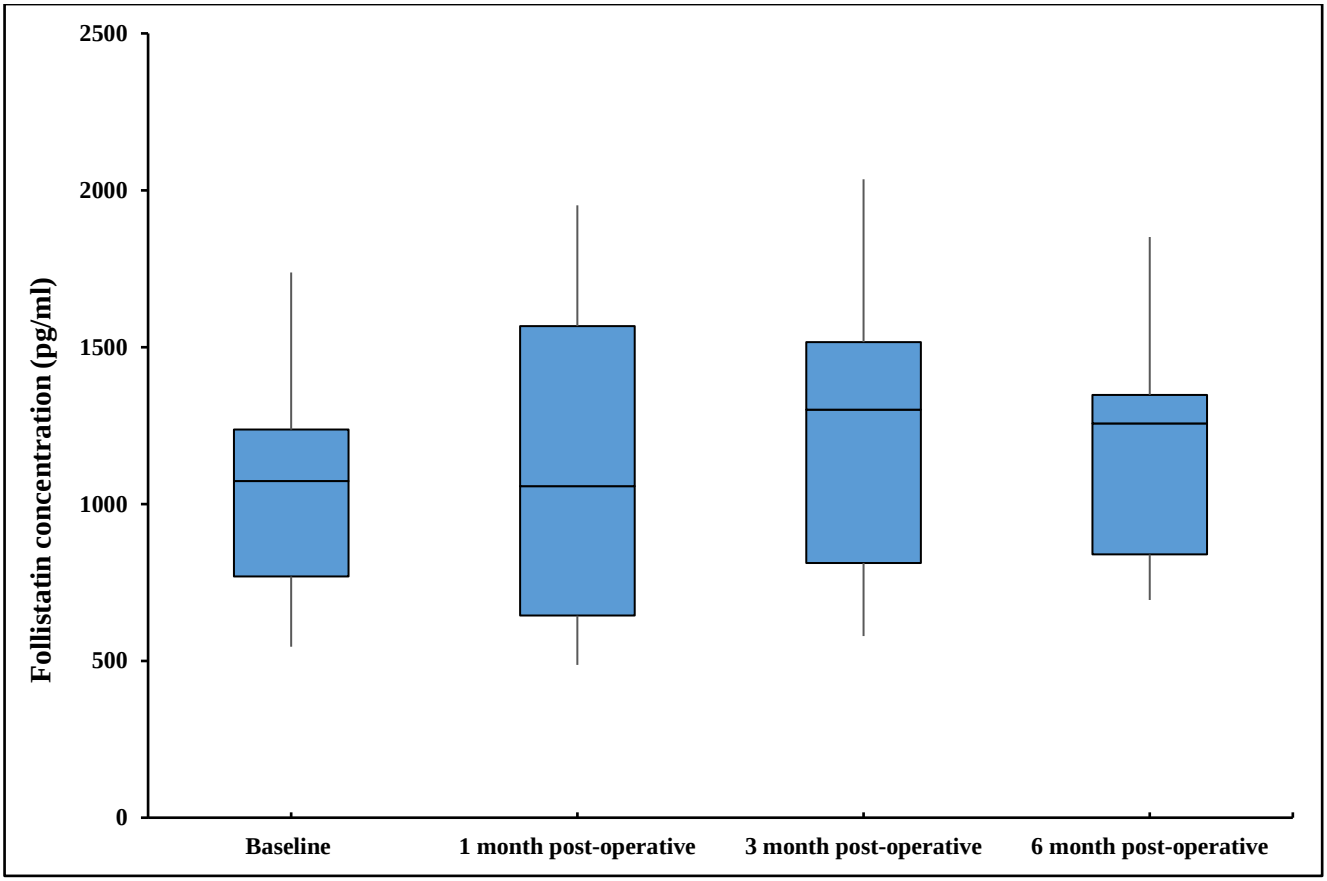

Figure 6. 4 The effect of TURBT on serum Follistatin concentration. The points represent median, (interquartile range) as determined by Friedman X2(3) = 2.91, p=0.403, n=40.

6.2.5 The effect of TURBT on HER-2/neu concentration

Figure 6.5 represents changes to serum HER-2/neu concentrations (pg/ml) in patients who had TURBT for the treatment of NMIBC. This parameter was measured as a potential biomarker for assessing cancer growth. HER-2/neu immunoreactivity is usually an indicator of cell proliferation and can be used to assess cancer growth. Data are presented in box plots using median (interquartile ranges). There was a trend of decreasing HER-2/neu concentration up to 6 months post-operatively. HER-2/neu serum concentration decreased from 5406 pg/ml, (3446-7823) at baseline, to 4157.43 pg/ml, (3309-7471) at 1-month post-operative. At 3-months post-operative however, HER-2/neu concentration increased to 4930 pg/ml, (4140-5884) before finally decreasing to at 6-months post-operative to 4396 pg/ml, (3752-5559). There was no statistical significance ($X^2(3) = 4.441$, p=0.22), as determined by the Friedman test.

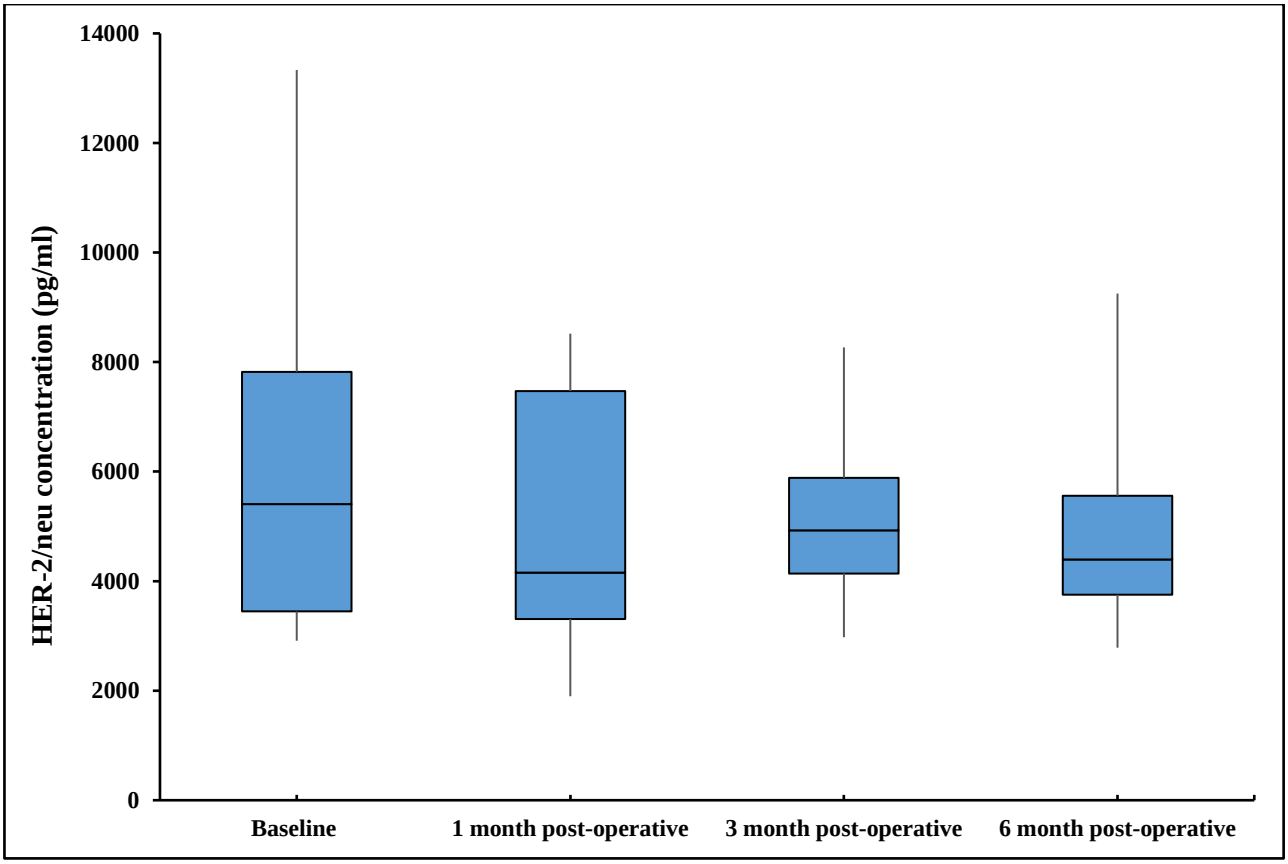

Figure 6. 5 The effect of TURBT on serum HER-2/neu concentration.
The points represent [Median, (interquartile range), X2(3) = 4.441, p=0.22], as determined by Friedman, n=40.

6.2.6 The effect of TURBT on sEGFR concentration

Figure 6.6 represents changes to sEGFR concentrations (pg/ml) in patients who had TURBT for the treatment of NMIBC. sEGFR was measured as potential biomarkers for cancer growth. Data are presented in box plots using median (interquartile ranges). sEGFR serum concentration decreased from 14384 pg/ml, (11930-22672) at baseline to 13093 pg/ml, (10539-19821) at 1-month post-operative. At 3-months post-operative, serum sEGFR concentration increased to 15148 pg/ml, (12081-19085) before decreasing to 14869 pg/ml, (12659-17502) at 6-months post-operative. There was no significant change in sEGFR concentrations ($X^2(3) = 5.26$, p=0.15) as determined by the Friedman test.

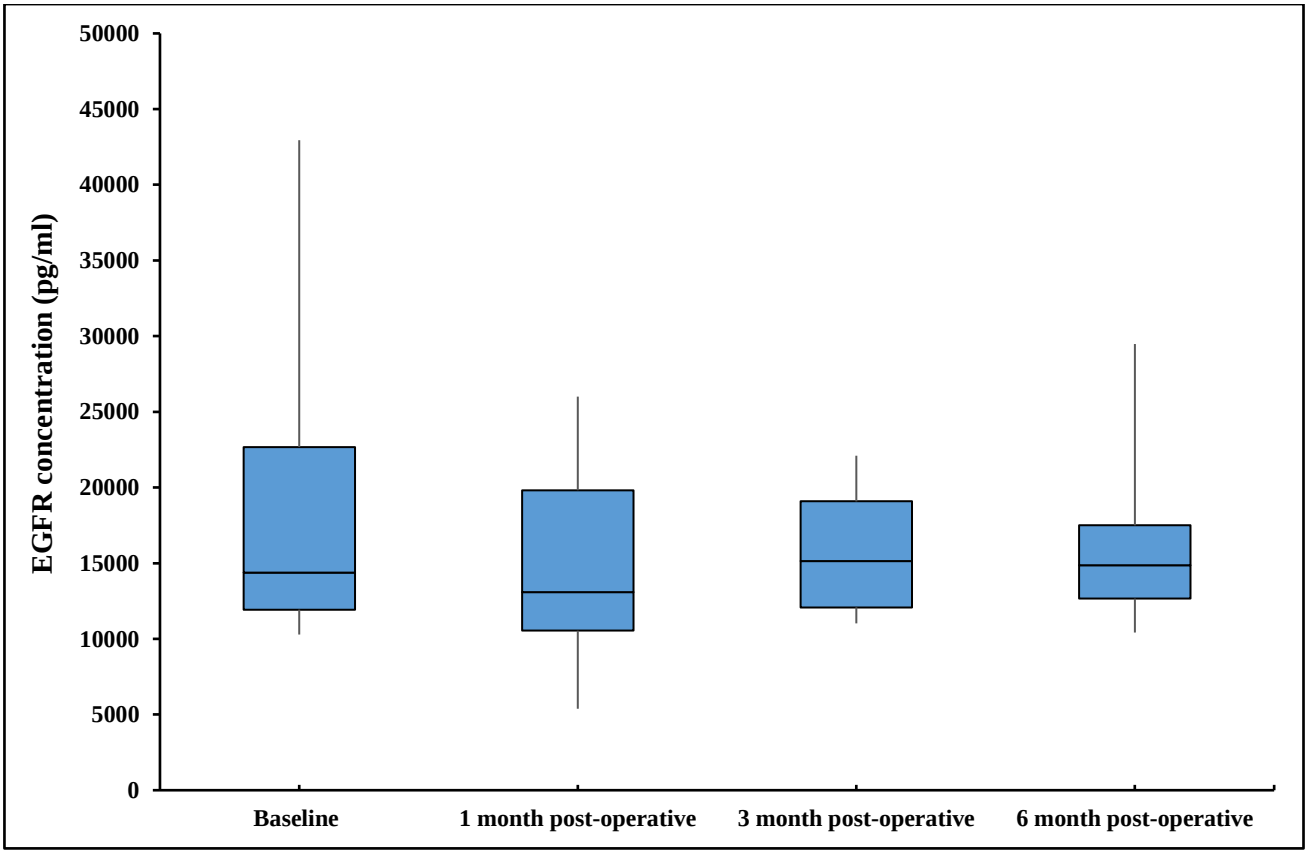

Figure 6. 6 The effect of TURBT on serum sEGFR concentration.
The points represent [Median, (interquartile range), ($X^2(3) = 5.26$, p=0.15 as determined by Friedman, n=40.

6.2.7 The effect of TURBT on EGF concentration

Figure 6.7 represents changes to EGF concentrations (pg/ml) in patients who had TURBT for the treatment of NMIBC. EGF was measured as potential biomarkers for cancer growth. Data are presented in box plots using mean (±SD). Serum EGF concentrations were relatively unchanged from baseline 120 (± 47) to 1-month post-operative (121 ± 51). At 3-months post-operative, serum EGF concentration decreased to 101 (± 47) and moderately increased at 6-months post-operative to 105 (± 51). Statistically, these changes were not significant, as determined by the Anova test (Wilk's Lambda= 0.67, $F_{(3,48)} = 2.839$, p=p=0.09).

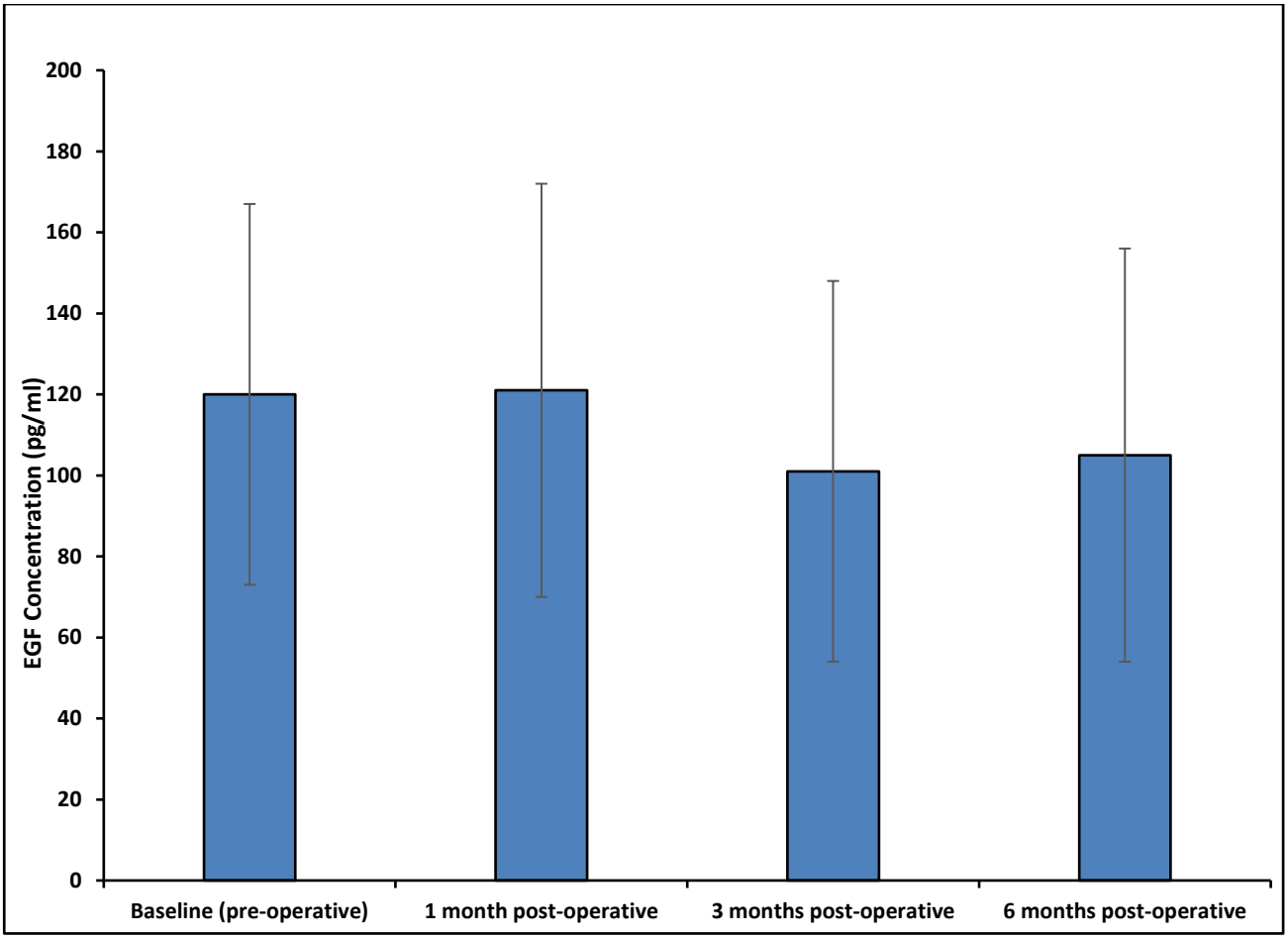

Figure 6. 7 The effect of TURBT on serum EGF concentration.
The points represent [Mean ± SD], Wilk's Lambda= 0.67, $F_{(3,48)} = 2.839$, p=0.09, as determined by Anova, n=40.

6.2.8 The effect of TURBT on TIE-2 concentration

Figure 6.8 represents changes to TIE-2 concentrations (pg/ml) in patients who had TURBT for the treatment of NMIBC. TIE-2 was measured as a potential biomarker for angiogenesis. Data are presented in box plots using median (interquartile ranges). TIE-2 concentration increased from 10896 pg/ml, (9504-12426) at baseline to 11139 pg/ml, (8620-13018) at 1-month post-operative. At 3-months post-operative, TIE-2 concentration decreased to 10620 pg/ml, (9302-13296) before increasing to 10723 pg/ml, (8974-13252) at 6-months post-operative. There was no statistical significance ($X^2(3) = 1.52$, p=0.68) as determined by the Friedman test.

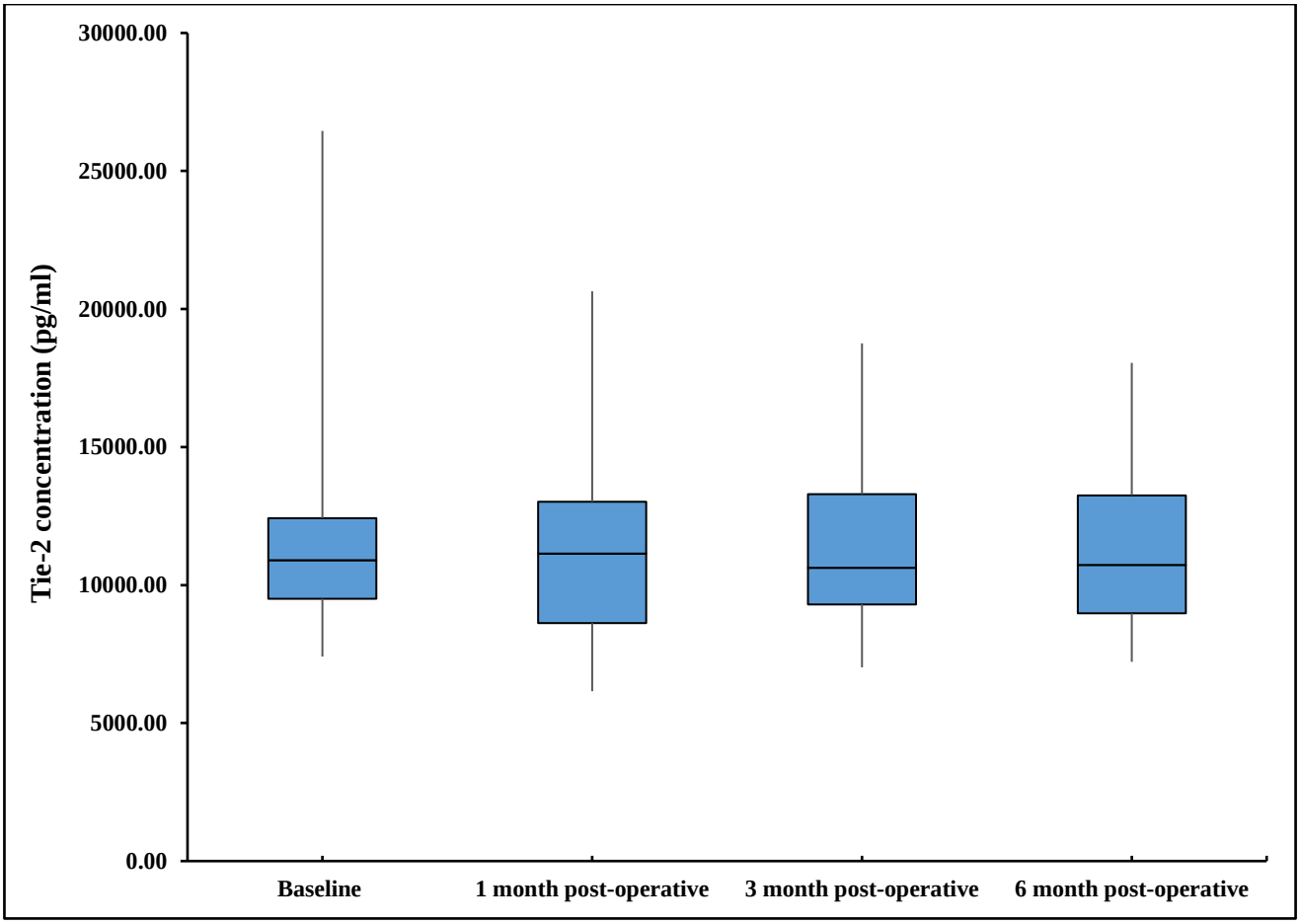

Figure 6. 8 The effect of TURBT on serum TIE-2 concentration. The points represent [Median, (interquartile range) $X^2(3) = 1.52$, p=0.68 as determined by Friedman, n=40.

6.2.9 The effect of TURBT on VEGF-A concentration

Figure 6.9 represents changes to VEGF-A concentrations (pg/ml) in patients who had TURBT for the treatment of NMIBC. This marker was investigated due to its roles in tumour growth and angiogenesis. Data are presented in box plots using median (interquartile ranges).

With regards to VEGF-A, baseline serum concentrations increased from 1244, (430-1441) (pg/ml) to 1255 (401-1472) (pg/ml) at 1-month post-operative. At 3-months post-operative, serum concentrations decreased to 1221 (336-1343) (pg/ml) and further decreased at 6-months post-operative to 1136 (330-1277) (pg/ml). There was no statistical significance in VEGF-A serum concentrations up to 6-months after TURBT ($X^2(3) = 3.776$, p=0.29), as determined by the Friedman test.

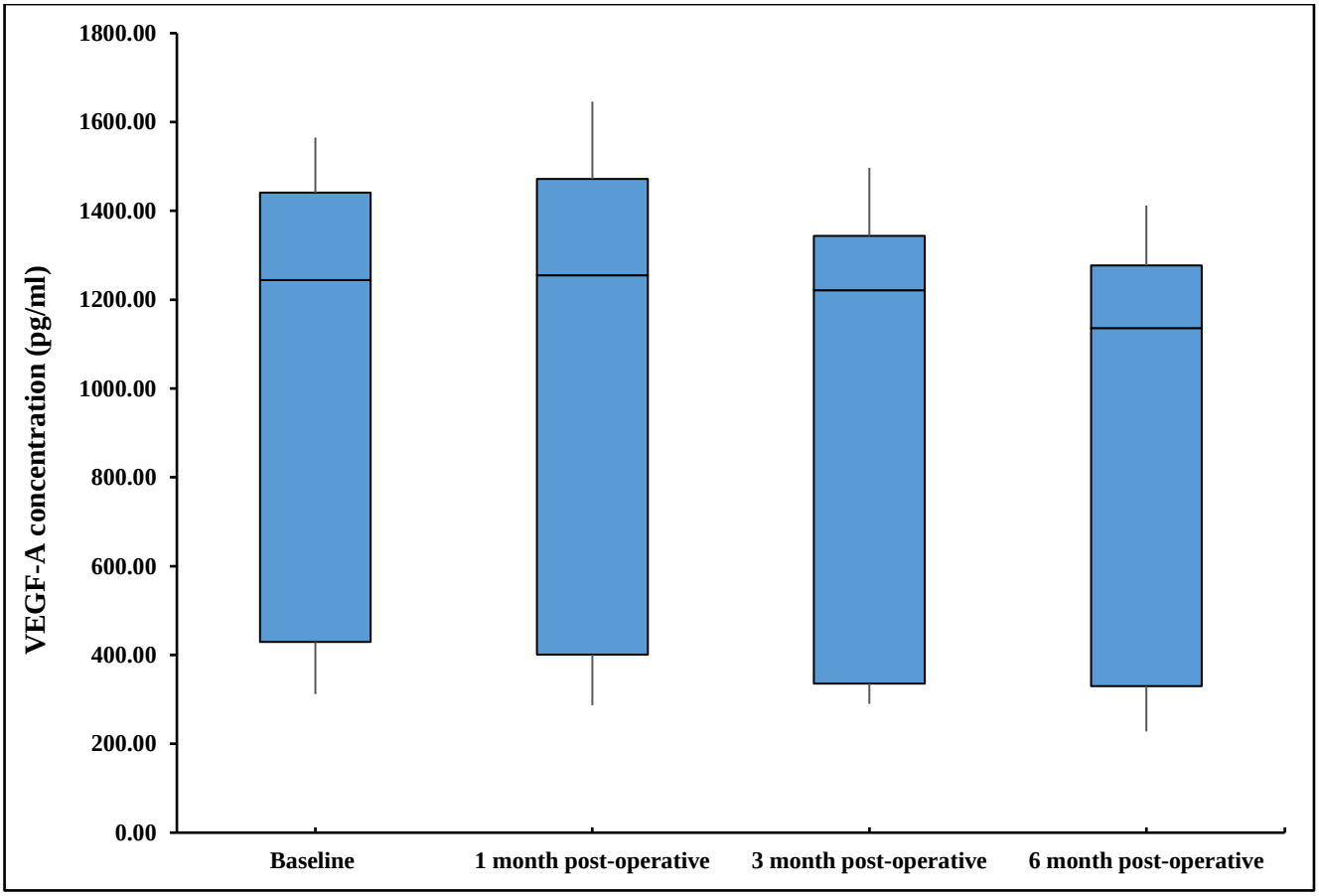

Figure 6. 9 The effect of TURBT on serum VEGF-A concentration
VEGF-A, points represent [Median, (interquartile range) $X^2(3) = 3.776$, p=0.29 as determined by Friedman, no=40

6.2.10 The effect of TURBT on VEGF-C concentration

Figure 6.9 represents changes to VEGF-C concentrations (pg/ml) in patients who had TURBT for the treatment of NMIBC. This marker was investigated due to its roles in tumour growth and angiogenesis. Data are presented in bar charts using mean (±SD).

There was a statistically significant decrease in serum VEGF-C concentration following TURBT [(Wilk's Lambda= 0.624, $F_{(3,48)} = 3.612$, p=0.04), as determined by Anova]. Serum VEGF-C concentration increased from 2711 (± 971) (pg/ml) at baseline to 2821 (± 988) (pg/ml) at 1-month post-operative. At 3-months post-operative, Serum VEGF-C concentrations decreased to 2406 (± 795), before moderately increasing to 2421 (± 785) at 6-month post-operative. On further statistical analysis using the Bonferoni post-hoc test. There was a significant difference between 1-month post-operative and 3-months post-operative serum VEGF-C concentrations (p=0.05).

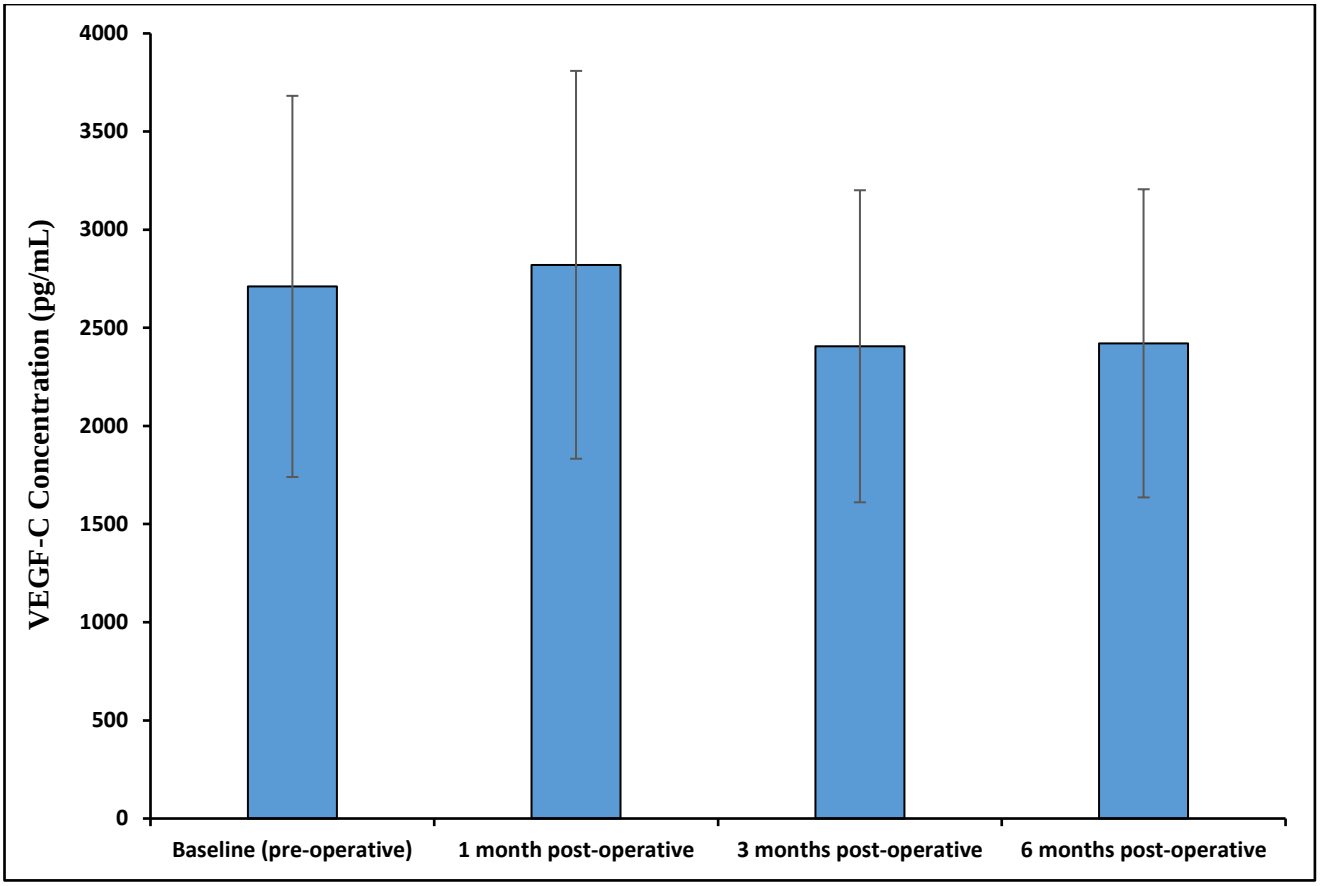

Figure 6. 10 The effect of TURBT on serum VEGF-C concentration
VEGF-C, points represent Mean ± SD, (Wilk's Lambda= 0.624, $F_{(3,48)}$ = 3.612, p=0.04). Significant change between 1-month and 3-months (p=0.05), as determined by Bonferroni test.

6.2.11 The effect of TURBT on VEGF-D concentration

Figure 6.11 represents changes to VEGF-D concentrations (pg/ml) in patients who had TURBT for the treatment of NMIBC. This marker was investigated due to its roles in tumour growth and angiogenesis. Data are presented in box plots using median (Inter Quartile Ranges). There was a slight increase in VEGF-D concentration from 2335 (649-2538) (pg/ml) to 2338 (695-2638) (pg/ml) at 1-month post-operative. VEGF-D concentrations then decreased at 3-months post-operative to 2259 (582-2482) (pg/ml) and further decreased to 2247 (594-2476) (pg/ml) at 6-months post-operative. There was no statistical significance ($X^2(3) = 2.012$, p=0.57), as determined by the Friedman test.

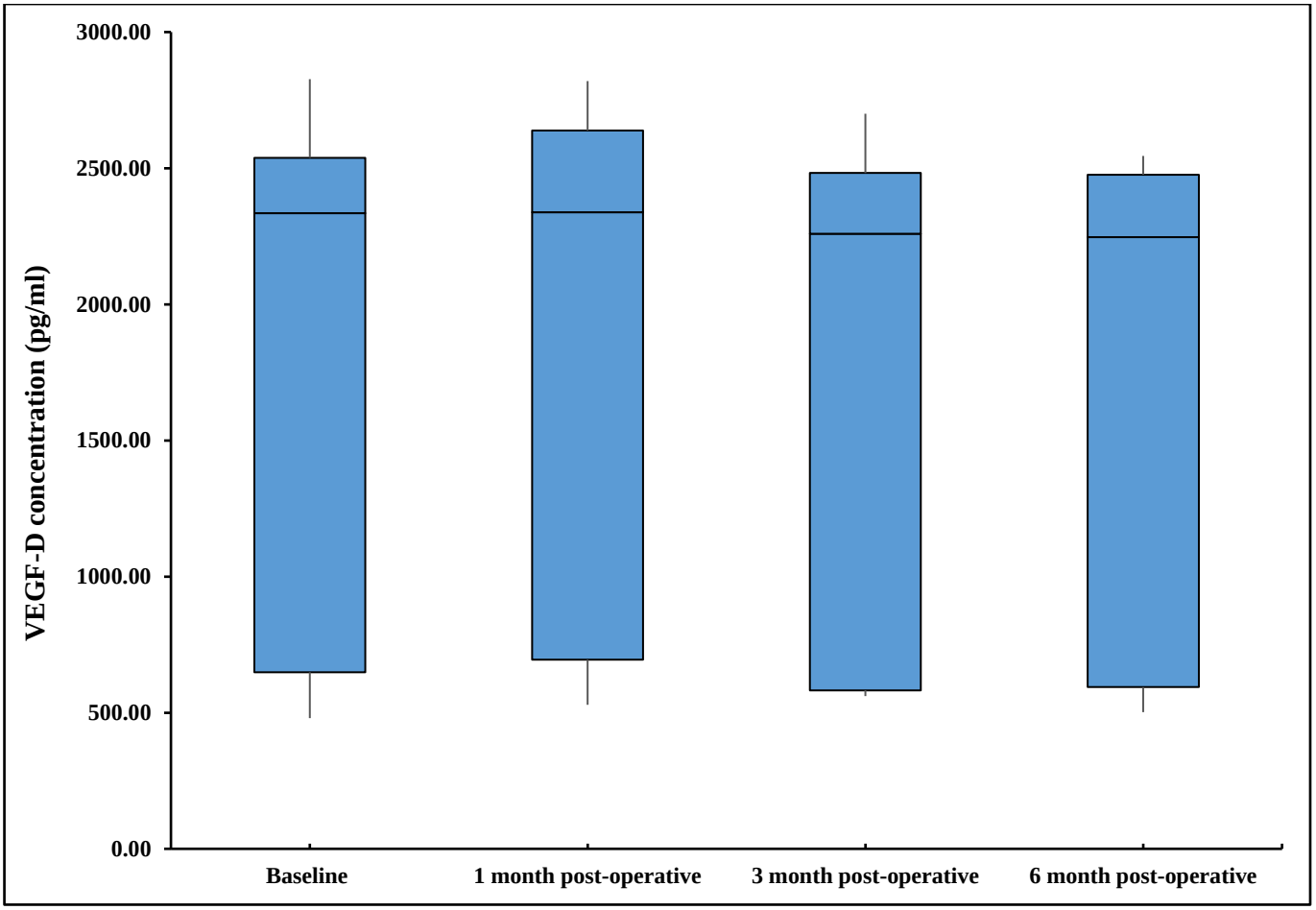

Figure 6. 11 The effect of TURBT on serum VEGF-D concentration
VEGF-D, points represent Median, (interquartile range), $X^2(3) = 2.012$, p=0.57, as determined by Friedman. n=40.

6.2.12 The effect of TURBT on VEGFR-1 concentration

Figure 6.12 represents changes to VEGFR-1 concentrations (pg/ml) in patients who had TURBT for the treatment of NMIBC. VEGFR-1 was measured as a potential biomarker for assessing cancer growth due to roles it plays in angiogenesis. Data are presented in bar charts using mean (±SD). The VEGFR-1 concentration increased from 1911 (± 208) pg/ml at baseline to 2247 (± 221) pg/ml at 1-month post-operative. At 3-months post-operative, VEGFR-1 concentration decreased to 2100 (± 188) pg/ml before peaking at 6-months post-operative 2251 (± 227) pg/ml. There was no statistical significance as determined by ANOVA test (Wilk's Lambda= 0.898, $F_{(3,48)} = 0.782$, p=0.15).

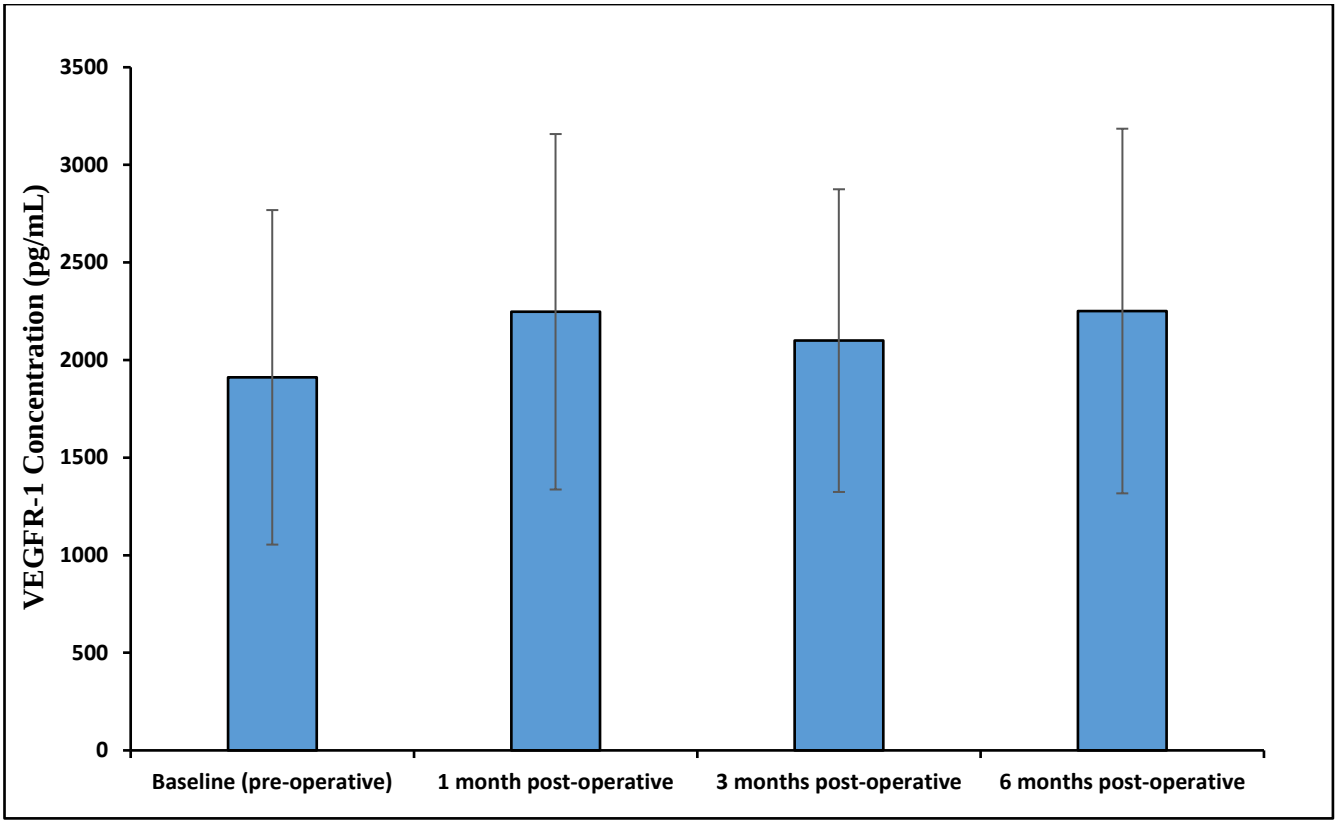

Figure 6. 12 The effect of TURBT on serum VEGFR-1 concentration.
The points represent [mean ± SE Mean), Wilk's Lambda= 0.898, $F_{(3,48)} = 0.782$, p=0.15), as determined by ANOVA, n=40.

6.2.13 The effect of TURBT on VEGFR-1 & 2 concentration

Figure 6.13 represents changes to VEGFR-2 concentrations (pg/ml) in patients who had TURBT for the treatment of NMIBC. VEGFR-2 was measured as a potential biomarker for assessing cancer growth due to roles it plays in angiogenesis. Data are presented in bar charts using mean (±SD). The VEGFR-2 concentration decreased from 5433 (± 470) pg/ml at baseline to 5266 (± 375) pg/ml at 1-month post-operative. VEGFR-2 concentration then increased at 3-months post-operative 6062 (± 465) pg/ml and peaked at 6-months post-operative 6371 (± 503) pg/ml. There was no statistical significance as determined by ANOVA test (Wilk's Lambda= 0.533, $F_{(3,48)} = 1.835$, p=0.15).

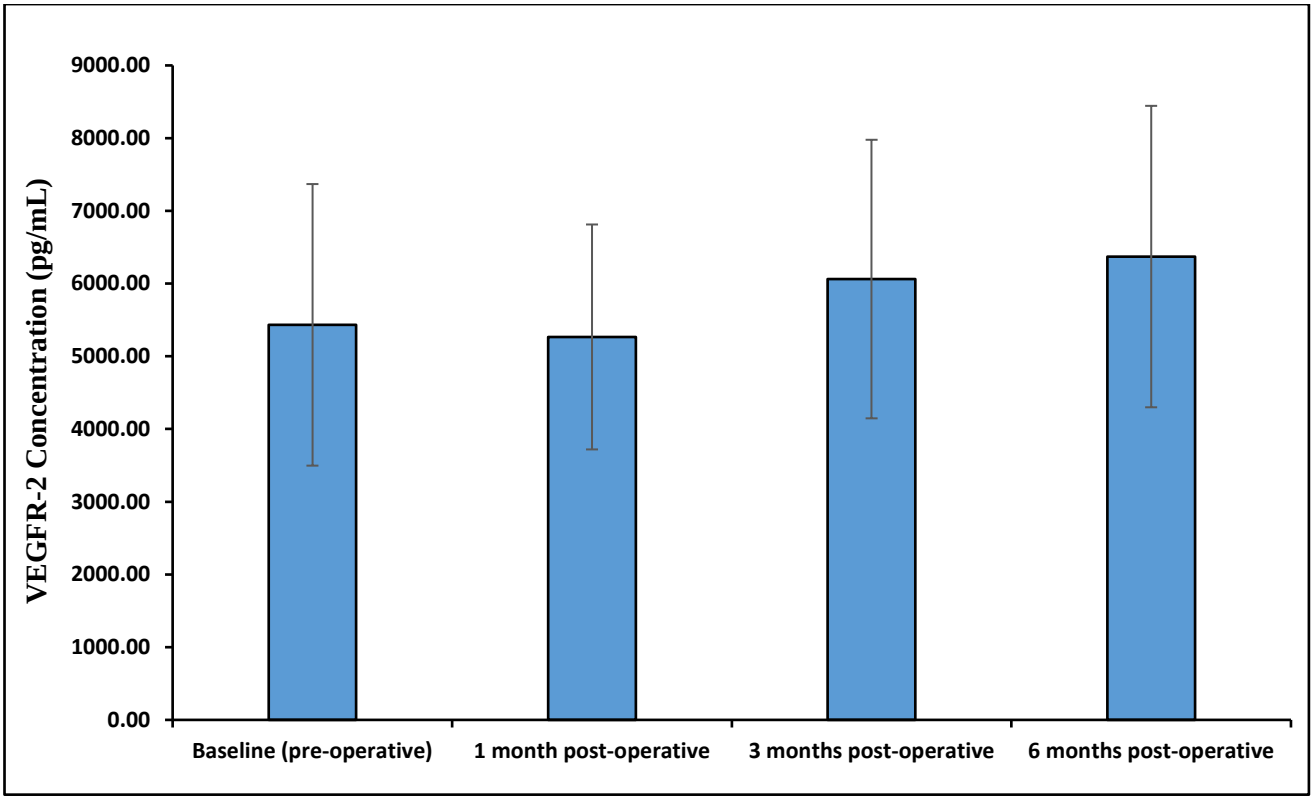

Figure 6. 13 The effect of TURBT on serum VEGFR-2 concentration.
The points represent [mean ± SE Mean), Wilk's Lambda= 0.533, $F_{(3,48)}$= 1.835, p=0.15 as determined by ANOVA, n=40.

6.3 Summary of results

The results presented above indicate changes in serum levels of various markers of angiogenesis and cancer growth in recruited BC patients following surgical treatment. Specifically

- There were significant changes in serum PDGF concentration ($X^2(3) = 10.91$, $p=0.012$).
- There were significant changes in serum SCF concentration ($X^2(3) = 8.79$, $p=0.032$).
- There were significant changes in serum VEGF-C concentration (Wilk's Lambda= 0.624, $F_{(3,48)} = 3.612$, $p=0.04$)
- There were trends of increasing concentrations in serum EGFR, HER-2/neu, VEGFR-1 and VEGFR-2
- There were also trends of increasing concentration in serum FGF-basic

7.0 Chapter Seven: The role of novel antibody immunoreactivity and their association with BC recurrence and progression

7.1 Synopsis

The main focus of this chapter was to evaluate the presence or levels of various tissue-based biomarkers in BC patients following TURBT. The selected biomarkers were investigated due their reported roles in angiogenesis and inflammation-associated cancer growth and progression.

During TURBT surgery, bladder tumour tissues taken in theatre were processed into FFPE blocks and used for the diagnosis and management of BC, according to NICE standard guidelines. 4 µm tissue sections were cut from FFPE blocks for each antibody and stained for the various antibodies using IHC.

The selective antibodies studied in this chapter are CD31, CD34, thrombomodulin, HER-2/neu, S100P, COX-2, SOX-2, CEACAM-1 and VEGFR-3. With regards to IHC analyses, each of these selective biomarkers was stained in FFPE bladder tissues from 35 patients (i.e. for CD31, 35 tissue sections were stained, one for each patient; for CD34, 35 tissue sections were stained, one for each patient, and so on).

In this present study, antibody immunoreactivity was analysed using IHC. Prior to staining patient tissues, validation of the IHC staining protocol was performed for each antibody and has been presented elsewhere (Section 3.1.8).

With the help of an experienced Senior Histologist (Alexander Makanga, HCPC Biomedical Scientist: BS61888) and a Consultant Pathologist, stained IHC slides were reported with careful consideration of Bladder tumours. IHC scores were reported as summarised in various tables below. Slides were reported as negative/zero, weak/+, ++ and +++, depending on the staining intensity and percentage immunoreactivity in Bladder tumour cells.

7.2 Results

7.2.1 Immunoreactivity of CD31 in BC patients

From an IHC perspective, CD31 may be used by pathologists in a range of clinical settings (e.g. haematological malignancies). This research focuses on their potential roles in tumour vascularisation in NMIBC, which is an indicator of angiogenesis.

The anti CD31 primary monoclonal antibody used in this study demonstrated cytoplasmic and membranous staining patterns in endothelial cells. IHC staining scores were obtained by examining each of the slides for the presence of antibody staining in endothelial cells close to tumour cells (Table 7.1) (Darai *et al.*, 1998; Wang *et al.*, 2008). A previous study has reported

CD31 staining patterns in normal human tissues (Pusztaszeri *et al.*, 2006) and tumour xenografts (Wang *et al.*, 2008).

The aim of this study was to initially identify the CD31 immunoreactivity in NMIBC tissue. The association between immunoreactivity and cancer recurrence and progression was then evaluated. Examples of each of the staining categories are presented in figures 7.1- 7.4, respectively.

Table 7. 1 Staining interpretation for IHC scores for anti-CD31
IHC immunoreactivity was determined by assessing the tumour cells staining intensity and percentage/quantity that were immunoreactive.

IHC Status	Meaning/Interpretation
Negative	No staining or Positive cytoplasmic/membranous staining in <5% of vascular endothelial cells in BC tumour
Positive (+)	Positive cytoplasmic/membranous staining in up to 20% vascular endothelial cells in Bladder tumour
Positive (++)	Positive cytoplasmic/membranous staining in up to 20-50% of vascular endothelial cells in Bladder tumour
Positive (+++)	Positive cytoplasmic/membranous staining in >50% of vascular endothelial cells in Bladder tumour

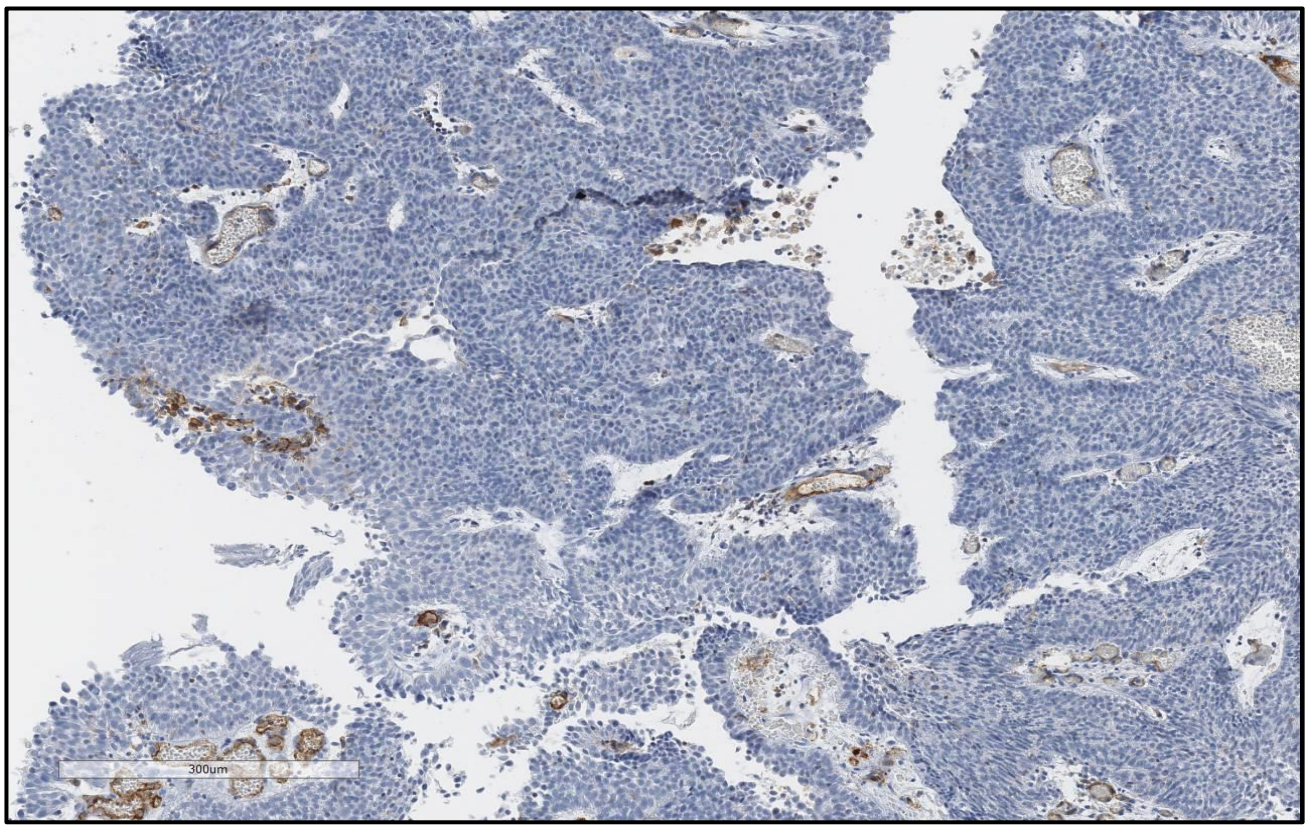

Figure 7. 1 Anti-CD31 antibody staining in BC tissues (negative).
No staining or positive cytoplasmic/membranous staining in <5% of endothelial cells in BC tissues. DAB detection. X100 magnification.

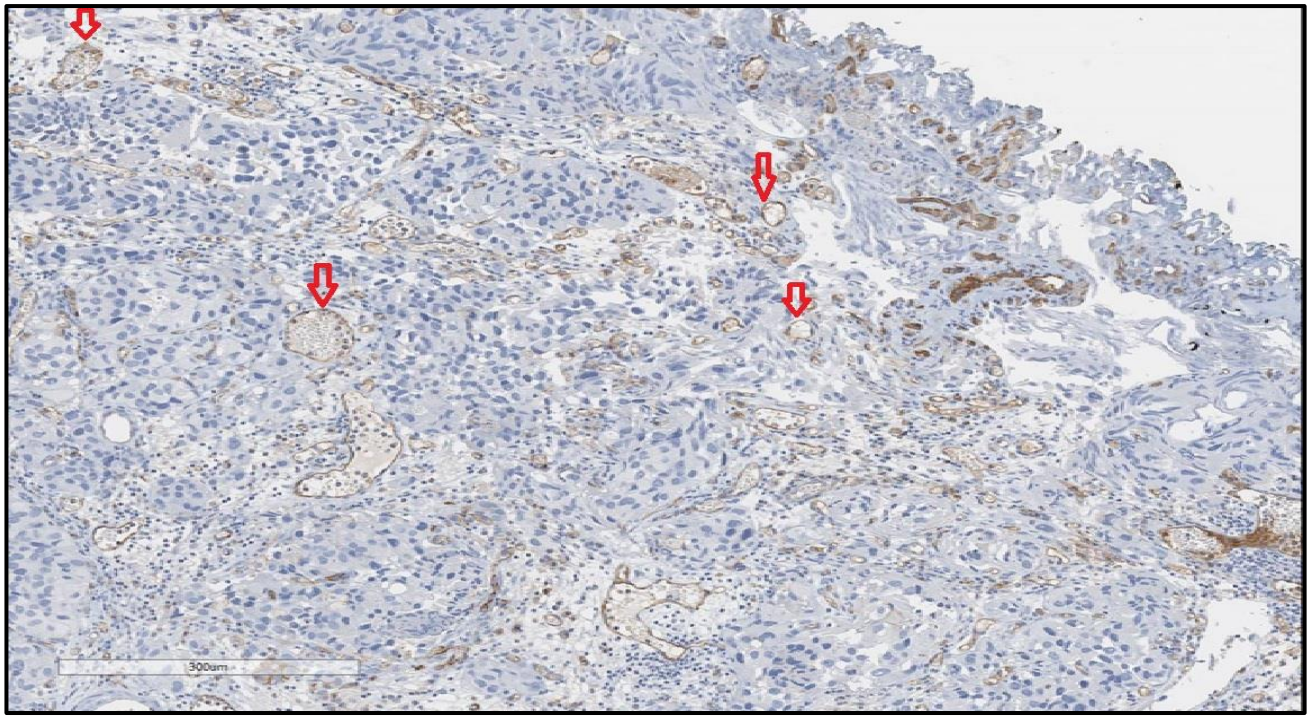

Figure 7. 2 Anti-CD31 antibody staining in BC tissues (IHC score= +).
Note the weak positive staining within vascular endothelial cells in the underlying muscle and stroma (Red arrows). Positive cytoplasmic/membranous staining in up to 20% of endothelial cells in bladder tumours. DAB detection. X100 magnification.

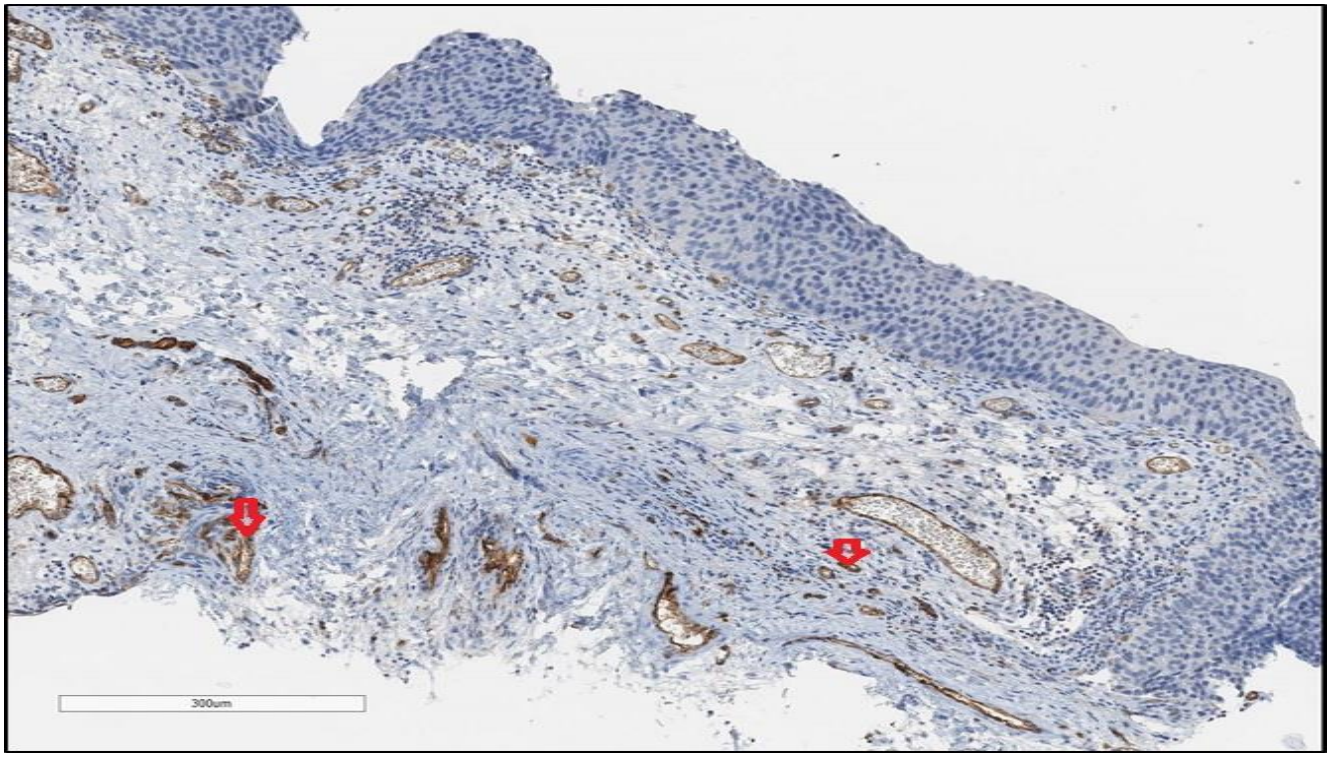

Figure 7. 3 Anti-CD31 antibody staining in BC tissues (IHC score= ++).
Red arrows show weak positive staining in vascular endothelial cells. Positive cytoplasmic/membranous staining in up to 20-50% of endothelial cells in Bladder tumour tissues. DAB detection. X100 magnification.

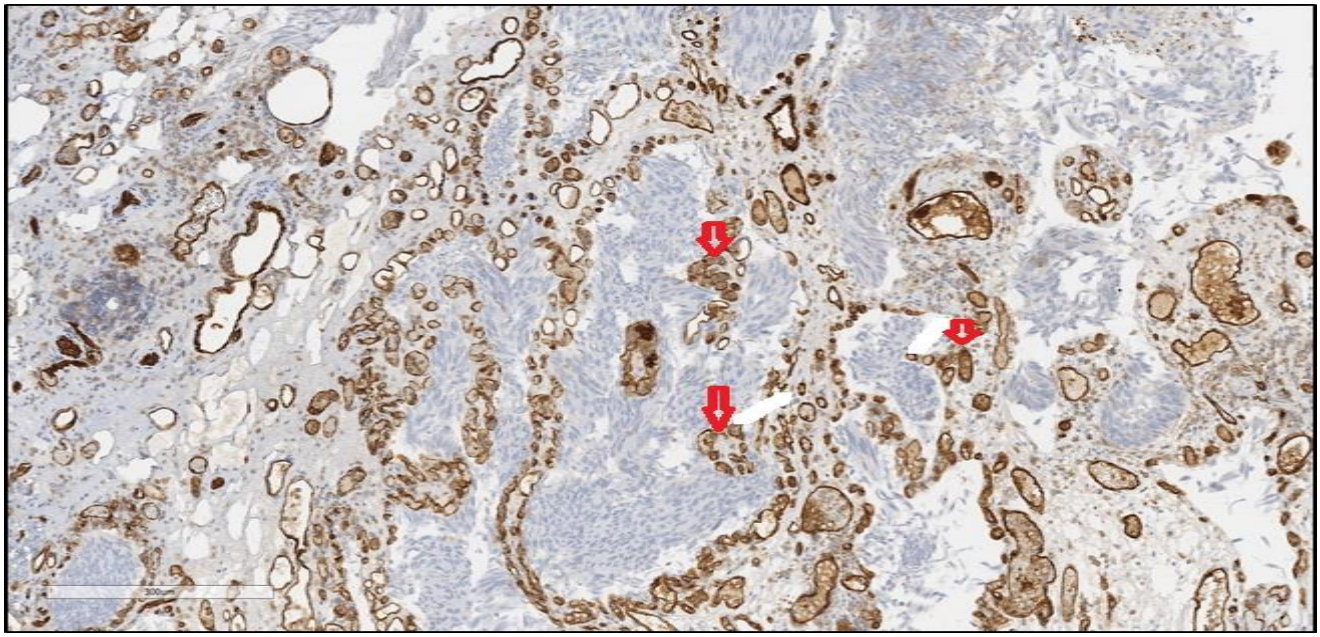

Figure 7. 4 Anti-CD31 antibody staining in BC tissues (IHC score= +++).
Note the positive staining (Red arrows) in vascular endothelial cells in vessels within tumour tissues. Positive cytoplasmic/membranous staining in >50% of endothelial cells in Bladder tumour tissues. DAB detection. X100 magnification.

Vascular endothelial cells in BC tissues had significantly higher anti CD31 immunoreactivity, compared to normal underlying tissues ($X^2(3) = 20.353$, $p< 0.001$), as determined by the Chi-square test (table 7.10).

With respect to cancer grading and staging, there was no significant association between patients' cancer grade and CD31 immunoreactivity ($X^2(2) = 2.719$, $p= 0.257$), as determined by the Kruskal-Wallis test. However, there was a significant association with cancer stage ($X^2(2)= 12.276$, $p= 0.002$), as determined by the Kruskal-Wallis test (table 7.10).

In the present study, 14 patients developed BC recurrence during the study period, all of which were diagnosed clinically during follow-up cystoscopies.

The relationship between antibody immunoreactivity (at diagnosis) vs BC recurrence was investigated via Mann-Whitney statistical test, and suggests that immunopositivity is not associated with an increased risk BC recurrence ($U= 102.00$, $p= 0.69$) (table 7.10).

7.2.2 Immunoreactivity CD34 in BC patients

From an IHC perspective, CD34 may be used by pathologists in a range of clinical settings (eg. Haematological malignancies), this research however focuses on their potential roles in tumour vascularisation, which is an indicator of angiogenesis.

The CD34 primary monoclonal antibody used in this study shows cytoplasmic and membranous staining patterns in vascular endothelial cells. IHC staining scores were obtained by examining each of the slides for the presence of antibody staining in vascular endothelial cells in BC tissues (Table 7.2) (Darai *et al.*, 1998; Wang *et al.*, 2008).

Table 7. 2 Staining interpretation for IHC scores for anti-CD34

IHC Status	Meaning/Interpretation
Negative	No staining or Positive cytoplasmic/membranous staining in <5% of vascular endothelial cells in BC tissues
Positive (+)	Positive cytoplasmic/membranous staining in up to 20% vascular endothelial cells in BC tissues
Positive (++)	Positive cytoplasmic/membranous staining in up to 20-50% vascular endothelial cells in BC tissues
Positive (+++)	Positive cytoplasmic/membranous staining in up to >50% vascular endothelial cells in BC tissues

The aim of this section was to initially identify CD34 immunoreactivity in NMIBC and subsequently compare these results in patients who had recurrence and progression. Examples of each of the staining categories are presented in figures 7.5- 7.8, respectively.

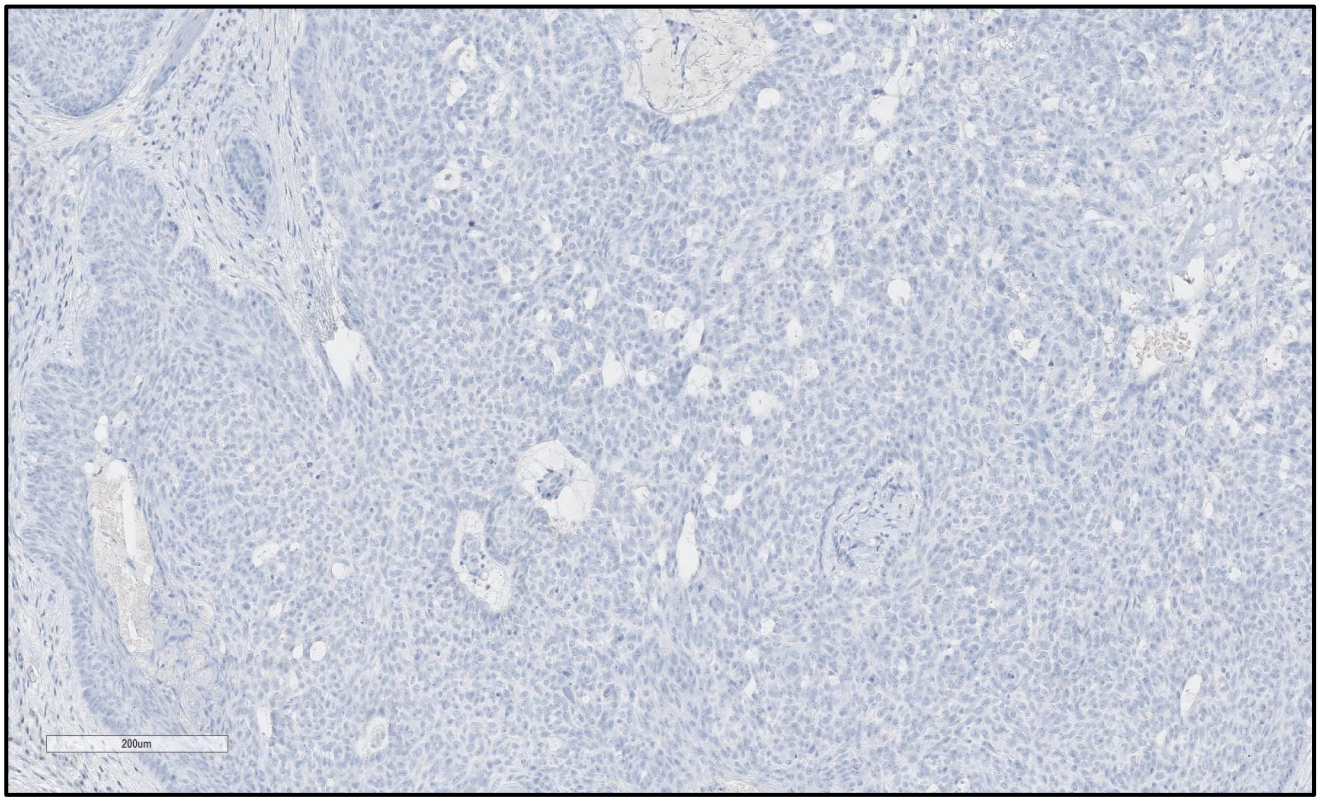

Figure 7. 5 Anti-CD34 antibody staining in BC tissues (negative).
Negative IHC staining in BC tissues. No staining or Positive cytoplasmic/membranous staining in <5% of endothelial cells in BC tissues. DAB detection. X100 magnification

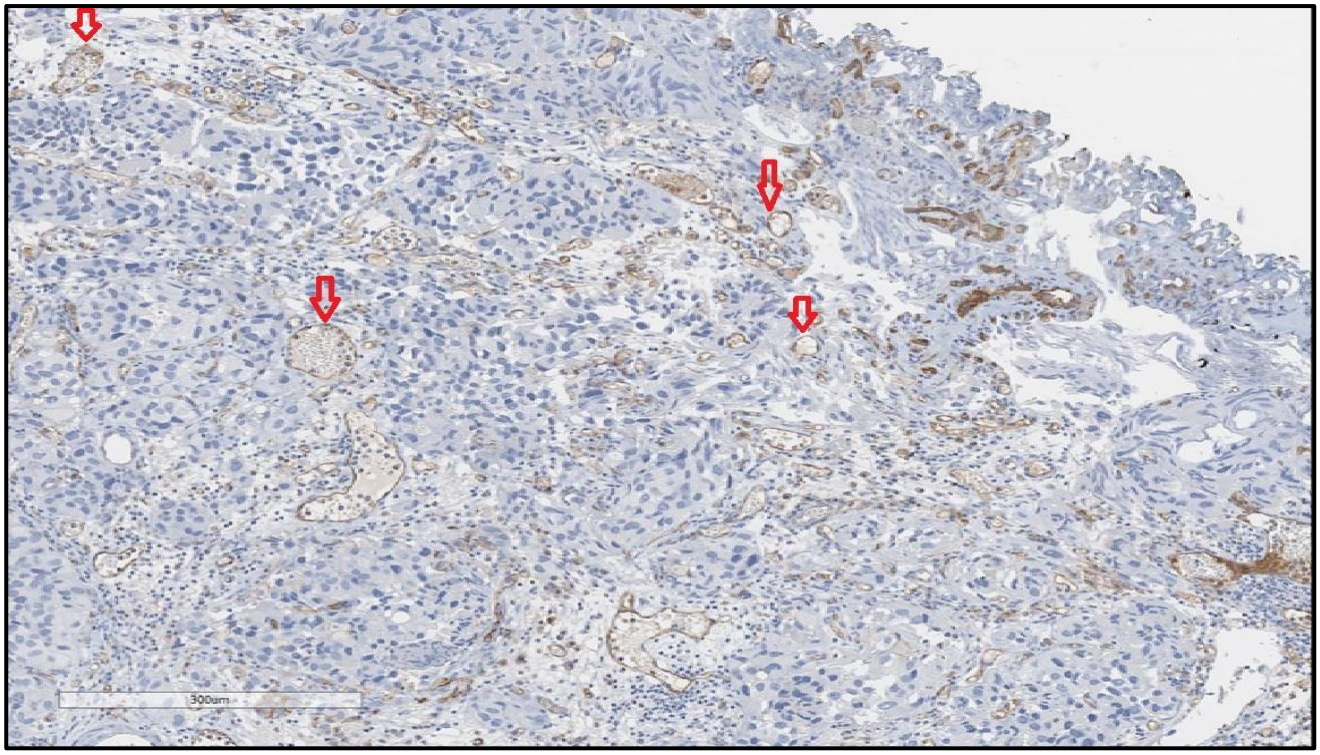

Figure 7. 6 Anti-CD34 antibody staining in BC tissues (IHC score= +).
Weak staining or positive cytoplasmic/membranous staining in up to 20% of endothelial cells in BC tissues. Note the weak positive staining in vascular endothelial cells (Red arrows) show. DAB detection. X100 magnification.

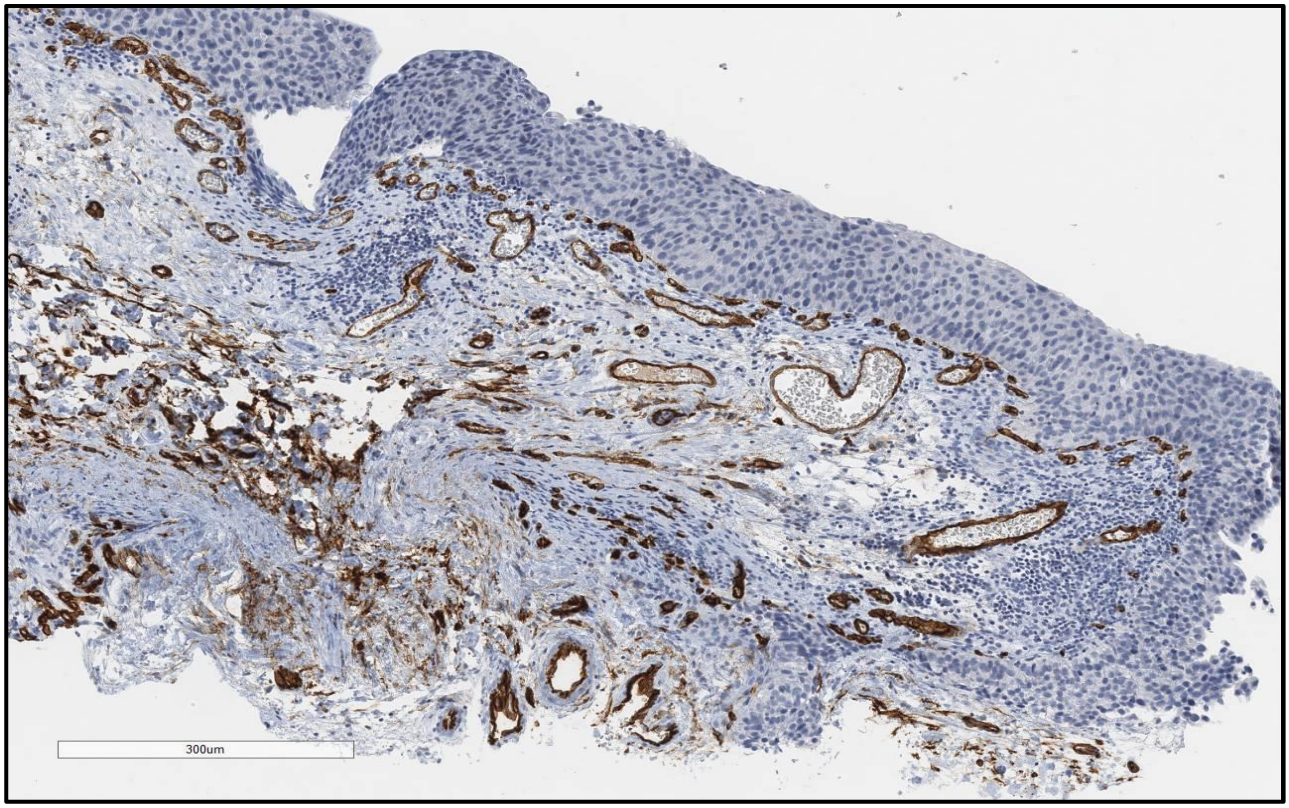

Figure 7. 7 Anti-CD34 antibody staining in BC tissues (IHC score= ++).
Positive cytoplasmic/membranous staining (Brown colour) in up to 20-50% of endothelial cells in BC tissues (brown colour). DAB detection. X100 magnification

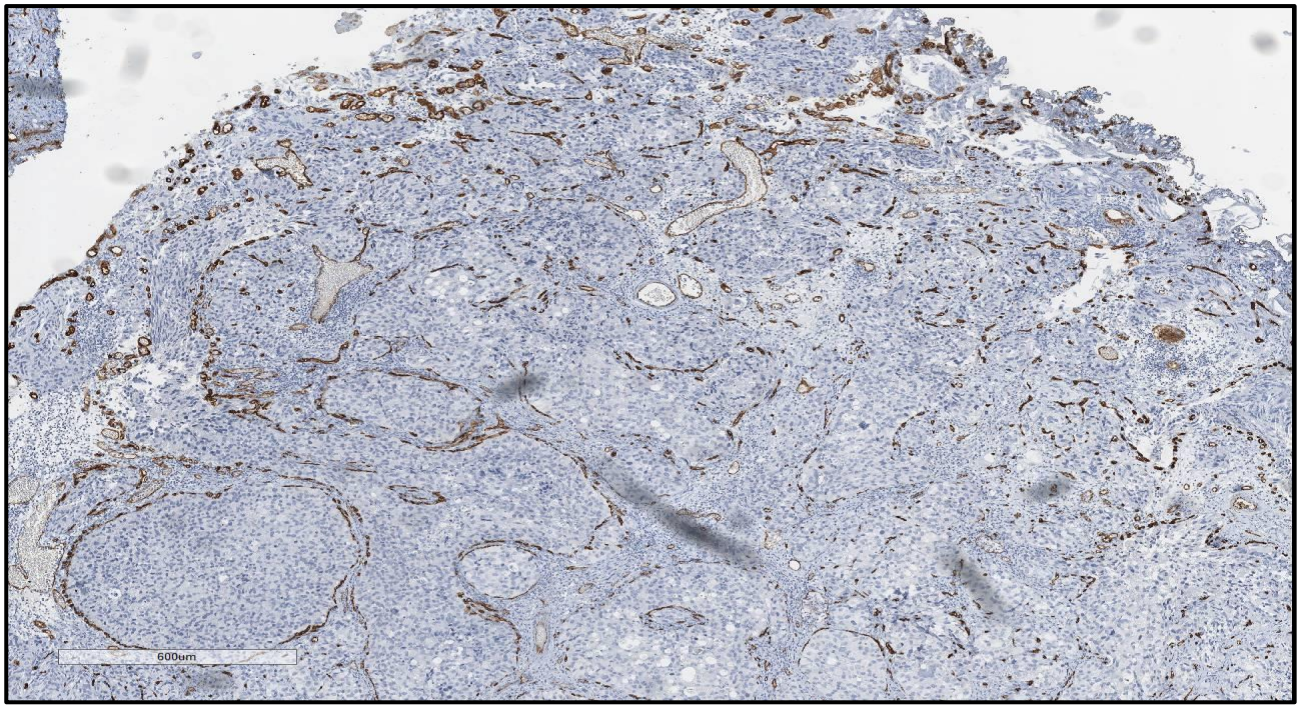

Figure 7. 8 Anti-CD34 antibody staining in BC tissues (IHC score= +++).
Positive cytoplasmic/membranous staining >50% of endothelial cells in BC tissues. Dab detection. X100 magnification

Vascular endothelial cells in BC tissues had significantly higher anti CD34 immunopositivity, compared to normal underlying tissues ($X^2(3) = 38.941$, $p< 0.001$), as determined by the Chi-square test (table 7.10).

With respect cancer to grading and staging, there was no significant association between patients' cancer grade and CD34 immunoreactivity ($X^2(2) = 1.95$, $p= 0.37$), as determined by the Kruskal-Wallis test. There was also no significant association between patient's cancer stage and CD34 immunoreactivity ($X^2(2) = 12.276$, $p= 0.17$), as determined by the Kruskal-Wallis test (table 7.10).

In the present study, 14 patients developed BC recurrence during the study period, all of which were diagnosed clinically during follow-up cystoscopies.

The relationship between antibody immunoreactivity (at diagnosis) vs BC recurrence was investigated via Mann-Whitney statistical test, and suggests that antibody immunoreactivity (CD34) is not associated with an increased risk BC recurrence ($U= 110.00$, $p= 0.97$).

7.2.3 Immunoreactivity of Thrombomodulin in BC patients

Thrombomodulin is an inflammatory marker but has been associated with tumour promotion and cancer growth (Greineder *et al.*, 2017; Song *et al.*, 2018)).

The anti-thrombomodulin primary monoclonal antibody used in this study shows membranous staining patterns in BC tissue sections. Positive membranous staining was reported based on colour intensity and percentage of cells that were immunoreactive. This Scoring system has previously been used by others and has been modified for this research (Hanly *et al.*, 2006; Paner *et al.*, 2014).

Table 7. 3 Staining interpretation for IHC scores for thrombomodulin

IHC Status	Meaning/Interpretation
Negative	Positive membranous staining in <5% of Bladder tumours
Positive (+)	Positive membranous staining in up to 20% of Bladder tumours
Positive (++)	Positive membranous staining in up to 20-50% of Bladder tumours
Positive (+++)	Positive membranous staining in >50% of Bladder tumours

The aim of this section was to initially identify immunoreactivity of thrombomodulin in NMIBC and subsequently compare these results in patients who had recurrence and progression. Examples of each of the staining categories are presented in figures 7.9-7.12, respectively.

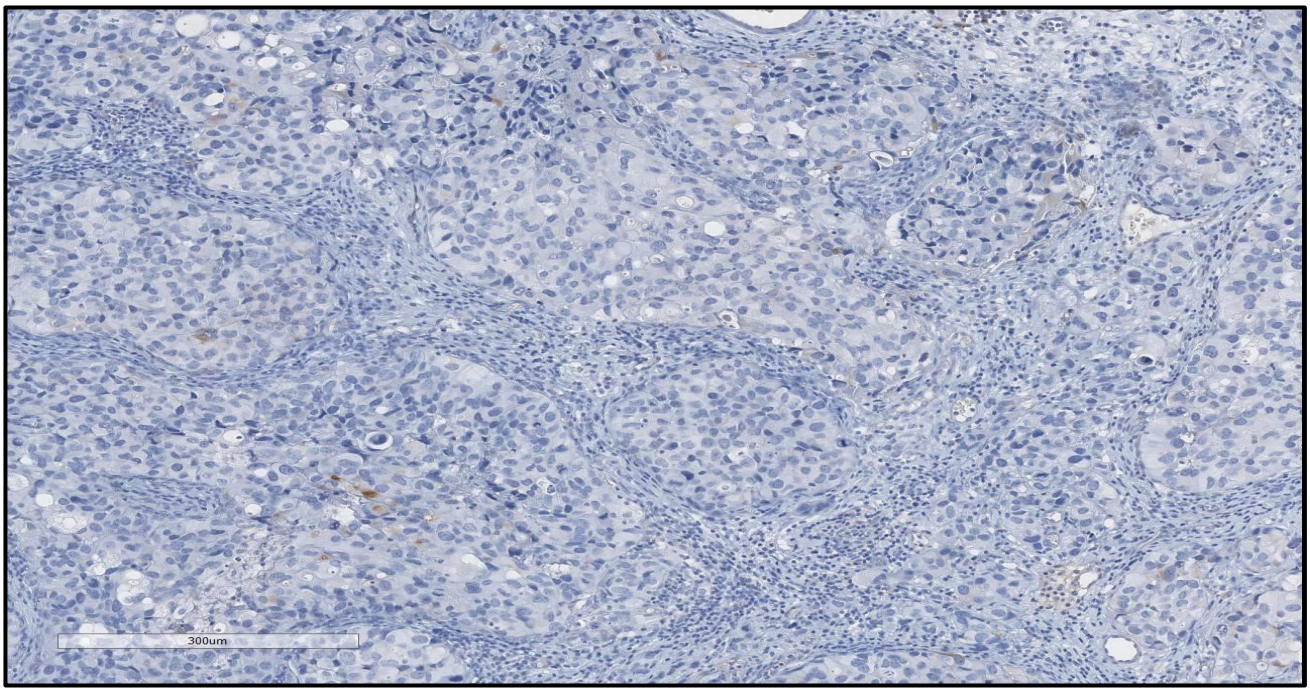

Figure 7. 9 Anti-thrombomodulin IHC staining in BC tissues (negative).
No staining/positive membranous staining in <5% of Bladder tumours. DAB detection. X100 magnification

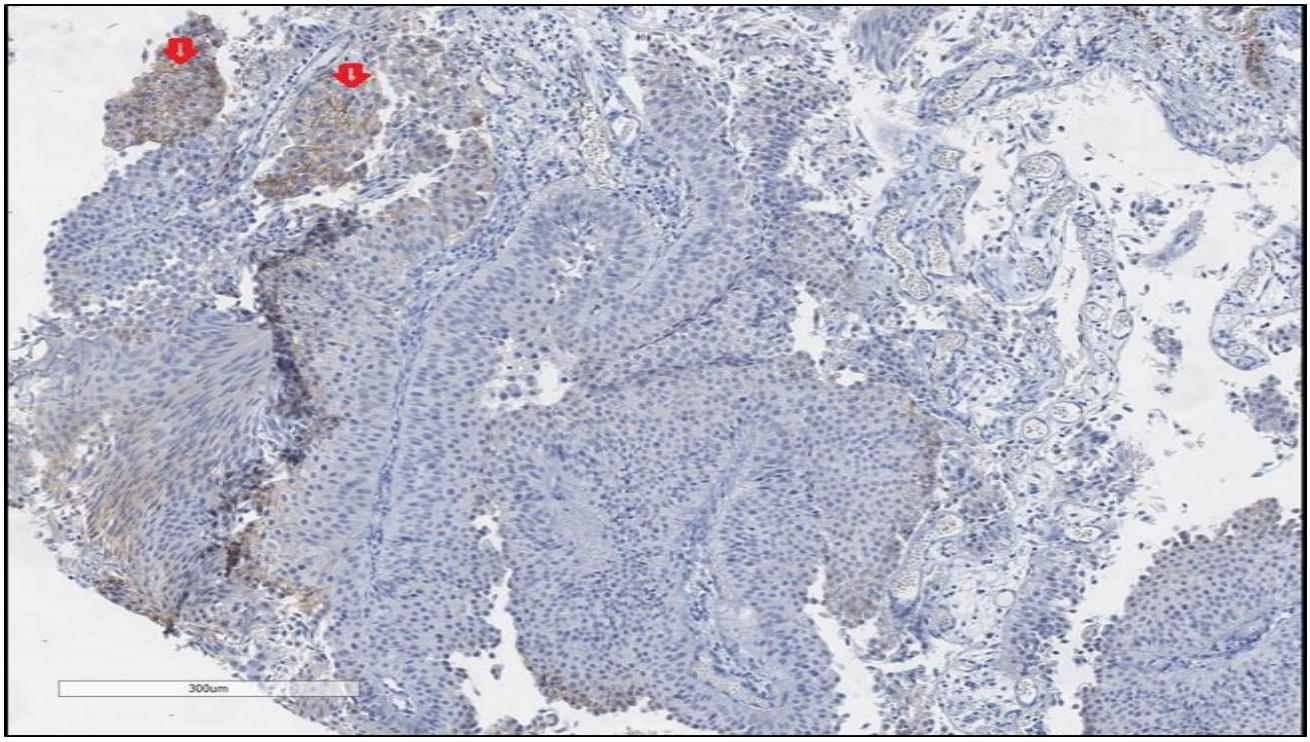

Figure 7. 10 Anti-thrombomodulin IHC staining in BC tissues (IHC score= +).
Positive membranous staining in up to 20% of Bladder tumours. Note the weak positive membranous staining (red arrows). Ventana ultraview DAB detection. X100 magnification.

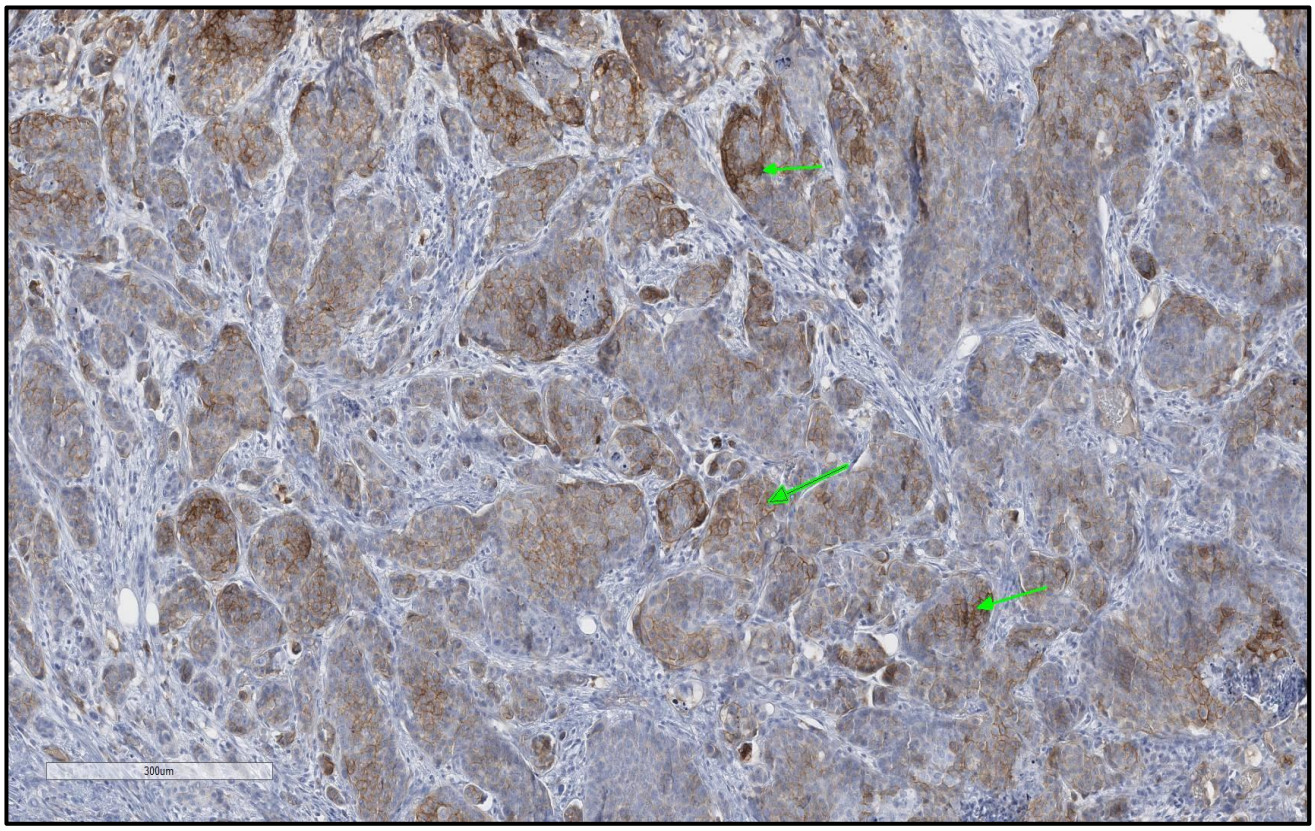

Figure 7. 11 Anti-thrombomodulin IHC staining in BC tissues (IHC score= ++).
Positive membranous staining in up to 20-50% of Bladder tumours. Note the Moderate colour intensity (green arrows). Ventana ultraview DAB detection. X40 magnification

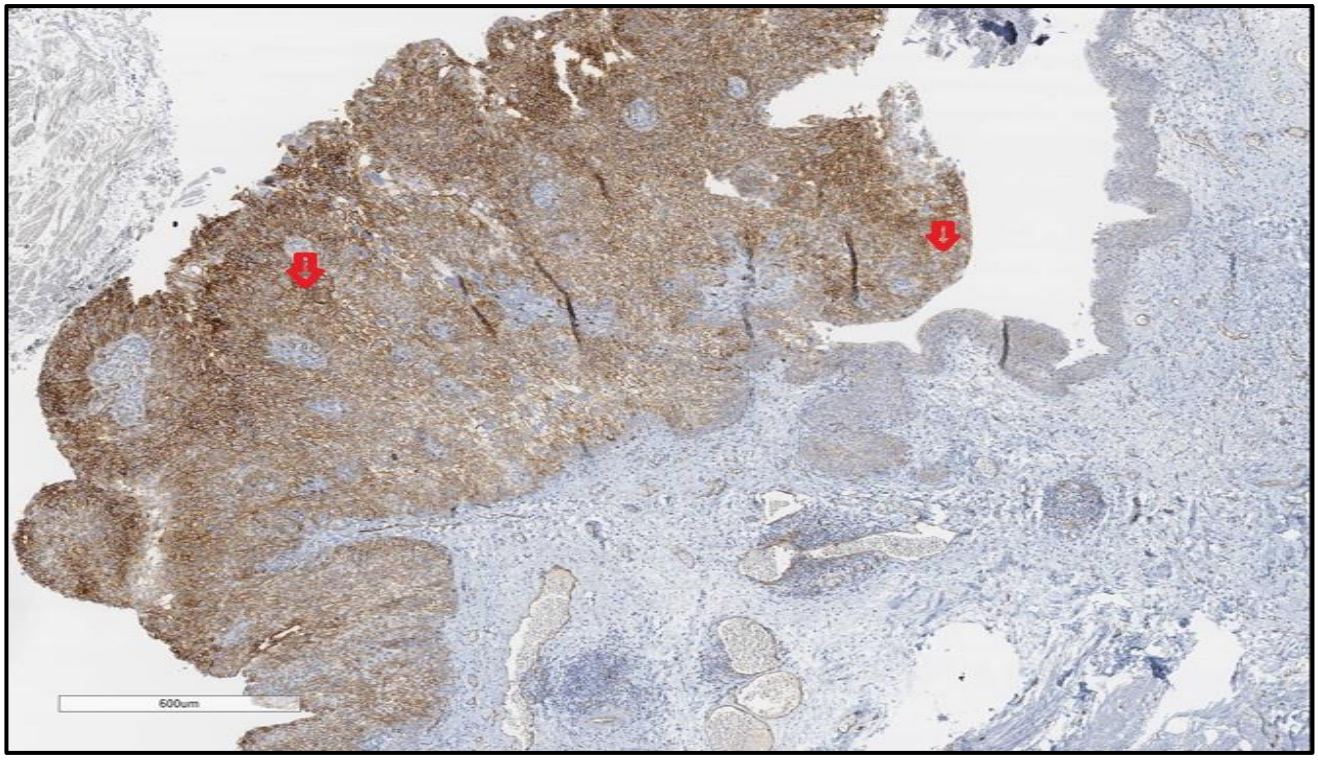

Figure 7. 12 Anti-thrombomodulin IHC staining in BC tissues (IHC score= +++).
Positive membranous staining in >50% of Bladder tumours. Note the high colour intensity (red arrows). Ventana ultraview DAB detection. X40 magnification.

Generally, there was a significantly higher thrombomodulin immunopositivity in Bladder tumours, compared to normal underlying tissues ($X^2(3) = 11.29$, $p< 0.010$), as determined by the Chi-square test (table 7.10).

With respect cancer grading and staging, there was no significant association between patients' cancer grade and thrombomodulin immunoreactivity ($X^2(2) = 0.380$, $p= 0.83$), as determined by the Kruskal-Wallis test. There was however a significant association between patient's cancer stage and thrombomodulin immunoreactivity ($X^2(2) = 6.50$, $p= 0.039$), as determined by the Kruskal-Wallis test (table 7.10).

In the present study, 14 patients developed BC recurrence during the study period, all of which were diagnosed clinically during follow-up cystoscopies.

The relationship between antibody immunoreactivity (at diagnosis) vs BC recurrence was investigated via Mann-Whitney statistical test. There was no significant association between thrombomodulin immunoreactivity vs BC ($U= 115.50$, $p= 0.88$) (table 7.10).

The relationship between antibody immunoreactivity (at diagnosis) vs BC recurrence was investigated via Mann-Whitney statistical test, and suggests that antibody immunoreactivity

(thrombomodulin) is not associated with an increased risk BC recurrence (U= 115.50, p= 0.88) (table 7.10).

7.2.4 Immunoreactivity of HER-2/neu in BC patients

HER-2 is a growth factor receptor implicated in tumour cell proliferation and growth through a series of complex pathways (Coussens *et al.*, 1985; Wang *et al.*, 2016b).

The anti-HER-2/neu primary monoclonal antibody used in this study shows membranous staining patterns in BC tissue sections. Positive membranous staining was reported based on colour intensity and percentage of cells staining positive. This Scoring system has previously been used by (Doval *et al.*, 2015; Gancberg et al., 2002) and is modified from the ASCO recommended scoring system used for the clinical management of invasive breast cancer.

Table 7. 4 Staining interpretation for anti-HER-2 antibody IHC scores

IHC Status	Meaning/Interpretation
Negative	No or weak membranous staining in <5% of BC tissues
Positive (+)	Positive membranous staining in up to 20% of BC tissues
Positive (++)	Positive membranous staining in 20-50% of BC tissues
Positive (+++)	Positive membranous staining in >50% of BC tissues

The aim of this section was to initially identify the immunoreactivity of HER-2/neu in NMIBC and subsequently compare this immunoreactivity in patients who had recurrence and progression. Examples of each of the staining categories are presented in figures 7.13-7.16, respectively.

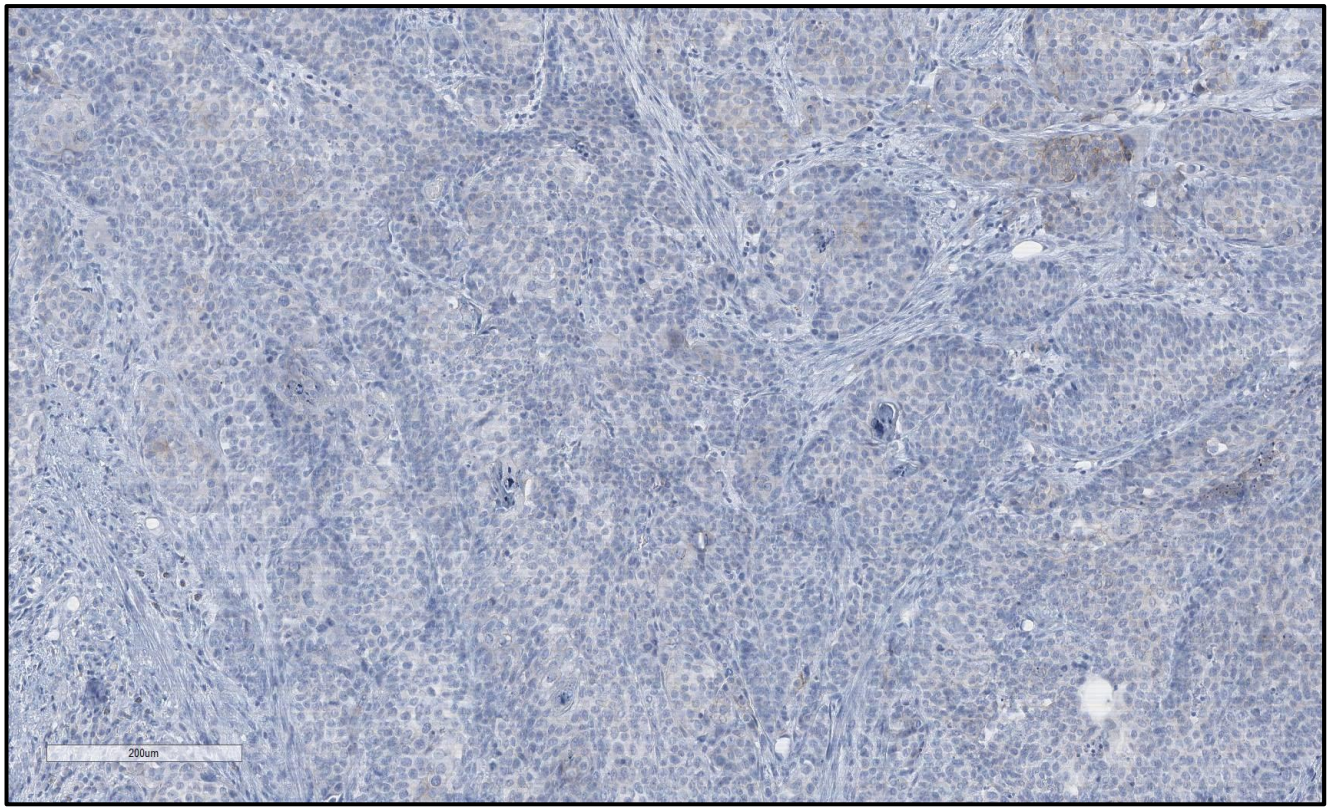

Figure 7. 13 Anti-HER-2/neu antibody staining in BC tissues (IHC score= negative).
No or weak membranous staining in <5% of BC tissues. DAB detection. X100 magnification

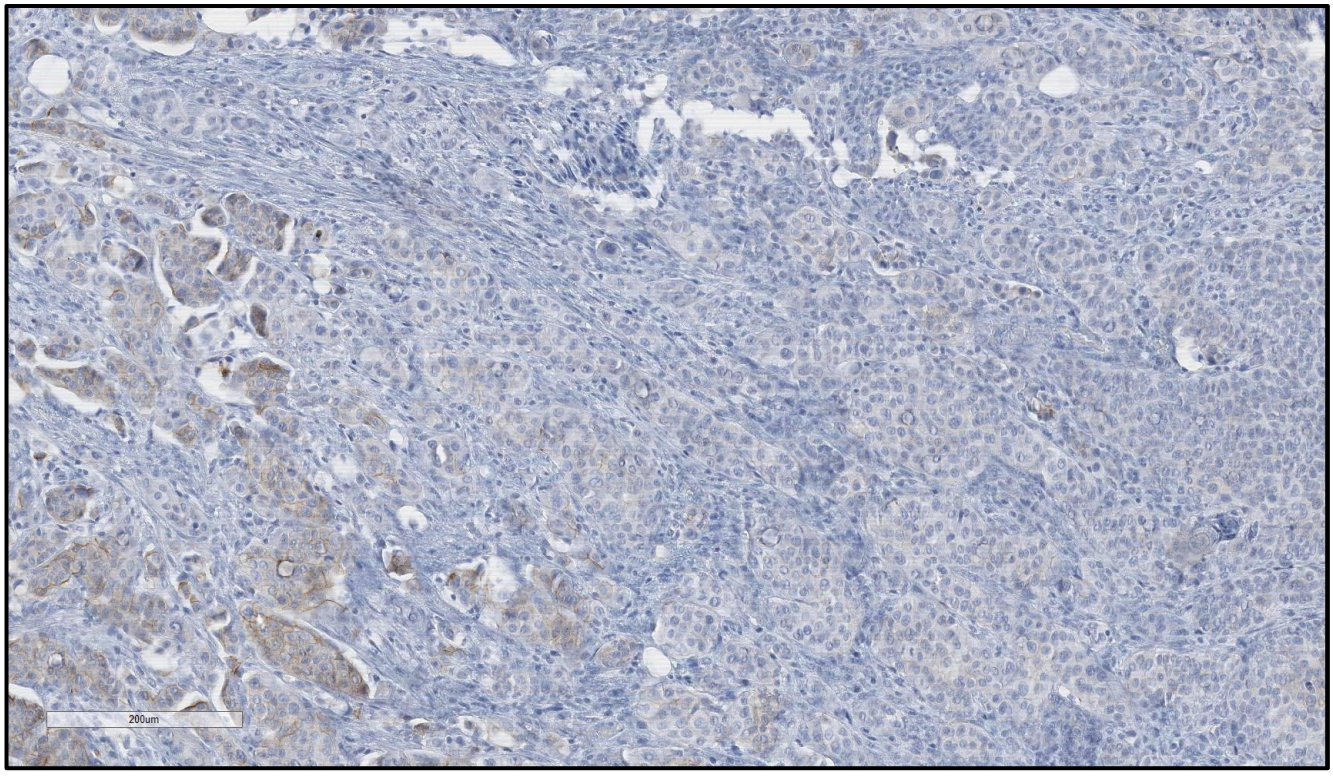

Figure 7. 14 Anti-HER-2/neu antibody staining in BC tissues (IHC score= +).
Weakly positive membranous staining in BC tumours. Ventana ultraview DAB detection. X40 magnification

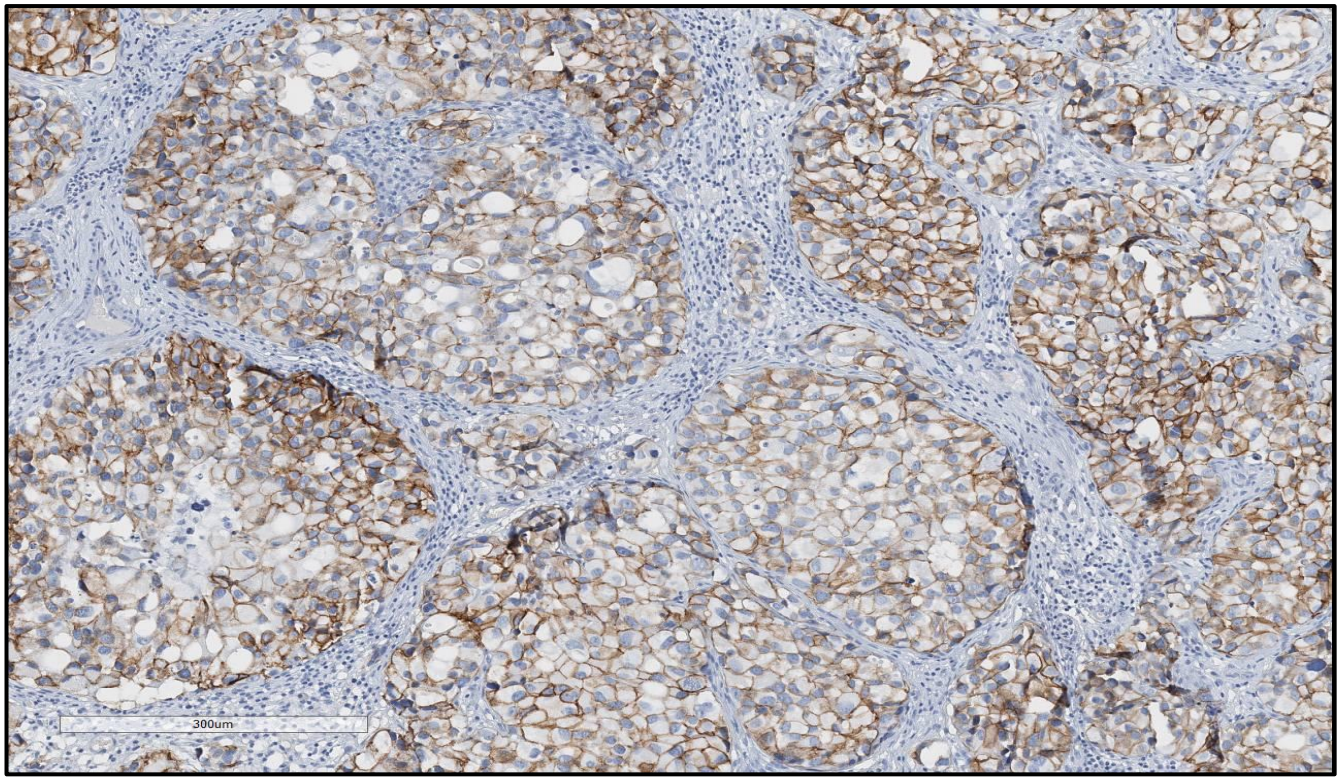

Figure 7. 15 Anti-HER-2/neu antibody staining in BC tissues (IHC score= ++).
Moderate positive membranous staining in 20-50% of BC tissues. (Brown). Ventana ultraview DAB detection. X100 magnification.

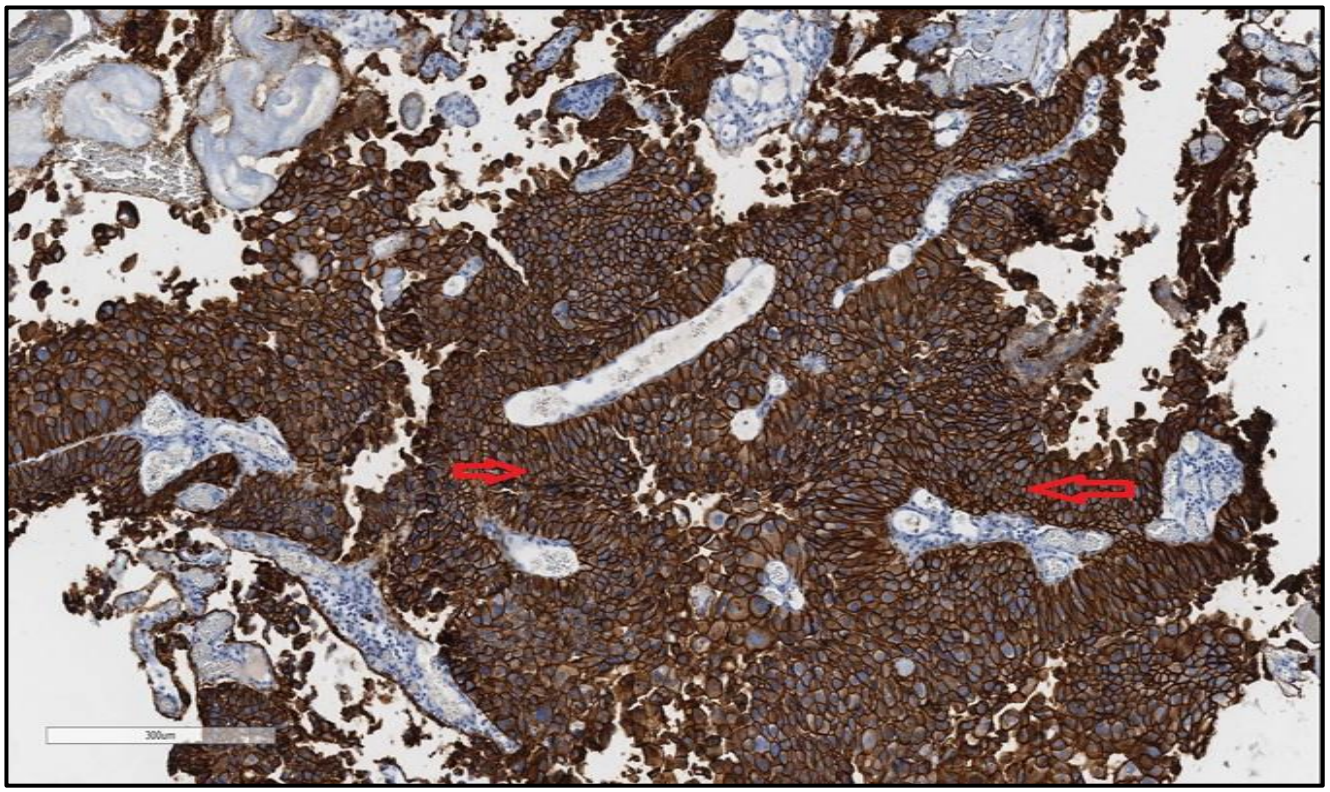

Figure 7. 16 Anti-HER-2/neu antibody staining in BC tissues (IHC score= +++).
Strong positive membranous staining in >50% of BC tissues (Brown colour, red arrows). Ventana ultraview DAB detection. X100 magnification.

Generally, there was a significantly higher HER-2/neu immunoreactivity in Bladder tumours, compared to normal underlying tissues ($X^2(3) = 8.82$, $p< 0.032$), as determined by the Chi-square test (table 7.10).

With respect cancer grading, there was a significant association between patients' cancer grade and HER-2/neu immunoreactivity ($X^2(2) = 11.407$, **p= 0.003**), as determined by the Kruskal-Wallis test. Further post-hoc testing using the Mann-Whitney test revealed significant difference between grade 1 and grade 2 (Z= -3.042, **p= 0.002**, r= 0.673) and a significant difference between grade 1 and grade 3 (Z= -2.843, **p= 0.004**, r= 0.606), both with a high Eta^2 effect size (table 7.10).

There was also a significant association between patient's cancer stage and HER-2/neu immunoreactivity ($X^2(2) = 16.092$, **p< 0.001**), as determined by the Kruskal-Wallis test (table 7.10).

In the present study, 14 patients developed BC recurrence during the study period, all of which were diagnosed clinically during follow-up cystoscopies.

The relationship between antibody immunoreactivity (at diagnosis) vs BC recurrence was investigated via Mann-Whitney statistical test, and suggests that antibody immunoreactivity (HER-2/neu) is not associated with an increased risk BC recurrence (U= 101.50, p= 0.91) (table 7.10).

7.2.5 Immunoreactivity of S100P in BC patients

S100P is a low molecular weight protein first purified from human placenta tissue (Emoto *et al.*, 1992). It has been implicated in various physiological processes such as cell cycle regulation as well as pathological conditions such as cancer (Jiang *et al.*, 2016).

The anti-S100p primary monoclonal antibody used in this study shows cytoplasmic and nuclear staining patterns in BC tissue sections. Positive membranous staining was reported based on colour intensity and percentage of tumour cells that were immunoreactive.

Table 7. 5 Staining interpretation for S100P staining in BC patient tissues
Positive membranous staining was reported based on colour intensity and percentage of immunoreactive tumour cells. Scoring system has previously been used by (Paner *et al.*, 2014).

IHC Status	Meaning/Interpretation
Negative	Positive cytoplasmic/nuclear staining in <5% of Bladder tumours
Positive (+)	Positive cytoplasmic/nuclear staining in up to 20% of Bladder tumours
Positive (++)	Positive cytoplasmic/nuclear staining in up to 20-50% of Bladder tumours
Positive (+++)	Positive cytoplasmic/nuclear staining in >50% of Bladder tumours

The aim of this section was to initially identify immunoreactivity of anti-S100P in NMIBC and subsequently compare this immunoreactivity in patients who had recurrence and progression. Examples of each of the staining categories are presented in figures 7.17-7.20, respectively.

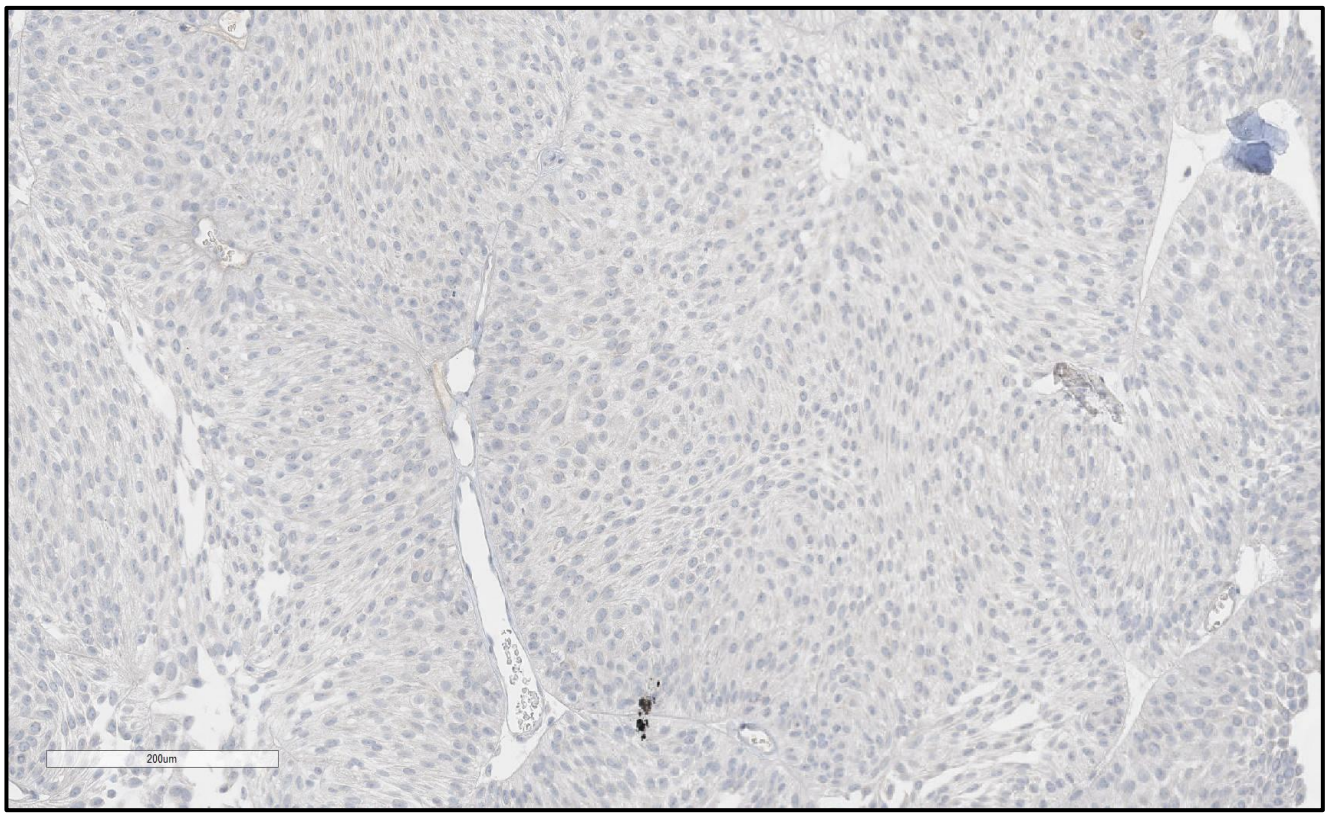

Figure 7. 17 Anti-S100P antibody staining in BC tissues (Negative control).
No staining or positive cytoplasmic/nuclear staining in <5% of Bladder tumours. Ventana ultraview DAB detection. X100 magnification

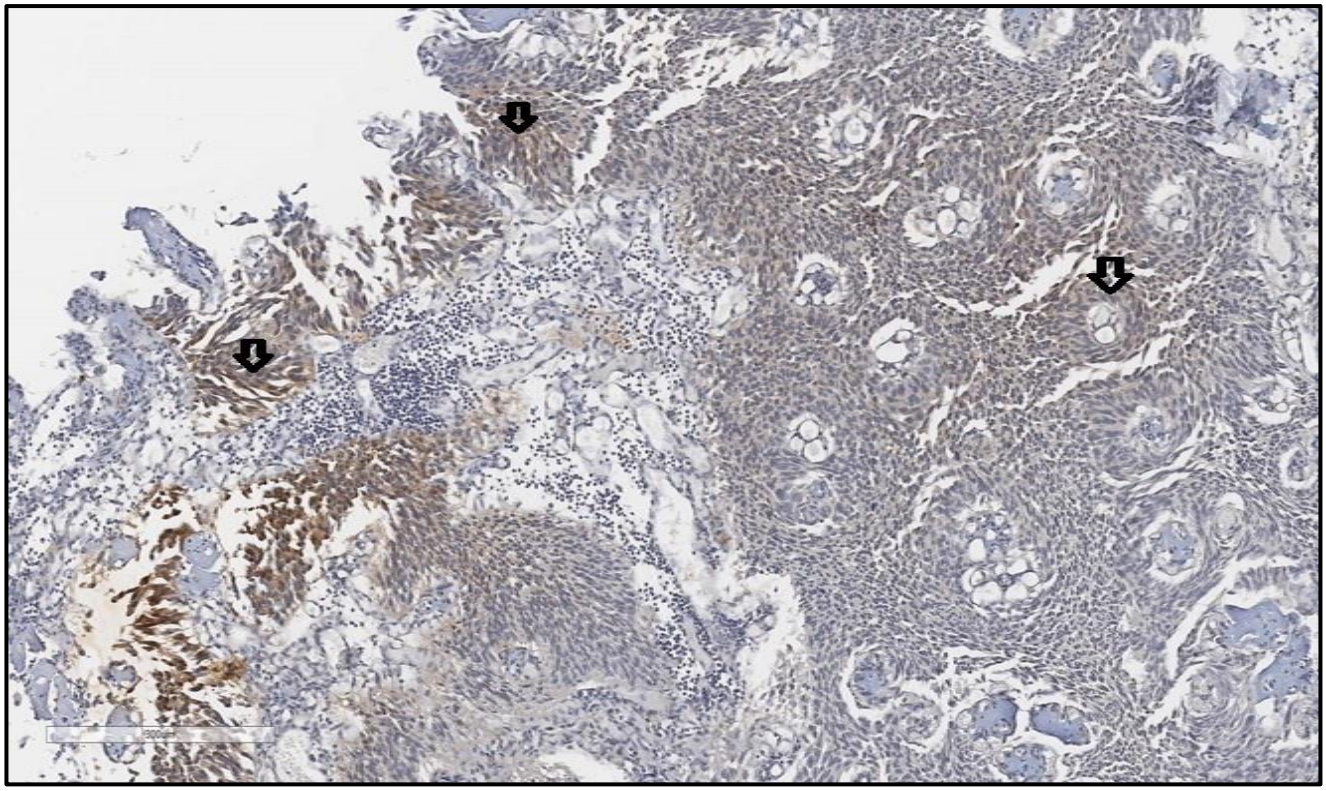

Figure 7. 18 Anti-S100P antibody staining in BC tissues (IHC score= +).
Weak Nuclear/cytoplasmic staining in up to 20% of Bladder tumours (black arrows). Ventana ultraview DAB detection. X100 magnification

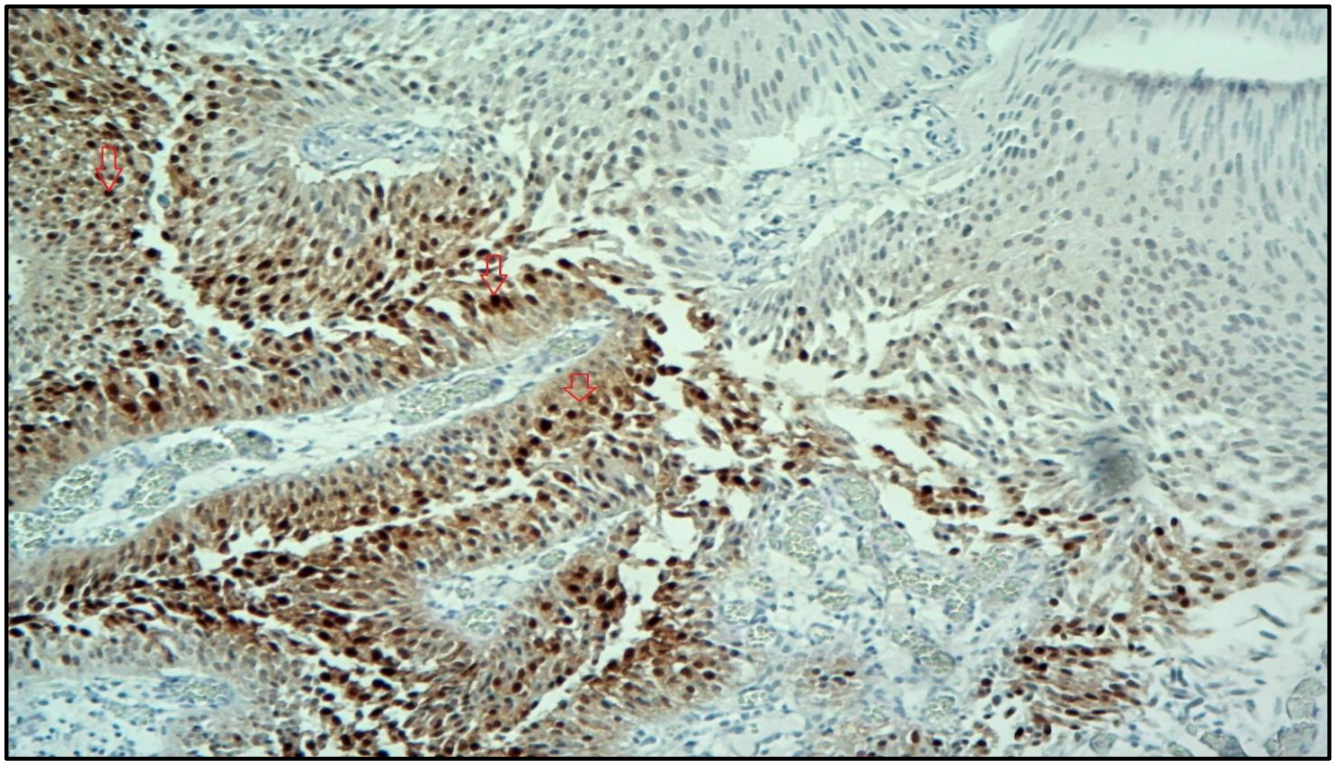

Figure 7. 19 Anti-S100P antibody staining in BC tissues (IHC score= ++).
Moderate/strong positive nuclear and cytoplasmic staining 20-50% of Bladder tumours (red arrows). Ventana ultraview DAB detection. X100 magnification

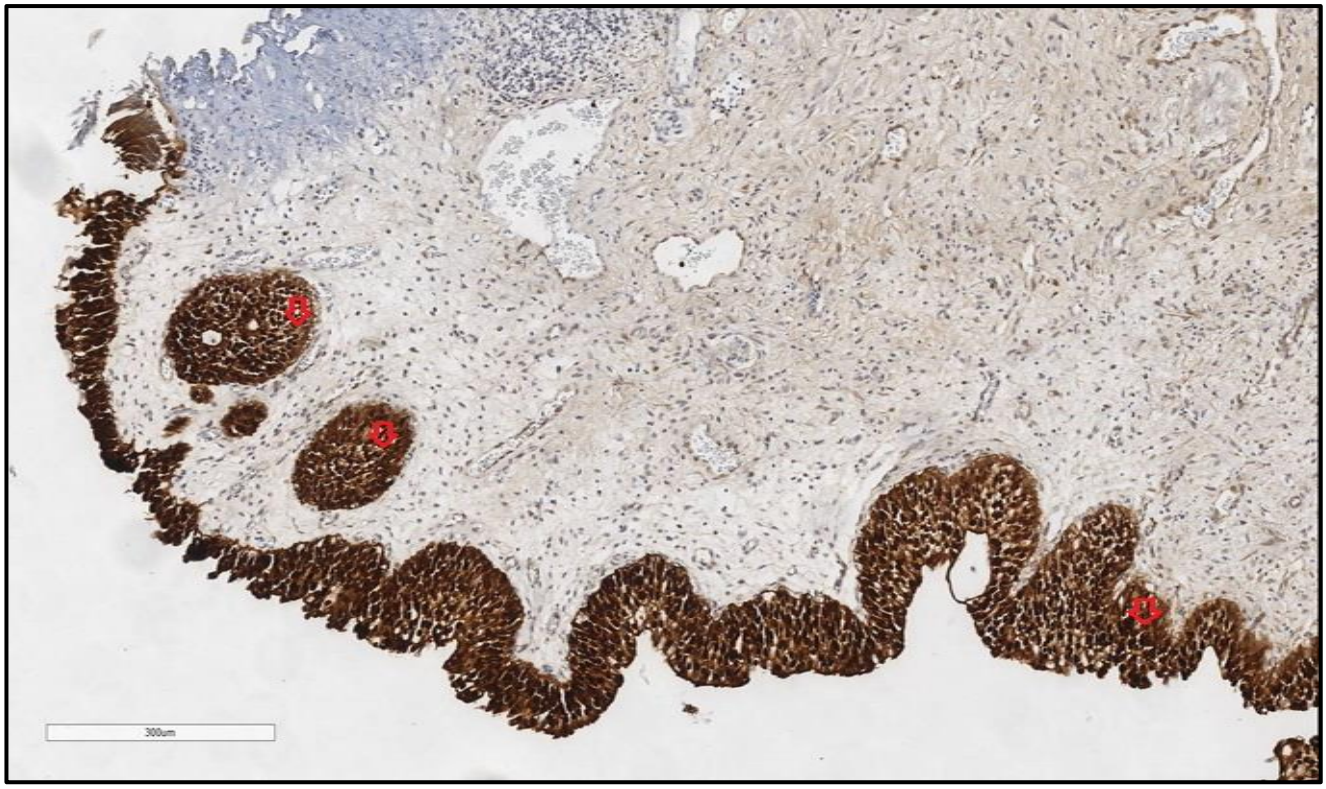

Figure 7. 20 Anti-S100P antibody staining in BC tissues (IHC score= +++).
Strong positive nuclear and cytoplasmic staining in >50% of Bladder tumours. Ventana ultraview DAB detection. X40 magnification.

Generally, there was a significant increase in S100P immunoreactivity in Bladder tumours compared to those in normal tissues (X2(3) = 41.686, p< 0.001), as determined by the Chi-square test (table 7.10).

With respect to cancer grading, there was no significant association between patients' cancer grade and anti-S100P immunoreactivity ($X^2(2) = 0.206$, p= 0.902), as determined by the Kruskal-Wallis. There was also no significant association between patient's cancer stage and S100P immunoreactivity ($X^2(2) = 2.134$, p= 0.344), as determined by the Kruskal-Wallis test (table 7.10).

In the present study, 14 patients developed BC recurrence during the study period, all of which were diagnosed clinically during follow-up cystoscopies.

The relationship between antibody immunoreactivity (at diagnosis) vs BC recurrence was investigated via Mann-Whitney statistical test, and suggests that antibody immunoreactivity (S100P) is not associated with an increased risk BC recurrence (U= 96.00, p= 0.23) (table 7.10).

7.2.6 Immunoreactivity of COX-2 in BC patients

COX-2 is a 70 kDa enzyme involved in inflammatory processes through the activities of prostaglandins (Mead *et al*., 1986). It is immunoreactive in BC and may potentially be a good marker for cancer recurrence.

The anti-COX-2 primary monoclonal antibody used in this study shows cytoplasmic and membranous staining patterns in BC tissue sections. Positive membranous and cytoplasmic staining was reported based on colour intensity and percentage of cells staining positive.

Evaluation of COX-2 staining was performed microscopically by assessing the percentage and intensity of staining observed in the cytoplasm and membranes of epithelial cells within tumours. Other scoring systems employing points for both stain percentage and intensity have been described by other researchers (Cai *et al*., 2017).

Table 7. 6 Staining interpretation for COX-2 staining in BC patient tissues

IHC Status	Meaning/Interpretation
Negative	Positive cytoplasmic/membranous staining in <5% of Bladder tumours
Positive (+)	Positive cytoplasmic/membranous staining in up to 20% of Bladder tumours
Positive (++)	Positive cytoplasmic/membranous staining in up to 20-50% of Bladder tumours
Positive (+++)	Positive cytoplasmic/membranous staining in >50% of Bladder tumours

The aim of this section was to initially identify the immunoreactivity of COX-2 in NMIBC and subsequently compare this immunoreactivity in patients who had recurrence and progression. Examples of each of the staining categories are presented in figures 7.21-7.24, respectively.

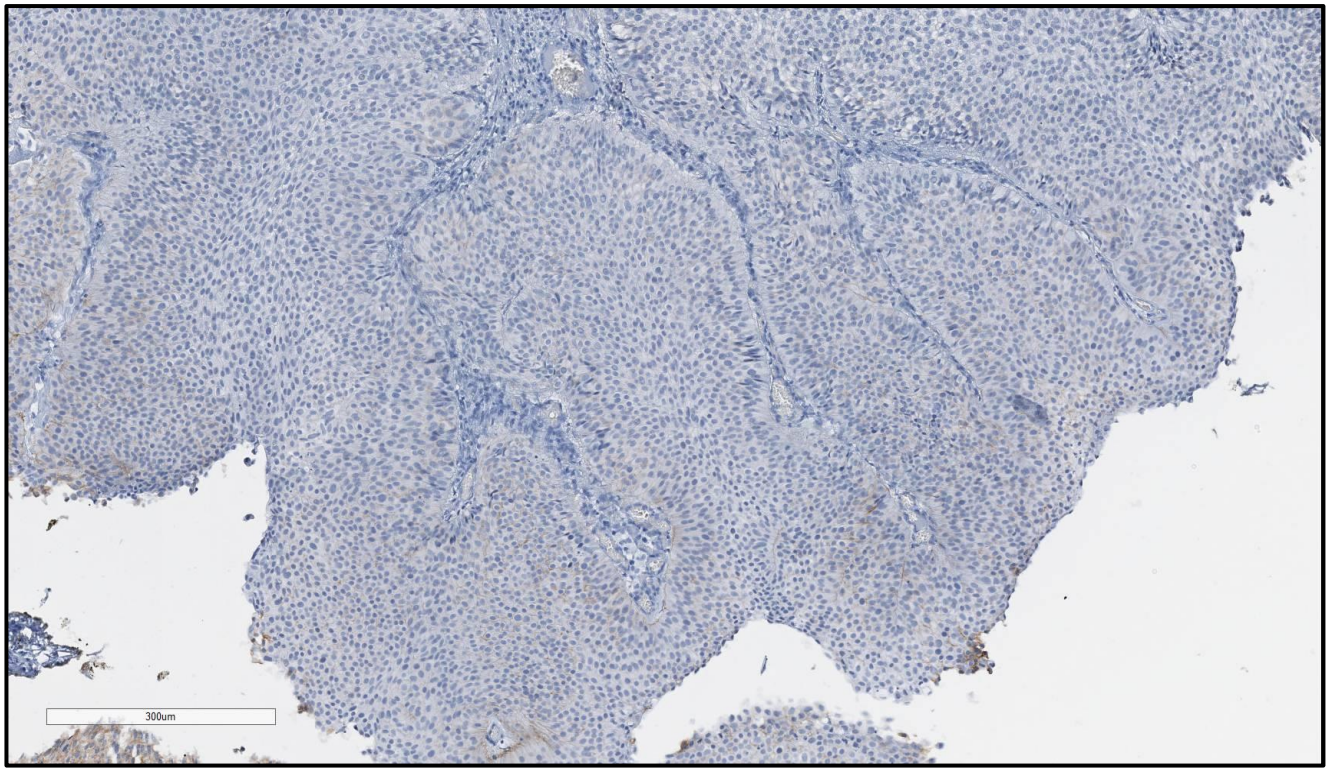

Figure 7. 21 Anti-COX-2 antibody staining in BC tissues (IHC score= NEG)
No staining/Positive cytoplasmic/membranous staining in <5% of Bladder tumours. Ventana Ultraview DAB. X100 magnification

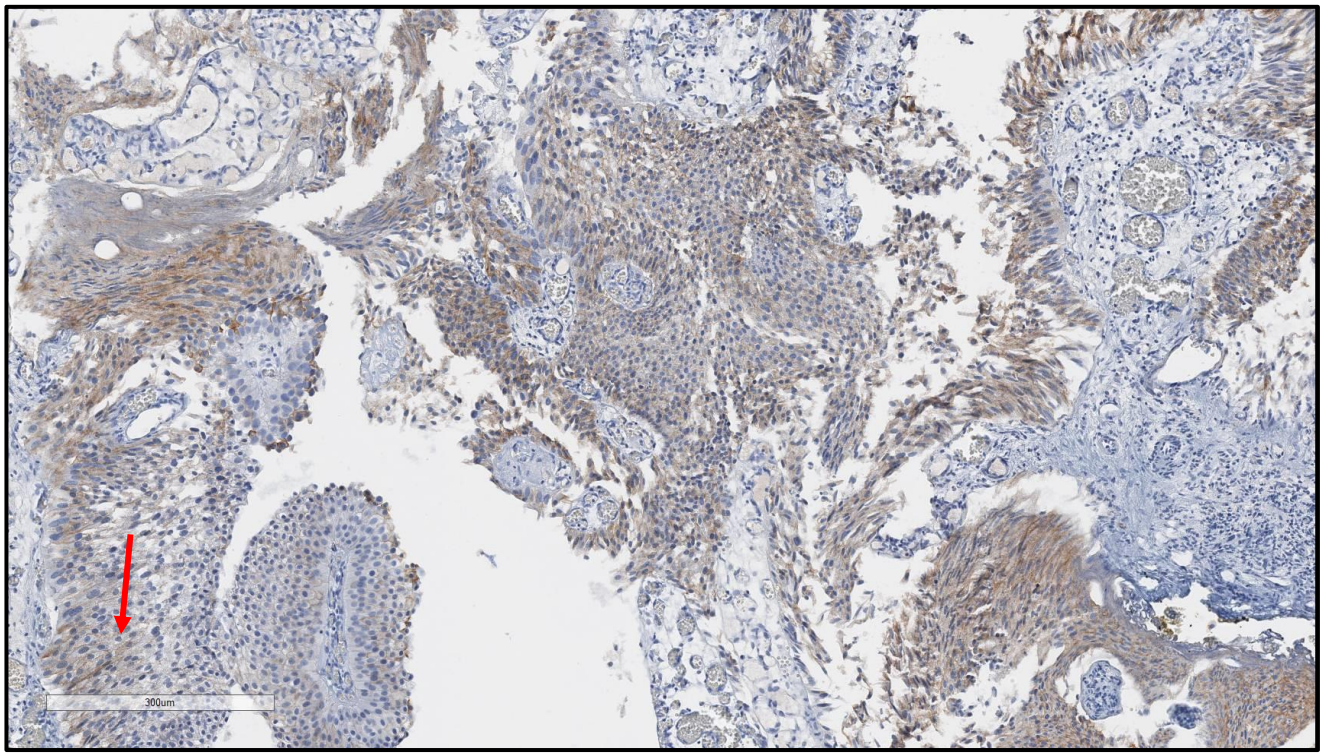

Figure 7. 22 Anti-COX-2 antibody staining in BC tissues (IHC score= +).
Weak positive cytoplasmic/membranous staining in up to 20% of Bladder tumour cells (Brown colour, red arrows). DAB detection. X100 magnification.

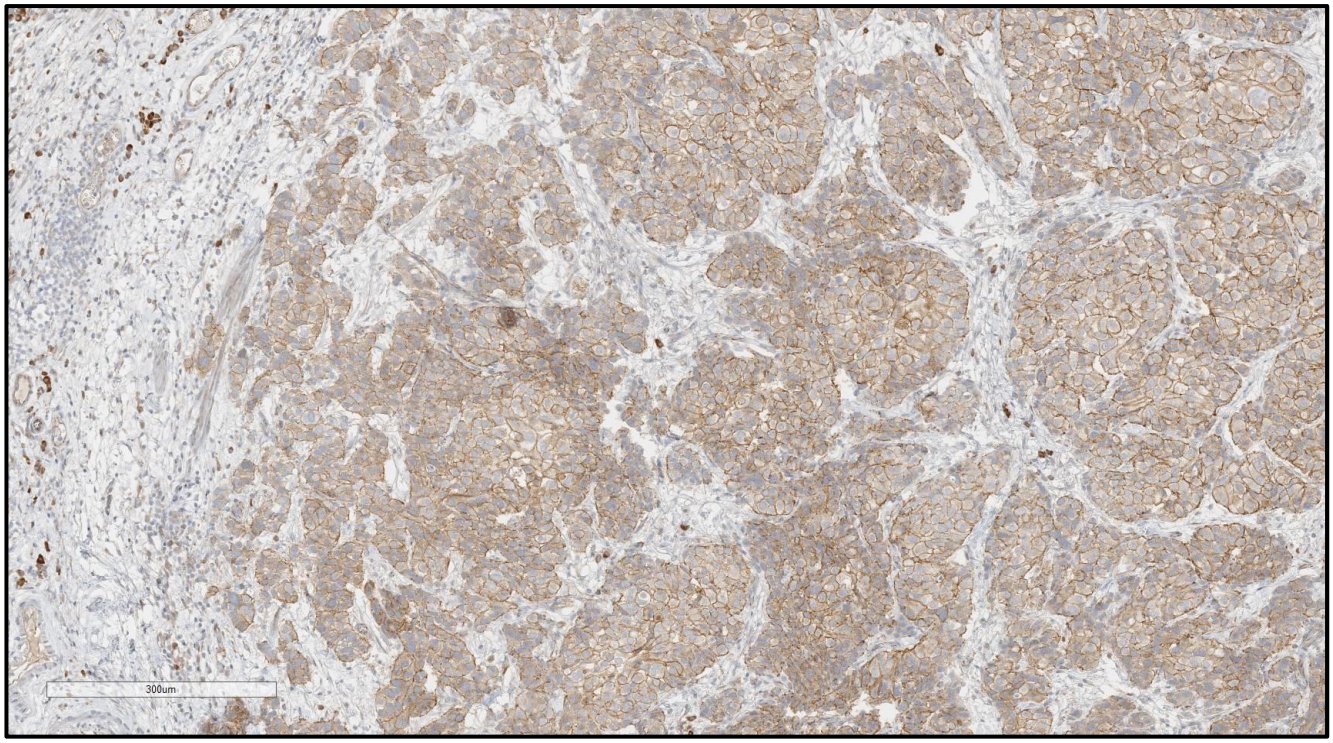

Figure 7. 23 Anti-COX-2 antibody staining in BC tissues (IHC score= ++).
Moderate/high positive cytoplasmic/membranous staining (brown colour) in in up to 20-50% of Bladder tumours. DAB detection. X100 magnification.

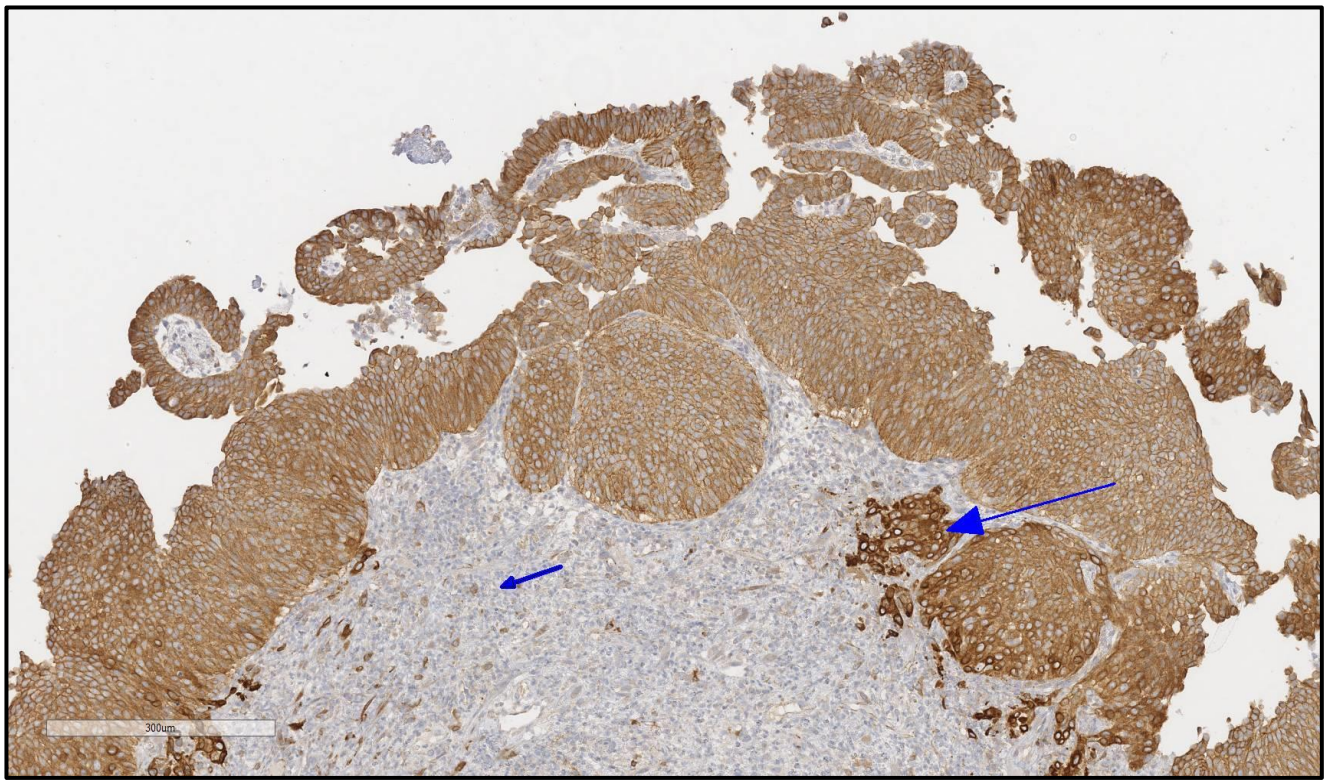

Figure 7. 24 Anti-COX-2 antibody staining in BC tissues (IHC score= +++).
Strong positive cytoplasmic/membranous staining in in up to >50% of Bladder tumours (bigger arrow). Note the absence of staining in underlying tissue (smaller arrow). Ventana Ultraview DAB. X100 magnification.

Generally, there was a significant increase in COX-2 immunoreactivity in Bladder tumours, compared to those in normal tissues (X2(3) = 19.97, p< 0.001), as determined by the Chi-square test (table 7.10).

With respect to cancer grading, there was no significant association between patients' cancer grade and anti-COX-2 immunoreactivity ($X^2(2) = 0.96$, p= 0.61), as determined by the Kruskal-Wallis test. There was also no significant association between patient's cancer stage and S100P immunoreactivity ($X^2(2) = 1.65$, p= 0.45), as determined by the Kruskal-Wallis test (table 7.10).

In the present study, 14 patients developed BC recurrence during the study period, all of which were diagnosed clinically during follow-up cystoscopies.

The relationship between antibody immunoreactivity (at diagnosis) vs BC recurrence was investigated via Mann-Whitney statistical test, and suggests that antibody immunoreactivity (COX-2) is not associated with an increased risk BC recurrence (U= 118.50, p= 0.98) (table 7.10).

7.2.7 Immunoreactivity of SOX-2 in BC patients

SOX-2 was analysed in this study due to its role in pathology such as cell proliferation (Masui *et al.*, 2007; Sarkar & Hochedlinger, 2013).Its immunoreactivity has been reported in several human cancers such as cervical squamous cell carcinoma, lung cancer and BC (Chang *et al.*, 2015; Kitamura *et al.*, 2013; Tsuta *et al.*, 2011).

The anti-SOX-2 primary monoclonal antibody used in this study shows nuclear staining patterns in BC tissue sections. Positive nuclear staining was reported based on colour intensity and percentage of cells staining positive.

Table 7. 7 Staining interpretation for SOX-2 staining in BC patient tissues

IHC Status	Meaning/Interpretation
Negative	<5% Stained Nuclei in any low power field
Positive (+)	<25% Nuclei staining in Bladder tumours
Positive (++)	25-50% nuclei staining in Bladder tumours
Positive (+++)	<75% Nuclei staining in Bladder tumours

The aim of this section was to initially identify the immunoreactivity of SOX-2 in NMIBC and subsequently compare this immunoreactivity in patients who had recurrence and progression. Examples of each of the staining categories are presented in figures 7.25- 7.28.

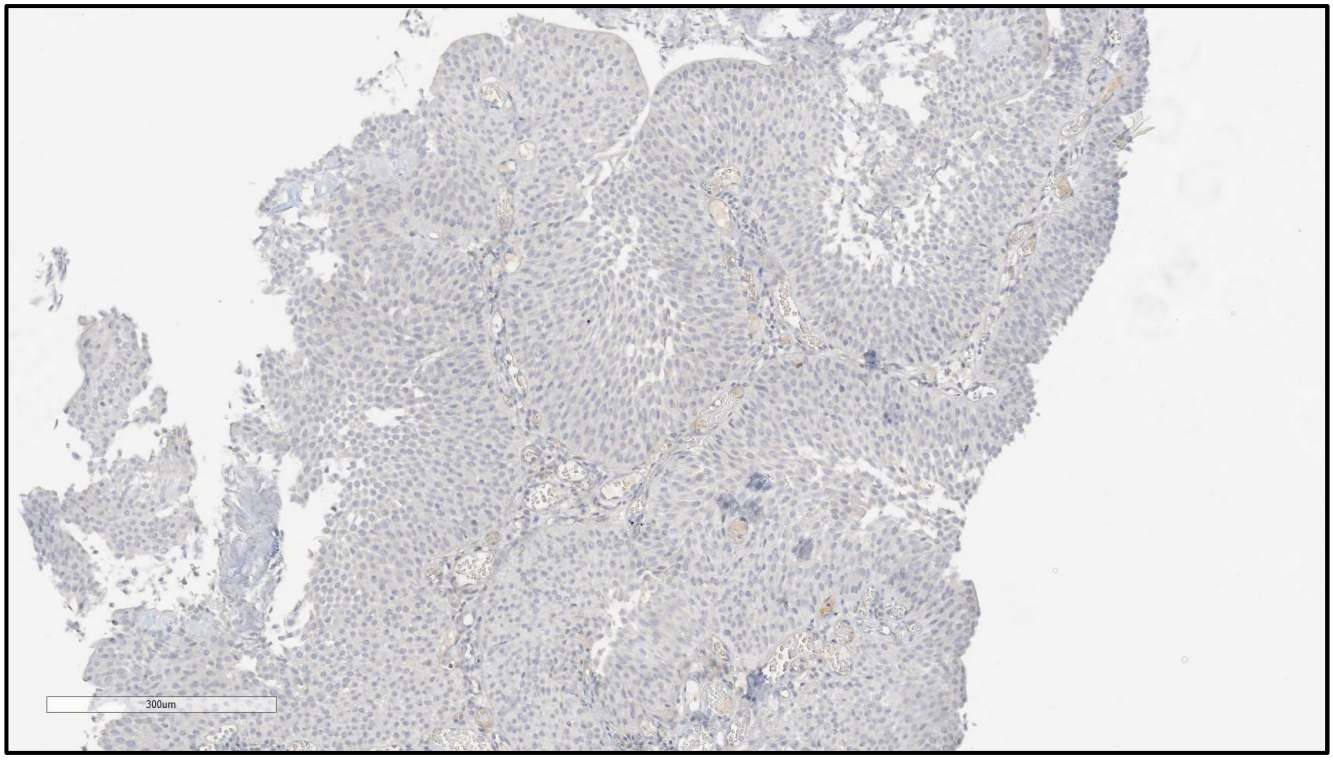

Figure 7. 25 Anti-SOX-2 antibody staining in BC tissues (IHC score= Negative)
<5% Stained Nuclei in any low power field. Ventana Ultraview DAB. X100 magnification

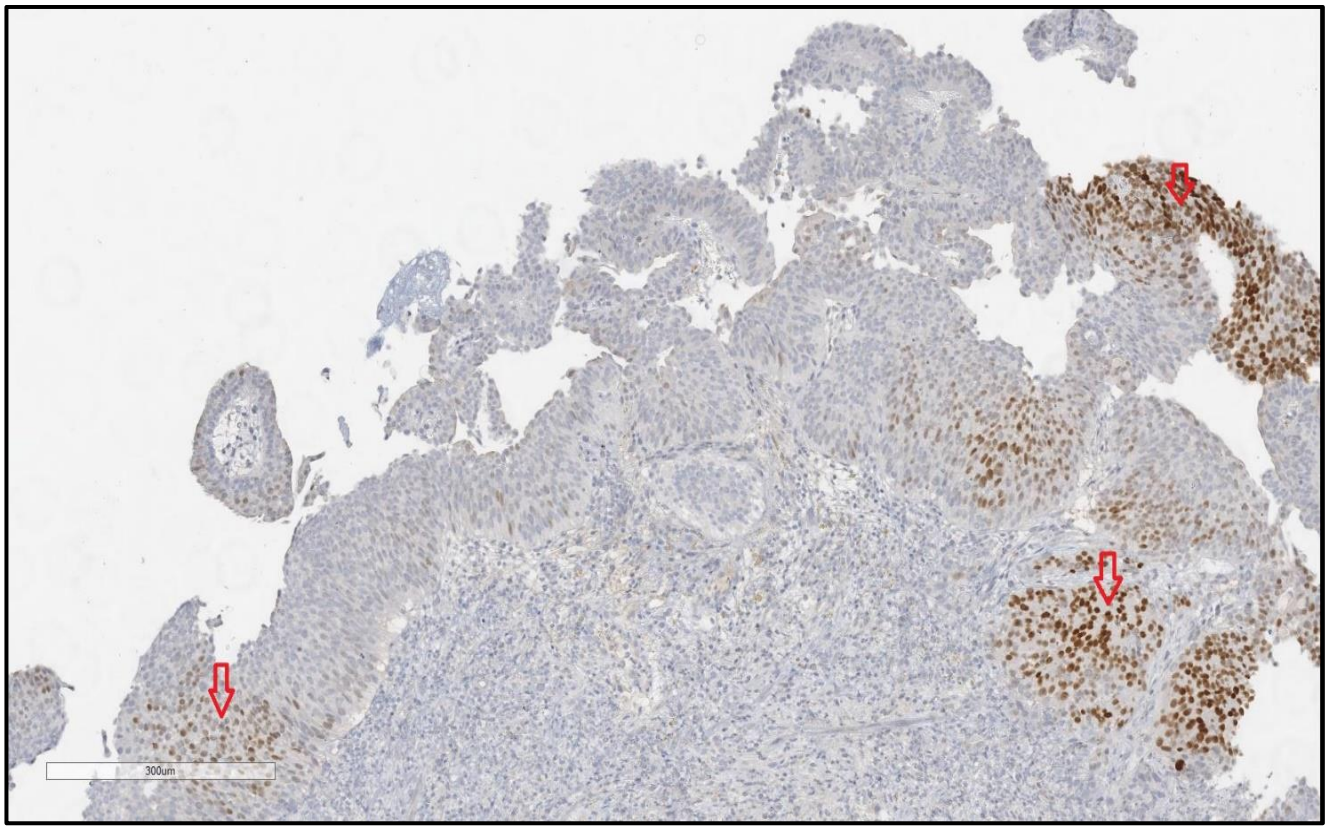

Figure 7. 26 Anti-SOX-2 antibody staining in BC tissues (IHC score= +).
Positive nuclear staining in <25% of Bladder tumours (red arrows). Ventana Ultraview DAB. X100 Magnification.

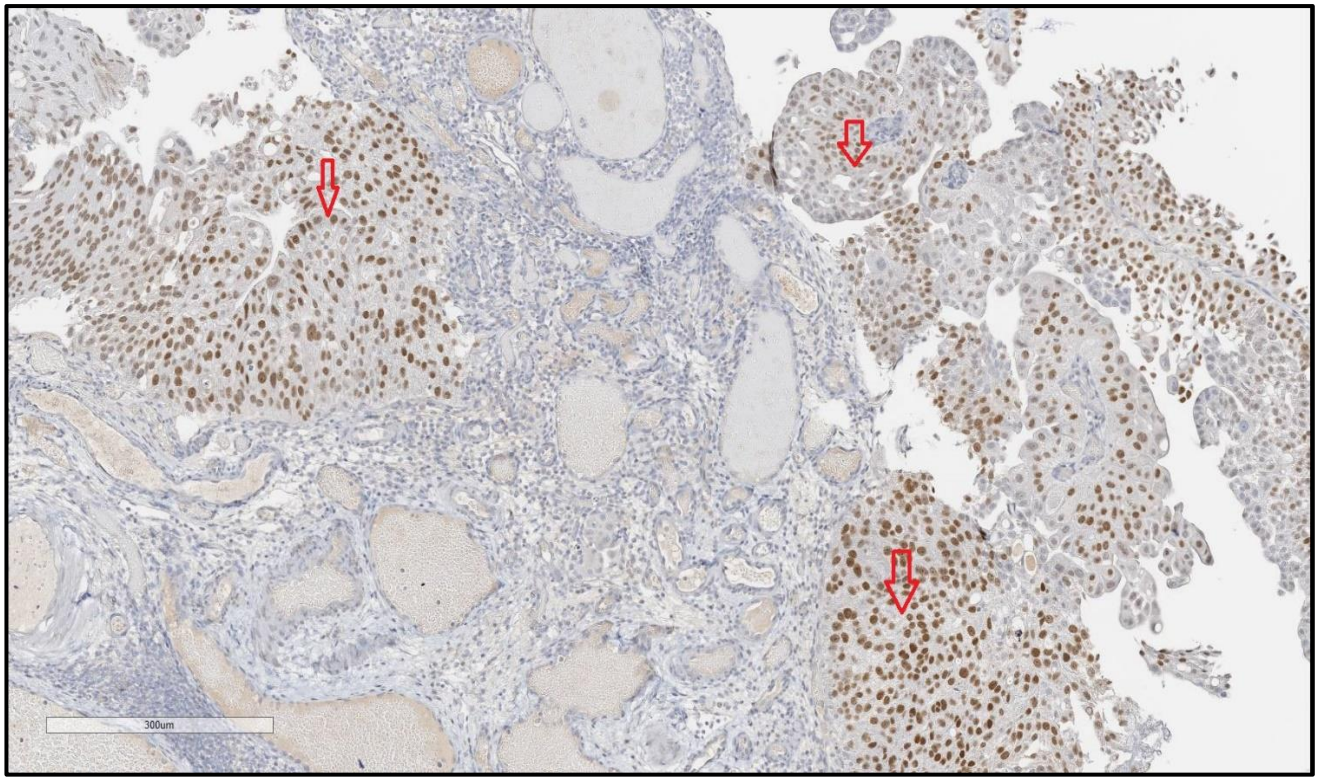

Figure 7. 27 Anti-SOX-2 antibody staining in BC tissues (IHC score= ++)
Positive nuclear staining in 25-50% of Bladder tumours (red arrows). Ventana Ultraview DAB. X100 Magnification

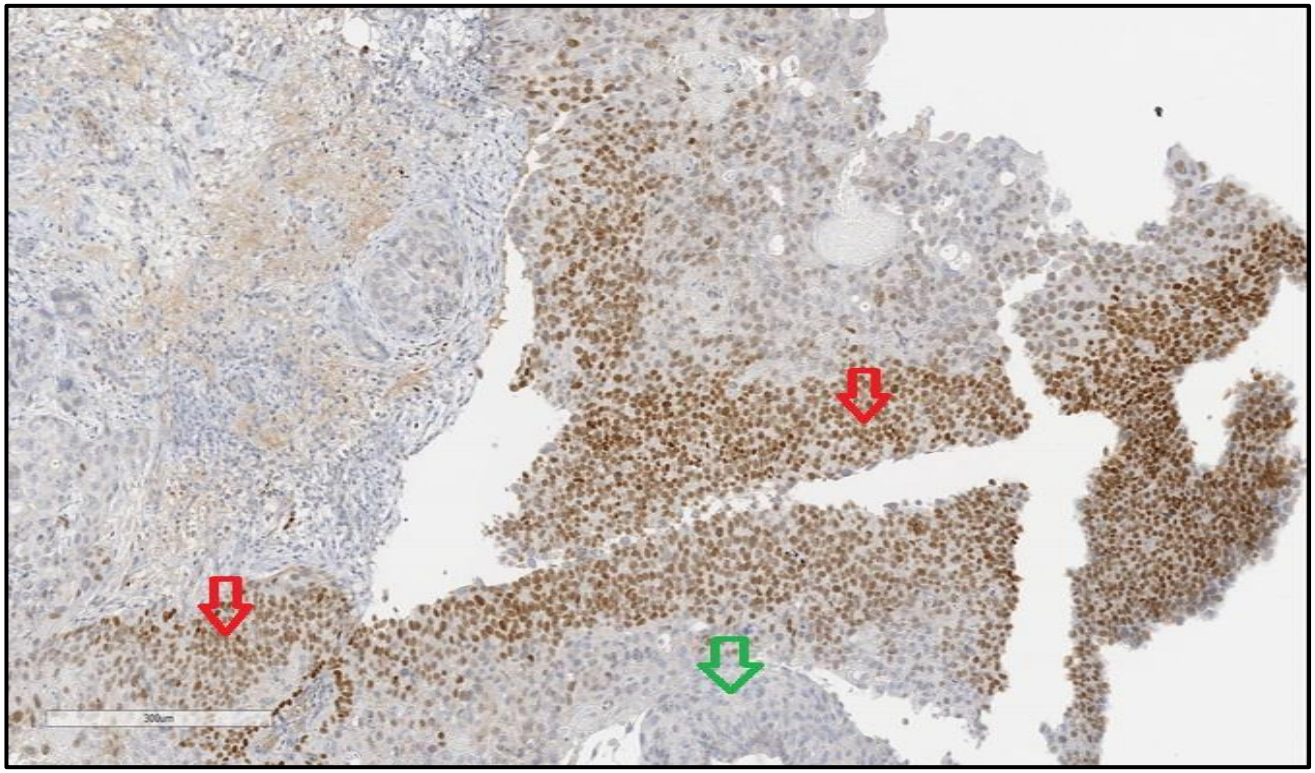

Figure 7. 28 Anti-SOX-2 antibody staining in BC tissues (IHC score= +++)
Positive nuclear staining in >50% Bladder tumour cells (red arrows). No staining in normal cells (Green arrows) Ventana Ultraview DAB. X100 Magnification

Generally, there was a significant increase in SOX-2 immunoreactivity in Bladder tumour, compared to normal tissues (X2(3) = 20.88, p< 0.001), as determined by the Chi-square test (table 7.10).

With respect to cancer grading, there was no significant association between patients' cancer grade and SOX-2 immunoreactivity ($X^2(2) = 5.45$, p= 0.06), as determined by the Kruskal-Wallis test. There was also no significant association between patient's cancer stage and SOX-2 immunoreactivity ($X^2(2) = 4.38$, p= 0.11), as determined by the Kruskal-Wallis test (table 7.10).

In the present study, 14 patients developed BC recurrence during the study period, all of which were diagnosed clinically during follow-up cystoscopies.

The relationship between antibody immunoreactivity (at diagnosis) vs BC recurrence was investigated via Mann-Whitney statistical test, and suggests that antibody immunoreactivity (SOX-2) is not associated with an increased risk BC recurrence (U= 111.50, p= 0.74) (table 7.10).

7.2.8 Immunoreactivity of anti-CEACAM-1 in BC patients

In this present study, the immunoreactivity of CEACAM-1 was analysed using IHC. Prior to staining patient tissues, validation of the IHC staining protocol was performed and has been presented elsewhere (Section 3.1.6).

The anti-CEACAM-1 primary monoclonal antibody used in this study shows cytoplasmic/membranous staining patterns in BC tissue sections. Positive staining was reported based on colour intensity and percentage of Bladder tumours staining positive.

Table 7. 8: Staining interpretation for IHC scores for CEACAM-1
The anti-CEACAM-1 primary monoclonal antibody used in this study shows cytoplasmic and membranous localisation BC tissue sections.

IHC Status	Meaning/Interpretation
Negative	Positive cytoplasmic/membranous staining in <5% of Bladder tumours
Positive (+)	Positive cytoplasmic/membranous staining in up to 20% of Bladder tumours
Positive (++)	Positive cytoplasmic/membranous staining in up to 20-50% of Bladder tumours
Positive (+++)	Positive cytoplasmic/membranous staining in >50% of Bladder tumours

The aim of this section was to initially identify the immunoreactivity of CEACAM-1 in NMIBC and subsequently compare this immunoreactivity in patients who had recurrence and

progression. Examples of the staining for negative and positive (+) categories are presented in figures 7.29 -7.31.

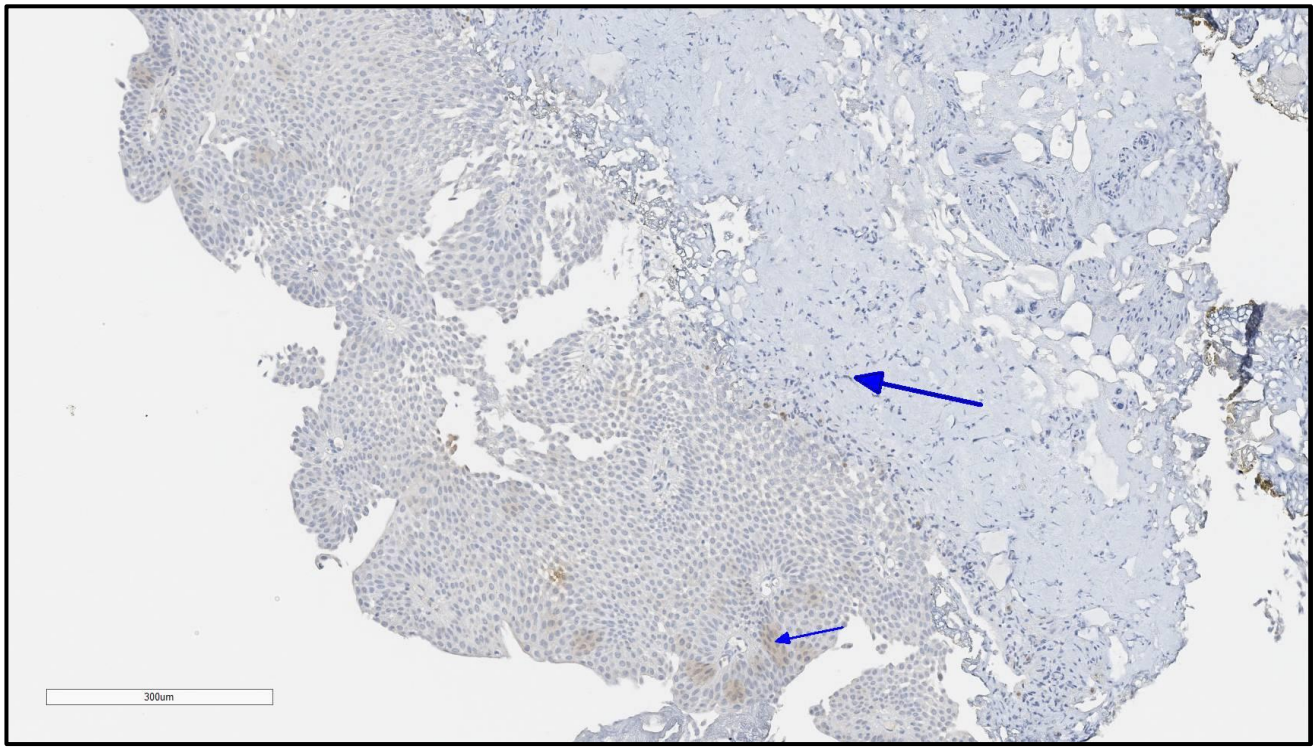

Figure 7. 29 Anti-CEACAM-1 antibody staining in BC tissues (IHC score= Negative). No staining/Positive membranous staining in <5% of Bladder tumours. Small blue arrow shows weakly immunoreactive bladder tumour. Bug blue arrow shows underlying connective tissue. Ventana Ultraview DAB. X100 magnification

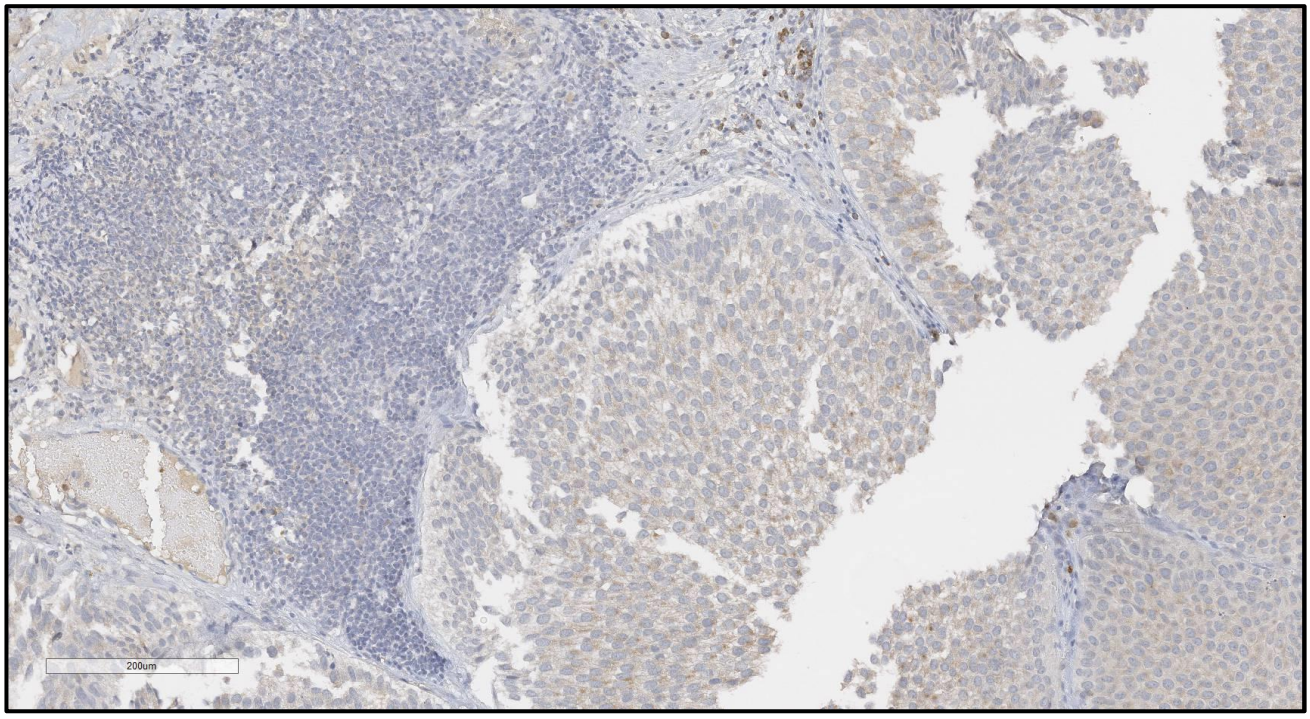

Figure 7. 30 Anti-CEACAM-1 antibody staining in BC tissues (IHC score= +). Moderate membranous staining in up to 20% of Bladder tumours. Ventana Ultraview DAB. X100 magnification

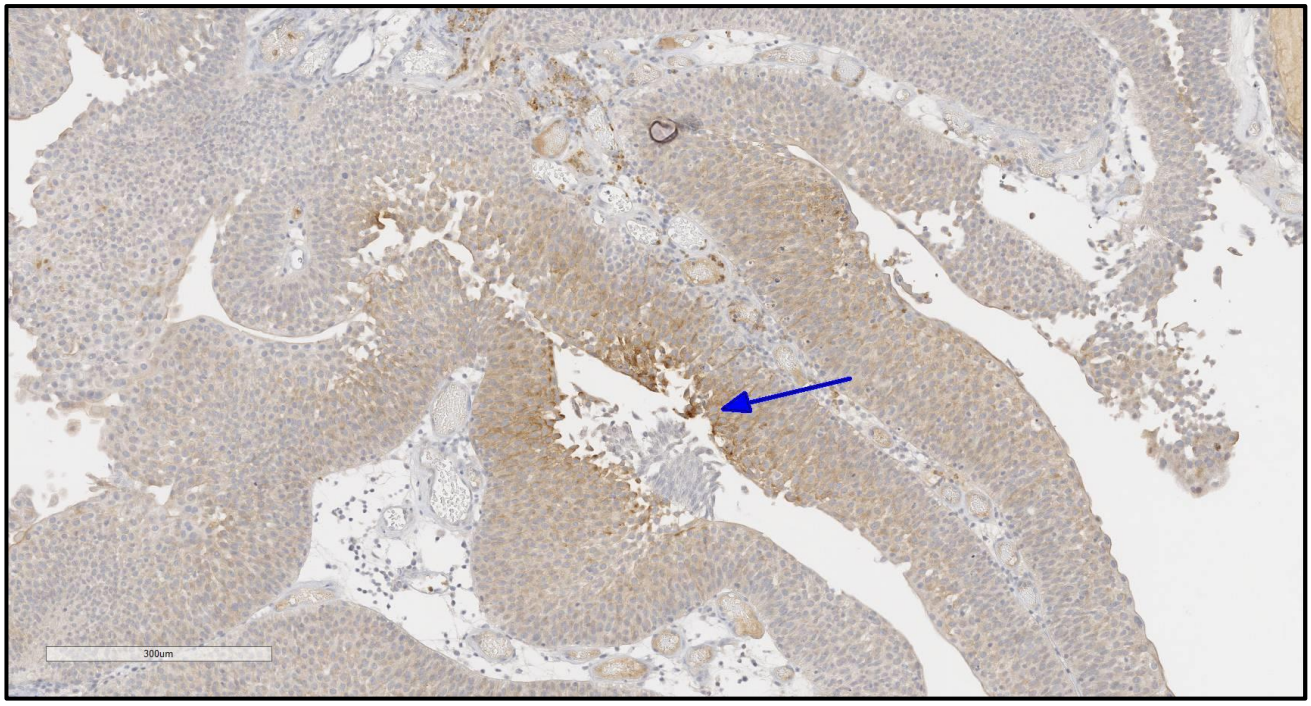

Figure 7. 31 Anti-CEACAM-1 antibody staining in BC tissues (IHC score= ++).
Positive membranous staining in 20-50% of Bladder tumour cells (Blue arrows). Ventana ultraview DAB detection. X100 magnification

Generally, there was a significant change (loss of immunoreactivity) in CEACAM-1 immunoreactivity in Bladder tumour, compared to normal tissues (X2(3) = 11.29, p< 0.001), as determined by the Chi-square test (table 7.10).

With respect to cancer grading, there was a significant association between patients' cancer grade and CEACAM-1 immunoreactivity ($X^2(2) = 6.19$, p= 0.045), as determined by the Kruskal-Wallis (table 7.10). Further post-hoc testing using the Mann-Whitney test revealed significant difference between grade 1 and grade 3 (Z= -2.444, p= 0.015, r= 0.509) (table 7.10).

With respect to cancer staging, there was a significant association between patient's cancer stage and CEACAM-1 immunoreactivity ($X^2(2) = 10.78$, p= 0.005), as determined by the Kruskal-Wallis test (table 7.10).

In the present study, 14 patients developed BC recurrence during the study period, all of which were diagnosed clinically during follow-up cystoscopies.

The relationship between antibody immunoreactivity (at diagnosis) vs BC recurrence was investigated via Mann-Whitney statistical test, and suggests that antibody immunoreactivity (CEACAM-1) is not associated with an increased risk BC recurrence (U= 103.00, p= 0.65) (table 7.10).

7.2.9 Immunoreactivity of anti-VEGFR-3 in BC patients

In this present study, immunoreactivity of VEGFR-3 antibody was analysed using IHC. Prior to staining patient tissues, validation of the IHC staining protocol was performed and has been presented elsewhere (Section 3.1.5).

The anti-VEGFR-3 primary monoclonal antibody used in this study shows nuclear and cytoplasmic staining patterns in BC tissue sections. Positive nuclear and cytoplasmic staining was reported based on colour intensity and percentage of bladder tumours staining positive.

Table 7. 9: Staining interpretation for VEGFR-3 staining in BC patient tissues

IHC Status	Meaning/Interpretation
Negative	No Staining or <5% nuclei/cytoplasmic staining in Bladder tumours
Positive (+)	<25% Nuclei/cytoplasmic staining in Bladder tumours
Positive (++)	25-50% nuclei/cytoplasmic staining in Bladder tumours
Positive (+++)	<75% Nuclei/cytoplasmic staining in Bladder tumours

Examples of each of the staining categories are presented in figures 7.32- 7.35.

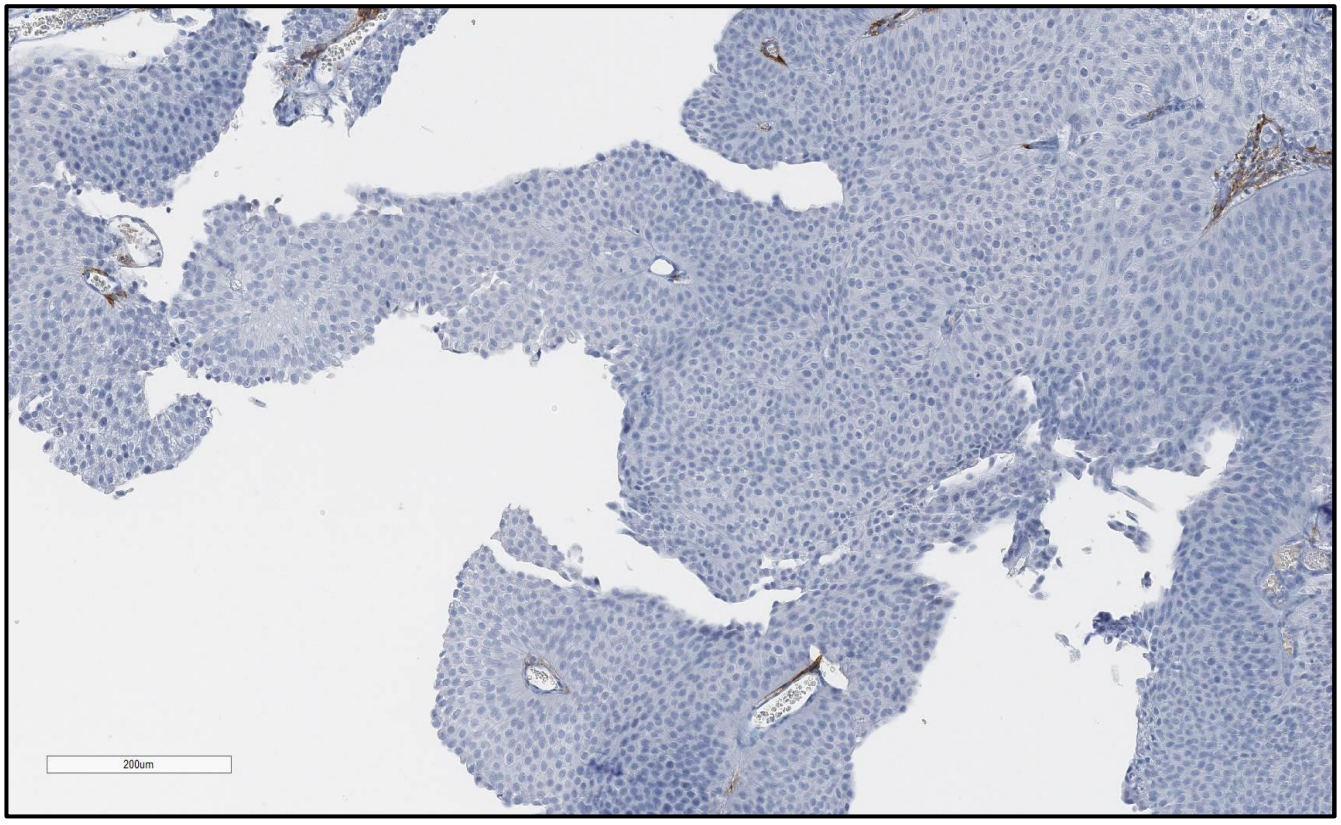

Figure 7. 32 Anti-VEGFR-3 antibody staining in BC tissues (Negative control).
No Staining or <5% nuclei/cytoplasmic staining in BC tissues. Ventana Ultraview DAB. X100 magnification.

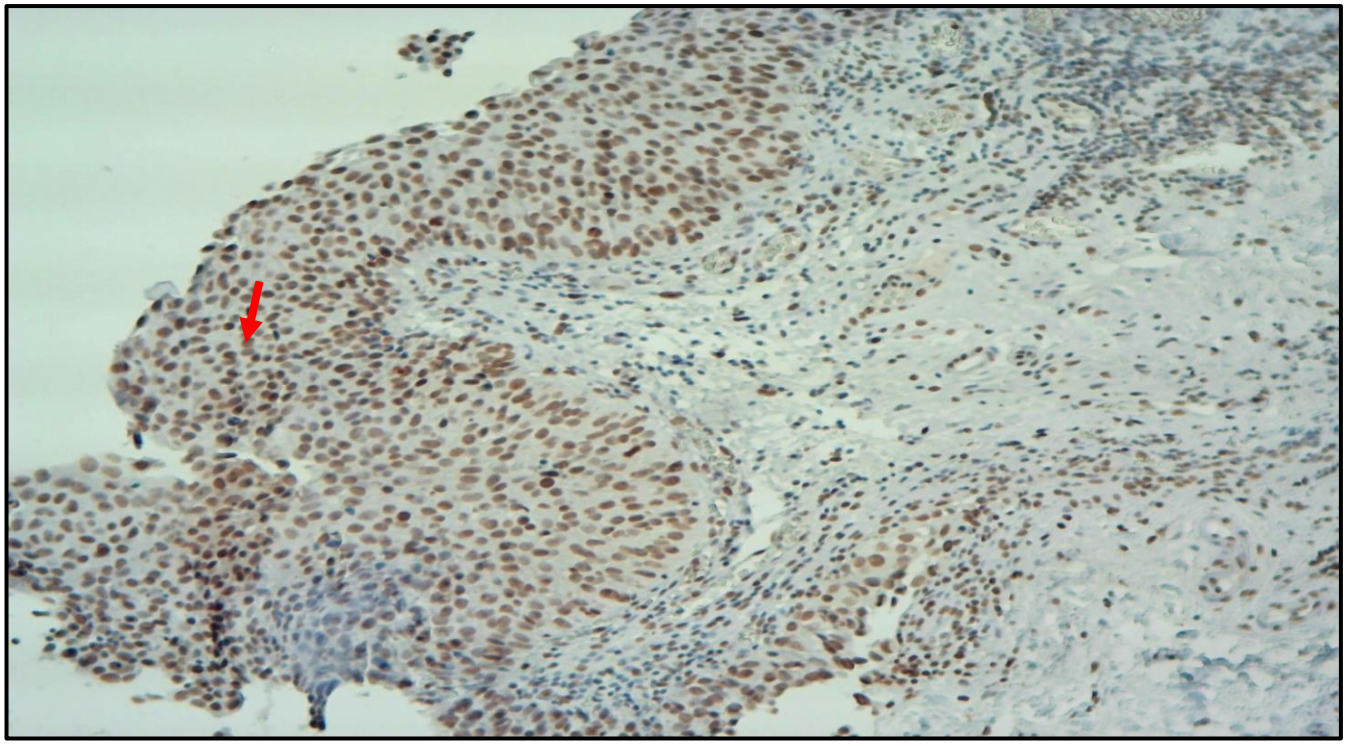

Figure 7. 33 Anti-VEGFR-3 antibody staining in BC tissues (IHC score= +).
Moderate positive cytoplasmic/membranous staining in <25% of Bladder tumours (red arrows). Ventana Ultraview DAB. X100 magnification.

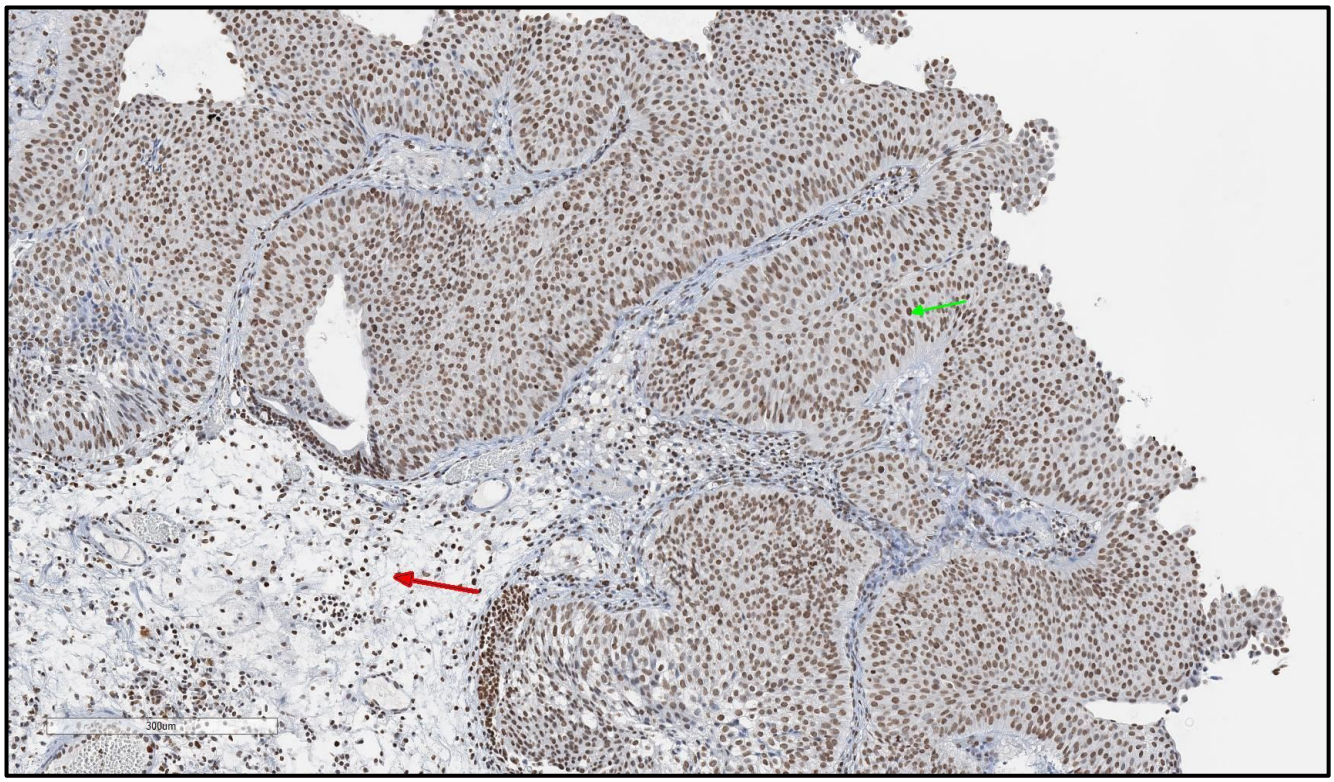

Figure 7. 34 Anti-VEGFR-3 antibody staining in BC tissues (IHC score= ++).
Moderate positive nuclear/cytoplasmic staining in 25-50% of Bladder tumours (Green arrows). Nonspecific staining in underlying stroma cells (red arrows). Ventana Ultraview DAB. X40 magnification.

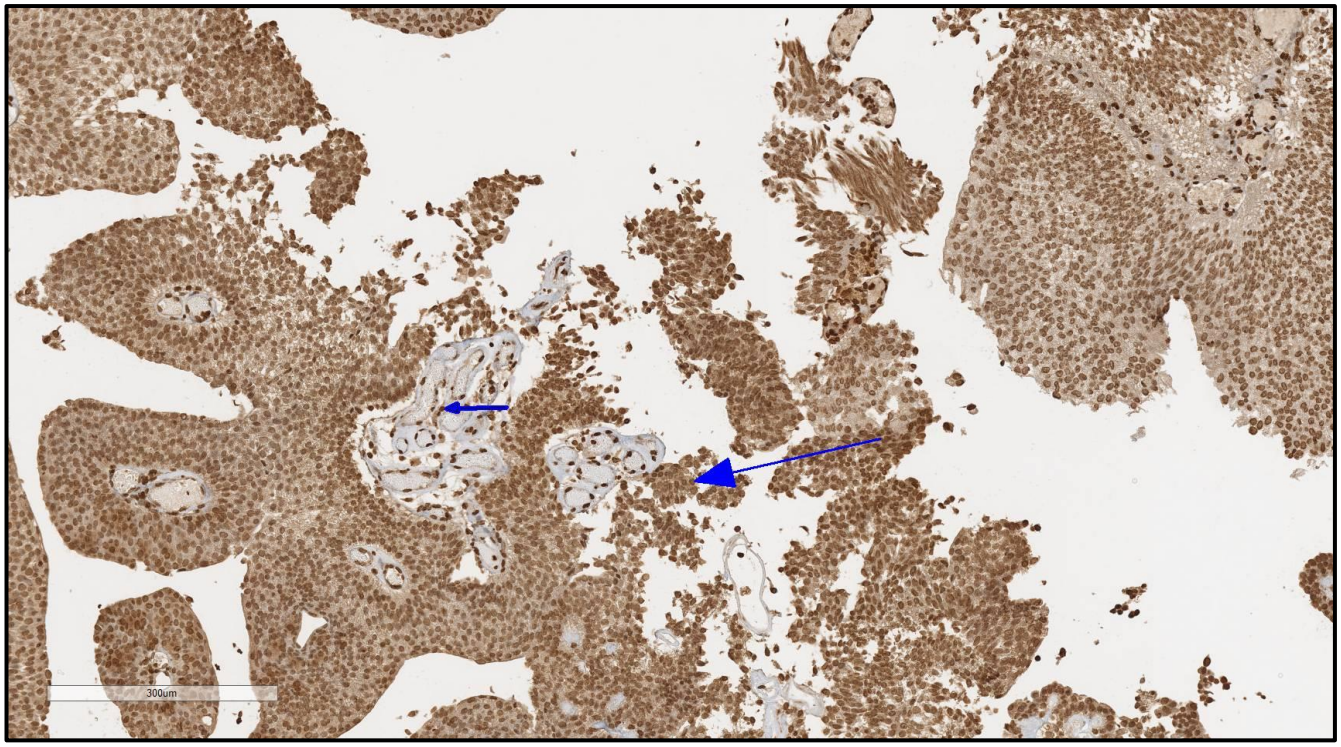

Figure 7. 35 Anti-VEGFR-3 antibody staining in BC tissues (IHC score= +++).
Strong nuclear/cytoplasmic staining in >50% of Bladder tumour (Blue arrows (big) smaller arrow shows nonspecific staining in stroma cells. Ventana Ultraview DAB. X40 magnification.

Generally, there was a significant increase in VEGFR-3 immunoreactivity in Bladder tumours, compared to normal tissues (X2(3) = 41.71, p< 0.001), as determined by the Chi-square test (table 7.10).

With respect to cancer grading, there was a significant association between patients' cancer grade and VEGFR-3 immunoreactivity ($X^2(2) = 4.18$, p= 0.12), as determined by the Kruskal-Wallis (table 7.10). There was also no significant association between patient's cancer stage and VEGFR-3 immunoreactivity ($X^2(2) = 2.94$, p= 0.23), as determined by the Kruskal-Wallis test (table 7.10).

In the present study, 14 patients developed BC recurrence during the study period, all of which were diagnosed clinically during follow-up cystoscopies.

The relationship between antibody immunoreactivity (at diagnosis) vs BC recurrence was investigated via Mann-Whitney statistical test, and suggests that antibody immunoreactivity (VEGFR-3) is not associated with an increased risk BC recurrence (U= 97.00, p= 0.38) (table 7.10).

Table 7. 10: summarised statistical results for antibody staining in BC

Antibody	Staining pattern in Bladder tumour	Antibody immunoreactivity (Chi square)	Antibody immunoreactivity vs BC grade (Kruskal-Wallis test)	Antibody immunoreactivity vs BC stage (Kruskal-Wallis test)	Antibody immunoreactivity vs Recurrence (Mann-Whitney test)
CD31	Increased immunoreactivity in vascular cells	$X^2(2) = 20.353$, $p< 0.001$	$X^2(2) = 2.719$, $p= 0.257$	$X^2(2) = 12.276$, $p= 0.002$	U= 102.00, p= 0.69)
CD34	Increased immunoreactivity in vascular cells	$X^2(2) = 38.941$, $p< 0.001$	$X^2(2) = 1.953$, $p= 0.377$	$X^2(2) = 3.596$, $p= 0.166$	U= 110.00, p= 0.97
Thrombomodulin	Reduced/loss of immunoreactivity	$X^2(2) = 11.286$, $p= 0.010$	$X^2(2) = 0.380$, $p= 0.827$	$X^2(2) = 6.498$, $p= 0.039$	U= 115.50, p= 0.89
HER-2	Increased immunoreactivity	$X^2(2) = 8.818$, $p= 0.032$	$X^2(2) = 11.407$, $p= 0.003$	$X^2(2) = 16.092$, $p< 0.001$	U= 101.50, p= 0.91
S100P	Increased immunoreactivity	$X^2(2) = 41.686$, $p< 0.001$	$X^2(2) = 0.206$, $p= 0.902$	$X^2(2) = 2.134$, $p= 0.344$	U=96.00, p= 0.23
CEACAM-1	Reduced/loss of immunoreactivity	$X^2(2) = 11.286$, $p< 0.001$	$X^2(2) = 6.192$, $p= 0.045$	$X^2(2) = 10.782$, $p= 0.005$	U= 103.00, p= 0.65
SOX-2	Increased immunoreactivity	$X^2(2) = 20.886$, $p< 0.001$	$X^2(2) = 5.451$, $p= 0.066$	$X^2(2) = 4.383$, $p= 0.112$	U= 111.50, p= 0.74
COX-2	Increased immunoreactivity	$X^2(2) = 19.971$, $p< 0.001$	$X^2(2) = 0.960$, $p= 0.619$	X2(2) = 1.648, p= 0.439	U= 118.50, p= 0.98
VEGFR-3	Increased immunoreactivity	$X^2(2) = 41.706$, $p< 0.001$	$X^2(2) = 4.184$, $p= 0.123$	$X^2(2) = 2.935$, $p= 0.231$	U= 97.00, p= 0.38

Table 7. 11: Raw data of antibody staining (at diagnosis) and recurrence in recruited BC patients

STUDY NUMBER	GRADE	STAGE	RECURRENCE	HER-2	SOX-2	COX-2	VEGFR-3	CEACAM-1	CD31	CD34	S100P	THROMBO
TURBT/001	G2	pTa	YES	++	+	+++	+++	neg	++	+++	++	++
TURBT/002	G3	pT2	NO	+++	neg	neg	+++	+	+	+	++	+++
TURBT/003	G3	Pt2	NO	neg	+++	++	+++	neg	+++	+++	neg	neg
TURBT/004	G1	pTa	NO	+	neg	+	++	neg	++	neg	++	neg
TURBT/005	G1	pTa	NO	+	neg	++	+++	neg	+	+	++	neg
TURBT/006	G3	pTa	NO	++	+	++	+++	neg	+++	+++	+++	neg
TURBT/007	G1	pTa	NO	neg	neg	+++	+++	neg	+++	+++	+++	+
TURBT/008	G3	pT1	NO	++	+	+++	+++	neg	+++	+++	+++	neg
TURBT/009	G2	pTa	NO	++	neg	++	++	neg	++	+++	+++	+++
TURBT/010	G1	pTa	NO	neg	neg	+++	+++	neg	++	+++	+++	neg
TURBT/011	G2	pTa	YES	++	neg	++	+++	neg	+++	+++	+++	neg
TURBT/012	G2	pT1	NO	+++	neg	+++	+++	neg	+++	+++	+++	+
TURBT/013	G1	pTa	YES	neg	+	++	++	neg	+	++	+++	+
TURBT/014	G3	pT1	NO	++	neg	+	+++	+	+++	+++	++	+
TURBT/015	G2	pTa	YES	++	++	+++	+++	++	++	+++	+++	neg
TURBT/016	G3	pTa	YES	++	++	+++	+++	neg	+++	++	+++	+
TURBT/017	G2	pTa	YES	++	neg	++	+++	neg	+	+++	++	neg
TURBT/018	G2	pTa	NO	++	++	++	+++	neg	+++	+++	+++	++
TURBT/019	G2	pTa	YES	++	neg	+++	+++	+	+++	+++	+++	+
TURBT/020		CIS pTa	YES	neg	neg	+					+	+
TURBT/021	G2	pTa	NO	neg	neg	+++	+++	neg	++	++	+++	neg
TURBT/022	G2	pTa	YES		neg	+++	+++	neg	+++	+++	+++	neg
TURBT/023	G3	pT2a	YES	NEG	+++	+++	+++	neg	+++	+++	neg	neg
TURBT/024	G1	pTa	NO	+	neg	++	+++	neg	+++	+++	+++	++
TURBT/025	G3	pT1	NO	++	neg	+++	+++	neg	++	++	+++	neg
TURBT/026	G3	pT2	NO	+++	+	+++	+++	+	++	+++	+++	++
TURBT/027	G2	pTa	YES	+	neg	+++	++	neg	++	++	+++	+
TURBT/028		SCC	YES	neg	+	neg	+	neg	Neg	neg	neg	+
TURBT/029		T CELL PAPILLOMA	NO	neg	+++	++	+++	neg	+++	+++	+++	neg
TURBT/030	G1	pTa	YES	neg	neg	+++	+++	neg	+++	+++	+++	+
TURBT/031	G3	pT1	NO	++	neg	++	+++	neg	+++	+++	+++	++
TURBT/032	G3	pTa	YES	+++	+	++	+++	+	+++	+++	+++	++
TURBT/033	G1	pTa	NO	neg	neg	+++	+++	neg	++	+++	+++	+
TURBT/034	G3	pT2	NO	neg	+	+++	+++	+	+++	+++	+++	+
TURBT/035	G3	pT1	NO	TBC	+++	+++	+++	+	++	++	+++	+

8.0 Chapter Eight: General Discussion

8.1 General research Overview

The focus of this research was to evaluate changes of selective biomarkers in BC patients, who had a transurethral resection of bladder tumour (TURBT) surgery for the diagnosis and treatment of BC. These biomarkers were investigated due to their roles in various mechanisms leading to cancer growth and proliferation. Following TURBT, patients were followed for a period of 6 months during which time, venous blood samples were obtained from each patient and analysed for monitoring changes in selective novel biomarkers. Various selected tissue-based biomarkers were also investigated in patient tissues following TURBT for the treatment of BC.

Initially antibody staining and IHC protocols were optimised (chapter 3), prior to undertaking four pilot clinical studies involving BC patients. Specifically, this research study aimed to investigate;

1. Changes in serum-based inflammatory markers in BC patients and their association with recurrence and progression

2. Changes in serum MMP-2, MMP-3, MMP-9 and CEACAM-1 in patients undergoing TURBT for the treatment of BC

3. The role of various serum-based angiogenic and growth biomarkers in NMIBC recurrence/progression

4. The role of novel antibody immunoreactivity and their association with BC recurrence and progression

8.1.1 Optimisation of protocols for Immunohistochemistry (Chapter 3)

The main aim of this chapter was to verify and optimise the protocols and antibodies used for assessing IHC staining of various antibodies in BC tissues. Following TURBT, bladder tissues were processed into Formalin-Fixed Paraffin-Embedded (FFPE) tissue blocks for H&E staining and interpretation. 4 µm serial sections were cut from each tissue and placed on positively charge microscope slides for IHC staining. Tissue sample preparation, sectioning, staining and analysis were carried within an UKAS ISO15189 accredited NHS histopathology department at the Glan Clwyd Hospital, North Wales. The antibodies optimised in this chapter include CEACAM-1, CD31, CD34, COX-2, HER-2/neu, S100P, SOX-2, Thrombomodulin and VEGFR-3. Optimisation of various antibodies for IHC was undertaken using recommended control sample tissues (Table 2.1).

During this research, the IHC process was optimised and validated by including both control and sample tissues on the same IHC microscope slide (Figure 2.1). This approach enhances internal quality control measures by exposing both control and sample tissues to same staining conditions, i.e. temperature, wash cycles, incubation time, etc. Although traditional IHC protocols also use control tissue samples, these samples are usually placed on separate microscope slides and included during the staining process. This therefore exposes the different microscope slides to potential variations in temperature, time of incubation and reporting. The presence of both control and sample tissues on the same slide, further enhances the reporting process as there will be no need to change microscope slides to compare staining in control slides with staining in patient tissues.

As the optimisation of IHC staining protocols and subsequent analyses of patient tissues were undertaken within an UKAS ISO15189 accredited histopathology laboratory, this further validates the IHC protocols to both clinical and laboratory standards. New knowledge gained from this rigorous process will shed more light on IHC staining and interpretation in Bladder tumour samples, and may be potentially welcomed by reputable bodies like EAU and NICE.

Optimisation of the S100P antibody required a modification of the recommended protocol (section 3.1.1). Specifically, primary antibody incubation time was increased to 24 minutes, a post-stain amplification step was included and duration of counterstaining was increased to 12 minutes. This resulted in clearer positive nuclear and cytoplasmic staining and reduced background staining, in trophoblastic epithelial cells of the human placenta control tissue (figures 3.2 & 3.3). The results from this optimisation protocol complements a study by Maciejczyk *et al.*, (2013) who verified anti-S100P immunoreactivity in human placenta tissues by observing positive nuclear and cytoplasmic staining. Our study, however, requires a shorter primary antibody incubation time (24 minutes), shorter antigen retrieval (8 minutes) and a shorter overall IHC process compared to the process reported by others (Maciejczyk *et al.*, 2013; Surowiak *et al.*, 2007) and could be used as an alternative methodology for assessing anti-S100P immunoreactivity in BC tissues.

With regards to VEGFR-3, the optimisation and verification of this biomarker was performed using human umbilical cord control samples (section 3.1.5). The staining results from experimental protocols 1-3 produced generally unspecific nuclei and cytoplasmic staining within normal endothelial cells, muscle tissue and other underlying stromal cells (Figures 3.16-3.18). These observations complement similar reports by Smith *et al.* (2010), who previously observed non-specific staining in 4 clones of VEGFR-3. With respect to the present study, optimised IHC staining (protocol 4) was however observed in nuclei and cytoplasm of vascular endothelial cells in human umbilical cord samples. The optimisation protocol used in this

research was performed on umbilical cord samples in contrast with breast and colorectal cancers used by Smith *et al.* (2010), providing further application for staining of this biomarker in other tissue sample types. With respect to staining VEGFR-3 in human bladder biopsies, this research therefore provides new and novel staining approach on the Roche Ventana XT or Roche Ventana ultra IHC platforms (optimised: experimental Protocol 4).

Optimisation of the COX-2 antibody has been described previously (section 3.1.2). Specifically, the optimised protocol (optimised: experimental protocol 2) required a longer antigen retrieval step (64 minutes) and longer primary antibody incubation time (32 minutes). Optimum cytoplasmic and membranous IHC staining in colonic crypts observed in this research study was used as a template for staining BC tissues. Although previous studies have assessed COX-2 IHC staining in human endometrial carcinoma and colorectal cancer tissues (Cai *et al.*, 2017; Hedaya *et al.*, 2015), optimisation results from this present study provides a new and novel method for performing IHC in human BC tissues. In contrast others (Hedaya *et al.*, 2015) who used an EDTA antigen retrieval method, the COX-2 antibody and IHC process used in this research study used a Heat Induced Epitope Retrieval (HIER) method for optimum staining. We provide further details of the staining process, sample micrographs of staining intensity, control and staining duration for optimum staining. This new approach and method for staining tissue COX-2, will help contribute into BC research for those operators using the Roche Ventana XT IHC autostainer or the Roche Ventana ultra IHC autostainer platforms.

With regards to CEACAM-1, optimisation and verification of the IHC protocol and antibody staining was performed using human colon adenocarcinoma control samples (section 3.1.6). Although the experimental protocols produced few overall variations, the optimum staining in human colon tissues was observed in experimental protocol 2. Previous research by Thom *et al.* (2009), reported a longer IHC protocol (2 days) and used only negative controls in contrast with our present study, which has a shorter protocol (3 hours). The CEACAM-1 IHC method developed in the present study, significantly reduces the protocol assay duration (2 days *vs* 3 hours) compared to the original method as described by Thom et al., (2009), and furthermore provides more detailed information about the staining patterns in control tissues. This method was subsequently used as a template to optimise for staining in bladder tumour samples.

HER-2/neu optimisation has been described previously (section 3.1.3). Using breast adenocarcinoma tissue samples, the optimised protocol (experimental protocol 2) had a shorter antigen retrieval step (4 minutes), primary antibody incubation time was 20 minutes, and an amplification step was also included. The optimised protocol (experimental protocol 2) was used for staining BC tissues. HER-2 IHC is currently used for clinical management of invasive breast cancer, and has therefore been studied by other research groups (Gheybi *et al.*, 2016; Ji

et al., 2014; Shirsat *et al.*, 2012). However, this current research provides new information with regards staining BC tissues using the Roche Ventana XT IHC autostainer and the Roche Ventana ultra IHC autostainer platforms.

Optimisation of CD31 and CD34 were performed using human appendix tissue samples as positive control. With the inclusion of an amplification step and an increased incubation time, optimum CD31 staining was observed within vascular endothelial cells in appendix tissues. In the same tissues, CD34 immunostaining produced higher colour intensity compared to CD31. This observation complements a similar study by (Krishnamoorthy *et al.*, 2015), who also reported that, CD34 immunostaining had a higher colour intensity in non-distended vein samples compared to CD31. The modified protocol for assessing CD31 and CD34 used in this research, therefore, may provide an alternative method for future researchers and will aid standardization of IHC protocols within pathology (clinical and research) laboratories.

With regards to thrombomodulin, non-specific binding was prevented by adding a blocking step to the IHC protocol. For the optimum protocol, primary antibody incubation time was also increased to 32 minutes, post-staining amplification was enhanced using Ventana amplifier and an Ultrawash step was included. These modifications resulted to enhanced membranous and cytoplasmic staining within Bladder epithelial cells. Membranous staining patterns observed in this present study complement results by (Song *et al.*, 2018) who also observed similar findings in Oral Squamous cell carcinoma. In contrast to this present study however, the study by (Song *et al.*, 2018) does not provide any information on control tissues, stain protocol and protocol duration. Detailed results from this current study may provide a suitable template for BC research on the Roche Ventana IHC autostainer.

SOX-2 optimisation has been described previously (section 3.1.4). Using human fallopian tube tissue samples, the optimised protocol (experimental protocol 2) had a longer antigen retrieval step (76 minutes), blocking step was included, primary antibody incubation time was 32 minutes, and an amplification step was also included. The optimised protocol (experimental protocol 2) produced cytoplasmic and nuclear staining patterns in fallopian tube tissues and complements results from a study by Capatina, Cimpean, Raica, Coculescu, & Poiana, (2019) who also reported similar staining patterns. In comparison with Capatina *et al.* (2019) however, the protocol developed in this current study had a shorter overall duration and is more suitable for BC research. Furthermore, this current research provides new information with regards staining BC tissues using the Roche Ventana XT IHC autostainer and the Roche Ventana ultra IHC autostainer platforms.

Variation in IHC may be caused by several factors and is one main sources of controversy limiting standardisation across laboratories, research groups and regulatory bodies. Although storage duration of FFPE tissues has been highlighted as a potential source of variation, Shi, Liu, & Taylor (2007) have recommended the need to optimise antigen retrieval techniques prior to staining sample tissues.

In summary, the present study has developed and optimised novel biomarker tissue staining methods that may be, in the future, used to screen, diagnose and monitor patients with BC.

8.1.2 Chapter Four: Changes in serum-based inflammatory markers in BC patients and their association with recurrence and progression

The main aim of this chapter was to identify changes in various inflammatory-related biomarkers in patients scheduled for surgical procedures for the treatment of BC. Venous blood samples were taken pre-operatively and at 1-month, 3-months and 6-months post-operatively. TURBT, the main surgical procedure for the diagnosis and treatment of BC, is an invasive technique usually performed under general anaesthesia. Inflammation-associated biomarkers, which may be significant in cancer promotion and growth, were therefore analysed and monitored up to six months following treatment.

MIP-2 was investigated in this research due to its association with inflammation and also its potential role in angiogenesis and tumourigenesis (Kollmar *et al.*, 2006). Serum MIP-2 concentration showed a significant decrease up to 6 months following TURBT ($p=0.001$). Furthermore, there were significant differences between baseline pre-operative serum MIP-2 concentrations and 6-month post-operative concentrations ($p<0.05$).

TURBT conducted under general anaesthesia is expected to initiate an inflammatory response which, in the presence of MIP-2, may lead to increased production of positive mediators of inflammation such as leucocytes and mast cells (Proudfoot *et al.*, 2003). Therefore, it can be appreciated that, MIP-2 concentrations will increase during this time, as evidenced by the increase in concentration at 1-month post-operative. However, 3 and 6-months following surgical treatment, MIP-2 serum concentration are expected to reduce, following resolution of acute inflammatory responses due to surgery. This expectation is evidence by the results from this study, which show decreases in MIP-2 concentration at 3-months post-operative and 6-months post-operative.

A mouse model evaluating changes in plasma MIP-2 levels following optical surgery, observed an increase in MIP-2 concentration up to 7 days post-operative (Avraham *et al.*, 2008). Findings from their study showed that activation of the inflammatory response following surgery resulted

in increased plasma MIP-2 concentration and therefore complements findings from this current study, which also observed increased MIP-2 concentrations at 1-month post-operative.

Furthermore, findings by Avraham *et al. (*2008) also showed a decrease in MIP-2 at 2-months post-operative, which also complements the findings from this current study. With regards to both studies however, longer follow up periods (12, 18 and 24 months) would be more effective for conclusive evaluation of MIP-2 changes and to rule out changes caused by physiological responses, such as wound healing and tissue repair. Nonetheless, our results provide new evidence of decreasing MIP-2 serum concentration in patients undergoing TURBT for BC treatment and diagnosis.

Although CD31 plays various roles in normal physiology (e.g. tissue repair), it was investigated in this research due to its role in angiogenesis and tumour growth (Cao *et al.*, 2002; Kiseleva *et al.*, 2018). With regards to this present study, serum CD31 (also known as PECAM-1) concentrations significantly increased up to 6 months post-operatively ($p=0.003$). Furthermore, there were significant differences between baseline (pre-operative) CD31 levels vs 3-months post-operative ($p=0.002$) and between baseline (pre-operative) CD31 levels vs 6-months post-operative ($p=0.001$).

The initial rise in CD31 concentration at 1-month post-operative could be due to increased tissue repair following the surgical procedures (Nolff *et al.*, 2018). Although serum CD31 concentrations continued to increase at 3 and 6-months post-operative, follow up data is unavailable to confirm association with recurrence and progression.

(Zheng, Chen, Wang, Wang, & Lei (2017) recently reported higher survival rates in metastatic breast cancer who had low serum pre-treatment serum CD31 concentrations suggesting that lower CD31 concentrations were associated with less aggressive tumour properties. In their study however, only pre-treatment CD31 concentrations were measured in recruited patients in contrast to this present study which measured serum changes at various time points following treatment and offers new information about CD31 in BC patients. Differences in treatment techniques (palliative vs TURBT) could also account for variations in their results compared to findings from this present study.

IL-6, IL-8 and TNF-α showed similar trends of decreasing concentration up to 6-months after surgical procedures for the diagnosis and treatment of BC. For IL-6, serum concentrations initially increased at 1-month post-operative, before decreasing at 3-months and 6-months post-operative toward baseline levels. In both *in vitro* and in vivo studies, IL-6, IL-8 and TNF-α have been characterised as acute phase proteins whose immunoreactivity is elevated

immediately following an inflammatory event (Campillo-Gimenez *et al.*, 2018; Papadopoulos, Karpouzis, Tentes, & Kouskoukis, 2014).

In agreement with others (Campillo-Gimenez *et al.*, 2018; Papadopoulos *et al.*, 2014), the present study reports an increased IL-6 concentration for up to 1 month following TURBT for the treatment of BC. Although IL-6 levels noticeably decreased towards basal levels at 6-months post-treatment, a possible explanation for this could potentially be due to the resolution of the initial inflammatory response after surgery.

In a recent study, Feng *et al.* (2018) reported an association between high pre-operative IL-6 and IL-8 serum concentrations and poor survival in pancreatic cancer, whilst high pre-diagnostic serum IL-8 levels have been associated with an increased risk (Trabert *et al.*, 2014), poor prognosis and overall survival (Kassim *et al.*, 2004) of ovarian cancer. In comparison with our current study, these provide no further information with regards to variations in cytokine concentration following surgical or adjuvant intervention. Our study highlights new knowledge with regards to IL-6 and IL-8 serum concentrations in BC and may be useful in developing a panel of biomarkers for assessing TURBT outcome.

With respect to CD40, this is a transmembrane protein member of the larger TNF superfamily and is usually located on the surfaces of platelets, activated B and T cells (van Kooten & Banchereau, 2000). Under certain conditions, such as an inflammatory response during immune activation, it may also be expressed on the surfaces of basophils, mast cells and NK cells (Blumberg *et al.*, 2006). No changes to sCD40 were reported during the present study, possibly suggesting a minimal inflammatory involvement during the post-operative period.

Angiopoietin-2 is expressed on endothelial cells and has been associated with inflammation and angiogenesis (Ju *et al.*, 2014; Lefere *et al.*, 2018). Despite an initial increase in Angiopoietin-2 at 1-month post TURBT, concentrations decreased at 6 months. A possible explanation for the observed rise in concentration at 1-month post-operative, could potentially be due to increased inflammation induced wound healing, tissue repair or vascular remodelling, which has also been reported by others (Bupathi, Kaseb, Meric-Bernstam, & Naing, 2015; Tanaka *et al.*, 1999).

In a recent study, Chen *et al.* (2018) reported significantly higher serum angiopoietin-2 levels in lung cancer patients compared to healthy controls. In agreement with our current study, they reported significant reduction in serum angiopoietin-2 concentration following surgical techniques. Our findings complement their observations that, following surgical techniques, serum angiopoietin-2 concentration reduce potentially because tumour cells that secrete angiopoietin-2 have been removed.

Osteopontin is a glycoprotein with multifunctional properties in inflammation, cell-cell interaction and bone remodelling (Fisher, Torchia, Fohr, Young, & Fedarko, 2001; Giachelli & Steitz, 2000; Lund *et al.*, 2009; Villanueva *et al.*, 2019). In the present study, serum osteopontin concentrations showed a trend of decreasing concentration up to 6-months post-operative. Interestingly however, serum concentrations increased moderately at 1-month and 3-months post-operative potentially indicating an elevated osteopontin-associated inflammatory response or increased cell-cell interaction due to tissue repair following TURBT. At 6-months post-operative, serum osteopontin levels reduced below pre-operative levels further confirming our suggestion that, the initial elevations were responses influenced by TURBT surgery.

In patients with active TCC, higher plasma osteopontin concentrations were observed in patients with high grade cancers and metastasis compared to patients with inactive TCC and healthy controls (Ang *et al.*, 2005), confirming tumourigenic properties in TCC especially in patients with superficial cancers. Osteopontin values reported in their study were markedly lower than the results observed in this present study which may be due to the different techniques employed (ELISA vrs Bioplex). As a secreted protein, sensitive methods are required for the accurate measurement of osteopontin in BC patients due to its potential utility for monitoring treatment outcome.

Findings from this current research complement similar results by Zhou *et al.* (2013) who reported increased 1 week and reduced 1 month and 2 months post-operative serum Osteopontin levels in patients with HCC. Our results are however novel in BC and provides new knowledge about changes in Osteopontin levels following TURBT for the diagnosis and treatment of BC. Validation of these findings using larger sample cohorts with longer follow up confirm Osteopontin as a novel biomarker for BC recurrence and progression.

In summary, it appears that changes to serum biological markers following TURBT for the diagnosis and treatment of BC followed a similar trend. In general, it appeared that most of the biological markers measured during these studies peaked at 1 month postoperatively, prior to decreasing at 3 and 6 months respectively. It is proposed that up to 1-month post-operative is when the most noticeable changes in biological markers occur. This study may therefore have clinical implications for understanding the development of an inflammatory response post-TURBT, and may help aid clinicians with regards to planning their post-operative management and patient care.

With regards to serum-based inflammatory markers, MIP-2 and CD31 have shown most promise following this study. Significant changes (increases in MIP-2 and decreases in CD31) were observed in BC patients following TUTBT. It can therefore be appreciated, that these

biomarkers, amongst the consideration of others, could potentially be considered as part of a BC biomarker profile. However, further investigation, involving larger cohorts, is required to fully establish the roles of these markers following TURBT for BC.

8.1.3 Chapter Five: Changes in serum Matrix Metalloproteinase 2, 3 and 9 (MMP-2, MMP-3 and MMP-9) and Carcinoembryonic Antigen-related Cell Adhesion Molecule-1 (CEACAM-1), in patients undergoing TURBT, for the treatment of NMIBC

The main focus of this chapter was to identify changes in serum MMP-2, MMP-3, MMP-9 and CEACAM-1 in patients undergoing TURBT, for the treatment of NMIBC. The MMPs are a group of proteinases involved in degradation of the Extra Cellular Matrix (ECM), an essential step in tumourigenesis and angiogenesis (Littlepage *et al.*, 2010; Lv *et al.*, 2018).

Some research studies have implicated MMPs in tumour growth (Chan *et al.*, 2017; Deng *et al.*, 2017) and therapeutic interventions targeting ECM degradation by MMPs have been developed for the management of certain pathological conditions (Alaseem *et al.*, 2017).

Generally, there was a trend of decreasing serum MMP-2 concentration up to 6 months following TURBT for the treatment of NMIBC. MMP-2 concentration decreased at 1-month post-operative, remained unchanged at 3-months post-operative and further decreased at 6-months post-operative. Following removal of the main cancer tumour through surgery, it can be appreciated that concentrations will fall post-operatively due to an absence of MMP secreting tumour stromal cells or reduced degradation of the ECM.

In breast cancer patients, Song *et al.* (2012) investigated MMP-2 and observed that higher pre-operative serum MMP-2 levels were significantly linked to poorer prognosis. Although Song et al. (2012) did not measure post-operative MMP-2 levels, our findings complement their results since the baseline MMP-2 results were higher than any of the results observed post-operatively. Since our study did not assess prognostic data following TURBT, we cannot directly compare serum concentrations and cancer prognosis or survival. Our study however further supports the observation that increased MMP-2 secretion occurs in the presence of tumour cells but adds new knowledge in BC research since no previous studies have monitored MMP-2 changes following TURBT treatment.

A study investigating serum MMP-2 observed lower concentrations in CRC patients compared to healthy controls as well as lower concentrations in patients with high grade tumours, advanced cancer stages and patients with metastatic disease (Groblewska *et al.*, 2014). One reason for this observation could be because high levels of MMP-2 lead to increased proteolysis and increased cell migration during metastasis, which potentially has the general effect of lowering the circulating MMP-2 levels in patients.

In similar study, Waas, Wobbes, Ruers, Lomme, & Hendriks (2006) also observed lower serum MMP-2 concentrations in patients with metastatic liver disease compared with healthy controls further suggesting that in high grade, stage and metastatic disease, increased activity within the ECM reduces serum MMP-2 concentrations. In comparison with both studies by Waas *et al.* (2006) and Groblewska *et al.* (2014), although cancer prognosis, metastasis and survival were beyond the scope of our study, we nonetheless report higher pre-operative serum MMP-2 concentrations compared to post-operative concentration in BC patients. These differences in our reports could be due to differences in patient cohorts (NMIBC vrs CRC) and test methods (ELISA vrs Bioplex assay).

With regards to serum MMP-3, there was a trend of decreasing serum MMP-3 concentration following TURBT in BC patients recruited into this study. There was however an initial increase in concentration from baseline to 1-month post-operative potentially due to ECM remodelling following surgical techniques. At 3 months and 6-months post-operative however, low MMP-3 concentrations are expected if there is no cancer recurrence or progression.

In a recent study Benoit *et al. (*2015) investigated serum MMP-3 levels in BC patients and reported decreased concentrations in patients with lymph node involvement at the time of radical cystectomy, indicating a potential role of MMP-3 in lymph node metastasis. The pre-operative serum MMP-3 levels reported in the study are lower than those observed in this present study, and may be due to differences in patient cohorts. Whilst their study included patients with metastasis, our current study only included superficial BC patients. Higher pre-operative serum MMP-3 may be due to presence of the tumour cells initiating cell proliferation, ECM degradation and angiogenesis (Littlepage *et al.*, 2010; Lv *et al.*, 2018)

In this study, serum MMP-9 concentrations showed a significant decrease up to 6-months post-operatively. Various researchers have investigated MMP-9 immunoreactivity in tissues, urine and serum samples of BC patients (Eissa, 2007; Hara, 2001; Reis *et al.*, 2012). In a study by Guan et al. (2003), pre-operative serum MMP-9 concentrations were significantly higher ($p<0.001$) in patients with TCC compared with healthy controls. The results from the present study complement these findings, in that, basal levels of MMP-9 were higher than those following resection of the tumour via TURBT. In this present study, serum MMP concentrations were measured using a bead-based flow cytometry method, which has been employed by other studies (Benoit *et al.*, 2015), confirming a reliable methodology for analysing this group of biomarkers.

A fundamental difference between the studies discussed above and our current study is the length of follow up. These studies only measured pre-operative serum MMPs levels, whereas

the present study made comparisons between pre-operative serum MMPs concentrations up to 6-months post-operatively. It can therefore be appreciated that excision or removal of bladder tumours during surgery, may eventually reduce serum MMP levels. This may be due to the fact that there is increased presence of MMPs within the tumour microenvironment. TURBT, which successfully removes Bladder tumours, will therefore reduce MMP presence within the tumour site and this could eventually lead a reduction in serum levels. It is for this reason, that measuring serum MMP levels in serum could potentially be considered a useful biomarker for monitoring patients with BC.

Although CEACAM-1 has pleiotropic effects (such as inducing apoptosis, regulation of cell migrations, inhibition of cell proliferation) (Gebauer *et al.*, 2014) in both physiology and pathological conditions, it was investigated in this present study due to its potential role as a marker of angiogenesis and tumour growth (Ergün *et al.*, 2000).

In this present study, although there were no significant changes in CEACAM-1 serum concentrations, there was trend of increasing concentration up to 6 months following TURBT for BC treatment. Since CEACAM-1 has been shown to induce apoptosis and inhibit proliferation in epithelial cells, the results from this present study suggests increasing serum concentrations may possess protective functions for BC patients.

Huajun *et al.* (2018) have suggested that, combined measurement of serum CEACAM-1 and APE1 has an increased potential of detecting colorectal cancer, since higher concentrations were observed in patients with colorectal cancer. Their findings are in disagreement with the results from this present study although they measured only one-time point (pre-treatment) CEACAM-1 concentration.

Although the association between serum CEACAM-1 and BC recurrence were not correlated in this present study, a recent study observed that patients with low serum CEACAM-1 had a prolonged overall survival rate confirmed with patients with higher concentrations (Gebauer *et al.*, 2014). These further suggest that CEACAM-1 has protective functions and warrants further study.

With regards to bladder specific research, there is limited evidence in literature on the effects of CEACAM-1 on BC stage, grade and recurrence. Therefore, this present study provides new information with regards to changes in serum CEACAM-1 concentration following TURBT for BC treatment and should be investigated further using larger sample cohorts and longer follow ups.

In summary, it is the MMP-9 biomarker that has shown most promise following this study. Significant changes (decreases) were observed in BC patients following TUTBT. It can

therefore be appreciated, that this biomarker, amongst the consideration of others, could potentially be considered as part of a BC biomarker profile.

8.1.4 Chapter Six: The role of various serum-based angiogenic and growth biomarkers in Non-Muscle Invasive BC recurrence/progression

The main focus of this chapter was to identify changes in various angiogenesis-related serum biomarkers in patients undergoing treatment for BC. The biomarkers analysed in this chapter are mainly associated with tumour growth and progression by influencing processes such as angiogenesis. Venous blood samples were taken pre-operatively and at 1-month, 3-months and 6-months post-operatively. TURBT, the main surgical procedure for the diagnosis and treatment of BC, is an invasive technique usually performed under general anaesthesia. The biomarkers measured in this chapter include growth factors, growth factor receptors and cell adhesion molecules.

The basic fibroblast growth factor (bFGF) is strongly pro-angiogenic and has been implicated in cell proliferation and cancer growth (Harney *et al.*, 2015; Lewis *et al.*, 2016). In this study, there was a trend of increasing serum bFGF concentration up to 6-months after TURBT, suggesting increased bFGF systemic or tumour activity following TURBT treatment.

Although the results observed in this present study were not statistically significant, the trend of increasing bFGF concentration could potentially be due to tissue remodelling, vascular repair or early cancer recurrence. In TCC patients, Szarvas *et al.* (2012) have previously shown that increased serum bFGF concentration is associated with angiogenesis. In comparison with Szarvas *et al.* (2012) however, follow up serum data was not provided, and conclusions with regards to angiogenesis may be inaccurate due the several other underlying factors such as chemotherapy. In this present study, although increased bFGF concentrations were observed post-operatively, conclusive evidence, may be produced, by increasing the length of follow up to 36-48 months following TURBT, in order to rule out influences of normal physiological repair following TURBT.

Although FGF has been investigated in several human cancers (Bremnes, Camps, & Sirera, 2006; Kawaguchi *et al.*, 2019; Student *et al.*, 2018), no evidence has been produced regarding post-operative serum changes in BC patients after TURBT. The studies mentioned above only measured either pre-operative serum levels or tissue immunoreactivity of FGF and did not perform any follow up serum bFGF concentration monitoring. Measuring only pre-operative bFGF concentrations does not provide enough evidence concerning post-operative changes and cannot explain the long-term effects of bFGF on tumour angiogenesis. The results reported in this present study therefore provide novel information and evidence that, bFGF serum

concentration increase in BC patients following TURBT and should be investigated further using larger sample cohorts.

PDGF is a growth factor involved in angiogenesis, cell proliferation and tumour growth (Holleran *et al.*, 2015; Jitariu *et al.*, 2018). In the present study, there was a significant decrease in serum PDGF concentration in BC patients, up to 6-months following surgical treatment via TURBT. Further statistical analysis showed that there were significant differences between baseline pre-operative and 3-months post-operative PDGF concentrations.

Pan et al. (2017), investigated PDGF in CRC patients and reported high pre-operative PDGF levels in patients those patients with liver metastasis (Pan *et al.*, 2017). Although this present study did not assess long-term treatment outcome, the present findings complement the findings by Pan et al. (2017) highlighting higher pre-operative concentrations in BC patients. It is suspected that, in the presence of high PDGF levels, there is increased cell proliferation and angiogenesis (Wang *et al.*, 2012a), as evidenced in the higher pre-operative concentrations observed in this present study.

In patients with ovarian tumours, increased serum levels of PDGF-AA and PDGF-BB were observed in patients with residual disease compared to those without residual disease (Madsen *et al.*, 2012) which suggests that PDGF activity in those patients with residual disease, contributed to the high serum concentrations reported. In the present study, PDGF serum concentrations increased moderately at 6-months post-operative probably due to early recurrence. However, this suggestion should be investigated further by including serum analysis at 12, 18 and 24 months post-operative to identify association with recurrence and progression.

Due to limited evidence concerning serum PDGF in BC, the findings from this present research provide new information on post-operative PDGF changes and should be considered in BC biomarker profiles for monitoring and management following TURBT.

Even though SCF is mainly involved in hematopoietic cell proliferation, there is evidence to suggest that hematopoietic cytokines can stimulate proliferation of non-hematopoietic cells leading to tumour progression (Turner *et al.*, 1992). In the present study, there was a significant increase in serum SCF concentration in BC patients following TURBT, the treatment of BC. Specifically, there was significant increase between baseline pre-operative and 3-months post-operative serum SCF concentrations. These results suggest that, following removal of bladder tumours via TURBT, serum SCF concentrations continued to increase up to 6 months post-operative and may be due to initial tissue remodelling after surgery. At 3 and 6 months post-

operative, the increase in SCF may be due to early recurrence or presence of residual disease following TURBT.

Although methodological differences exist between this present study and a study by (Mroczko *et al.*, 2005), the results from both studies complement each other with regards to low pre-treatment SCF levels. It can be appreciated that, following removal of tumour cells, any sustained increase in serum SCF concentration beyond the initial physiological response, may be an indicator of tumour-related angiogenesis. This observation however requires more investigation with larger sample sizes.

With regards to pre-operative serum SCF concentrations, the results from this present study also complement (Łukaszewicz-Zając, Mroczko, Kozłowski, & Szmitkowski, 2017) who observed lower serum SCF levels in oesophageal cancer patients compared to normal controls. In this present study, the increased concentration at 1-month post-operative may be due to initial physiological responses (such as wound healing or remodelling) caused by TURBT surgery.

Presently, due to limited evidence from literature with regards to serum SCF concentration in BC patients, the findings from this present research provide new information on post-operative serum SCF changes and should be considered in BC biomarker profiles for monitoring and management following TURBT.

Follistatin was investigated in this research because it is a regulatory glycoprotein associated with tumour angiogenesis and cell promotion in various cancers (Ren *et al.*, 2012; Zabkiewicz *et al.*, 2017) whiles tumour suppressor properties have been reported by other studies (An *et al.*, 2017; Razanajaona *et al.*, 2007). Although not statistically significant, serum Follistatin concentrations investigated in this study showed a trend of increasing concentration following TURBT treatment suggesting that Follistatin was secreted into circulation at 3 months and 6-months after surgical techniques.

In a recent study, serum Follistatin levels were higher in patients with lung cancer compared with normal controls (Zhang, Ruan, Xiao, Chen, & Zhang, 2018b). The study however only measured one time point in comparison with our study which measured 4 different time points. Furthermore, normal controls were not included in our present study since baseline pre-operative concentrations were compared with post-operative concentrations.

In another study, (Ren *et al.*, 2012) also reported higher serum Follistatin levels in patients with ovarian cancer indicating a potential role in tumour growth due to increased angiogenesis. In this present study, higher serum Follistatin levels at 3 and 6-months post-operative potentially suggests tumour associated angiogenesis. However, follow up recurrence data was beyond the

scope of the study. This study nonetheless provides new information about serum Follistatin changes in bladder cancer patients undergoing TURBT and requires further investigation.

HER-2/neu is a transmembrane protein involved in signal activation leading to tumour growth (Coussens *et al.*, 1985; Semba *et al.*, 1985; Siddiqa *et al.*, 2008; Wang *et al.*, 2016b). Although most research on HER-2 has focussed on tissue immunoreactivity in various cancers (Hammam *et al.*, 2015; Slamon *et al.*, 2001; Smith *et al.*, 2007), serum HER-2 was measured in this present research because serum biomarkers are cheaper, less invasive and less time consuming and may therefore provide an alternative tool for management of BC.

Although there was a trend of decreasing serum HER-2 concentration up to 6 months following TURBT for the treatment of BC, these findings were not statistically significant. As a marker of cell proliferation, it can be appreciated that serum HER-2 concentrations will increase in the presence of cancer cells. Indeed in BC tissues, a recent a study has observed higher HER-2 immunoreactivity in high grade tumours compared to low grade further confirming HER-2 as a marker of cancer cell proliferation (Hammam *et al.*, 2015).

The main vascular endothelial growth factors (VEGFs) (VEGF-A, VEGF-B, VEGF-C and VEGF-D) and their transmembrane receptors (VEGFR-1, 2 and 3) are important mediators of angiogenesis and vasculogenesis and have been studied in various human conditions (Benjamin *et al.*, 1999; Gerhardt *et al.*, 2003; Shibuya, 2011; Yang *et al.*, 2018a). These markers were therefore investigated in this present study, due to their roles in tumour growth through angiogenesis.

In this present, similar trends of decreasing serum VEGF-A, VEGF-C and VEGF-D concentrations were observed in BC patients up to 6 months following TURBT treatment. (pg/ml) in patients who had TURBT for the treatment of NMIBC. Interestingly however, these biomarkers increased at 1-month post-operative suggesting increased activity probably due to physiological response to TURBT surgery. As vascular endothelial markers involved in other physiological processes, such as wound healing, physiological angiogenesis (Shigetomi *et al.*, 2018) etc, it can be appreciated that serum concentrations will rise initially as a response to surgery.

Although the trends observed for serum VEGF-C and VEGF-D concentrations in this present study suggest normal physiological responses to surgery, test inaccuracy or sensitivity may potentially be a source of variation. It has been suggested that VEGF-C and VEGF-D are mostly released as immature isoforms which can be proteolytically cleaved to produce active forms (McColl *et al.*, 2007). The method used in measuring VEGF-C and VEGF-D in this present

study, is not specific for active isoforms. Therefore, validation of the present results using a more sensitive method as well as larger sample sizes, will provide more information.

With regards to pre-operative serum concentrations, the results observed in this present study complement (Seker *et al.*, 2013), who observed high VEGF concentration in CRC and lung cancer patients undergoing chemotherapy. With regards to the study by (Seker *et al.*, 2013) however, the lower post-treatment concentrations may potentially be due to repeated chemotherapy in their patients cohorts. Since most of the patients included in the present study only had TURBT surgery (with adjuvant immunotherapy), the observed serum changes at 3- and 6-months post-operative are not likely to be influenced by other external factors.

In a recent study, (Benoit *et al.*, 2015), observed a significant association between serum VEGF-A and VEGF-C levels and tumour invasion in patients with superficial BC. Although similar cancer cohorts were used (NMIBC), the findings disagree probably due to the different laboratory test methods used in analysing the serum-based biomarkers (Bioplex vrs flow cytometry). The present study further differs from by measuring follow up serum concentrations up to 6 months after treatment.

With respect to VEGFR-1 and VEGFR-2, the serum concentrations observed in this present study, showed a general trend of increasing concentration up to 6 months following treatment via TURBT. These findings seem to suggests that these receptors have an inverse relationship with the growth factors (VEGF-A, VEGF-C and VEGF-D).

Lack of correlation between the serum-based growth factors and receptors the tissue-based receptor, could possibly be due to the presence of a different influencing factor. Therefore, further analysis of serum concentrations up to 4 years following TURBT could provide more information.

TIE-2 is a small receptor protein for angiopoietin-2 and has been shown to play important roles in cancer proliferation and growth (Ju *et al.*, 2014). In this present study TIE-2 was measured as a potential biomarker for angiogenesis. Although there was an initial increase in serum concentration at 1-month post-operative, TIE-2 showed a trend of decreasing concentration up to 6 months post-operative. These results for TIE-2 observed in this present study also complement the trend reported for angiopoietin-2 (its receptor) and suggest initial response (such as tissue repair) following TURBT.

Szarvas *et al.* (2008) have previously shown that NMIBC patients have higher TIE-2 levels compared to MIBC suggesting that TIE-2 may have aggressive tumour properties due to increased angiogenesis. These observations were however not observed in this present study

due to shorter follow up. It does however appear that, up to 6 months after TURBT, TIE-2 concentrations reduce below baseline levels and should be investigated further.
In summary, the results from this present study suggests that changes to serum-based biological markers following TURBT for the diagnosis and treatment of BC followed a similar trend. With regards to serum-based angiogenic and growth markers, PDGF and SCF have shown most promise following this study. Significant changes (increases) were observed in BC patients following TURBT. It can therefore be appreciated, that this biomarker, amongst the consideration of others, could potentially be considered as part of a BC biomarker profile. However, further investigation, involving larger cohorts, is required to fully establish the roles of these markers following TURBT for BC.

8.1.5 Chapter Seven: The role of novel antibody immunoreactivity and their association with BC recurrence and progression

The main aim of this chapter was to evaluate the role of various selective antibodies in BC recurrence and progression. This was done by assessing IHC staining of various selected biomarkers in patient tissues following TURBT for the treatment of BC. Prior to performing IHC on patient tissues, antibody staining and IHC protocols were optimised using recommended control tissues (chapter 3).

Biomarkers studied in this chapter were selected, due to their involvement in cancer growth and progression, through hallmarks such as angiogenesis and inflammation. Indeed, previous studies using animal models, human tissues and cell culture have reported important roles of inflammation and angiogenesis in tumourigenesis, cancer growth and progression (Grimm *et al.*, 2010; Mao, Jiang, Sun, & Peng, 2015; Nowak *et al.*, 2018; Perkhofer *et al.*, 2016; Tung *et al.*, 2013).

CD31 is a transmembrane cell adhesion molecule with roles in leucocyte migration, angiogenesis and cell proliferation and can be useful as a potential marker of angiogenesis (Stockinger *et al.*, 1990). Tissue immunoreactivity patterns of CD31 and CD34 have been reported by (Pusztaszeri *et al.*, 2006).

With regards to CD31, the results from this present study showed a significant increase in CD31 immunoreactivity in vascular endothelial cells located in bladder tumour cells with some staining also located close to the tumour cells. As a marker of angiogenesis, these findings potentially show the presence of increased angiogenesis within the Bladder tumours. The scoring system used in this research examines both staining intensity and percentage positivity in tumour cells and has been used by others (Usuda *et al.*, 2018).

The CD31 immunoreactivity patterns reported in this study further complement results by (Qian *et al.*, 2018) who also reported increased CD31 immunoreactivity in all tumour vessels. Contrast to their study however, this present study used different patient cohorts (hepatocellular carcinoma *vrs* transitional cell carcinoma). Both studies however show that, CD31 in a good marker for measuring angiogenesis using IHC.

Results from this present study also showed that, there was no association between CD31 immunoreactivity and cancer grade. These findings disagree with a previous study by (Kuang *et al.*, 2013), who reported significant association between CD31 immunoreactivity in tumour grades. A possible explanation for the different findings could be scoring systems used for assessing CD31 immunoreactivity. Whereas this present study using a simple scoring system (using staining intensity and tumour cell percentage), (Kuang *et al.*, 2013) measured MVD using a specialised imaging software. Using MVD analysis, significant CD31 immunoreactivity has also been observed in high grade tumours by other researchers (Mohamed, Mohammed, Ibrahim, Mohamed, & Salah, 2017b). It is therefore possible that, different reporting or scoring systems will cause variations in reporting CD31 staining and potentially hinder validation across research groups and laboratories.

In this present study, patients with cancer stage pTa presented with higher CD31 immunoreactivity compared to other BC stages. These findings suggest that increased CD31 immunoreactivity in low pTa tumours may have an association with angiogenesis. These observations complement a recent study which reported, that high CD31 immunoreactivity in Laryngeal Squamous Cell Carcinoma are associated with low stage cancers and early recurrence (Schluter *et al.*, 2018). The results from this study also complement earlier results by El Gehani *et al.* (2011) that observed higher CD31 immunoreactivity in BC patients. Whereas this present study used a scoring system based on staining intensity and percentage however, El Gehani *et al.* (2011) measured microvessel density which is sometimes prone to variation. Several other studies have linked CD31 immunoreactivity to poor prognosis, metastasis, recurrence and survival (Deliu *et al.*, 2016; Diana *et al.*, 2016; Virman *et al.*, 2015; Wermker *et al.*, 2015).

With regards to recurrence, there was no association between CD31 immunoreactivity (at diagnosis) and BC recurrence and progression following TURBT treatment. It is suggested that any future research evaluation the association between CD31 immunoreactivity and BC recurrence should consider analysing BC tissues at baseline and up to 24-36 months following TURBT. This approach will provide more detailed information with regards to changes in CD31 immunoreactivity.

In summary, the results from this present study highlight increased CD31 immunoreactivity in vascular cells in BC tumours and provides an approach to evaluating angiogenesis. The findings provide new information with respect to CD31 staining in BC patients following TURBT treatment. Although no association was observed with cancer recurrence, the findings require further investigation using larger sample cohorts as well as longer follow up periods.

CD34 is also a transmembrane protein expressed on hematopoietic stem cells, vascular endothelial progenitors and embryonic fibroblasts (Brown *et al.*, 1991; Fina *et al.*, 1990; Patry *et al.*, 2018). In this present study, higher CD34 immunoreactivity was observed in endothelial cells within BC cells compared to other areas. As a marker of the endothelium, this observation suggests increased activity probably due to angiogenesis in BC cells. In agreement with other researchers (Giulioni *et al.*, 2019), this provides potentially useful information which can be exploited for developing anti-cancer therapies by targeting anti-angiogenic pathways.

Results from our present study further complement findings by others who reported no association between CD34 immunoreactivity and tumour grade and stage in patients with oesophageal and oral squamous cell carcinoma (Shahsavari, Farhadi, Sadri, & Sedehi, 2015). Although they measured vascular density in their patient cohorts, the findings nonetheless indicate no association with various clinicopathological features and suggests CD34 may not be a good biomarker for monitoring treatment.

Other studies have investigated CD34 immunoreactivity by evaluating microvessel density in tissues (Moghadam, Abadi, & Mokhtari, 2015; Sarmadi *et al.*, 2017). In comparison with these studies, the present study used a scoring system based on staining intensity and cell percentage. Both methods are subject to variation and requires validation for clinical utility. With regards to our study however, we provide new information with regards to CD34 immunoreactivity in BC and therefore recommend validation of these findings with larger sample sizes and longer follow ups.

With regards to cancer recurrence, there was no association between CD34 immunoreactivity (at diagnosis) and cancer recurrence after treatment with TURBT. Our findings are in disagreement with earlier reports by (Tsuji, Ishiguro, Sasaki, & Kudo, 2013) who observed a significant relationship between high CD34 immunoreactivity and cancer recurrence in patients with HCC. These differences between findings may be explained by the patient cohorts employed in the 2 studies. Whilst Tsuji *et al.* (2013) compared CD34 immunoreactivity between 2 different patient cohorts (patients with HCC recurrence following repeated examination of tissue biopsies vs patients with 5 year history of disease free recurrence post-surgical treatment), this present study used only one patient cohort by analysing CD34

immunoreactivity (at diagnosis) and comparing immunoreactivity patterns with treatment outcome.

In summary, the results from this present study highlight increased CD34 immunoreactivity in vascular cells in BC tumours and provides an approach to evaluating angiogenesis. The findings provide new information with respect to CD34 staining in BC patients following TURBT treatment. Although no association was observed with cancer recurrence, the findings require further investigation using larger sample cohorts as well as longer follow up periods.

Thrombomodulin is a 74kDa protein implicated in inflammation and other cancer-related processes (Horowitz & Palumbo, 2012; Zhang *et al.*, 1998). The results obtained from this research showed a significant difference in thrombomodulin immunoreactivity in BC tissue cells compared to normal Bladder tissues. Specifically, Bladder tumour cells showed loss of immunoreactivity or reduced thrombomodulin immunoreactivity within bladder tumour cells. Due to its tumour suppressive properties (Tanaka *et al.*, 2017), loss of thrombomodulin immunoreactivity observed in this present study, could potentially cause increased tissue differentiation, metastasis and recurrence.

Although the exact mechanisms through which thrombomodulin mediate cancer growth are not fully understood, earlier cell culture and animal studies have shown that, thrombomodulin maintains cell-cell interactions and also inhibits degradation of the ECM; important factors in cancer proliferation (Koutsi, Papapanagiotou, & Papavassiliou, 2008; Weiler *et al.*, 2001).

In both human tissues and BC cell lines, Wu *et al.* (2014) have demonstrated an inverse relationship between thrombomodulin immunoreactivity and aggressive tumour behaviour of BC. Using cell lines, Zheng *et al.* (2016) also reported a reduction in cell proliferation and angiogenesis in the presence of increased thrombomodulin whilst its absence was associated with increased tumour growth, cell migration and invasion. Our findings therefore further complement these earlier studies by highlighting the loss of Thrombomodulin immunoreactivity within BC cells. In terms of Bladder specific research however, our research provides new information on Thrombomodulin staining patterns in bladder tumours.

Our current study also investigated the association between cancer stage and thrombomodulin immunoreactivity. Patients with high stage BC were significantly associated with reduced thrombomodulin immunoreactivity suggesting that there was reduced cell to cell interaction due to the absence of thrombomodulin. This observation is in agreement with an earlier study which reported that, decreased thrombomodulin immunoreactivity was significantly correlated with high cancer stage, differentiation and 5 year survival (Hanly *et al.*, 2006). With regards to

cancer stage therefore, findings from this present study complement their findings and suggests that loss of thrombomodulin immunoreactivity in cancer cells results in higher rates of differentiation which can potentially lead to metastasis and recurrence.

In this current study, there was no association between thrombomodulin immunoreactivity (at diagnosis) and cancer recurrence. This observation should however be further investigated using larger sample sizes and increasing the length of follow up.

Even though their exact physiological role has not been fully understood, CEA and its cell adhesion molecules have been associated with several cancers in both tissue culture and animal model studies (Dango *et al*., 2008; Gebauer *et al*., 2014; Thoem *et al*., 2009). CEACAM-1 was investigated in this present study due to its potential role as a marker of angiogenesis and tumour growth (Ergün *et al.*, 2000).

The results from this present study showed a loss of CEACAM-1 immunoreactivity in Bladder tumour cells compared to other tissues. Due to its angiogenic properties, an increased immunoreactivity of CECAM-1, was expected in BC patients before TURBT. Indeed, the findings from this present study disagree with earlier investigations by other researchers who observed that, increased tissue immunoreactivity of CEACAM-1 are associated with angiogenesis in lung cancer (Dango *et al.*, 2008). Furthermore, the two IHC reporting systems (traditional scoring system using stain intensity/percentage vrs MVD) produced different results and raises further issues with validation.

Although some studies have associated CEACAM-1 immunoreactivity with aggressive tumour behaviour (ie high grade, advanced stage, metastasis, survival etc) in different human cancers, (Thies *et al.*, 2002; Thom *et al.*, 2009), findings from this current study disagree with their observations. Although similar reporting systems were used, variations in the findings could be due to sample sizes and patient cohorts. We nonetheless provide new information with regards to CEACAM-1 immunoreactivity in BC patients undergoing TURBT treatment.

COX-2 is an enzyme homodimer involved in inflammation by catalysing the production of prostaglandins from arachidonic acid (Mead *et al.*, 1986). In studies using cell culture, animal models and human tissues, a significant link between COX-2 and inflammation-associated tumour properties have been identified (Anderson *et al.*, 1996; Crofford, 1997; Giovannucci *et al.*, 1995; Giovannucci *et al.*, 1994). These earlier studies provided a depth of knowledge for current research in BC. COX-2 was therefore included in this present study due to its links with inflammation and cancer growth.

The results from this study showed that, there was generally a significant increase in COX-2 immunoreactivity in Bladder tumour cells, compared to those in normal tissues. These findings are in agreement with a recent study by (Hedaya *et al.,* 2015) who also observed higher COX-2 immunoreactivity in colonic adenocarcinoma tissues in comparison with normal tissues. These findings suggest that tumour cells of epithelial origin express high levels of COX-2 probably due to chronic inflammation and may potentially be a good biomarker. Furthermore, high stage and high grade patients presented with high staining intensity and percentage of tumour cells (Hedaya *et al.,* 2015). These observations were also present in the current study and suggests that COX-2 immunoreactivity in cancer tissues (especially staining intensity) should be further investigated in BC.

With regards to cancer stage, the results from this study are in contrast to (Cai *et al.,* 2017) who reported significant associations between COX-2 immunoreactivity and cancer stage. Although both endometrial carcinoma (EC) and BC are of epithelial origin, differences in sample size (183 EC vrs 35 BC), duration of follow up (5 yrs for EC vrs 2 yrs for BC) and different antibody clones, may explain the differences in results reported by both studies.

The relationship between antibody immunoreactivity (at diagnosis) vs BC recurrence was not significant. Nonetheless, the immunoreactivity patterns of COX-2 in BC, reported in this present study, should be investigated further using larger sample sizes and longer follow up periods. COX-2 seems to be epithelial cancer specific and may be a useful marker for monitoring and management of BC patients following TURBT.

The S100P protein is a small kDa protein which was initially purified from human placenta (Emoto *et al.*, 1992) but has been shown to play key roles in cellular processes like regulation of cell cycle, growth, transcription and differentiation (Jiang *et al.,* 2016). It was investigated in this present study because its cellular immunoreactivity may interact with growth factors and growth factor receptors, leading to several effects such as tumour proliferation (Jiang *et al.*, 2016).

The results from this present study showed that S100P was significantly immunoreactive in BC cells in comparison with normal Bladder tissue and suggests this protein may be a good marker for identification of BC. In a similar study, S100A8 (which belongs to the same family as S100P) was highly immunoreactive in TCC tissues compared to normal cells (CUI *et al.*, 2012). In disagreement with that study however, there was no correlation between S100P immunoreactivity and patients' cancer grade and stage in this present study.

Although it can be appreciated that S100P immunoreactivity will be higher in high grade tumours due to increased cell proliferation, that observation was not made in this present study

and could potentially be due to low sample size. Furthermore, comparing S100P immunoreactivity at diagnosis, with S100P immunoreactivity at 2-5 years following treatment, may provide confirmatory information with regards to recurrence and long-term outcome measures.

In agreement with this present study, an evaluation of S100P immunoreactivity revealed increased nuclear and cytoplasmic staining in tumour cells in an earlier study by (Yuan *et al.*, 2013). Furthermore, there was heterogeneous S100P immunoreactivity across tissue components as well as some degree of nonspecific staining in inflammatory cells located within tumour cells (Yuan *et al.*, 2013). These observations further confirm our suggestions that S100P as an inflammatory marker may potentially be useful in BC management and monitoring following surgical treatment.

With regards to recurrence however, the findings from this present study disagree with (Yuan *et al.*, 2013) who observed that positive S100P immunoreactivity was strongly associated with early recurrence in HCC patients. Difference in patient cohorts and sample sizes may explain these variations. The results from this study nonetheless provides new information with regards to S100P staining in bladder tumour cells as well as its association with cancer grade, stage and recurrence following treatment via TURBT.

SOX2 is a transcription factor and plays important roles in the development of embryonic stem stems and other growth processes (Masui *et al.*, 2007; Sarkar & Hochedlinger, 2013). It was investigated during this research study due to its potential utility as a biomarker of cancer growth and progression.

With regards to this present study, there was a significant increase in SOX-2 immunoreactivity in Bladder tumour cells, compared to those in normal tissues suggesting that, there was potentially an increased rate of cell proliferation due to increased transcription in bladder tumour cells. These findings complement a reports from a recent study which reported that tumour cells expressing SOX2 contributed to increased BC tumour proliferation (Zhu *et al.*, 2017a). the results further complement earlier an earlier study in cervical squamous cell carcinoma (SCC) where SOX2 was observed to be highly immunoreactive in the SCC tissues compared with normal cervical tissues (Chang *et al.*, 2015). Results from the present study however, provides more information about the stain protocols, optimisation of IHC (described in chapter 3) and representative micrographs of the stain scores. This therefore provides anew template for future research on BC using the Roche Ventana IHC platforms.

In a meta-analysis of seven studies which included 1,944 patients with non-small cell lung cancer (NSCLC), increased immunoreactivity of SOX2 was associated with favourable

prognosis (Shao, Chen, & He, 2015). In this present study, there was no association between SOX-2 immunoreactivity and cancer recurrence. In this regards, although the follow up period was shorter (less than 2 yrs.), findings from this current study are in agreement with the results from (Shao *et al.*, 2015).

In light of our current understanding of SOX2 activities in cancer, it may be utilised as a prognostic tool or therapeutic intervention.

HER-2/neu is a transmembrane protein involved in signal activation leading to tumour growth (Coussens *et al.*, 1985; Semba *et al.*, 1985; Siddiqa *et al.*, 2008; Wang *et al.*, 2016b). In various human cancers, different HER-2 immunoreactivity rates and patterns have been reported (Hammam *et al.*, 2015; Slamon *et al.*, 2001; Smith *et al.*, 2007). HER-2 immunoreactivity was therefore investigated in this present study due to its links to cancer growth in various human cancers, especially its utility in breast cancer treatment and management.

In this present study, HER-2 was significantly immunoreactive in Bladder tumour cells, compared to normal tissues. As a protein involved in signal transduction leading to increased cell proliferation, the increased immunoreactivity observed in this present study potentially implicates HER-2 in BC growth. These observations complement results by (Hasan *et al.*, 2018) who reported higher HER-2 immunoreactivity in colorectal cancer cells compared to normal controls. In contrast however, (Hasan *et al.*, 2018) assessed HER-2 immunoreactivity using an image analysis software (Image J) compared with the present study which measured HER-2 immunoreactivity using modified reporting system.

Furthermore, the results from this present study complements results by (Du, Xu, Fang, & Qi, 2012) who have previously reported similar findings (higher HER-2 immunoreactivity) in breast cancer patients. The differences between the studies however is that, this present study provides detailed information with regards to antibody clone, scoring system and optimises IHC protocol to the Ventana IHC autostainer.

With respect patients' cancer grade, there was a significant association with HER-2 immunoreactivity. Specifically, the results show that high grade (G3) patients presented with higher HER-2 immunoreactivity compared with low grade (G1) and are thus, in agreement with (Jana *et al.*, 2012), although their observations were made in breast cancer patients. These findings nonetheless suggest that HER-2 immunoreactivity results in higher rate of cell differentiation that potentially leads to increased risk of recurrence and metastasis in BC patients.

In this present study, high stage tumours (e.g. pT1/pT2 in BC) presented with high HER-2 immunoreactivity, complementing similar findings breast cancer (Jana *et al.*, 2012). It can be appreciated that, increasing HER-2 immunoreactivity will lead to increased activation of the so-called MAPK pathway, which explains the association with aggressive tumour behaviour. Indeed other researchers have highlighted the link between HER-2 and metstasis and survival (dos Santos *et al.*, 2017; Prins, Ruurda, van Diest, van Hillegersberg, & Ten Kate, 2013).

With regards to cancer recurrence, the results from this present study did not identify an association with HER-2 tissue immunoreactivity. These findings are in disagreement with Rouanet *et al.* (2014) who observed a significant association between HER-2 immunoreactivity and recurrence in breast Cancer. In comparison with that study however, different antibody clones, scoring systems, and slightly different stain protocols were used in both studies. Although long-term treatment outcome (overall survival, prognosis) were beyond the scope of this present study, the present findings are in agreement with others (Baiocchi *et al.*, 2017) who reported no significant association between HER-2 immunoreactivity and recurrence patients with cervical cancers. The differences between both methods (such as small sample sizes, short follow up periods) may explain the difference.

VEGFR-3 is a transmembrane receptor kinase implicated in tumour associated angiogenesis and cell promotion (Cartland *et al.*, 2016; Shibuya, 2011). In this present study, there was a significant increase in VEGFR-3 immunoreactivity in Bladder tumour cells, compared to those in normal tissues.

In a study by Hedaya *et al.* (2015), VEGF immunoreactivity in colonic adenocarcinoma showed intensely positive staining compared to normal control tissues. However, control tissues were moderately positive for VEGF indicating the potential likelihood of false positive reporting. In this present study, there was also nonspecific VEGFR-3 staining within nuclei of some underlying muscle cells, lymphatic endothelial cells and basal tissue cells. This observation in this and other study highlights the unspecific nature of VEGF staining and raises the issues with standardisation in reporting slides.

In agreement with this present study, VEGFR-3 immunoreactivity was significantly localised to the vascular endothelial cells within tumours compared to normal cells in a previous study (Smith *et al.*, 2010). A similar scoring system was used in both studies which suggests that results may potentially be standardised across laboratories. However, the present study also observed nonspecific nuclei and cytoplasmic staining in noncancerous tissues, an observation which has also been reported by (Petrova *et al.*, 2008) in an assessment of several research studies which used the same VEGFR-3 antibody clone (54703/MAB3491).

During this study, interpretation of IHC slides was performed by careful consideration of the stain intensity and percentage of tumour cells staining positive. A significant source of variation and controversy in IHC is the type of scoring system, which also hinders standardisation of reporting within and across laboratories. Some authors have however reported consistent results using both automated and traditional scoring systems (Choudhury, Yagle, Swanson, Krohn, & Rajendran, 2010). Taking these factors into consideration nonetheless, this present research took into consideration, important factors such as control tissues, protocol verification/optimisation, experience of reporting histologist/consultant and cancer cohort. Some of the results produced in this present study are therefore novel whiles other complement or disagree with other researchers.

In summary, it can be appreciated that monitoring of tissue immunoreactivity of HER-2 and thrombomodulin may show promise for the management of patients with BC. Overall, and with respect to all of the serum and tissue biomarkers investigated in this study, it is proposed that changes in the measured parameters may not be due to a single factor, but due to a number of factors that may result following TURBT surgery such as: tissue damage, wound repair, and removal of the tumour (resection).

The present study, although with its limitations, does provide a novel approach to IHC methodology by introducing new biomarkers (e.g. HER-2 and thrombomodulin) that may become useful tools for the monitoring of patients with BC. In addition, serum-based biomarkers such as CD31, MMP-9, PDGF, SCF and MIP-2 could also be considered for future studies involving BC patients, and may help form the basis for biomarker profile for BC.

8.2 Study Limitations & Future Direction

It is acknowledged that this clinical pilot-study had limitations to include, sample size, measuring both serum and tissue-based biomarkers on all samples collected, and to assess changes to biomarkers following the 6 months' follow-up period.

With respect to the serum and tissue biological markers (e.g. thrombomodulin, MMP-9, MIP-2, etc.) measured in the present study, it would have been interesting to have measured these biomarkers in serum and tissue for all patients. The results generated could have provided complementary information involving the serum and tissue-based biomarker, for example, an increased tissue immunoreactivity of a specific biomarker may have resulted in a decrease secretion into the serum. Measuring urine samples in any future study, would also be useful and provide supportive information to data generated from the present study. However, due to time and financial constraints it was difficult to measure serum and tissue markers for all samples in the present study, and analysing urine samples would have doubled the costs.

In the present study, 40 patients were recruited from a single site hospital, namely Wrexham Maelor, North Wales. It would have been beneficial if more patients were recruited from other hospital sites across North Wales, which may have provided additional information that could have had an effect on the outcome of some of the statistical analysis undertaken on the biomarker data.

As means of a future direction for the study, it would be interesting to follow-up the patients beyond the 6 months' period, possibly up to 24-36 months' post TURBT. Gaining additional information at these time points may highlight any sustained changes to the various biomarkers and their association with clinical outcome measures.

With respect to the biomarkers measured during this study, it would also be interesting in any future studies to consider molecular markers such as FGFR-3, E-Cadherin, Tropomyosin. Measuring some molecular markers that have been reported to play a role in BC, could be complementary to the markers that have been investigated in the present study.

The present study has provided a sound foundation to undertake future work involving multi-centre studies, which may be able to help validate the IHC methods undertaken during this thesis. They could also aid and provide further evidence for developing a specific panel of biomarkers that could be used in addition to, or in combination with, current management protocols, for the identification of patients at risk of developing recurrence and progression.

8.3 Conclusion

The main aim of this research study was to evaluate the role of novel biomarkers (serum and tissue based) and their association with recurrence and progression in BC.

With regards to laboratory investigations, currently there are no routine biomarkers available for monitoring BC patients at increased risk of developing recurrence and progression. By monitoring changes in various biomarkers post-TURBT, any sustained increase may be a predictor of cancer recurrence or progression.

The findings from this study suggest that serum and tissue-based biomarkers such as MIP-2, MMP-9, HER-2, thrombomodulin and CD31 may provide a way of assessing patients post-TURBT, and would allow urological surgeons a biomarker profile to monitor patients during the management and surveillance of their BC.

Collectively, findings from the present study may indicate an alternative approach in the monitoring and management of patients with BC. It is proposed that by allowing urological surgeons access to laboratory markers such as MIP-2, MMP-9, HER-2, Thrombomodulin and CD31, potentially, in the future, these biomarkers may be used in addition to, or in combination with, currently used scoring systems to predict cancer recurrence and progression. Since current management of BC mainly involves imaging and resection, measuring a biomarker profile capable of detecting recurrence, could provide an alternative route for managing patients.

Ultimately, our research findings may allow current NHS post-operative care protocols to be revised, improved and implemented within 6-8 years, although larger studies are needed in this area of research in order to make an impact on a national scale, and to promote good practice in the field of urology, pertaining to BC.

9.0 Chapter Nine: References

Abubaker, K., Luwor, R. B., Escalona, R., McNally, O., Quinn, M. A., Thompson, E. W., . . . Ahmed, N. (2014). Targeted Disruption of the JAK2/STAT3 Pathway in Combination with Systemic Administration of Paclitaxel Inhibits the Priming of Ovarian Cancer Stem Cells Leading to a Reduced Tumor Burden. *Front Oncol, 4*, 75. doi:10.3389/fonc.2014.00075

Aggarwal, B. B., Vijayalekshmi, R., & Sung, B. (2009). Targeting inflammatory pathways for prevention and therapy of cancer: short-term friend, long-term foe. *Clinical Cancer Research, 15*(2), 425-430.

Alaseem, A., Alhazzani, K., Dondapati, P., Alobid, S., Bishayee, A., & Rathinavelu, A. (2017). *Matrix Metalloproteinases: A challenging paradigm of cancer management.* Paper presented at the Seminars in Cancer Biology.

Alberg, A. J., Kouzis, A., Genkinger, J. M., Gallicchio, L., Burke, A. E., Hoffman, S. C., . . . Comstock, G. W. (2007). A prospective cohort study of bladder cancer risk in relation to active cigarette smoking and household exposure to secondhand cigarette smoke. *American Journal of Epidemiology, 165*(6), 660-666.

Alexander, P. B., Yuan, L., Yang, P., Sun, T., Chen, R., Xiang, H., . . . Wang, X.-F. (2014). EGF promotes mammalian cell growth by suppressing cellular senescence. *Cell Research, 25*, 135. doi:10.1038/cr.2014.141

https://www.nature.com/articles/cr2014141#supplementary-information

An, J., Wang, L., Zhao, Y., Hao, Q., Zhang, Y., Zhang, J., . . . Gao, Y. (2017). Effects of FSTL1 on cell proliferation in breast cancer cell line MDAMB231 and its brain metastatic variant MDAMB231BR. *Oncol Rep, 38*(5), 3001-3010. doi:10.3892/or.2017.6004

Anderson, G. D., Hauser, S. D., McGarity, K. L., Bremer, M. E., Isakson, P. C., & Gregory, S. A. (1996). Selective inhibition of cyclooxygenase (COX)-2 reverses inflammation and immunoreactivity of COX-2 and interleukin 6 in rat adjuvant arthritis. *J Clin Invest, 97*(11), 2672-2679. doi:10.1172/jci118717

Andersson, K.-E., & Arner, A. (2004). Urinary bladder contraction and relaxation: physiology and pathophysiology. *Physiological reviews, 84*(3), 935-986.

Ang, C., Chambers, A. F., Tuck, A. B., Winquist, E., & Izawa, J. I. (2005). Plasma osteopontin levels are predictive of disease stage in patients with transitional cell carcinoma of the bladder. *BJU Int, 96*(6), 803-805. doi:10.1111/j.1464-410X.2005.05716.x

Antoni, S., Ferlay, J., Soerjomataram, I., Znaor, A., Jemal, A., & Bray, F. (2017). Bladder Cancer Incidence and Mortality: A Global Overview and Recent Trends. *European Urology, 71*(1), 96-108. doi:10.1016/j.eururo.2016.06.010

Apollo, A., Ortenzi, V., Scatena, C., Zavaglia, K., Aretini, P., Lessi, F., . . . Naccarato, A. G. (2019). Molecular characterization of low grade and high grade bladder cancer. *PLoS One, 14*(1), e0210635. doi:10.1371/journal.pone.0210635

Avraham, B. C., Dotan, G., Hasanreisoglu, M., Kramer, M., Monselise, Y., Cohen, Y., . . . Goldenberg-Cohen, N. (2008). Increased plasma and optic nerve levels of IL-6, TNF-alpha, and MIP-2 following induction of ischemic optic neuropathy in mice. *Curr Eye Res, 33*(4), 395-401. doi:10.1080/02713680801932891

Babjuk, M., Böhle, A., Burger, M., Capoun, O., Cohen, D., Compérat, E. M., . . . Zigeuner, R. (2017). EAU Guidelines on Non–Muscle-invasive Urothelial Carcinoma of the Bladder: Update 2016. *European Urology, 71*(3), 447-461. doi:https://doi.org/10.1016/j.eururo.2016.05.041

Babjuk, M., Burger, M., Zigeuner, R., Shariat, S. F., van Rhijn, B. W., Compérat, E., . . . Redorta, J. P. (2013). EAU guidelines on non–muscle-invasive urothelial carcinoma of the bladder: update 2013. *European Urology, 64*(4), 639-653.

Baeriswyl, V., & Christofori, G. (2009). The angiogenic switch in carcinogenesis. *Seminars in Cancer Biology, 19*(5), 329-337. doi:https://doi.org/10.1016/j.semcancer.2009.05.003

Baiocchi, G., Begnami, M. D., Chen, M. J., Fukazawa, E. M., Badiglian-Filho, L., Pellizzon, A. C. A., . . . Lopes, A. (2017). HER-2 Immunoreactivity and Response to Radiotherapy in Patients with Advanced Cervical Cancer. *J Reprod Med, 62*(5-6), 234-240.

Balkwill, F. (2002). Tumor necrosis factor or tumor promoting factor? *Cytokine & growth factor reviews, 13*(2), 135-141. doi:http://dx.doi.org/10.1016/S1359-6101(01)00020-X

Balkwill, F., & Mantovani, A. (2001). Inflammation and cancer: back to Virchow? *The lancet, 357*(9255), 539-545.

Balkwill, F. R., & Mantovani, A. (2012). *Cancer-related inflammation: common themes and therapeutic opportunities.* Paper presented at the Seminars in Cancer Biology.

Balmain, A., Barrett, J. C., Moses, H., & Renan, M. J. (1993). How many mutations are required for tumorigenesis? Implications from human cancer data. *Molecular carcinogenesis, 7*(3), 139-146.

Bansal, N., Gupta, A., Sankhwar, S. N., & Mahdi, A. A. (2014). Low- and high-grade bladder cancer appraisal via serum-based proteomics approach. *Clinica chimica acta, 436*, 97-103. doi:http://dx.doi.org/10.1016/j.cca.2014.05.012

Barden, A., Phillips, M., Hill, L. M., Fletcher, E. M., Mas, E., Loh, P. S., . . . Corcoran, T. B. (2018). Antiemetic doses of dexamethasone and their effects on immune cell populations and plasma mediators of inflammation resolution in healthy volunteers. *Prostaglandins Leukot Essent Fatty Acids, 139*, 31-39. doi:10.1016/j.plefa.2018.11.004

Basilico, C., & Moscatelli, D. (1992). The FGF family of growth factors and oncogenes *Advances in cancer research* (Vol. 59, pp. 115-165): Elsevier.

Benjamin, L. E., Golijanin, D., Itin, A., Pode, D., & Keshet, E. (1999). Selective ablation of immature blood vessels in established human tumors follows vascular endothelial growth factor withdrawal. *The Journal of clinical investigation, 103*(2), 159-165.

Benoit, T., Keller, E. X., Wolfsgruber, P., Hermanns, T., Günthart, M., Banzola, I., . . . Poyet, C. (2015). High VEGF-D and Low MMP-2 Serum Levels Predict Nodal-Positive Disease in Invasive Bladder Cancer. *Medical Science Monitor: International Medical Journal Of Experimental And Clinical Research, 21*, 2266-2274. doi:10.12659/MSM.894383

Berglin, L., Sarman, S., van der Ploeg, I., Steen, B., Ming, Y., Itohara, S., . . . Kvanta, A. (2003). Reduced choroidal neovascular membrane formation in matrix metalloproteinase-2-deficient mice. *Invest Ophthalmol Vis Sci, 44*(1), 403-408.

Beutler, B. (1999). The role of tumor necrosis factor in health and disease. *The journal of rheumatology. Supplement, 57*, 16-21.

Bishop, G. A., Moore, C. R., Xie, P., Stunz, L. L., & Kraus, Z. J. (2007). TRAF proteins in CD40 signaling. *Adv Exp Med Biol, 597*, 131-151. doi:10.1007/978-0-387-70630-6_11

Blackwell, K. L., Burstein, H. J., Storniolo, A. M., Rugo, H., Sledge, G., Koehler, M., . . . O'Shaughnessy, J. (2010). Randomized study of Lapatinib alone or in combination with trastuzumab in women with ErbB2-positive, trastuzumab-refractory metastatic breast cancer. *J Clin Oncol, 28*(7), 1124-1130. doi:10.1200/jco.2008.21.4437

Blackwell, K. L., Burstein, H. J., Storniolo, A. M., Rugo, H. S., Sledge, G., Aktan, G., . . . Bischoff, J. (2012). Overall survival benefit with lapatinib in combination with trastuzumab for patients with human epidermal growth factor receptor 2–positive metastatic breast cancer: final results from the EGF104900 study. *Journal of Clinical Oncology, 30*(21), 2585-2592.

Blumberg, N., Gettings, K. F., Turner, C., Heal, J. M., & Phipps, R. P. (2006). An association of soluble CD40 ligand (CD154) with adverse reactions to platelet transfusions. *Transfusion, 46*(10), 1813-1821. doi:10.1111/j.1537-2995.2006.00979.x

Bouck, N., Stellmach, V., & Hsu, S. C. (1996). How tumors become angiogenic *Advances in cancer research* (Vol. 69, pp. 135-174): Elsevier.

Bowcock, A., Kidd, J., Lathrop, G., Daneshvar, L., May, L., Ray, A., . . . Cavalli-Sforza, L. (1988). The human "interferon-β 2/hepatocyte stimulating factor/interleukin-6" gene: DNA polymorphism studies and localization to chromosome 7p21. *Genomics, 3*(1), 8-16.

Boyanton, B. L., & Blick, K. E. (2002). Stability studies of twenty-four analytes in human plasma and serum. *Clinical chemistry, 48*(12), 2242-2247.

Brausi, M., Collette, L., Kurth, K., van der Meijden, A. P., Oosterlinck, W., Witjes, J. A., . . . Sylvester, R. J. (2002). Variability in the recurrence rate at first follow-up cystoscopy after TUR in stage Ta T1 transitional cell carcinoma of the bladder: a combined analysis of seven EORTC studies. *Eur Urol, 41*(5), 523-531.

Bremnes, R. M., Camps, C., & Sirera, R. (2006). Angiogenesis in non-small cell lung cancer: The prognostic impact of neoangiogenesis and the cytokines VEGF and bFGF in tumours and blood. *Lung Cancer, 51*(2), 143-158. doi:https://doi.org/10.1016/j.lungcan.2005.09.005

Bridge, J. A., Lee, J. C., Daud, A., Wells, J. W., & Bluestone, J. A. (2018). Cytokines, Chemokines, and Other Biomarkers of Response for Checkpoint Inhibitor Therapy in Skin Cancer. *Frontiers in medicine, 5*, 351-351. doi:10.3389/fmed.2018.00351

Brown, J., Greaves, M., & Molgaard, H. (1991). The gene encoding the stem cell antigen, CD34, is conserved in mouse and expressed in haemopoietic progenitor cell lines, brain, and embryonic fibroblasts. *International Immunology, 3*(2), 175-184.

Brown, T., Slack, R., Rushton, L., & Group, w. t. B. O. C. B. S. (2012). Occupational cancer in Britain: Urinary tract cancers: bladder and kidney. *British journal of cancer, 107*(Suppl 1), S76.

Bupathi, M., Kaseb, A., Meric-Bernstam, F., & Naing, A. (2015). Hepatocellular carcinoma: Where there is unmet need. *Molecular oncology, 9*(8), 1501-1509.

Burger, M., Catto, J. W., Dalbagni, G., Grossman, H. B., Herr, H., Karakiewicz, P., . . . Shariat, S. (2013). Epidemiology and risk factors of urothelial bladder cancer. *European Urology, 63*(2), 234-241.

Cai, S., Zhang, Y.-x., Han, K., & Ding, Y.-q. (2017). Immunoreactivitys and clinical significance of COX-2, VEGF-C, and EFGR in endometrial carcinoma. *Archives of Gynecology and Obstetrics, 296*(1), 93-98. doi:10.1007/s00404-017-4386-9

Campillo-Gimenez, L., Renaudin, F., Jalabert, M., Gras, P., Gosset, M., Rey, C., . . . Ea, H. K. (2018). Inflammatory Potential of Four Different Phases of Calcium Pyrophosphate Relies on NF-kappaB Activation and MAPK Pathways. *Front Immunol, 9*, 2248. doi:10.3389/fimmu.2018.02248

Cao, G., O'Brien, C. D., Zhou, Z., Sanders, S. M., Greenbaum, J. N., Makrigiannakis, A., & DeLisser, H. M. (2002). Involvement of human PECAM-1 in angiogenesis and in vitro endothelial cell migration. *American Journal of Physiology-Cell Physiology, 282*(5), C1181-C1190.

Capatina, C., Cimpean, A. M., Raica, M., Coculescu, M., & Poiana, C. (2019). SOX 2 Immunoreactivity in Human Pituitary Adenomas-Correlations With Pituitary Function. *In Vivo, 33*(1), 79-83. doi:10.21873/invivo.11442

Cardoso, H. J., Figueira, M. I., & Socorro, S. (2017). The stem cell factor (SCF)/c-KIT signalling in testis and prostate cancer. *Journal of cell communication and signaling, 11*(4), 297-307.

Cartland, S. P., Genner, S. W., Zahoor, A., & Kavurma, M. M. (2016). Comparative Evaluation of TRAIL, FGF-2 and VEGF-A-Induced Angiogenesis In Vitro and In Vivo. *Int J Mol Sci, 17*(12). doi:10.3390/ijms17122025

Cerdan, C., Rouleau, A., & Bhatia, M. (2004). VEGF-A165 augments erythropoietic development from human embryonic stem cells. *Blood, 103*(7), 2504-2512.

Chamie, K., Litwin, M. S., Bassett, J. C., Daskivich, T. J., Lai, J., Hanley, J. M., . . . Saigal, C. S. (2013). Recurrence of high-risk bladder cancer: a population-based analysis. *Cancer, 119*(17), 3219-3227. doi:10.1002/cncr.28147

Chan, O. T. M., Furuya, H., Pagano, I., Shimizu, Y., Hokutan, K., Dyrskjot, L., . . . Rosser, C. J. (2017). Association of MMP-2, RB and PAI-1 with decreased recurrence-free survival and overall survival in bladder cancer patients. *Oncotarget, 8*(59), 99707-99721. doi:10.18632/oncotarget.20686

Chang, X., Zhang, J., Huang, C., Pang, X., Luo, Q., Zhang, H., & Zhang, S. (2015). Sex-determining region Y-related high mobility group box (SOX)-2 is overexpressed in cervical squamous cell carcinoma and contributes cervical cancer cell migration and invasion in vitro. *Tumor Biology, 36*(10), 7725-7733. doi:10.1007/s13277-015-3450-y

Chang, Y. J., Cheng, Y. W., Lin, R. K., Huang, C. C., Chen, W. T., Ke, T. W., & Wei, P. L. (2016). Thrombomodulin Influences the Survival of Patients with Non-Metastatic Colorectal Cancer through Epithelial-To-Mesenchymal Transition (EMT). *PLoS One, 11*(8), e0160550. doi:10.1371/journal.pone.0160550

Chen, Y., Wu, Y., Zhang, X., Zeng, H., Liu, Y., Wu, Q., . . . Sun, F. (2018). Angiopoietin-2 (Ang-2) is a useful serum tumor marker for liver cancer in the Chinese population. *Clinica chimica acta, 478*, 18-27. doi:https://doi.org/10.1016/j.cca.2017.12.017

Chou, R., Selph, S., Buckley, D. I., Fu, R., Griffin, J. C., Grusing, S., & Gore, J. L. (2017). Comparative Effectiveness of Fluorescent Versus White Light Cystoscopy for Initial Diagnosis or Surveillance of Bladder Cancer on Clinical Outcomes: Systematic Review and Meta-Analysis. *The Journal of urology, 197*(3, Part 1), 548-558. doi:https://doi.org/10.1016/j.juro.2016.10.061

Choudhury, K. R., Yagle, K. J., Swanson, P. E., Krohn, K. A., & Rajendran, J. G. (2010). A robust automated measure of average antibody staining in immunohistochemistry images. *Journal of Histochemistry & Cytochemistry, 58*(2), 95-107.

Colomiere, M., Ward, A. C., Riley, C., Trenerry, M. K., Cameron-Smith, D., Findlay, J., . . . Ahmed, N. (2009). Cross talk of signals between EGFR and IL-6R through JAK2/STAT3 mediate epithelial-mesenchymal transition in ovarian carcinomas. *Br J Cancer, 100*(1), 134-144. doi:10.1038/sj.bjc.6604794

Colquhoun, A. J., & Mellon, J. K. (2002). Epidermal growth factor receptor and bladder cancer. *Postgraduate Medical Journal, 78*(924), 584-589. doi:10.1136/pmj.78.924.584

Colville-Nash, P. R., & Scott, D. L. (1992). Angiogenesis and rheumatoid arthritis: pathogenic and therapeutic implications. *Annals of the Rheumatic Diseases, 51*(7), 919-925. doi:10.1136/ard.51.7.919

Coquet, J. M., Rausch, L., & Borst, J. (2015). The importance of co-stimulation in the orchestration of T helper cell differentiation. *Immunol Cell Biol, 93*(9), 780-788. doi:10.1038/icb.2015.45

Coussens, L., Yang-Feng, T. L., Liao, Y.-C., Chen, E., Gray, A., McGrath, J., . . . Francke, U. (1985). Tyrosine kinase receptor with extensive homology to EGF receptor shares chromosomal location with neu oncogene. *Science, 230*(4730), 1132-1139.

Coussens, L. M., & Werb, Z. (2002). Inflammation and cancer. *Nature, 420*(6917), 860-867. doi:10.1038/nature01322

Cresswell, J., Robertson, H., Neal, D. E., Griffiths, T. R. L., & Kirby, J. A. (2001). Distribution of lymphocytes of the αEβ7 phenotype and E-cadherin in normal human urothelium and bladder carcinomas. *Clinical & Experimental Immunology, 126*(3), 397-402. doi:10.1046/j.1365-2249.2001.01652.x

Crivelli, J. J., Xylinas, E., Kluth, L. A., Rieken, M., Rink, M., & Shariat, S. F. (2014). Effect of Smoking on Outcomes of Urothelial Carcinoma: A Systematic Review of the Literature. *European Urology, 65*(4), 742-754. doi:https://doi.org/10.1016/j.eururo.2013.06.010

Crofford, L. (1997). COX-1 and COX-2 tissue immunoreactivity: implications and predictions. *The Journal of Rheumatology. Supplement, 49*, 15-19.

Cruz, P. V., Wakai, T., Shirai, Y., Yokoyama, N., & Hatakeyama, K. (2005). Loss of carcinoembryonic antigen-related cell adhesion molecule 1 immunoreactivity is an adverse prognostic factor in hepatocellular carcinoma. *Cancer, 104*(2), 354-360. doi:10.1002/cncr.21159

Cui, Y.Y., Shi, A.P., & Xu, N. (2012). Immunoreactivity of S100A8 protein in human bladder cancer and its clinical significance. *Chinese Journal of Laboratory Diagnosis, 2*, 017.

Cumberbatch, M. G. K., Jubber, I., Black, P. C., Esperto, F., Figueroa, J. D., Kamat, A. M., . . . Catto, J. W. F. (2018). Epidemiology of Bladder Cancer: A Systematic Review and Contemporary Update of Risk Factors in 2018. *Eur Urol, 74*(6), 784-795. doi:10.1016/j.eururo.2018.09.001

Dango, S., Sienel, W., Schreiber, M., Stremmel, C., Kirschbaum, A., Pantel, K., & Passlick, B. (2008). Elevated immunoreactivity of carcinoembryonic antigen-related cell adhesion molecule 1 (CEACAM-1) is associated with increased angiogenic potential in non-small-cell lung cancer. *Lung Cancer, 60*(3), 426-433.

Darai, E., Bringuier, A. F., Walker-Combrouze, F., Fauconnier, A., Couvelard, A., Feldmann, G., . . . Scoazec, J. Y. (1998). CD31 immunoreactivity in benign, borderline, and malignant epithelial ovarian tumors: an immunohistochemical and serological analysis. *Gynecol Oncol, 71*(1), 122-127. doi:10.1006/gyno.1998.5118

David, J., Nandakumar, A., Muniroh, M., Akiba, S., Yamamoto, M., & Koriyama, C. (2017). Suppression of methylmercury-induced MIP-2 immunoreactivity by N-acetyl-L-cysteine in murine RAW264.7 macrophage cell line. *Eur J Med Res, 22*(1), 45. doi:10.1186/s40001-017-0287-4

De Palma, M., Biziato, D., & Petrova, T. V. (2017). Microenvironmental regulation of tumour angiogenesis. *Nature Reviews Cancer, 17*(8), 457.

Dede, D. S., Gumuskaya, B., Guler, G., Onat, D., Altundag, K., & Ozisik, Y. (2013). Evaluation of changes in biologic markers ER, PR, HER 2 and Ki-67 index in breast cancer with administration of neoadjuvant dose dense doxorubicin, cyclophosphamide followed by paclitaxel chemotherapy. *J buon, 18*(2), 366-371.

Deliu, I. C., Neagoe, C. D., Bezna, M., Genunche-Dumitrescu, A. V., Toma, S. C., Ungureanu, B. S., . . . ForTofoiu, M. (2016). Correlations between endothelial cell markers CD31, CD34 and CD105 in colorectal carcinoma. *Rom J Morphol Embryol, 57*(3), 1025-1030.

Deng, J., Chen, W., Du, Y., Wang, W., Zhang, G., Tang, Y., . . . Zhou, Y. (2017). Synergistic efficacy of Cullin1 and MMP-2 immunoreactivitys in diagnosis and prognosis of colorectal cancer. *Cancer Biomark, 19*(1), 57-64. doi:10.3233/cbm-160341

Diana, A., Wang, L. M., D'Costa, Z., Azad, A., Silva, M. A., Soonawalla, Z., . . . Fokas, E. (2016). Prognostic role and correlation of CA9, CD31, CD68 and CD20 with the desmoplastic stroma in pancreatic ductal adenocarcinoma. *Oncotarget, 7*(45), 72819-72832. doi:10.18632/oncotarget.12022

Ditre, J. W., Gonzalez, B. D., Simmons, V. N., Faul, L. A., Brandon, T. H., & Jacobsen, P. B. (2011). Associations between pain and current smoking status among cancer patients. *PAIN, 152*(1), 60-65. doi:https://doi.org/10.1016/j.pain.2010.09.001

Dixon, J. S., & Gosling, J. A. (1983). Histology and fine structure of the muscularis mucosae of the human urinary bladder. *J Anat, 136*(Pt 2), 265-271.

Dmitrieva, O. S., Shilovskiy, I. P., Khaitov, M. R., & Grivennikov, S. I. (2016). Interleukins 1 and 6 as Main Mediators of Inflammation and Cancer. *Biochemistry (Mosc), 81*(2), 80-90. doi:10.1134/s0006297916020024

Doat, S., Marous, M., Rebillard, X., Tretarre, B., Lamy, P. J., Soares, P., . . . Menegaux, F. (2018). Prostatitis, other genitourinary infections and prostate cancer risk: Influence of non-steroidal anti-inflammatory drugs? Results from the EPICAP study. *Int J Cancer*. doi:10.1002/ijc.31565

Dobrzycka, B., Mackowiak-Matejczyk, B., Kinalski, M., & Terlikowski, S. J. (2013). Pretreatment serum levels of bFGF and VEGF and its clinical significance in endometrial carcinoma. *Gynecol Oncol, 128*(3), 454-460. doi:10.1016/j.ygyno.2012.11.035

dos Santos, G. T., Camillo, N. D., Berto, M. D., Prolla, J. C., da Cruz, I. B. M., Roehe, A. V., . . . Bica, C. G. (2017). Impact of Her-2 over expression on Survival of Patients with Metastatic Breast Cancer. *Asian Pac J Cancer Prev, 18*(10), 2673-2678. doi:10.22034/apjcp.2017.18.10.2673

Doval, D. C., Sharma, A., Sinha, R., Kumar, K., Dewan, A. K., Chaturvedi, H., . . . Mehta, A. (2015). Immunohistochemical Profile of Breast Cancer Patients at a Tertiary Care Hospital in New Delhi, India. *Asian Pac J Cancer Prev, 16*(12), 4959-4964.

Drejer, D., Béji, S., Munk Nielsen, A., Høyer, S., Wrist Lam, G., & Jensen, J. B. (2017). Clinical relevance of narrow-band imaging in flexible cystoscopy: the DaBlaCa-7 study. *Scandinavian Journal of Urology, 51*(2), 120-123. doi:10.1080/21681805.2017.1295101

Drewes, C. C., Dias, R. Y., Hebeda, C. B., Simons, S. M., Barreto, S. A., Ferreira, J. M., Jr., . . . Farsky, S. H. (2012). Actions of the Kunitz-type serine protease inhibitor Amblyomin-X on VEGF-A-induced angiogenesis. *Toxicon, 60*(3), 333-340. doi:10.1016/j.toxicon.2012.04.349

Du, J. W., Xu, K. Y., Fang, L. Y., & Qi, X. L. (2012). Clinical significance of Mena and Her-2 immunoreactivity in breast cancer. *Eur J Gynaecol Oncol, 33*(5), 455-458.

Eble, J., Sauter, G., Epstein, J., & Sesterhenn, I. (2004). Tumours of the urinary system and male genital organs: pathology and genetics. *World Health Organization Classification of Tumours. Lyon*.

Eissa, S. (2007). Noninvasive diagnosis of bladder cancer by detection of matrix metalloproteinases (MMP-2 and MMP-9) and their inhibitor (TIMP-2) in urine. *European Urology, 52*(5), 1388-1396. doi:10.1016/j.eururo.2007.04.006

El Gehani, K., Al-Kikhia, L., Mansuri, N., Syrjanen, K., Al-Fituri, O., & Elzagheid, A. (2011). Angiogenesis in urinary bladder carcinoma as defined by microvessel density (MVD) after immunohistochemical staining for Factor VIII and CD31. *Libyan J Med, 6*. doi:10.3402/ljm.v6i0.6016

Emoto, Y., Kobayashi, R., Akatsuka, H., & Hidaka, H. (1992). Purification and characterization of a new member of the S-100 protein family from human placenta. *Biochemical and biophysical research communications, 182*(3), 1246-1253.

Epstein, J. I., Amin, M. B., Reuter, V. R., Mostofi, F. K., & Committee, B. C. C. (1998). The World Health Organization/International Society of Urological Pathology consensus

classification of urothelial (transitional cell) neoplasms of the urinary bladder. *The American journal of surgical pathology, 22*(12), 1435-1448.

Ergün, S., Kilic, N., Ziegeler, G., Hansen, A., Nollau, P., Götze, J., . . . Fernando, M. (2000). CEA-related cell adhesion molecule 1: a potent angiogenic factor and a major effector of vascular endothelial growth factor. *Molecular cell, 5*(2), 311-320.

Erin, N., Nizam, E., Tanriover, G., & Koksoy, S. (2015). Autocrine control of MIP-2 secretion from metastatic breast cancer cells is mediated by CXCR2: a mechanism for possible resistance to CXCR2 antagonists. *Breast Cancer Res Treat, 150*(1), 57-69. doi:10.1007/s10549-015-3297-3

Eroglu, A., Ersoz, C., Karasoy, D., & Sak, S. (2017). Vascular endothelial growth factor (VEGF)-C, VEGF-D, VEGFR-3 and D2-40 immunoreactivitys in primary breast cancer: Association with lymph node metastasis. *Adv Clin Exp Med, 26*(2), 245-249. doi:10.17219/acem/58784

Esmon, N. L., Owen, W., & Esmon, C. (1982). Isolation of a membrane-bound cofactor for thrombin-catalyzed activation of protein C. *Journal of Biological Chemistry, 257*(2), 859-864.

Fedarko, N. S., Jain, A., Karadag, A., & Fisher, L. W. (2004). Three small integrin binding ligand N-linked glycoproteins (SIBLINGs) bind and activate specific matrix metalloproteinases. *The FASEB journal, 18*(6), 734-736.

Feng, L., Qi, Q., Wang, P., Chen, H., Chen, Z., Meng, Z., & Liu, L. (2018). Serum levels of IL-6, IL-8, and IL-10 are indicators of prognosis in pancreatic cancer. *Journal of International Medical Research, 46*(12), 5228-5236.

Ferlay, J., Soerjomataram, I., Ervik, M., Dikshit, R., Eser, S., Mathers, C., . . . Bray, F. (2013). GLOBOCAN 2012 v1. 0, cancer incidence and mortality worldwide: IARC CancerBase No. 11 [internet]. International Agency for Research on Cancer, Lyon. *globocan. iarc. fr (accessed 10 October 2014)*.

Fina, L., Molgaard, H. V., Robertson, D., Bradley, N. J., Monaghan, P., Delia, D., . . . Greaves, M. F. (1990). Immunoreactivity of the CD34 gene in vascular endothelial cells. *Blood, 75*(12), 2417-2426.

Fisher, L. W., Jain, A., Tayback, M., & Fedarko, N. S. (2004). Small integrin binding ligand N-linked glycoprotein gene family immunoreactivity in different cancers. *Clin Cancer Res, 10*(24), 8501-8511. doi:10.1158/1078-0432.ccr-04-1072

Fisher, L. W., Torchia, D. A., Fohr, B., Young, M. F., & Fedarko, N. S. (2001). Flexible structures of SIBLING proteins, bone sialoprotein, and osteopontin. *Biochem Biophys Res Commun, 280*(2), 460-465. doi:10.1006/bbrc.2000.4146

Folkman, J. (1971). Tumor angiogenesis: therapeutic implications. *New England Journal of Medicine, 285*(21), 1182-1186.

Fouad, H., Salem, H., Ellakwa, D. E., & Abdel-Hamid, M. (2018). MMP-2 and MMP-9 as prognostic markers for the early detection of urinary bladder cancer. *J Biochem Mol Toxicol*, e22275. doi:10.1002/jbt.22275

Foulds, L. (1954). The experimental study of tumor progression: a review. *Cancer Research, 14*(5), 327-339.

Freedman, N. D., Silverman, D. T., Hollenbeck, A. R., Schatzkin, A., & Abnet, C. C. (2011). Association between smoking and risk of bladder cancer among men and women. *Jama, 306*(7), 737-745.

Gancberg, D., Järvinen, T., Di Leo, A., Rouas, G., Cardoso, F., Paesmans, M., ... & Larsimont, D. (2002). Evaluation of HER-2/NEU protein immunoreactivity in breast cancer by immunohistochemistry: an interlaboratory study assessing the reproducibility of HER-2/NEU testing. *Breast cancer research and treatment*, *74*(2), 113-120.

García-Tello, A., Angulo, J. C., Andrés, G., Ramón de Fata, F., Sánchez-Chapado, M., & López, J. I. (2014). Impact of p53, MIB-1 and PECAM-1 immunoreactivity on the prognosis of urothelial carcinoma of the renal pelvis. *Actas Urológicas Españolas (English Edition), 38*(8), 506-514. doi:https://doi.org/10.1016/j.acuroe.2014.07.005

Gasche, J. A., Hoffmann, J., Boland, C. R., & Goel, A. (2011). Interleukin-6 promotes tumorigenesis by altering DNA methylation in oral cancer cells. *Int J Cancer, 129*(5), 1053-1063. doi:10.1002/ijc.25764

Gazzaniga, P., Gandini, O., Gradilone, A., Silvestri, I., Giuliani, L., Magnanti, M., . . . Agliano, A. M. (1999). Detection of basic fibroblast growth factor mRNA in urinary bladder cancer: correlation with local relapses. *Int J Oncol, 14*(6), 1123-1127.

Gebauer, F., Wicklein, D., Horst, J., Sundermann, P., Maar, H., Streichert, T., . . . Schumacher, U. (2014). Carcinoembryonic antigen-related cell adhesion molecules (CEACAM) 1, 5 and 6 as biomarkers in pancreatic cancer. *PLoS One, 9*(11), e113023. doi:10.1371/journal.pone.0113023

Gerhardt, H., Golding, M., Fruttiger, M., Ruhrberg, C., Lundkvist, A., Abramsson, A., . . . Shima, D. (2003). VEGF guides angiogenic sprouting utilizing endothelial tip cell filopodia. *The Journal of cell biology, 161*(6), 1163-1177.

Gheybi, M. K., Baradaran, A., Mohajeri, M. R., Ostovar, A., Hajalikhani, P., & Farrokhi, S. (2016). Validity of immunohistochemistry method in predicting HER-2 gene status and association of clinicopathological variables with it in invasive breast cancer patients. *Apmis, 124*(5), 365-371. doi:10.1111/apm.12518

Giachelli, C. M., & Steitz, S. (2000). Osteopontin: a versatile regulator of inflammation and biomineralization. *Matrix Biol, 19*(7), 615-622.

Gibadulinova, A., Tothova, V., Pastorek, J., & Pastorekova, S. (2011). Transcriptional regulation and functional implication of S100P in cancer. *Amino acids, 41*(4), 885-892.

Giovannucci, E., Egan, K. M., Hunter, D. J., Stampfer, M. J., Colditz, G. A., Willett, W. C., & Speizer, F. E. (1995). Aspirin and the risk of colorectal cancer in women. *N Engl J Med, 333*(10), 609-614. doi:10.1056/nejm199509073331001

Giovannucci, E., Rimm, E. B., Stampfer, M. J., Colditz, G. A., Ascherio, A., & Willett, W. C. (1994). Aspirin use and the risk for colorectal cancer and adenoma in male health professionals. *Ann Intern Med, 121*(4), 241-246.

Giulioni, M., Marucci, G., Cossu, M., Tassi, L., Bramerio, M., Barba, C., . . . Marras, C. E. (2019). CD34 Immunoreactivity in Low-Grade Epilepsy-Associated Tumors: Relationships with Clinicopathologic Features. *World Neurosurg, 121*, e761-e768. doi:10.1016/j.wneu.2018.09.212

Gospodarowicz, D. (1975). Purification of a fibroblast growth factor from bovine pituitary. *Journal of Biological Chemistry, 250*(7), 2515-2520.

Greineder, C. F., Johnston, I. H., Villa, C. H., Gollomp, K., Esmon, C. T., Cines, D. B., . . . Muzykantov, V. R. (2017). ICAM-1-targeted thrombomodulin mitigates tissue factor-driven inflammatory thrombosis in a human endothelialized microfluidic model. *Blood Adv, 1*(18), 1452-1465. doi:10.1182/bloodadvances.2017007229

Gril, B., Palmieri, D., Bronder, J. L., Herring, J. M., Vega-Valle, E., Feigenbaum, L., . . . Steeg, P. S. (2008). Effect of lapatinib on the outgrowth of metastatic breast cancer cells to the brain. *J Natl Cancer Inst, 100*(15), 1092-1103. doi:10.1093/jnci/djn216

Grimm, M., Kim, M., Rosenwald, A., Heemann, U., Germer, C. T., Waaga-Gasser, A. M., & Gasser, M. (2010). Toll-like receptor (TLR) 7 and TLR8 immunoreactivity on CD133+ cells in colorectal cancer points to a specific role for inflammation-induced TLRs in tumourigenesis and tumour progression. *Eur J Cancer, 46*(15), 2849-2857. doi:10.1016/j.ejca.2010.07.017

Groblewska, M., Mroczko, B., Gryko, M., Pryczynicz, A., Guzińska-Ustymowicz, K., Kędra, B., . . . Szmitkowski, M. (2014). Serum levels and tissue immunoreactivity of matrix metalloproteinase 2 (MMP-2) and tissue inhibitor of metalloproteinases 2 (TIMP-2) in colorectal cancer patients. *Tumor Biology, 35*(4), 3793-3802.

Grossman, H. B., Gomella, L., Fradet, Y., Morales, A., Presti, J., Ritenour, C., . . . Group, P. B. S. (2007). A phase III, multicenter comparison of hexaminolevulinate fluorescence cystoscopy and white light cystoscopy for the detection of superficial papillary lesions in patients with bladder cancer. *The Journal of urology, 178*(1), 62-67.

Guan, K.-P., Ye, H.-Y., Yan, Z., Wang, Y., & Hou, S.-K. (2003). Serum levels of endostatin and matrix metalloproteinase-9 associated with high stage and grade primary transitional cell carcinoma of the bladder. *Urology, 61*(4), 719-723.

Guo, A., Liu, A., & Teng, X. (2016). The pathology of urinary bladder lesions with an inverted growth pattern. *Chin J Cancer Res, 28*(1), 107-121. doi:10.3978/j.issn.1000-9604.2016.02.01

Guo, L., Chen, S., Jiang, H., Huang, J., Jin, W., & Yao, S. (2014a). The immunoreactivity of S100P increases and promotes cellular proliferation by increasing nuclear translocation of beta-catenin in endometrial cancer. *Int J Clin Exp Pathol, 7*(5), 2102-2112.

Guo, S., Tao, X., Wang, Y., Tang, J., Shen, L., & Song, C. (2014b). [SCF/c-Kit signaling promotes invasion of T24 cells via PI3K pathway]. *Nan Fang Yi Ke Da Xue Xue Bao, 34*(4), 507-510.

Gupta, M., Milbar, N., Tema, G., Pederzoli, F., Chappidi, M., Kates, M., . . . Bivalacqua, T. J. (2019). Impact of intravesical therapy for non-muscle invasive bladder cancer on the accuracy of urine cytology. *World J Urol*. doi:10.1007/s00345-018-02624-3

Hadler-Olsen, E., Fadnes, B., Sylte, I., Uhlin-Hansen, L., & Winberg, J. O. (2011). Regulation of matrix metalloproteinase activity in health and disease. *The FEBS journal, 278*(1), 28-45.

Hammam, O., Nour, H. H., Mosaad, M., Akl, M., Khalil, H., al Ganzory, H., & Hindawi, A. (2015). The clinical significance of HER2 protein amplification/immunoreactivity in

urinary bladder lesion. *Arab Journal of Urology, 13*(2), 146-152. doi:https://doi.org/10.1016/j.aju.2015.01.004

Hanahan, D., & Weinberg, R. A. (2000). The hallmarks of cancer. *Cell, 100*(1), 57-70.

Hanahan, D., & Weinberg, Robert A. (2011). Hallmarks of Cancer: The Next Generation. *Cell, 144*(5), 646-674. doi:http://dx.doi.org/10.1016/j.cell.2011.02.013

Hanly, A., Redmond, M., Winter, D., Brophy, S., Deasy, J., Bouchier-Hayes, D., & Kay, E. (2006). Thrombomodulin immunoreactivity in colorectal carcinoma is protective and correlates with survival. *British journal of cancer, 94*(9), 1320.

Hara, I. (2001). Significance of matrix metalloproteinases and tissue inhibitors of metalloproteinase immunoreactivity in the recurrence of superficial transitional cell carcinoma of the bladder. *The Journal of urology, 165*(5), 1769-1772.

Hardbower, D. M., de Sablet, T., Chaturvedi, R., & Wilson, K. T. (2013). Chronic inflammation and oxidative stress: the smoking gun for Helicobacter pylori-induced gastric cancer? *Gut Microbes, 4*(6), 475-481. doi:10.4161/gmic.25583

Harney, A. S., Arwert, E. N., Entenberg, D., Wang, Y., Guo, P., Qian, B.-Z., . . . Condeelis, J. S. (2015). Real-time imaging reveals local, transient vascular permeability, and tumor cell intravasation stimulated by TIE2hi macrophage–derived VEGFA. *Cancer discovery*.

Hasan, R., Bhatt, D., Khan, S., Khan, V., Verma, A. K., Anees, A., & Dev, K. (2018). Association of Her-2 Immunoreactivity and Clinicopathological Parameters in Colorectal Carcinoma in Indian Population. *Open access Macedonian journal of medical sciences, 7*(1), 6-11. doi:10.3889/oamjms.2019.008

Health, U. D. o., & Services, H. (2004). *The health consequences of smoking: a report of the Surgeon General* (Vol. 62): US Department of Health and Human Services, Centers for Disease Control and ….

Health, U. D. o., & Services, H. (2014). The health consequences of smoking—50 years of progress: a report of the Surgeon General. *Atlanta, GA: US Department of Health and Human Services, Centers for Disease Control and Prevention, National Center for Chronic Disease Prevention and Health Promotion, Office on Smoking and Health, 17*.

Hedaya, M., Helmy, A., Ezzat, H., & Hammam, O. (2015). Cyclo-oxygenase-2 and vascular endothelial growth factor immunoreactivity in colorectal cancer patients. *The Egyptian Journal of Surgery, 34*(1), 35-40. doi:10.4103/1110-1121.153369

Herr, H. W., & Donat, S. M. (2008). A comparison of white-light cystoscopy and narrow-band imaging cystoscopy to detect bladder tumour recurrences. *BJU international, 102*(9), 1111-1114.

Hirama, M., Takahashi, F., Takahashi, K., Akutagawa, S., Shimizu, K., Soma, S., . . . Fukuchi, Y. (2003). Osteopontin overproduced by tumor cells acts as a potent angiogenic factor contributing to tumor growth. *Cancer letters, 198*(1), 107-117.

Holleran, G., Hall, B., O'Regan, M., Smith, S., & McNamara, D. (2015). Immunoreactivity of angiogenic factors in patients with sporadic small bowel angiodysplasia. *Journal of clinical gastroenterology, 49*(10), 831-836.

Horowitz, N. A., & Palumbo, J. S. (2012). Mechanisms coupling thrombomodulin to tumor dissemination. *Thrombosis research, 129*, S119-S121.

Huajun, W., Ying, F., Hongxing, Z., Weifeng, S., Pingyang, S., Mingde, H., & Guoguang, L. (2018). Clinical value of combined detection of serum APE1-Aabs and CEACAM-1 in the diagnosis of colorectal cancer. *Eur Rev Med Pharmacol Sci, 22*(5), 1286-1289. doi:10.26355/eurrev_201803_14469

Huddart, R., Jones, R., & Choudhury, A. (2015). A new dawn for bladder cancer? recommendations from the National Institute for Health and Care Excellence (NICE) on managing bladder cancer. *Clinical Oncology*.

Hudziak, R. M., Schlessinger, J., & Ullrich, A. (1987). Increased immunoreactivity of the putative growth factor receptor p185HER2 causes transformation and tumorigenesis of NIH 3T3 cells. *Proceedings of the National Academy of Sciences, 84*(20), 7159-7163.

Huijbers, E. J. M., van Beijnum, J. R., Thijssen, V. L., Sabrkhany, S., Nowak-Sliwinska, P., & Griffioen, A. W. (2016). Role of the tumor stroma in resistance to anti-angiogenic therapy. *Drug Resistance Updates, 25*, 26-37. doi:https://doi.org/10.1016/j.drup.2016.02.002

Humphrey, P. A., Moch, H., Cubilla, A. L., Ulbright, T. M., & Reuter, V. E. (2016). The 2016 WHO Classification of Tumours of the Urinary System and Male Genital Organs—Part B: Prostate and Bladder Tumours. *European Urology, 70*(1), 106-119. doi:https://doi.org/10.1016/j.eururo.2016.02.028

Hurwitz, H., Fehrenbacher, L., Novotny, W., Cartwright, T., Hainsworth, J., Heim, W., . . . Kabbinavar, F. (2004). Bevacizumab plus irinotecan, fluorouracil, and leucovorin for metastatic colorectal cancer. *N Engl J Med, 350*(23), 2335-2342. doi:10.1056/NEJMoa032691

Iqbal, N., & Iqbal, N. (2014). Human epidermal growth factor receptor 2 (HER2) in cancers: over expression and therapeutic implications. *Molecular biology international, 2014*.

Jana, D., Mandal, S., Mukhopadhyay, M., Mitra, D., Mukhopadhyay, S. K., & Sarkar, D. K. (2012). Prognostic significance of HER-2/neu and survival of breast cancer patients attending a specialized breast clinic in Kolkata, Eastern India. *Asian Pac J Cancer Prev, 13*(8), 3851-3855.

Ji, Y., Sheng, L., Du, X., Qiu, G., Chen, B., & Wang, X. (2014). Clinicopathological variables predicting HER-2 gene status in immunohistochemistry-equivocal (2+) invasive breast cancer. *Journal of thoracic disease, 6*(7), 896-904. doi:10.3978/j.issn.2072-1439.2014.07.27

Jiang, H., Hu, H., Lin, F., Lim, Y. P., Hua, Y., Tong, X., & Zhang, S. (2016). S100P is Overexpressed in Squamous Cell and Adenosquamous Carcinoma Subtypes of Endometrial Cancer and Promotes Cancer Cell Proliferation and Invasion. *Cancer Invest, 34*(10), 477-488. doi:10.1080/07357907.2016.1212206

Jiang, X. (2007). *Fluid intake, micturition habits, associated medications and conditions as potential risk factors for bladder cancer*. University of Southern California.

Jitariu, A. A., Raica, M., Cimpean, A. M., & Suciu, S. C. (2018). The role of PDGF-B/PDGFR-BETA axis in the normal development and carcinogenesis of the breast. *Crit Rev Oncol Hematol, 131*, 46-52. doi:10.1016/j.critrevonc.2018.08.002

Josh, F., Tobita, M., Tanaka, R., Orbay, H., Ogata, K., Suzuki, K., . . . Mizuno, H. (2013). Concentration of PDGF-AB, BB and TGF-β1 as Valuable Human Serum Parameters in Adipose-derived Stem Cell Proliferation. *Journal of Nippon Medical School, 80*(2), 140-147. doi:10.1272/jnms.80.140

Jost, S. P., Gosling, J. A., & Dixon, J. S. (1989). The morphology of normal human bladder urothelium. *J Anat, 167*, 103.

Ju, R., Zhuang, Z. W., Zhang, J., Lanahan, A. A., Kyriakides, T., Sessa, W. C., & Simons, M. (2014). Angiopoietin-2 secretion by endothelial cell Exosomes Regulation by the phosphatidylinositol 3-kinase (Pi3k)/akt/endothelial nitric oxide synthase (enos) and syndecan-4/syntenin pathways. *Journal of Biological Chemistry, 289*(1), 510-519.

Karashima, T., Sweeney, P., Kamat, A., Huang, S., Kim, S. J., Bar-Eli, M., . . . Dinney, C. P. N. (2003). Nuclear Factor-κB Mediates Angiogenesis and Metastasis of Human Bladder Cancer through the Regulation of Interleukin-8. *Clinical Cancer Research, 9*(7), 2786-2797.

Kassim, S. K., El-Salahy, E. M., Fayed, S. T., Helal, S. A., Helal, T., Azzam, E. E.-d., & Khalifa, A. (2004). Vascular endothelial growth factor and interleukin-8 are associated with poor prognosis in epithelial ovarian cancer patients. *Clinical biochemistry, 37*(5), 363-369.

Kaulfuβ, S., Seemann, H., Kampe, R., Meyer, J., Dressel, R., König, B., . . . Burfeind, P. (2013). Blockade of the PDGFR family together with SRC leads to diminished proliferation of colorectal cancer cells. *Oncotarget, 4*(7), 1037.

Kawaguchi, K., Sakurai, M., Yamamoto, Y., Suzuki, E., Tsuda, M., Kataoka, T. R., . . . Toi, M. (2019). Alteration of specific cytokine immunoreactivity patterns in patients with breast cancer. *Sci Rep, 9*(1), 2924. doi:10.1038/s41598-019-39476-9

Kessenbrock, K., Wang, C.-Y., & Werb, Z. (2015). Matrix metalloproteinases in stem cell regulation and cancer. *Matrix biology, 44*, 184-190.

Kilic, N., Oliveira-Ferrer, L., Wurmbach, J.-H., Loges, S., Chalajour, F., Vahid, S. N., . . . Ergun, S. (2005). Pro-angiogenic signaling by the endothelial presence of CEACAM1. *Journal of Biological Chemistry, 280*(3), 2361-2369.

Kiseleva, R. Y., Greineder, C., Villa, C., Marcos-Contreras, O., Hood, E., Shuvaev, V., . . . Muzykantov, V. (2018). Vascular endothelial effects of collaborative binding to platelet/endothelial cell adhesion molecule-1 (PECAM-1). *Scientific reports, 8*(1), 1510.

Kitamura, H., Torigoe, T., Hirohashi, Y., Asanuma, H., Inoue, R., Nishida, S., . . . Sato, N. (2013). Prognostic impact of the immunoreactivity of ALDH1 and SOX2 in urothelial cancer of the upper urinary tract. *Modern Pathology, 26*(1), 117.

Kollmar, O., Menger, M. D., & Schilling, M. K. (2006). Macrophage inflammatory protein-2 contributes to liver resection-induced acceleration of hepatic metastatic tumor growth. *World J Gastroenterol, 12*(6), 858-867.

Korkolopoulou, P., Christodoulou, P., Kapralos, P., Exarchakos, M., Bisbiroula, A., Hadjiyannakis, M., . . . Thomas-Tsagli, E. (1997). The role of p53, MDM2 and c-erb B-2 oncoproteins, epidermal growth factor receptor and proliferation markers in the

prognosis of urinary bladder cancer. *Pathol Res Pract, 193*(11-12), 767-775. doi:10.1016/s0344-0338(97)80055-6

Koutros, S., Silverman, D. T., Alavanja, M. C. R., Andreotti, G., Lerro, C. C., Heltshe, S., . . . Beane Freeman, L. E. (2016). Occupational exposure to pesticides and bladder cancer risk. *International Journal of Epidemiology, 45*(3), 792-805. doi:10.1093/ije/dyv195

Koutsi, A., Papapanagiotou, A., & Papavassiliou, A. G. (2008). Thrombomodulin: from haemostasis to inflammation and tumourigenesis. *The international journal of biochemistry & cell biology, 40*(9), 1669-1673.

Krishnamoorthy, B., Critchley, W., Barnard, J., Waterworth, P., Caress, A., Fildes, J., & Yonan, N. (2015). *Validation of the endothelial staining markers CD31 and CD34 in immunohistochemistry of the long saphenous vein.* Paper presented at the Journal of cardiothoracic surgery.

Kuang, B. H., Wen, X. Z., Ding, Y., Peng, R. Q., Cai, P. Q., Zhang, M. Q., . . . Zhang, X. (2013). The prognostic value of platelet endothelial cell adhesion molecule-1 in non-small-cell lung cancer patients. *Med Oncol, 30*(2), 536. doi:10.1007/s12032-013-0536-5

Kuespert, K., Pils, S., & Hauck, C. R. (2006). CEACAMs: their role in physiology and pathophysiology. *Current opinion in cell biology, 18*(5), 565-571.

Kwan, M. L., Kushi, L. H., Danforth, K. N., Roh, J. M., Ergas, I. J., Lee, V. S., . . . Tang, L. (2019). The Be-Well Study: a prospective cohort study of lifestyle and genetic factors to reduce the risk of recurrence and progression of non-muscle-invasive bladder cancer. *Cancer Causes Control*. doi:10.1007/s10552-019-1130-8

Lammers, R. J., Palou, J., Witjes, W. P., Janzing-Pastors, M. H., Caris, C. T., & Witjes, J. A. (2014). Comparison of expected treatment outcomes, obtained using risk models and international guidelines, with observed treatment outcomes in a Dutch cohort of patients with non-muscle-invasive bladder cancer treated with intravesical chemotherapy. *BJU Int, 114*(2), 193-201.

Lee, D. H., Yoon, H., Park, S., Kim, J. S., Ahn, Y. H., Kwon, K., . . . Kim, K. H. (2018). Urinary Exosomal and cell-free DNA Detects Somatic Mutation and Copy Number Alteration in Urothelial Carcinoma of Bladder. *Sci Rep, 8*(1), 14707. doi:10.1038/s41598-018-32900-6

Lee, S., Chen, T. T., Barber, C. L., Jordan, M. C., Murdock, J., Desai, S., . . . Iruela-Arispe, M. L. (2007). Autocrine VEGF signaling is required for vascular homeostasis. *Cell, 130*(4), 691-703.

Lefere, S., Van de Velde, F., Hoorens, A., Raevens, S., Van Campenhout, S., Vandierendonck, A., . . . Devisscher, L. (2018). Angiopoietin-2 promotes pathological angiogenesis and is a novel therapeutic target in murine non-alcoholic fatty liver disease. *Hepatology*. doi:10.1002/hep.30294

Lemoli, R. M., Fortuna, A., Grande, A., Gamberi, B., Bonsi, L., Fogli, M., . . . Tura, S. (1994). Immunoreactivity and functional role of c-kit ligand (SCF) in human multiple myeloma cells. *Br J Haematol, 88*(4), 760-769.

Lewis, C. E., Harney, A. S., & Pollard, J. W. (2016). The multifaceted role of perivascular macrophages in tumors. *Cancer cell, 30*(1), 18-25.

Li, X., Yang, H., Zhang, Z., Yan, Z., Lv, H., Zhang, Y., & Wu, B. (2019). Concentrated growth factor exudate enhances the proliferation of human periodontal ligament cells in the presence of TNFalpha. *Mol Med Rep, 19*(2), 943-950. doi:10.3892/mmr.2018.9714

Liang, N., Li, Y., & Chung, H. Y. (2017). Two natural eudesmane-type sesquiterpenes from Laggera alata inhibit angiogenesis and suppress breast cancer cell migration through VEGF- and Angiopoietin 2-mediated signaling pathways. *Int J Oncol, 51*(1), 213-222. doi:10.3892/ijo.2017.4004

Liang, W., & Ferrara, N. (2016). The complex role of neutrophils in tumor angiogenesis and metastasis. *Cancer immunology research, 4*(2), 83-91.

Lipponen, P., & Eskelinen, M. (1994). Immunoreactivity of epidermal growth factor receptor in bladder cancer as related to established prognostic factors, oncoprotein (c-erbB-2, p53) immunoreactivity and long-term prognosis. *Br J Cancer, 69*(6), 1120-1125.

Liss, M. A., White, M., Natarajan, L., & Parsons, J. K. (2016). Exercise Decreases and Smoking Increases Bladder Cancer Mortality. *Clinical Genitourinary Cancer*.

Littlepage, L. E., Sternlicht, M. D., Rougier, N., Phillips, J., Gallo, E., Yu, Y., . . . Werb, Z. (2010). Matrix metalloproteinases contribute distinct roles in neuroendocrine prostate carcinogenesis, metastasis, and angiogenesis progression. *Cancer Res, 70*(6), 2224-2234. doi:10.1158/0008-5472.can-09-3515

Liu, Y., Wang, C., Shan, X., Wu, J., Liu, H., Liu, H., . . . Fan, J. (2017). S100P is associated with proliferation and migration in nasopharyngeal carcinoma. *Oncol Lett, 14*(1), 525-532. doi:10.3892/ol.2017.6198

Liukkonen, T., Rajala, P., Raitanen, M., Rintala, E., Kaasinen, E., & Lipponen, P. (1999). Prognostic value of MIB-1 score, p53, EGFr, mitotic index and papillary status in primary superficial (Stage pTa/T1) bladder cancer: a prospective comparative study. The Finnbladder Group. *Eur Urol, 36*(5), 393-400. doi:20039

Lopez-Beltran, A., & Montironi, R. (2004). Non-Invasive Urothelial Neoplasms: According to the Most Recent WHO Classification. *European Urology, 46*(2), 170-176. doi:https://doi.org/10.1016/j.eururo.2004.03.017

Lorente, L., Rodriguez, S. T., Sanz, P., Pérez-Cejas, A., Padilla, J., Díaz, D., . . . Barrera, M. A. (2018). High serum soluble CD40L levels previously to liver transplantation in patients with hepatocellular carcinoma are associated with mortality at one year. *Journal of Critical Care, 43*, 316-320. doi:https://doi.org/10.1016/j.jcrc.2017.09.032

Losa, A., Hurle, R., & Lembo, A. (2000). Low dose bacillus Calmette-Guerin for carcinoma in situ of the bladder: long-term results. *J Urol, 163*(1), 68-71; discussion 71-62.

Lotan, Y., & Roehrborn, C. G. (2002). Cost-effectiveness of a modified care protocol substituting bladder tumor markers for cystoscopy for the followup of patients with transitional cell carcinoma of the bladder: a decision analytical approach. *The Journal of urology, 167*(1), 75-79.

Łukaszewicz-Zając, M., Mroczko, B., Kozłowski, M., & Szmitkowski, M. (2017). Stem cell factor in the serum of patients with esophageal cancer in relation to its histological types. *Archives of medical science: AMS, 13*(6), 1357.

Lund, S. A., Giachelli, C. M., & Scatena, M. (2009). The role of osteopontin in inflammatory processes. *J Cell Commun Signal, 3*(3-4), 311-322. doi:10.1007/s12079-009-0068-0

Luo, W., Tapolsky, M., Earley, K., Wood, C. G., Wilson, D. R., Logothetis, C. J., & Lin, S.-H. (1999). Tumor-suppressive activity of CD66a in prostate cancer. *Cancer gene therapy, 6*(4), 313.

Luster, A. D. (1998). Chemokines—chemotactic cytokines that mediate inflammation. *New England Journal of Medicine, 338*(7), 436-445.

Lv, Y., Zhao, X., Zhu, L., Li, S., Xiao, Q., He, W., & Yin, L. (2018). Targeting intracellular MMPs efficiently inhibits tumor metastasis and angiogenesis. *Theranostics, 8*(10), 2830-2845. doi:10.7150/thno.23209

Maciejczyk, A., Lacko, A., Ekiert, M., Jagoda, E., Wysocka, T., Matkowski, R., . . . Surowiak, P. (2013). Elevated nuclear S100P immunoreactivity is associated with poor survival in early breast cancer patients. *Histol Histopathol, 28*(4), 513-524. doi:10.14670/hh-28.513

Madsen, C. V., Steffensen, K. D., Olsen, D. A., Waldstrom, M., Smerdel, M., Adimi, P., . . . Jakobsen, A. (2012). Serial measurements of serum PDGF-AA, PDGF-BB, FGF2, and VEGF in multiresistant ovarian cancer patients treated with bevacizumab. *J Ovarian Res, 5*(1), 23. doi:10.1186/1757-2215-5-23

Maeshima, Y., Colorado, P. C., Torre, A., Holthaus, K. A., Grunkemeyer, J. A., Ericksen, M. B., . . . Kalluri, R. (2000). Distinct antitumor properties of a type IV collagen domain derived from basement membrane. *Journal of Biological Chemistry, 275*(28), 21340-21348.

Mantovani, A. (2009). Cancer: inflaming metastasis. *Nature, 457*(7225), 36.

Mantovani, A., Allavena, P., Sica, A., & Balkwill, F. (2008). Cancer-related inflammation. *Nature, 454*(7203), 436.

Mao, A. W., Jiang, T. H., Sun, X. J., & Peng, J. (2015). Application of chemokine receptor antagonist with stents reduces local inflammation and suppresses cancer growth. *Tumour Biol, 36*(11), 8637-8643. doi:10.1007/s13277-015-3557-1

Mariappan, P., Zachou, A., & Grigor, K. M. (2010). Detrusor muscle in the first, apparently complete transurethral resection of bladder tumour specimen is a surrogate marker of resection quality, predicts risk of early recurrence, and is dependent on operator experience. *European Urology, 57*(5), 843-849.

Masson, V., de la Ballina, L. R., Munaut, C., Wielockx, B., Jost, M., Maillard, C., . . . Itohara, S. (2005). Contribution of host MMP-2 and MMP-9 to promote tumor vascularization and invasion of malignant keratinocytes. *The FASEB journal, 19*(2), 234-236.

Masui, S., Nakatake, Y., Toyooka, Y., Shimosato, D., Yagi, R., Takahashi, K., . . . Sharov, A. A. (2007). Pluripotency governed by Sox2 via regulation of Oct3/4 immunoreactivity in mouse embryonic stem cells. *Nature cell biology, 9*(6), 625.

Mazoochi, T., Karimian, M., Ehteram, H., & Karimian, A. (2019). Survivin c.-31G>C (rs9904341) gene transversion and urinary system cancers risk: a systematic review and a meta-analysis. *Per Med, 16*(1), 67-78. doi:10.2217/pme-2018-0053

McColl, B. K., Paavonen, K., Karnezis, T., Harris, N. C., Davydova, N., Rothacker, J., . . . Hibbs, M. L. (2007). Proprotein convertases promote processing of VEGF-D, a critical step for binding the angiogenic receptor VEGFR-2. *The FASEB journal, 21*(4), 1088-1098.

McCormack, V. A., Agudo, A., Dahm, C. C., Overvad, K., Olsen, A., Tjonneland, A., . . . Almquist, M. (2010). Cigar and pipe smoking and cancer risk in the European Prospective Investigation into Cancer and Nutrition (EPIC). *International journal of cancer, 127*(10), 2402-2411.

McDermott, R. S., Deneux, L., Mosseri, V., Védrenne, J., Clough, K., Fourquet, A., . . . Beuzeboc, P. (2002). Circulating macrophage colony stimulating factor as a marker of tumour progression. *European cytokine network, 13*(1), 121-127.

Mead, J., Alfin-Slater, R., Howton, D., & Popjak, G. (1986). Prostaglandins, thromboxanes, and prostacyclin. *Lipids: Chemistry, Biochemistry, and Nutrition*, 149-216.

Mhawech, P., Iselin, C., & Pelte, M.-F. (2002). Value of immunohistochemistry in staging T1 urothelial bladder carcinoma. *European Urology, 42*(5), 459-463.

Millan-Rodriguez, F., Chechile-Toniolo, G., Salvador-Bayarri, J., Palou, J., & Vicente-Rodriguez, J. (2000). Multivariate analysis of the prognostic factors of primary superficial bladder cancer. *The Journal of urology, 163*(1), 73-78.

Miller, D. L., Yaron, R., & Yellin, M. J. (1998). CD40L-CD40 interactions regulate endothelial cell surface tissue factor and thrombomodulin immunoreactivity. *J Leukoc Biol, 63*(3), 373-379.

Moens, S., Goveia, J., Stapor, P. C., Cantelmo, A. R., & Carmeliet, P. (2014). The multifaceted activity of VEGF in angiogenesis–implications for therapy responses. *Cytokine & growth factor reviews, 25*(4), 473-482.

Moghadam, S. A., Abadi, A. M., & Mokhtari, S. (2015). Immunohistochemical analysis of CD34 immunoreactivity in salivary gland tumors. *J Oral Maxillofac Pathol, 19*(1), 30-33. doi:10.4103/0973-029x.157197

Mohamed, S. Y., Mohammed, H. L., Ibrahim, H. M., Mohamed, E. M., & Salah, M. (2017a). Role of VEGF, CD105, and CD31 in the Prognosis of Colorectal Cancer Cases. *Journal of gastrointestinal cancer*, 1-12.

Mohamed, S. Y., Mohammed, H. L., Ibrahim, H. M., Mohamed, E. M., & Salah, M. (2017b). Role of VEGF, CD105, and CD31 in the Prognosis of Colorectal Cancer Cases. *Journal of gastrointestinal cancer*. doi:10.1007/s12029-017-0014-y

Mohammed, S. I., Knapp, D. W., Bostwick, D. G., Foster, R. S., Khan, K. N. M., Masferrer, J. L., . . . Koki, A. T. (1999). Immunoreactivity of Cyclooxygenase-2 (COX-2) in Human Invasive Transitional Cell Carcinoma (TCC) of the Urinary Bladder. *Cancer Research, 59*(22), 5647-5650.

Mostofi, F. K., Sobin, L. H., Torloni, H., & Organization, W. H. (1973). Histological typing of urinary bladder tumours.

Mowatt, G., Zhu, S., Kilonzo, M., Boachie, C., Fraser, C., Griffiths, T. R., . . . Vale, L. (2010). Systematic review of the clinical effectiveness and cost-effectiveness of photodynamic diagnosis and urine biomarkers (FISH, ImmunoCyt, NMP22) and cytology for the

detection and follow-up of bladder cancer. *Health Technol Assess, 14*(4), 1-331, iii-iv. doi:10.3310/hta14040

Mroczko, B., Szmitkowski, M., WereszczyńSka-Siemiątkowska, U., & Okulczyk, B. (2005). Stem cell factor (SCF) and interleukin 3 (IL-3) in the sera of patients with colorectal cancer. *Digestive diseases and sciences, 50*(6), 1019-1024.

Muller, W. J., Sinn, E., Pattengale, P. K., Wallace, R., & Leder, P. (1988). Single-step induction of mammary adenocarcinoma in transgenic mice bearing the activated c-neu oncogene. *Cell, 54*(1), 105-115.

Munn, L. L. (2017). Cancer and inflammation. *Wiley Interdisciplinary Reviews: Systems Biology and Medicine, 9*(2), e1370.

Nagase, H., Visse, R., & Murphy, G. (2006). Structure and function of matrix metalloproteinases and TIMPs. *Cardiovascular research, 69*(3), 562-573.

Neumaier, M., Paululat, S., Chan, A., Matthaes, P., & Wagener, C. (1993). Biliary glycoprotein, a potential human cell adhesion molecule, is down-regulated in colorectal carcinomas. *Proceedings of the National Academy of Sciences, 90*(22), 10744-10748.

Ng M, Freeman MK, Fleming TD, et al. Smoking Prevalence and Cigarette Consumption in 187 Countries, 1980-2012. *JAMA.* 2014;311(2):183–192. doi:10.1001/jama.2013.284692

Newby, A. C. (2005). Dual role of matrix metalloproteinases (matrixins) in intimal thickening and atherosclerotic plaque rupture. *Physiological reviews, 85*(1), 1-31.

Nolff, M., Albert, R., Wohlsein, P., Baumgartner, W., Reese, S., & Meyer-Lindenberg, A. (2018). Histomorphometric evaluation of MMP-9 and CD31 immunoreactivity during healing under Negative Pressure Wound Therapy in dogs. *Schweiz Arch Tierheilkd, 160*(9), 525-532. doi:10.17236/sat00173

Nowak, A., Grzegrzolka, J., Kmiecik, A., Piotrowska, A., Matkowski, R., & Dziegiel, P. (2018). Role of nestin immunoreactivity in angiogenesis and breast cancer progression. *Int J Oncol, 52*(2), 527-535. doi:10.3892/ijo.2017.4223

Nowell, P. C. (1976). The clonal evolution of tumor cell populations. *Science, 194*(4260), 23-28.

O'Brien, C. D., Lim, P., Sun, J., & Albelda, S. M. (2003). PECAM-1-dependent neutrophil transmigration is independent of monolayer PECAM-1 signaling or localization. *Blood, 101*(7), 2816-2825. doi:10.1182/blood-2002-08-2396

Office of national statistic, (2019). Cancer survival in England: adult, stage at diagnosis and childhood - patients followed up to 2018. Assessed from https://www.ons.gov.uk/peoplepopulationandcommunity/healthandsocialcare/conditionsanddiseases/bulletins/cancersurvivalinengland/stageatdiagnosisandchildhoodpatientsfollowedupto2018 on 5th September 2019.

Ohno-Matsui, K., Uetama, T., Yoshida, T., Hayano, M., Itoh, T., Morita, I., & Mochizuki, M. (2003). Reduced retinal angiogenesis in MMP-2-deficient mice. *Invest Ophthalmol Vis Sci, 44*(12), 5370-5375.

Ohtsuka, Y., Lee, J., Stamm, D., & Sanderson, I. (2001a). MIP-2 secreted by epithelial cells increases neutrophil and lymphocyte recruitment in the mouse intestine. *Gut, 49*(4), 526-533.

Ohtsuka, Y., Lee, J., Stamm, D. S., & Sanderson, I. R. (2001b). MIP-2 secreted by epithelial cells increases neutrophil and lymphocyte recruitment in the mouse intestine. *Gut, 49*(4), 526-533.

Okada-Ban, M., Thiery, J. P., & Jouanneau, J. (2000). Fibroblast growth factor-2. *The international journal of biochemistry & cell biology, 32*(3), 263-267.

Pan, H.-D., Peng, Y.-F., Xiao, G., & Gu, J. (2017). High levels of serum platelet-derived growth factor-AA and human epidermal growth factor receptor-2 are predictors of colorectal cancer liver metastasis. *World J Gastroenterol, 23*(7), 1233.

Paner, G. P., Annaiah, C., Gulmann, C., Rao, P., Ro, J. Y., Hansel, D. E., . . . Luthringer, D. J. (2014). Immunohistochemical evaluation of novel and traditional markers associated with urothelial differentiation in a spectrum of variants of urothelial carcinoma of the urinary bladder. *Human pathology, 45*(7), 1473-1482.

Papadopoulos, J., Karpouzis, A., Tentes, J., & Kouskoukis, C. (2014). Assessment of Interleukins IL-4, IL-6, IL-8, IL-10 in Acute Urticaria. *J Clin Med Res, 6*(2), 133-137. doi:10.14740/jocmr1645w

Parkin, D. M. (2008). The global burden of urinary bladder cancer. *Scandinavian journal of urology and nephrology, 42*(sup218), 12-20.

Parkin, D. M. (2011). 1. The fraction of cancer attributable to lifestyle and environmental factors in the UK in 2010. *British journal of cancer, 105*, S2-S5.

Parkin, D. M., Sitas, F., Chirenje, M., Stein, L., Abratt, R., & Wabinga, H. (2008). Part I: Cancer in Indigenous Africans—burden, distribution, and trends. *The lancet oncology, 9*(7), 683-692.

Patry, C., Remme, C., Betzen, C., Tonshoff, B., Yard, B. A., Beck, G., & Rafat, N. (2018). VCAM-1 immunoreactivity is upregulated by CD34+/CD133+-stem cells derived from septic patients. *PLoS One, 13*(3), e0195064. doi:10.1371/journal.pone.0195064

Pereira, L. M. C., Bersano, P. R. O., Rocha, D. D., & Lopes, M. D. (2018). Effect of EGF on immunoreactivity and localization of maturation-promoting factor, mitogen-activated protein kinase, p34(cdc2) and cyclin B during different culture periods on in vitro maturation of canine oocytes. *Reprod Domest Anim*. doi:10.1111/rda.13365

Perkhofer, L., Walter, K., Costa, I. G., Carrasco, M. C., Eiseler, T., Hafner, S., . . . Muller, M. (2016). Tbx3 fosters pancreatic cancer growth by increased angiogenesis and activin/nodal-dependent induction of stemness. *Stem Cell Res, 17*(2), 367-378. doi:10.1016/j.scr.2016.08.007

Perletti, G., Monti, E., Magri, V., Cai, T., Cleves, A., Trinchieri, A., & Montanari, E. (2017). The association between prostatitis and prostate cancer. Systematic review and meta-analysis. *Arch Ital Urol Androl, 89*(4), 259-265. doi:10.4081/aiua.2017.4.259

Petrova, T. V., Bono, P., Holnthoner, W., Chesnes, J., Pytowski, B., Sihto, H., . . . Alitalo, K. (2008). VEGFR-3 immunoreactivity is restricted to blood and lymphatic vessels in solid tumors. *Cancer cell, 13*(6), 554-556.

Potente, M., & Carmeliet, P. (2017). The link between angiogenesis and endothelial metabolism. *Annual review of physiology, 79*, 43-66.

Prall, F., Nollau, P., Neumaier, M., Haubeck, H.-D., Drzeniek, Z., Helmchen, U., . . . Wagener, C. (1996). CD66a (BGP), an adhesion molecule of the carcinoembryonic antigen family, is expressed in epithelium, endothelium, and myeloid cells in a wide range of normal human tissues. *Journal of Histochemistry & Cytochemistry, 44*(1), 35-41.

Presta, M., Foglio, E., Churruca Schuind, A., & Ronca, R. (2018). Long Pentraxin-3 Modulates the Angiogenic Activity of Fibroblast Growth Factor-2. *Front Immunol, 9*, 2327. doi:10.3389/fimmu.2018.02327

Prins, M. J., Ruurda, J. P., van Diest, P. J., van Hillegersberg, R., & Ten Kate, F. J. (2013). The significance of the HER-2 status in esophageal adenocarcinoma for survival: an immunohistochemical and an in situ hybridization study. *Ann Oncol, 24*(5), 1290-1297. doi:10.1093/annonc/mds640

Proudfoot, A. E. I., Handel, T. M., Johnson, Z., Lau, E. K., LiWang, P., Clark-Lewis, I., . . . Kosco-Vilbois, M. H. (2003). Glycosaminoglycan binding and oligomerization are essential for the in vivo activity of certain chemokines. *Proceedings of the National Academy of Sciences, 100*(4), 1885-1890. doi:10.1073/pnas.0334864100

Pusztaszeri, M. P., Seelentag, W., & Bosman, F. T. (2006). Immunohistochemical Immunoreactivity of Endothelial Markers CD31, CD34, von Willebrand Factor, and Fli-1 in Normal Human Tissues. *Journal of Histochemistry & Cytochemistry, 54*(4), 385-395. doi:10.1369/jhc.4A6514.2005

Qian, H., Yang, L., Zhao, W., Chen, H., & He, S. (2018). A comparison of CD105 and CD31 immunoreactivity in tumor vessels of hepatocellular carcinoma by tissue microarray and flow cytometry. *Exp Ther Med, 16*(4), 2881-2888. doi:10.3892/etm.2018.6553

Rabindran, S. K., Discafani, C. M., Rosfjord, E. C., Baxter, M., Floyd, M. B., Golas, J., . . . Wissner, A. (2004). Antitumor activity of HKI-272, an orally active, irreversible inhibitor of the HER-2 tyrosine kinase. *Cancer Res, 64*(11), 3958-3965. doi:10.1158/0008-5472.can-03-2868

Raica, M., & Cimpean, A. M. (2010). Platelet-derived growth factor (PDGF)/PDGF receptors (PDGFR) axis as target for antitumor and antiangiogenic therapy. *Pharmaceuticals, 3*(3), 572-599.

Rajcani, J., Kajo, K., Adamkov, M., Moravekova, E., Lauko, L., Felcanova, D., & Bencat, M. (2013). Immunohistochemical characterization of urothelial carcinoma. *Bratislavske lekarske listy, 114*(8), 431-438.

Razanajaona, D., Joguet, S., Ay, A.-S., Treilleux, I., Goddard-Léon, S., Bartholin, L., & Rimokh, R. (2007). Silencing of FLRG, an antagonist of activin, inhibits human breast tumor cell growth. *Cancer Research, 67*(15), 7223-7229.

Reis, S. T., Leite, K. R. M., Piovesan, L. F., Pontes-Junior, J., Viana, N. I., Abe, D. K., . . . Dall'Oglio, M. F. (2012). Increased immunoreactivity of MMP-9 and IL-8 are correlated with poor prognosis of Bladder Cancer. *BMC Urology, 12*(1), 18. doi:10.1186/1471-2490-12-18

Ren, P., Chen, F.-F., Liu, H.-Y., Cui, X.-L., Sun, Y., Guan, J.-L., . . . Wang, Y.-N. (2012). High Serum Levels of Follistatin in Patients with Ovarian Cancer. *Journal of International Medical Research, 40*(3), 877-886. doi:10.1177/147323001204000306

Reulen, R. C., Kellen, E., Buntinx, F., Brinkman, M., & Zeegers, M. P. (2008). A meta-analysis on the association between bladder cancer and occupation. *Scandinavian journal of urology and nephrology, 42*(sup218), 64-78.

Riese, D. J., & Stern, D. F. (1998). Specificity within the EGF family/ErbB receptor family signaling network. *Bioessays, 20*(1), 41-48.

Righi, L., Deaglio, S., Pecchioni, C., Gregorini, A., Horenstein, A. L., Bussolati, G., . . . Malavasi, F. (2003). Role of CD31/platelet endothelial cell adhesion molecule-1 immunoreactivity in in vitro and in vivo growth and differentiation of human breast cancer cells. *The American Journal of Pathology, 162*(4), 1163-1174.

Risau, W. (1997). Mechanisms of angiogenesis. *Nature, 386*(6626), 671.

Roskoski Jr, R. (2005). Signaling by Kit protein-tyrosine kinase—the stem cell factor receptor. *Biochemical and biophysical research communications, 337*(1), 1-13.

Rot, A., & Andrian, U. H. v. (2004). Chemokines in Innate and Adaptive Host Defense: Basic Chemokinese Grammar for Immune Cells. *Annual Review of Immunology, 22*(1), 891-928. doi:10.1146/annurev.immunol.22.012703.104543

Rouanet, P., Roger, P., Rousseau, E., Thibault, S., Romieu, G., Mathieu, A., . . . Maran-Gonzalez, A. (2014). HER 2 over expression a major risk factor for recurrence in pT1a-bN0M0 breast cancer: results from a F rench regional cohort. *Cancer medicine, 3*(1), 134-142.

Säemann, M. D., Diakos, C., Kelemen, P., Kriehuber, E., Zeyda, M., Böhmig, G. A., . . . Zlabinger, G. J. (2003). Prevention of CD40-triggered dendritic cell maturation and induction of T-cell hyporeactivity by targeting of Janus kinase 3. *American Journal of Transplantation, 3*(11), 1341-1349.

Sarkar, A., & Hochedlinger, K. (2013). The sox family of transcription factors: versatile regulators of stem and progenitor cell fate. *Cell stem cell, 12*(1), 15-30.

Sarmadi, S., Izadi-Mood, N., Movarei, F., Sefidbakht, S., Sotoudeh, K., & Jahanzad, E. (2017). Association of Neo Angiogenesis by CD34 Immunoreactivity and Clinicopathologic Features in Squamous Cell Carcinoma of Cervix. *Acta Med Iran, 55*(5), 282-289.

Sathishkumar, C., Prabu, P., Balakumar, M., Lenin, R., Prabhu, D., Anjana, R. M., . . . Balasubramanyam, M. (2016). Augmentation of histone deacetylase 3 (HDAC3) epigenetic signature at the interface of proinflammation and insulin resistance in patients with type 2 diabetes. *Clin Epigenetics, 8*, 125. doi:10.1186/s13148-016-0293-3

Sauter, G., Algaba, F., Amin, M., Busch, C., Cheville, J., Gasser, T., . . . Epstein, J. (2004). Tumours of the urinary system: non-invasive urothelial neoplasias. *WHO Classification of Tumours of the Urinary System and Male Genital Organs, IARCC Press, Lyon*, 90-150.

Savant, S. S., Sriramkumar, S., & O'Hagan, H. M. (2018). The Role of Inflammation and Inflammatory Mediators in the Development, Progression, Metastasis, and

Chemoresistance of Epithelial Ovarian Cancer. *Cancers (Basel), 10*(8). doi:10.3390/cancers10080251

Schetter, A. J., Heegaard, N. H., & Harris, C. C. (2009). Inflammation and cancer: interweaving microRNA, free radical, cytokine and p53 pathways. *Carcinogenesis, 31*(1), 37-49.

Schluter, A., Weller, P., Kanaan, O., Nel, I., Heusgen, L., Hoing, B., . . . Brandau, S. (2018). CD31 and VEGF are prognostic biomarkers in early-stage, but not in late-stage, laryngeal squamous cell carcinoma. *18*(1), 272. doi:10.1186/s12885-018-4180-5

Sciannameo, V., Carta, A., d'Errico, A., Giraudo, M. T., Fasanelli, F., Arici, C., . . . Ricceri, F. (2018). New insights on occupational exposure and bladder cancer risk: a pooled analysis of two Italian case-control studies. *Int Arch Occup Environ Health*. doi:10.1007/s00420-018-1388-2

Seker, M., Sancaktar, E., Acibucu, D., Filiz, A., Deveci, K., Bahceci, A., . . . Yuce, S. (2013). Prognostic value of serum Tie-2 and vascular endothelial growth factor levels in cancer patients. *Eur Rev Med Pharmacol Sci, 17*(21), 2929-2932.

Semba, K., Kamata, N., Toyoshima, K., & Yamamoto, T. (1985). A v-erbB-related protooncogene, c-erbB-2, is distinct from the c-erbB-1/epidermal growth factor-receptor gene and is amplified in a human salivary gland adenocarcinoma. *Proceedings of the National Academy of Sciences, 82*(19), 6497-6501.

Senger, D. R., Galli, S. J., Dvorak, A. M., Perruzzi, C. A., Harvey, V. S., & Dvorak, H. F. (1983). Tumor cells secrete a vascular permeability factor that promotes accumulation of ascites fluid. *Science, 219*(4587), 983-985.

Senger, D. R., Wirth, D. F., & Hynes, R. O. (1979). Transformed mammalian cells secrete specific proteins and phosphoproteins. *Cell, 16*(4), 885-893.

Sha, Q. Q., Wei, Q. Z., Zhu, J. K., Wang, K. X., Wang, C., Liu, H. T., . . . Zhang, G. Y. (2012). Loss of membranous carcinoembryonic antigen-related cell adhesion molecule 1 immunoreactivity is related to decreased relapse-free survival of hepatocellular carcinoma following liver transplantation. *Chin Med J (Engl), 125*(16), 2841-2845.

Shahsavari, F., Farhadi, S., Sadri, D., & Sedehi, M. (2015). Evaluation of Microvascularity by CD34 Immunoreactivity in Esophagus and Oral Squamous Cell Carcinoma. *J Contemp Dent Pract, 16*(6), 458-462.

Shao, W., Chen, H., & He, J. (2015). The role of SOX-2 on the survival of patients with non-small cell lung cancer. *Journal of thoracic disease, 7*(7), 1113.

Shchors, K., Nozawa, H., Xu, J., Rostker, F., Swigart-Brown, L., Evan, G., & Hanahan, D. (2013). Increased invasiveness of MMP-9-deficient tumors in two mouse models of neuroendocrine tumorigenesis. *Oncogene, 32*(4), 502.

Sheelam, S., Reddy, S. P., Kulkarni, P. G., Nandan, S., Keerthi, M., & Raj, G. S. (2018). Role of cell proliferation and vascularity in malignant transformation of potentially malignant disorders. *J Oral Maxillofac Pathol, 22*(2), 281. doi:10.4103/jomfp.JOMFP_182_17

Shi, J. F., Xu, S. X., He, P., & Xi, Z. H. (2014). Immunoreactivity of carcinoembryonic antigen-related cell adhesion molecule 1(CEACAM1) and its correlation with angiogenesis in gastric cancer. *Pathol Res Pract, 210*(8), 473-476. doi:10.1016/j.prp.2014.03.014

Shi, S.-R., Liu, C., & Taylor, C. R. (2007). Standardization of immunohistochemistry for formalin-fixed, paraffin-embedded tissue sections based on the antigen-retrieval technique: from experiments to hypothesis. *Journal of Histochemistry & Cytochemistry, 55*(2), 105-109.

Shibuya, M., & Claesson-Welsh, L. (2006). Signal transduction by VEGF receptors in regulation of angiogenesis and lymphangiogenesis. Experimental cell research, 312(5), 549-560.

Shibuya, M. (2011). Vascular endothelial growth factor (VEGF) and its receptor (VEGFR) signaling in angiogenesis: a crucial target for anti-and pro-angiogenic therapies. *Genes & cancer, 2*(12), 1097-1105.

Shiels, M. S., Katki, H. A., Hildesheim, A., Pfeiffer, R. M., Engels, E. A., Williams, M., . . . Chaturvedi, A. K. (2015). Circulating inflammation markers, risk of lung cancer, and utility for risk stratification. *J Natl Cancer Inst, 107*(10), djv199.

Shigetomi, S., Imanishi, Y., Shibata, K., Sakai, N., Sakamoto, K., Fujii, R., . . . Ogawa, K. (2018). VEGF-C/Flt-4 axis in tumor cells contributes to the progression of oral squamous cell carcinoma via upregulating VEGF-C itself and contactin-1 in an autocrine manner. *Am J Cancer Res, 8*(10), 2046-2063.

Shirai, Y., Uwagawa, T., Shiba, H., Shimada, Y., Horiuchi, T., Saito, N., . . . Yanaga, K. (2017). Recombinant thrombomodulin suppresses tumor growth of pancreatic cancer by blocking thrombin-induced PAR1 and NF-kappaB activation. *Surgery, 161*(6), 1675-1682. doi:10.1016/j.surg.2016.12.008

Shirsat, H. S., Epari, S., Shet, T., Bagal, R., Hawaldar, R., & Desai, S. B. (2012). HER 2 status in invasive breast cancer: immunohistochemistry, fluorescence in-situ hybridization and chromogenic in-situ hybridization. *Indian J Pathol Microbiol, 55*(2), 175-179. doi:10.4103/0377-4929.97855

Siddiqa, A., Long, L. M., Li, L., Marciniak, R. A., & Kazhdan, I. (2008). Immunoreactivity of HER-2 in MCF-7 breast cancer cells modulates anti-apoptotic proteins Survivin and Bcl-2 via the extracellular signal-related kinase (ERK) and phosphoinositide-3 kinase (PI3K) signalling pathways. *BMC cancer, 8*, 129. doi:10.1186/1471-2407-8-129

Simons, K. H., Aref, Z., Peters, H. A. B., Welten, S. P., Nossent, A. Y., Jukema, J. W., . . . Quax, P. H. A. (2018). The role of CD27-CD70-mediated T cell co-stimulation in vasculogenesis, arteriogenesis and angiogenesis. *International Journal of Cardiology, 260*, 184-190. doi:10.1016/j.ijcard.2018.02.015

Sinnamon, M. J., Carter, K. J., Fingleton, B., & Matrisian, L. M. (2008). Matrix metalloproteinase-9 contributes to intestinal tumourigenesis in the adenomatous polyposis coli multiple intestinal neoplasia mouse. *International journal of experimental pathology, 89*(6), 466-475.

Slamon, D. J., Leyland-Jones, B., Shak, S., Fuchs, H., Paton, V., Bajamonde, A., . . . Pegram, M. (2001). Use of chemotherapy plus a monoclonal antibody against HER2 for metastatic breast cancer that overexpresses HER2. *New England Journal of Medicine, 344*(11), 783-792.

Smith, I., Procter, M., Gelber, R. D., Guillaume, S., Feyereislova, A., Dowsett, M., . . . Baselga, J. (2007). 2-year follow-up of trastuzumab after adjuvant chemotherapy in HER2-positive breast cancer: a randomised controlled trial. *The lancet, 369*(9555), 29-36.

Smith, N. D., Prasad, S. M., Patel, A. R., Weiner, A. B., Pariser, J. J., Razmaria, A., . . . Steinberg, G. D. (2016). Bladder Cancer Mortality in the United States: A Geographic and Temporal Analysis of Socioeconomic and Environmental Factors. *The Journal of urology, 195*(2), 290-296. doi:https://doi.org/10.1016/j.juro.2015.07.091

Smith, N. R., Baker, D., James, N. H., Ratcliffe, K., Jenkins, M., Ashton, S. E., . . . Womack, C. (2010). Vascular Endothelial Growth Factor Receptors VEGFR-2 and VEGFR-3 Are Localized Primarily to the Vasculature in Human Primary Solid Cancers. *Clinical Cancer Research, 16*(14), 3548-3561. doi:10.1158/1078-0432.ccr-09-2797

Song, J., Ma, D., Liu, X., Chen, Y., Fang, J., Lui, V. W. Y., . . . Wang, Z. (2018). Thrombomodulin (TM) in tumor cell differentiation and periphery blood immune microenvironment in oral squamous cell carcinoma. *Clinical Immunology, 191*, 27-33. doi:https://doi.org/10.1016/j.clim.2018.02.011

Song, N., Sung, H., Choi, J.-Y., Han, S., Jeon, S., Song, M., . . . Lee, K.-M. (2012). Preoperative serum levels of matrix metalloproteinase-2 (MMP-2) and survival of breast cancer among Korean women. *Cancer Epidemiology and Prevention Biomarkers*.

Spinale, F. G. (2002). Matrix metalloproteinases: regulation and dysregulation in the failing heart. *Circulation research, 90*(5), 520-530.

Stamler, R., Keutmann, H. T., Sidis, Y., Kattamuri, C., Schneyer, A., & Thompson, T. B. (2008). The Structure of FSTL3· Activin A Complex DIFFERENTIAL BINDING OF N-TERMINAL DOMAINS INFLUENCES FOLLISTATIN-TYPE ANTAGONIST SPECIFICITY. *Journal of Biological Chemistry, 283*(47), 32831-32838.

Stein, J. P., Lieskovsky, G., Cote, R., Groshen, S., Feng, A. C., Boyd, S., . . . Skinner, D. G. (2001). Radical cystectomy in the treatment of invasive bladder cancer: long-term results in 1,054 patients. *J Clin Oncol, 19*(3), 666-675.

Stockinger, H., Gadd, S. J., Eher, R., Majdic, O., Schreiber, W., Kasinrerk, W., . . . Knapp, W. (1990). Molecular characterization and functional analysis of the leukocyte surface protein CD31. *The Journal of Immunology, 145*(11), 3889-3897.

Student, V., Andrys, C., Soucek, O., Spacek, J., Tosner, J., & Sedlakova, I. (2018). Importance of basal fibroblast growth factor levels in patients with ovarian tumor. *Ceska Gynekol, 83*(3), 169-176.

Sun, H. J., Cai, W. W., Gong, L. L., Wang, X., Zhu, X. X., Wan, M. Y., . . . Qiu, L. Y. (2017). FGF-2-mediated FGFR1 signaling in human microvascular endothelial cells is activated by vaccarin to promote angiogenesis. *Biomed Pharmacother, 95*, 144-152. doi:10.1016/j.biopha.2017.08.059

Surowiak, P., Maciejczyk, A., Materna, V., Drag-Zalesińska, M., Wojnar, A., Pudelko, M., . . . Zabel, M. (2007). Unfavourable prognostic significance of S100P immunoreactivity in ovarian cancers. *Histopathology, 51*(1), 125-127.

Sylvester, R. J., van der Meijden, A., Witjes, J. A., Jakse, G., Nonomura, N., Cheng, C., . . . Kurth, K. H. (2005). High-grade Ta urothelial carcinoma and carcinoma in situ of the bladder. *Urology, 66*(6 Suppl 1), 90-107. doi:10.1016/j.urology.2005.06.135

Sylvester, R. J., van der Meijden, A. P., Oosterlinck, W., Witjes, J. A., Bouffioux, C., Denis, L., . . . Kurth, K. (2006). Predicting recurrence and progression in individual patients

with stage Ta T1 bladder cancer using EORTC risk tables: a combined analysis of 2596 patients from seven EORTC trials. *European Urology, 49*(3), 466-477.

Szarvas, T., Jäger, T., Droste, F., Becker, M., Kovalszky, I., Romics, I., . . . Rübben, H. (2008). Serum Levels of Angiogenic Factors and their Prognostic Relevance in Bladder Cancer. *Pathology & Oncology Research, 15*(2), 193. doi:10.1007/s12253-008-9107-z

Szarvas, T., Jäger, T., Laszlo, V., Kramer, G., Klingler, H. C., Vom Dorp, F., . . . Rübben, H. (2012). Circulating angiostatin, bFGF, and Tie2/TEK levels and their prognostic impact in bladder cancer. *Urology, 80*(3), 737. e713-737. e718.

Tabrizi, M. E. A., Lancaster, T. L., Ismail, T. M., Georgiadou, A., Ganguly, A., Mistry, J. J., . . . Ahmad, S. (2018). S100P enhances the motility and invasion of human trophoblast cell lines. *8*(1), 11488. doi:10.1038/s41598-018-29852-2

Tammela, T., Zarkada, G., Wallgard, E., Murtomäki, A., Suchting, S., Wirzenius, M., . . . Peltonen, R. (2008). Blocking VEGFR-3 suppresses angiogenic sprouting and vascular network formation. *Nature, 454*(7204), 656.

Tanaka, K., Salunya, T., Motomiya, Y., Motomiya, Y., Oyama, Y., Yamakuchi, M., & Maruyama, I. (2017). Decreased Immunoreactivity of Thrombomodulin in Endothelial Cells by Fibroblast Growth Factor-23/alpha-Klotho. *Ther Apher Dial, 21*(4), 395-404. doi:10.1111/1744-9987.12524

Tanaka, S., Mori, M., Sakamoto, Y., Makuuchi, M., Sugimachi, K., & Wands, J. R. (1999). Biologic significance of angiopoietin-2 immunoreactivity in human hepatocellular carcinoma. *The Journal of clinical investigation, 103*(3), 341-345. doi:10.1172/JCI4891

Thies, A., Moll, I., Berger, J., Wagener, C., Brummer, J., Schulze, H. J., . . . Schumacher, U. (2002). CEACAM1 immunoreactivity in cutaneous malignant melanoma predicts the development of metastatic disease. *J Clin Oncol, 20*(10), 2530-2536. doi:10.1200/jco.2002.05.033

Thoem, I., Schult-Kronefeld, O., Burkholder, I., Schuch, G., Andritzky, B., Kastendieck, H., . . . Schumacher, U. (2009). Immunoreactivity of CEACAM-1 in pulmonary adenocarcinomas and their metastases. *Anticancer Res, 29*(1), 249-254.

Thom, I., Schult-Kronefeld, O., Burkholder, I., Schuch, G., Andritzky, B., Kastendieck, H., . . . Laack, E. (2009). Immunoreactivity of CEACAM-1 in pulmonary adenocarcinomas and their metastases. *Anticancer Res, 29*(1), 249-254.

Trabert, B., Pinto, L., Hartge, P., Kemp, T., Black, A., Sherman, M. E., . . . Chaturvedi, A. K. (2014). Pre-diagnostic serum levels of inflammation markers and risk of ovarian cancer in the prostate, lung, colorectal and ovarian cancer (PLCO) screening trial. *Gynecologic oncology, 135*(2), 297-304.

Tsuji, N., Ishiguro, S., Sasaki, Y., & Kudo, M. (2013). CD34 immunoreactivity in noncancerous liver tissue predicts multicentric recurrence of hepatocellular carcinoma. *Dig Dis, 31*(5-6), 467-471. doi:10.1159/000355246

Tsuta, K., Tanabe, Y., Yoshida, A., Takahashi, F., Maeshima, A. M., Asamura, H., & Tsuda, H. (2011). Utility of 10 immunohistochemical markers including novel markers (desmocollin-3, glypican 3, S100A2, S100A7, and Sox-2) for differential diagnosis of

squamous cell carcinoma from adenocarcinoma of the Lung. *Journal of Thoracic Oncology, 6*(7), 1190-1199.

Tung, Y. T., Chen, H. L., Yen, C. C., Lee, P. Y., Tsai, H. C., Lin, M. F., & Chen, C. M. (2013). Bovine lactoferrin inhibits lung cancer growth through suppression of both inflammation and immunoreactivity of vascular endothelial growth factor. *J Dairy Sci, 96*(4), 2095-2106. doi:10.3168/jds.2012-6153

Turner, A. M., Zsebo, K. M., Martin, F., Jacobsen, F. W., Bennett, L. G., & Broudy, V. C. (1992). Nonhematopoietic tumor cell lines express stem cell factor and display c-kit receptors. *Blood, 80*(2), 374-381.

Usuda, K., Iwai, S., Funasaki, A., Sekimura, A., Motono, N., Ueda, Y., . . . Uramoto, H. (2018). Immunoreactivity and Prognostic Impact of VEGF, CD31 and alphaSMA in Resected Primary Lung Cancers. *Anticancer Res, 38*(7), 4057-4063. doi:10.21873/anticanres.12695

van Kooten, C., & Banchereau, J. (2000). CD40-CD40 ligand. *J Leukoc Biol, 67*(1), 2-17.

van Mourik, J. A., Leeksma, O., Reinders, J., De Groot, P. G., & Zandbergen-Spaargaren, J. (1985). Vascular endothelial cells synthesize a plasma membrane protein indistinguishable from the platelet membrane glycoprotein IIa. *Journal of Biological Chemistry, 260*(20), 11300-11306.

van Osch, F. H. M., Vlaanderen, J., Jochems, S. H. J., Bosetti, C., Polesel, J., Porru, S., . . . Zeegers, M. P. (2018). Modeling the complex exposure history of smoking in predicting bladder cancer: a pooled analysis of 15 case-control studies. *Epidemiology*. doi:10.1097/ede.0000000000000964

van Sleen, Y., Sandovici, M., Abdulahad, W. H., Bijzet, J., van der Geest, K. S. M., Boots, A. M. H., & Brouwer, E. (2019). Markers of angiogenesis and macrophage products for predicting disease course and monitoring vascular inflammation in giant cell arteritis. *Rheumatology (Oxford)*. doi:10.1093/rheumatology/kez034

Vasiliades, G., Kopanakis, N., Vasiloglou, M., Zografos, G., Margaris, H., Masselou, K., . . . Liakakos, T. (2012). Role of the hematopoietic cytokines SCF, IL-3, GM-CSF and M-CSF in the diagnosis of pancreatic and ampullary cancer. *The International journal of biological markers, 27*(3), 186-194.

Vihinen, P., & Kähäri, V. M. (2002). Matrix metalloproteinases in cancer: prognostic markers and therapeutic targets. *International journal of cancer, 99*(2), 157-166.

Villanueva, F., Araya, H., Briceno, P., Varela, N., Stevenson, A., Jerez, S., . . . Galindo, M. (2019). The cancer-related transcription factor RUNX2 modulates immunoreactivity and secretion of the matricellular protein osteopontin in osteosarcoma cells to promote adhesion to endothelial pulmonary cells and lung metastasis. *J Cell Physiol*. doi:10.1002/jcp.28046

Virman, J., Bono, P., Luukkaala, T., Sunela, K., Kujala, P., & Kellokumpu-Lehtinen, P. L. (2015). VEGFR3 and CD31 as prognostic factors in renal cell cancer. *Anticancer Res, 35*(2), 921-927.

Waas, E., Wobbes, T., Ruers, T., Lomme, R., & Hendriks, T. (2006). Circulating gelatinases and tissue inhibitor of metalloproteinase-1 in colorectal cancer metastatic liver disease. *European Journal of Surgical Oncology (EJSO), 32*(7), 756-763.

Wang, D., Stockard, C. R., Harkins, L., Lott, P., Salih, C., Yuan, K., . . . Siegal, G. P. (2008). Immunohistochemistry in the evaluation of neovascularization in tumor xenografts. *Biotech Histochem, 83*(3-4), 179-189. doi:10.1080/10520290802451085

Wang, H., Yin, Y., Li, W., Zhao, X., Yu, Y., Zhu, J., . . . Lu, W. (2012a). Over-immunoreactivity of PDGFR-β promotes PDGF-induced proliferation, migration, and angiogenesis of EPCs through PI3K/Akt signaling pathway. *PLoS One, 7*(2), e30503.

Wang, Y.-q., Jin, C., Zheng, H.-m., Zhou, K., Shi, B.-b., Zhang, Q., . . . Lin, F. (2016a). A novel prognostic inflammation score predicts outcomes in patients with ovarian cancer. *Clinica chimica acta, 456*, 163-169.

Wang, Y., Li, L., Guo, X., Jin, X., Sun, W., Zhang, X., & Xu, R. C. (2012b). Interleukin-6 signaling regulates anchorage-independent growth, proliferation, adhesion and invasion in human ovarian cancer cells. *Cytokine, 59*(2), 228-236. doi:10.1016/j.cyto.2012.04.020

Wang, Z., Wang, W., Xu, S., Wang, S., Tu, Y., Xiong, Y., . . . Wang, C. (2016b). The role of MAPK signaling pathway in the Her-2-positive meningiomas. *Oncol Rep, 36*(2), 685-695. doi:10.3892/or.2016.4849

Wang, Z., Wu, P., Wu, D., Zhang, Z., Hu, G., Zhao, S., . . . Huang, J. (2015). Prognostic and clinicopathological significance of serum interleukin-6 immunoreactivity in colorectal cancer: a systematic review and meta-analysis. *Onco Targets Ther, 8*, 3793-3801. doi:10.2147/ott.s93297

Wei, R., Wong, J. P. C., & Kwok, H. F. (2017). Osteopontin -- a promising biomarker for cancer therapy. *Journal of Cancer, 8*(12), 2173-2183. doi:10.7150/jca.20480

Weiler, H., Lindner, V., Kerlin, B., Isermann, B. H., Hendrickson, S. B., Cooley, B. C., . . . Post, M. J. (2001). Characterization of a mouse model for thrombomodulin deficiency. *Arteriosclerosis, Thrombosis, and Vascular Biology, 21*(9), 1531-1537.

Wermker, K., Brauckmann, T., Klein, M., Hassfeld, S., Schulze, H. J., & Hallermann, C. (2015). Prognostic value of S100/CD31 and S100/podoplanin double immunostaining in mucosal malignant melanoma of the head and neck. *Head Neck, 37*(9), 1368-1374. doi:10.1002/hed.23761

Wong, M. C., Fung, F. D., Leung, C., Cheung, W. W., Goggins, W. B., & Ng, C. F. (2018). The global epidemiology of bladder cancer: a joinpoint regression analysis of its incidence and mortality trends and projection. *Scientific reports, 8*(1), 1129.

World Health Organisation (2019). International agency for research on cancer. Population fact sheets. United Kingdom. Accessed from http://gco.iarc.fr/today/fact-sheets-populations on 19th June 2019.

Wright, C., Mellon, K., Johnston, P., Lane, D. P., Harris, A. L., Horne, C. H., & Neal, D. E. (1991). Immunoreactivity of mutant p53, c-erbB-2 and the epidermal growth factor receptor in transitional cell carcinoma of the human urinary bladder. *Br J Cancer, 63*(6), 967-970.

Wu, C.-T., Chang, Y.-H., Lin, P.-Y., Chen, W.-C., & Chen, M.-F. (2014). Thrombomodulin immunoreactivity regulates tumorigenesis in bladder cancer. *BMC cancer, 14*(1), 375.

Wu, Y., Stabach, P., Michaud, M., & Madri, J. A. (2005). Neutrophils lacking platelet-endothelial cell adhesion molecule-1 exhibit loss of directionality and motility in CXCR2-mediated chemotaxis. *The Journal of Immunology, 175*(6), 3484-3491.

Wu, Z., He, D., Zhao, S., & Wang, H. (2018). IL-17A/IL-17RA promotes invasion and activates MMP-2 and MMP-9 immunoreactivity via p38 MAPK signaling pathway in non-small cell lung cancer. *Mol Cell Biochem*. doi:10.1007/s11010-018-3483-9

Xu, J., Guo, X., Jing, M., & Sun, T. (2018). Prediction of tumor mutation burden in breast cancer based on the immunoreactivity of ER, PR, HER-2, and Ki-67. *Onco Targets Ther, 11*, 2269-2275. doi:10.2147/ott.s159830

Yafi, F. A., Brimo, F., Steinberg, J., Aprikian, A. G., Tanguay, S., & Kassouf, W. (2015). Prospective analysis of sensitivity and specificity of urinary cytology and other urinary biomarkers for bladder cancer. *Urol Oncol, 33*(2), 66 e25-31. doi:10.1016/j.urolonc.2014.06.008

Yang, H., Dinney, C. P., Ye, Y., Zhu, Y., Grossman, H. B., & Wu, X. (2008). Evaluation of Genetic Variants in MicroRNA-Related Genes and Risk of Bladder Cancer. *Cancer Research, 68*(7), 2530-2537. doi:10.1158/0008-5472.can-07-5991

Yang, J. G., Wang, L. L., & Ma, D. C. (2018a). Effects of vascular endothelial growth factors and their receptors on megakaryocytes and platelets and related diseases. *Br J Haematol, 180*(3), 321-334. doi:10.1111/bjh.15000

Yang, X., Zhang, H., Shi, Y., Yu, Z., Yan, H., Ni, Z., . . . Fang, W. (2018b). Association of serum angiopoietin-2 with malnutrition, inflammation, atherosclerosis and valvular calcification syndrome and outcome in peritoneal dialysis patients: a prospective cohort study. *J Transl Med, 16*(1), 312. doi:10.1186/s12967-018-1687-0

Yang, Y., Cheng, B. J., & Lu, S. (2017). Thrombomodulin regulates doxorubicin sensitivity through epithelial-mesenchymal transition in non-small cell lung cancer. *Eur Rev Med Pharmacol Sci, 21*(1), 95-101.

Yu, S. M., & Kim, S. J. (2010). Endoplasmic reticulum stress (ER-stress) by 2-deoxy-D-glucose (2DG) reduces cyclooxygenase-2 (COX-2) immunoreactivity and N-glycosylation and induces a loss of COX-2 activity via a Src kinase-dependent pathway in rabbit articular chondrocytes. *Experimental & molecular medicine, 42*(11), 777.

Yuan, R. H., Chang, K. T., Chen, Y. L., Hsu, H. C., Lee, P. H., Lai, P. L., & Jeng, Y. M. (2013). S100P immunoreactivity is a novel prognostic factor in hepatocellular carcinoma and predicts survival in patients with high tumor stage or early recurrent tumors. *PLoS One, 8*(6), e65501. doi:10.1371/journal.pone.0065501

Yuge, R., Kitadai, Y., Shinagawa, K., Onoyama, M., Tanaka, S., Yasui, W., & Chayama, K. (2015). mTOR and PDGF pathway blockade inhibits liver metastasis of colorectal cancer by modulating the tumor microenvironment. *Am J Pathol, 185*(2), 399-408. doi:10.1016/j.ajpath.2014.10.014

Zabkiewicz, C., Resaul, J., Hargest, R., Jiang, W. G., & Ye, L. (2017). Increased immunoreactivity of follistatin in breast cancer reduces invasiveness and clinically correlates with better survival. *Cancer Genomics-Proteomics, 14*(4), 241-251.

Zhang, H., Ye, Y. L., Li, M. X., Ye, S. B., Huang, W. R., Cai, T. T., . . . Li, J. (2017). CXCL2/MIF-CXCR2 signaling promotes the recruitment of myeloid-derived

suppressor cells and is correlated with prognosis in bladder cancer. *Oncogene, 36*(15), 2095-2104. doi:10.1038/onc.2016.367

Zhang, L., Chen, Y., Li, G., Chen, M., Huang, W., Liu, Y., & Li, Y. (2016). TGF-beta1/FGF-2 signaling mediates the 15-HETE-induced differentiation of adventitial fibroblasts into myofibroblasts. *Lipids Health Dis, 15*, 2. doi:10.1186/s12944-015-0174-3

Zhang, L., Wang, Y., Qin, Z., Li, R., Cong, R., Ji, C., . . . Song, N. (2018a). TP53 codon 72 Polymorphism and bladder cancer risk: a meta-analysis and emphasis on the role of tumor or smoking status. *J Cancer, 9*(19), 3522-3531. doi:10.7150/jca.26264

Zhang, P., Ruan, Y., Xiao, J., Chen, F., & Zhang, X. (2018b). Association of serum follistatin levels with histological types and progression of tumor in human lung cancer. *Cancer Cell Int, 18*, 162. doi:10.1186/s12935-018-0664-2

Zhang, Y., Weiler-Guettler, H., Chen, J., Wilhelm, O., Deng, Y., Qiu, F., . . . Böhrer, H. (1998). Thrombomodulin modulates growth of tumor cells independent of its anticoagulant activity. *The Journal of clinical investigation, 101*(7), 1301-1309.

Zheng, L.-F., Chen, P., Wang, Z., Wang, X.-J., & Lei, L. (2017). Preliminary study on the role of serum PECAM-1 in metastatic breast cancer. *Translational Cancer Research, 6*(6), 1207-1213.

Zheng, N., Huo, Z., Zhang, B., Meng, M., Cao, Z., Wang, Z., & Zhou, Q. (2016). Thrombomodulin reduces tumorigenic and metastatic potential of lung cancer cells by up-regulation of E-cadherin and down-regulation of N-cadherin immunoreactivity. *Biochemical and biophysical research communications, 476*(4), 252-259.

Zhou, C., Zhou, H.-J., Zhang, X.-F., Lou, L.-L., Ye, Q.-H., Zheng, Y., . . . Jia, H.-L. (2013). Postoperative Serum Osteopontin Level is a Novel Monitor for Treatment Response and Tumor Recurrence after Resection of Hepatitis B–related Hepatocellular Carcinoma. *Annals of surgical oncology, 20*(3), 929-937.

Zhou, M., Jin, Z., Liu, Y., He, Y., Du, Y., Yang, C., . . . Cao, M. (2017). Up-regulation of carcinoembryonic antigen-related cell adhesion molecule 1 in gastrointestinal cancer and its clinical relevance. *Acta Biochim Biophys Sin (Shanghai), 49*(8), 737-743. doi:10.1093/abbs/gmx060

Zhu, F., Qian, W., Zhang, H., Liang, Y., Wu, M., Zhang, Y., . . . Li, Y. (2017a). SOX2 is a marker for stem-like tumor cells in bladder cancer. *Stem cell reports, 9*(2), 429-437.

Zhu, M., Miao, B., Zhu, J., Wang, H., & Zhou, Z. (2017b). Transplantation of periodontal ligament cell sheets expressing human betadefensin3 promotes antiinflammation in a canine model of periodontitis. *Mol Med Rep, 16*(5), 7459-7467. doi:10.3892/mmr.2017.7514

10.0 Chapter Ten: Grants, publications & Conferences

10.1 Grants Awarded

Wrexham Maelor Voluntary Service (MVS) Equipment Grant. PE-tongwiis (2019). Funding for new clinical research analyser for the North Wales Clinical Research Centre. (Award: £48,631).

Betsi Cadwaldr University Health Board (BCUHB) Research and Development Pathway to Portfolio (P2P) funding. PE-tongwiis I. Shergill & SF Hughes (2016)**.** Evaluation of selective biomarkers and clinical outcome measures for the treatment of non-muscle invasive bladder cancer: A clinical feasibility-study. One-year project award (£30,000).

NISCHR AHSC Equipment Call. SF. Hughes, PE-tongwiis & I. Shergill. The immunoreactivity of biomarkers and clinical outcome measures pre and post-surgical treatment of prostate bladder and penile cancers. (Award: £39,936.42; 2015-2016). Grant for capital equipment.

Betsi Cadwaldr University Health Board (BCUHB) Research and Development Pathway to Portfolio (P2P) funding. SF Hughes, PE-tongwiis & I. Shergill. Changes in selective biomarkers after transurethral resection of a bladder tumour (TURBT) and their association with non-muscle invasive bladder cancer (NMIBC) recurrence and progression, as well as post-operative complications. Two-year project award (£16,960; 2014-2016).

Government of Ghana (Ghana Education Trust Fund)
Full Scholarship for PhD studies (£75,000)

10.2 Publications

Alyson J. Moyes, Rebecca M. Lamb, **Peter Ella-Tongwiis**, Anish Pushkaran, Issam Ahmed, Iqbal Shergill, & **Stephen F. Hughes** (2017). A pilot study evaluating changes to haematological and biochemical tests after Flexible Ureterorenoscopy for the treatment of kidney stones. *PLOS ONE*. PONE-D-16-40339.

Peter Ella-Tongwiis & Stephen Fôn Hughes (2016). The Effect of Storage on Various Haematological and Biochemical Parameters of NHSBT Donor Blood. *J J Hemato.*, 2(2): 029.

Rebecca J. Edge, **Peter Ella-Tongwiis**, Robert C. Coleman and Stephen F. Hughes. Mild-Tourniquet Induced Ischaemia-reperfusion Injury Results in Changes to Haematological, Haemostatic and Inflammatory Parameters. *British Journal of Medicine & Medical Research*; *4(13): 2470-2482*. DOI: 10.9734/BJMMR/2014/8387 (2014).

10.3 Conferences

Ella-tongwiis PE, Lamb RM, Shergill I. & Hughes SF. (2017). Trans-Urethral Resection of the Bladder tumour (TURBT) surgery,for the treatment of Non-Muscle Invasive Bladder cancer(NMIBC), results in changes to selective biochemical parameters. 35th World Congress of Endourology, Vancouver, Canada 12-16th September 2017 (Podium)

Ella-tongwiis PE, Lamb RM, Shergill I. & Hughes SF. (2017). Tissue Immunoreactivity of Novel Biomarkers and their Association with Non-Muscle Invasive Bladder cancer (NMIBC) Recurrence and Progression. Welsh Urological Society Spring Meeting. 9 & 10th March 2017. Caernarfon, North Wales. (Podium)

Lamb RM, Ella-tongwiis PE, Moyes AJ, Pushkaran A, Stainer V, Ahmed I, Shergill I. & Hughes SF. (2016). Changes in routine, cellular & molecular biomarkers following TURBT for NMIBC: A pilot study. Welsh Surgical & Welsh Urological Societies Meeting. November 2016. (PODIUM).

Ella-tongwiis PE, Moyes AJ. & Lamb RM. (2016). The North Wales & North West Urological Research Centre (NW2URC): An overview of our current clinical research studies. Poster. British Association of Urological Surgeons (BAUS). BT Convention Centre, Liverpool, UK. July 2016. (POSTER).

Ella-tongwiis PE, Shergill I. & Hughes SF. (2015). Changes in selective biomarkers after Transurethral Resection of a Bladder tumour (TURBT) in Non-Muscle Invasive Bladder cancer (NMIBC) and their association with bladder cancer recurrence and progression, as well as post-operative complications. University of Chester, Annual Faculty of Life Science: Postgraduate Conference. (PODIUM).

Total word count (including references) = 62,667
Word count (excluding references) = 49,376